

**Design and Application of Responsive Composite Particles for Multiphase Separations of
Bitumen Emulsions in Bituminous (Oil) Sands Extraction**

by

Chen Liang

A thesis submitted in partial fulfillment of the requirements for the degree of

Doctor of Philosophy

in

Chemical Engineering

Department of Chemical and Materials Engineering
University of Alberta

© Chen Liang, 2016

Abstract

The development of more environmentally-friendly and cost-effective extraction and production technologies is a key to sustaining heavy oil and bitumen production. The high viscosity of the heavily degraded petroleum requires additional processing in order to recover such challenging resources from both shallow surface deposits and deeper underground deposits. Intensive processing conditions require substantially more energy while the degraded nature of the heavy crude and bitumen leads to a lower price. The extraction involves numerous processes that separate valuable hydrocarbons from water and solids. Complete separation of heavy oil (bitumen) is not typically possible, due to the complexity of the bituminous (oil) sand ore. As a result, multiphase waste streams are generated at each step, which require a special treatment and/or complex disposal protocols. The dispersed nature of the waste makes its management difficult and expensive. Preparing specially designed composite particles by combining the properties of different materials may provide an effective method for such challenging tasks, by taking advantage of desirable and suppressing undesirable properties. Responsive behaviour can be incorporated into the composite particle to prepare smart materials tailored to the specific applications. To this end, various types of responsive particles were prepared and tested in this thesis research, including:

1. **Particles with Switchable Wettability.** Particles with switchable wettability were prepared from silica by chemical functionalization of its surface with CO₂-switchable amidine moieties. The surface of switchable particles, under CO₂, is more hydrophilic due to the ionized surface groups while, in the absence of CO₂, it is less hydrophilic as surface group revert back to their

basic non-ionic state. Both switchable oil-in-water and water-in-oil emulsions were thus stabilized/destabilized using solid particles with switchable and tunable wettability.

2. **Responsive Absorbent Particles.** Changes to the surface properties of particles can induce changes to colloidal stability. Composite absorbent particles consisting of an absorbent core coated by an interfacially active material were prepared by emulsion droplet dehydration of specially formulated emulsions. The composite absorbent particles with initial intermediate wettability were effectively dispersed in non-aqueous environment such as oil-continuous emulsions (*e.g.*, bitumen emulsions) and attached to emulsified water droplets. The surface of the composite absorbent particles became more hydrophilic and formed large aggregates following absorption of water. Large aggregates of spent absorbent particles were much easier to separate.
3. **Interfacially active Magnetic Particles.** Interfacially active particles were prepared by sequential adsorption of different cellulosic materials onto magnetic iron oxide (Fe_3O_4) particles. Interfacially active magnetic particles were effectively attached to the oil-water interface and imparted magnetic susceptibility to the biphasic mixture. Adding such interfacially active magnetic particles to biphasic waste (*e.g.*, emulsion droplets, rag layers and sludge) allowed biphasic waste to be magnetically separated.

The ability to induce a response in the properties or function (*e.g.*, emulsion or colloidal stability) of a particle can result in smarter processes that are specifically designed to take advantages of changing process conditions. Alternatively, manipulation and separation of responsive (*i.e.*, magnetic) particles can be facilitated by applying an external force (*i.e.*, a magnetic field). By matching a process with an appropriate responsive particle, it is possible to design processes with

reduced operating cost, less waste, and fewer environmental and health risks. Specifically, different responsive composite particles were designed and prepared to dewater bitumen emulsions by absorption and enable magnetic separation of emulsions droplets, rag layer and sludge.

Preface

The work described herein was carried out independently by the author, under the supervision of Prof. Z. Xu and Prof. Q. Liu. This dissertation is a compilation of both original work, published in journal papers, or in the form of manuscripts submitted for consideration of publication. Portions of the materials presented in Chapters 2, 4 and 5 have been previously published in various peer-reviewed journals. The following list specifies contributions of the author to each chapter:

- **Chapter 1: *Introduction*.** This section is an original work by the author, C. Liang.
- **Chapter 2: *Problem Description*.** This section is an original work by the author, C. Liang.
 - **Chapter 2.1: Particle-Stabilized Emulsions.** A version of this section has been published as D. Harbottle, C. Liang, N. El-Thaher, Q. Liu, J. Masliyah and Z. Xu “CHAPTER 11: Particle-Stabilized Emulsions in Heavy Oil Processing” in Particle-Stabilized Emulsions and Colloids: Formation and Application by the Royal Society of Chemistry with DOI:10.1039/9781782620143-00283. D. Harbottle and C. Liang jointly prepared the majority of the manuscript with additional contributions from N. El-Thaher, Q. Liu, J. Masliyah and Z. Xu. Z. Xu, J. Masliyah and Q. Liu provided guidance, supervision, and review of the manuscript.
- **Chapter 3: *Experimental*.** This section is an original work by the author, C. Liang.
- **Chapter 4: *Responsive Composite Particles*.** A version of this section has been published as C. Liang, Q. Liu and Z. Xu “Surfactant-Free Switchable Emulsions Using CO₂-Responsive Particles” in Volume 6, Issue 9 of *ACS Applied Materials & Interfaces* by the American Chemical Society with DOI:10.1021/am5007113. C. Liang was responsible for experimental design, data collection and interpretation, as well as preparation of the manuscript. Z. Xu and Q. Liu provided guidance, supervision, and review of the manuscript.
- **Chapter 5: *Dehydration of Emulsion Droplets*.** A version of this section has been published as C. Liang, Q. Liu and Z. Xu “Synthesis of Surface-Responsive Composite Particles by Dehydration of Water-in-Oil Emulsions” in Volume 7, Issue 37 of *ACS Applied Materials & Interfaces* published by the American Chemical Society with

DOI:10.1021/acsami.5b05093. C. Liang was responsible for experimental design, data collection and interpretation, as well as preparation of the manuscript. Z. Xu and Q. Liu provided guidance, supervision, and review of the manuscript.

- **Chapter 6:** *Absorptive Emulsion Dewatering*. A version of this section has been published as C. Liang, Q. Liu and Z. Xu “Dewatering Bitumen Emulsions using Interfacially Active Organic Composite Absorbent Particles” in Volume 30, Issue 7 of *Energy & Fuels* by the American Chemical Society with **DOI:**10.1021/acs.energyfuels.6b00228. C. Liang was responsible for experimental design, data collection and interpretation, as well as preparation of the manuscript. Z. Xu and Q. Liu provided guidance, supervision, and review of the manuscript.
- **Chapter 7:** *Interfacially active Magnetic Particles*. A version of this section has been submitted for consideration of publication. C. Liang was responsible for experimental design, data collection and interpretation, as well as preparation of the manuscript. X. He assisted in data collection. Z. Xu and Q. Liu provided guidance, supervision, and review of the manuscript.
- **Chapter 8:** *Summary and Future Work*. This section is an original work by the author, C. Liang.
- **Appendix A:** *General Background*. This section is an original work by the author, C. Liang.

Dedicated to
my mother and my father,
and to my brother;
to whom I owe everything.

Acknowledgements

The author acknowledges the financial support of the NSERC Industrial Chair Program in Oil Sands Engineering and all of its sponsors including Syncrude Canada Ltd., Suncor Energy Inc., Shell Canada - Albian Sands Energy Inc., Canadian Natural Resources Ltd., Fort Hills Energy Ltd., Teck Resources Ltd., Petro-Canada, Champion Technologies, Baker Petrolite Corporation, Nalco Canada Inc., Alberta Energy Research Institute (now Alberta Innovates - Energy and Environmental Solutions), and the University of Alberta. The author acknowledges the material support of Syncrude Canada Ltd., Nalco Canada Inc., Teck Resources Ltd., and Alberta Innovates Technology Futures Ltd. The author acknowledges the generous support and guidance of Dr. Z. Xu and Dr. Q. Liu. The author is gracious for the support of the Department of Chemical and Materials Engineering, the Department of Mechanical Engineering, NanoFAB and the Faculty of Graduate and Research Studies at the University of Alberta located in Edmonton, Alberta.

Table of Contents

Abstract.....	ii
Preface	v
Acknowledgements.....	viii
Table of Contents.....	ix
List of Figures	xiv
List of Tables	xvii
List of Abbreviations	xix
Chapter 1. Introduction	1
1.1 References	4
Chapter 2. Problem Description	6
2.1 Particle-Stabilized Emulsions	6
2.1.1 Introduction	6
2.1.2 Theory of Particle-Stabilized Emulsions.....	7
2.1.3 Asphaltenes.....	12
2.1.4 Particles.....	24
2.1.5 Rag Layers	29
2.1.6 Demulsification	32
2.1.7 Summary	44
2.2 Problem Statement and Objective	45
2.2.1 Preparing Composite Particles.....	46
2.2.2 Multiphase Waste.....	49
2.3 Multiphase Separation in Surface Mining	52

2.3.1	Surface Wettability Response.....	52
2.3.2	Magnetically Response	54
2.4	References	56
	Chapter 2.1.....	56
	Chapter 2.2.....	61
Chapter 3.	Experimental.....	63
3.1	Materials	63
3.1.1	Chemical Reagents.....	63
3.1.2	Bitumen Samples	65
3.1.3	Process Water Samples.....	66
3.2	Instrumentation	66
3.2.1	Physical Properties.....	66
3.2.2	Chemical Properties.....	67
3.3	Procedures	69
3.3.1	Diluted-Bitumen Emulsion.....	69
3.3.2	Silica-Coating.....	70
3.3.3	Silica-Functionalization	70
3.3.4	Emulsion Dehydration.....	72
3.4	Environmental Health and Safety.....	73
3.5	References	76
Chapter 4.	CO ₂ -Responsive Stabilizing Particles.....	77
4.1	Introduction	77
4.2	Concept of Switchable Particle	79
4.3	Experimental.....	80
4.4	Results and Discussion	82

4.5	Conclusions	91
4.6	References	91
Chapter 5.	Emulsion Droplet Dehydration	95
5.1	Introduction	95
5.2	Experimental	101
5.3	Results and Discussion	103
5.4	Conclusions	115
5.5	References	116
Chapter 6.	Absorptive Emulsion Dewatering	119
6.1	Introduction	119
6.2	Experimental	121
6.3	Results and Discussion	123
6.4	Conclusions	132
6.5	References	133
Chapter 7.	Interfacially Active Magnetic Particles.....	135
7.1	Introduction	135
7.2	Experimental	140
7.3	Results and Discussion	142
7.4	Conclusions	152
7.5	References	153
Chapter 8.	Summary and Future Work.....	155
8.1	Summary	155

8.1.1	CO ₂ -Responsive Stabilizing Particles.....	158
8.1.2	Dehydration of Emulsion Droplets	160
8.1.3	Absorptive Emulsion Dewatering	163
8.1.4	Interfacially Active Magnetic Particles.....	165
8.2	Future Work: Responsive Composite Particles.....	166
8.2.1	Composite Absorbent Particles	167
8.2.2	Interfacially Active Magnetic Particles.....	168
8.3	Future Work: In-Situ Production.....	169
8.3.1	Triggered Blocking Agent	169
8.3.2	Triggered Polymer Degradation.....	172
8.4	References	174
Works Cited.....		175
Chapter 1.....		175
Chapter 2.1.....		175
Chapter 2.2.....		180
Chapter 3.....		181
Chapter 4.....		182
Chapter 5.....		185
Chapter 6.....		188
Chapter 7.....		189
Chapter 8.....		191
Appendix A.	General Background	192
A.1	Bituminous (Oil) Sands.....	192
A.1.1	Bitumen Properties.....	194
A.1.2	Bitumen Blending.....	199
A.2	Surface Mining	200
A.2.1	Bitumen Ore Conditioning	201

A.2.2	Bitumen Recovery.....	204
A.2.3	Froth Treatment.....	207
A.2.4	Tailings Management.....	208
A.3	<i>In-situ</i> Extraction.....	210
A.3.1	Cyclic Steam Stimulation.....	212
A.3.2	Steam-Assisted Gravity Drainage.....	212
A.3.3	<i>In-situ</i> Combustion.....	213
A.4	Bitumen Upgrading and Synthetic Crude.....	213
A.4.1	Separation Processes.....	214
A.4.2	Thermal Cracking and Coking.....	215
A.4.3	Hydrogen Processes.....	216
A.5	Colloid and Interface Chemistry.....	216
A.5.1	Surface Activity.....	217
A.5.2	Surfactants.....	218
A.5.3	Emulsification.....	223
A.5.4	Emulsion Stability.....	224
A.5.5	Pickering Emulsions.....	227
A.5.6	Breaking Emulsions (Demulsification).....	229
A.6	Particle Engineering.....	230
A.6.1	Particle Properties.....	230
A.6.2	Micro- and Nano- Particles.....	232
A.6.3	Colloidal Stability.....	233
A.6.4	Particle Dynamics.....	235
A.6.5	Particle Synthesis.....	239
A.7	References.....	242

List of Figures

Figure 2-1. Preferential particle location at the oil-water interface	8
Figure 2-2. Scaled energy of particle detachment from the oil-water interface	9
Figure 2-3. Geometry of a Janus particle partitioning at the oil-water interface	10
Figure 2-4. Variation in particle detachment energy	12
Figure 2-5. Proposed molecular architecture of asphaltenes	13
Figure 2-6. Dynamic interfacial tension for asphaltene	16
Figure 2-7. Water droplet-in-diluted bitumen and interfacial crumpling	18
Figure 2-8. Comparison of asphaltene layers measured by dilatational and shear rheology.....	20
Figure 2-9. Shear viscoelastic properties of an aging asphaltene film	21
Figure 2-10. Thin liquid film apparatus.....	22
Figure 2-11. Thin film drainage of flexible and rigid interfacial skins.....	23
Figure 2-12. Schematic view of asphaltene nanoaggregates	25
Figure 2-13. Structure of kaolinite clays exhibiting three different surface characteristics	26
Figure 2-14. A schematic diagram of the vessel for generation of petroleum rag layer	30
Figure 2-15. Chemical structure of DETA-based block copolymer with EO/PO units	33
Figure 2-16. Structure of EC with a degree of substitution of 2.....	35
Figure 2-17. Interfacial tension between naphtha and water and micrographs of emulsions....	36
Figure 2-18. Water content of emulsion as a function of EC dosage	37
Figure 2-19. Interactions of water droplets visualized using the micropipette technique.....	39
Figure 2-20. AFM topography images of asphaltene-coated surfaces soaked in EC	40
Figure 2-21. Schematics of asphaltene displacement by EC on a hydrophilic solid surface.....	41
Figure 2-22. Schematic illustration of the synthesis of magnetic ethylcellulose nanoparticles ..	42
Figure 2-23. Water content at different depths of diluted bitumen emulsions	44
Figure 2-24. Illustration of composite particles with contrasting structures.....	47
Figure 2-25. Magnified images of emulsified water droplets in diluted bitumen	50
Figure 2-26. High viscosity persistent rag layer	51
Figure 2-27. Emulsion dewatering using responsive composite absorbent particles.....	55
Figure 2-28. Magnetic removal of sludge tagged with interfacially active magnetic particles....	55

Figure 2-29. Magnetic removal of rag layer tagged with interfacially active magnetic particles	55
Figure 3-1. The general chemical structure of cellulose ethers	64
Figure 4-1. Illustration of particles of different wettability at the oil-water interface	79
Figure 4-2. Illustration of the concept of switchable particles	79
Figure 4-3. Modifying the surface of CO ₂ -responsive particles	83
Figure 4-4. TEM micrograph of silica particles	83
Figure 4-5. FTIR spectra and TGA of functionalized silica particles	84
Figure 4-6. Images of different types of emulsions stabilized by different particles	88
Figure 4-7. Images of switchable emulsions stabilized by particles with switchable wettability	90
Figure 5-1. Composite particle produced after removal of water from emulsion droplet	100
Figure 5-2. Composite particles with absorbent interior and interfacially active surface	100
Figure 5-3. Preparation of CMC-EC composite particles by emulsion dehydration	104
Figure 5-4. Infrared spectra of CMC-EC composite absorbent particles	105
Figure 5-5. Thermogravimetric analysis of CMC-EC composite absorbent particles	106
Figure 5-6. Particle size distribution of CMC-EC composite absorbent particles	108
Figure 5-7. Particle size distribution and SEM micrograph of CMC-EC particles	110
Figure 5-8. Dispersability of CMC-EC composite particles before and after absorbing water	112
Figure 5-9. Water-in-mineral oil emulsion stabilized by CMC-EC composite particles	113
Figure 5-10. Dewatering mineral oil emulsion using composite absorbent particles	114
Figure 6-1. Emulsion dewatering using responsive composite absorbent particles	121
Figure 6-2. Magnetic removal of sludge tagged with interfacially active magnetic particles	126
Figure 6-3. Magnetic removal of rag layer tagged with interfacially active magnetic particles	128
Figure 6-4. Preparation of magnetically responsive composite absorbent particles	129
Figure 6-5. Dewatering diluted bitumen emulsion with composite absorbent particles	131
Figure 7-1. Two approaches to preparing composite interfacially active magnetic particles	139
Figure 7-2. The size distribution of various iron oxide nanoparticles	143
Figure 7-3. Sedimentation of various high concentration iron oxide particles suspensions	144
Figure 7-4. Surface charge of iron oxide nanoparticles adsorption of cellulose derivatives	145
Figure 7-5. Particle size distribution of interfacially active magnetic particles	147

Figure 7-6. Magnetic manipulation of a mixture of high-solids content mineral oil sludge	150
Figure 7-7. Magnetically-assisted separation of a process water and diluted-bitumen.....	152
Figure 8-1. Triggered blocking agent suitable for blocking the lower region of the formation.	171
Figure 8-2. Production fluid from <i>in-situ</i> operations to recover bitumen	173
Figure A-1. Schematic representation of the bitumen extraction process	194
Figure A-2. Typical structures of interfacially active naphthenic acids	197
Figure A-3. Schematic representation of oil sands ore conditioning	202
Figure A-4. Cross-sectional diagram of a typical tailings pond.....	209
Figure A-5. Diagram of a vertical well and a horizontal well.....	211
Figure A-6. Illustration of the solubility behaviour of a typical surfactant in solution	221
Figure A-7. Surfactant molecules with hydrophobic and hydrophilic moieties	222
Figure A-8. Illustration of the emulsification process and subsequent phase separation.....	223
Figure A-9. Illustration of the various mechanisms in phase separation of emulsions	225
Figure A-10. Illustration of the diffuse electric double layer	226
Figure A-11. Illustration of the effect of wetting in stabilizing emulsions with particles	228
Figure A-12. Illustration of coalescence of two emulsion droplets.....	228
Figure A-13. Illustration of various types of particles prepared with organized structure.....	232
Figure A-14. Illustration of two interacting particles	234
Figure A-15. Illustration of a cyclone separator	236
Figure A-16. Illustration of a charged particle under the influence of an electric field	237
Figure A-17. Illustration of magnetic field lines	238

List of Tables

Table 3-1. Chemical compounds and reagents used during the course of the investigation.....	63
Table 3-2. Cellulose derivatives used during the course of the investigation	65
Table 3-3. Selected chemical and physical properties of different oil sand ore samples.....	65
Table 3-4. The typical chemical composition of process water sample.....	66
Table 3-5. Materials and chemical reagents used for silica coating	70
Table 3-6. Materials and chemical reagents used for chemical functionalization of silica.....	71
Table 4-1. Zeta-potential of particles functionalized with CO ₂ -responsive surface groups.....	85
Table 4-2. Contact angle of silica wafer functionalized with CO ₂ -responsive surface groups.....	86
Table 5-1. Properties of various micron size CMC-EC composite particles.....	107
Table 5-2. Absorbent properties of micron size CMC-EC composite particles	110
Table 5-3. Properties of substrates prepared with CMC and EC.....	111
Table 6-1. Properties of composite absorbent particles prepared using cellulosic materials...	122
Table 6-2. Properties of hydrated composite absorbent particle aggregates	132
Table 7-1. Properties of particles prepared by adsorption of different cellulosic materials	146
Table 7-2. Colloidal stability of magnetically-responsive and interfacially active particles.....	149
Table 7-3. Recycle of magnetically-responsive and interfacially active particles	151
Table A-1. Typical physical properties of various types of crude oil	195
Table A-2. Density and viscosity of bitumen and water at different temperatures	195
Table A-3. Typical composition of bitumen from oil sands.....	196
Table A-4. Surface tension and interfacial tension of bitumen and various fluids	198
Table A-5. Typical thermal properties of oil sands ore constituents.	198
Table A-6. Typical bitumen blends for pipeline transport.....	199
Table A-7. Temperature of different oil sands ore slurries preparations	204
Table A-8. Composition of various streams leaving primary separation vessel	205
Table A-9. Common examples of different surfactants and their chemical structures.....	219
Table A-10. Hydrophilic-lipophilic balance (HLB) value of a surfactant	221
Table A-11. Comparison of different particle size measurement techniques	231
Table A-12. The characteristic point of zero charge for different materials.....	235

Table A-13. Curie temperature of different magnetic materials	238
Table A-14. Various techniques used to engineer particles.....	239
Table A-15. Various methods of polymerization in dispersed phase.....	242

List of Abbreviations

BHA	:	bottom hole assembly
BIT	:	bitumen
cmc	:	critical micelle concentration
CMC	:	sodium carboxymethyl cellulose
CVD	:	chemical vapour deposition
CSS	:	cyclic steam stimulation
DETA	:	diethylenetriamine
DMA-DMA	:	<i>N,N</i> -dimethylacetamide dimethylacetal
DMSO	:	dimethylsulfoxide
DRIFTS	:	diffuse reflectance infrared Fourier-transform spectroscopy
DS	:	degree substitution
DSA	:	drop shape analyzer
DVLO	:	Derjaguin, Landau, Verwey and Overbeek
DWR	:	double wall ring
EC	:	ethylcellulose
EDS	:	electron dispersion spectroscopy
EO	:	ethylene oxide
FFT	:	fluid fine tailings
FTIR	:	Fourier-transform infrared
HLB	:	hydrophilic-lipophilic balance
HPLC	:	high-performance liquid chromatography
ITFDA	:	integrated thin film drainage apparatus
LCST	:	lower critical solution temperature
MFT	:	mature fine tailings
MW	:	molecular weight
O/W	:	oil-in-water
O/W/O	:	oil-in-water-in-oil
PDI	:	polydispersity index

PEO	:	polyethyleneoxide
PO	:	propylene oxide
PPO	:	polypropyleneoxide
PSV	:	primary separation vessel
PTES	:	phenyltriethoxysilane
RSN	:	relative solubility number
SAGD	:	steam-assisted gravity drainage
SARA	:	saturate, aromatic, resin and asphaltene
SEM	:	scanning electron microscope
SPAN 80	:	sorbitan oleate
SPR	:	surface plasmon resonance
TEM	:	transmission electron microscope
TGA	:	thermogravimetric analysis
THAI	:	toe-to-heel air injection
TIOC	:	toluene-insoluble organic carbon
UV-VIS	:	ultraviolet-visible
VAPEX	:	vapour recovery extraction
W/O	:	water-in-oil
W/O/W	:	water-in-oil-in-water

Chapter 1. Introduction

Bituminous sands, oil sands or tar sands are a strategically important resource for Canada and will likely be one of the last remaining major reserves of petroleum hydrocarbons.¹⁻⁴ In addition to making fuels, petroleum resources serve as a feed stock for the production of important materials including monomers and organic building blocks for chemical manufacturing. Therefore, unlocking the wealth of the oil sands represents both a strategic and economic advantage. However, several technological challenges remain regarding the extraction, processing and the negative environmental impact of this unique unconventional petroleum resource.¹ Addressing these challenges has been the focus of many years of both academic and industrial research. The commercial value of the oil sands industry remains a large part of the Canadian economy and is unlikely to diminish in face of ever-growing global population and demand for improved living standards. The complicated reality also encompasses numerous political challenges, with many groups opposing the exploitation of the oil sands resource and placing pressure on government officials and policy makers.^{5,6} Unfortunately, few groups suggest credible alternatives and often overlook our universal dependency on cheap and abundant sources of energy, citing future technologies still well in their infancy. The focus of our society must be on serving both future and current needs. It is unethical to deny the basic necessities and reasonable luxuries we are accustomed to for the sake of meeting ideological initiatives. Challenges exist to be overcome; through better technology, the industry continues to strive to become more sustainable and efficient.

The following thesis describes the bitumen extraction process by surface mining and *in-situ* production methods used to commercially recover bitumen. The concept of responsiveness is explored in terms of the physicochemical changes encountered during the recovery process. Various types of specially-designed composite responsive particles are prepared in order to manage different multiphase systems encountered throughout the bitumen extraction process; including emulsions, rag layers and sludge. **Chapter 2** summarizes different challenges related to recovery of bitumen from oil sands including the formation of undesirable emulsions and the role of fine solids in enhancing emulsion stability. Multiphase separation problems including dewatering of bitumen froth as well as separation of rag layers and sludge are further described

in more detail. **Chapter 3** provides an overview of materials and instruments used over the course of various experiments as well as different experimental protocols used through the course of the current investigation.

The use of chemical additives can be challenging due to the complexity of bitumen recovery processes. Often, an additive beneficial in one step will have a detrimental effect on a subsequent step, if not adequately removed. Carefully prepared composite responsive materials are capable of adopting more than one effective function or exhibiting different properties under different conditions. Composite responsive materials can be engineered to meet the specification of various steps and are therefore of interest to bitumen recovery processes including multiphase separation such as breaking stable emulsions.

Chapter 4 and **Chapter 5** describe preparation procedures for responsive composite particles. The complex behaviour of composite particles is obtained by combining materials with different properties. The particle surface is most critical in determining its colloidal properties. Specifically, in **Chapter 4**, responsive particles are prepared from silica through chemical functionalization of silica surface with CO₂-responsive moieties to produce emulsions of switchable stability.⁷ Particles, chemically functionalized with surface groups having switchable charge, experience a change to its surface properties sufficient to alter its wettability. The change in wettability of switchable particles caused emulsions, stabilized by particles with appropriate wettability, to destabilize upon inducing a change to particle wettability. Additionally, in **Chapter 5**, responsive particles are also prepared from contrasting cellulosic materials by dehydration of emulsion droplets to produce readily-separated absorbent particles for removal of emulsified water from non-aqueous systems.⁸ In both systems, magnetic iron oxide can be incorporated into the composite particles to further impart magnetic responsiveness and facilitate their separation.

Chapter 6 and **Chapter 7** describe the use of responsive composite particles for managing different emulsions encountered during bitumen extraction by surface mining. Specially prepared absorbent particles are used to remove emulsified water from non-aqueous systems through absorption.⁹ The properties of the composite absorbent particles described in **Chapter 6** are ideally suited for removal of emulsified water. The surface of the composite absorbent

particles remains permeable to water, allowing emulsified water to be absorbed by the water-absorbent core. Composite absorbent particles also disperse effectively in non-polar solvents and attach to the oil-water interface. However, the surface of the composite absorbent particles undergoes a change after absorbing emulsified water that causes absorbent particles to lose colloidal stability. Following loss of colloidal stability, formation of larger aggregates greatly facilitates subsequent separation by sedimentation and/or screening. In **Chapter 7**, magnetic particles are treated using cellulosic materials in order to produce an interfacially active surface that can readily adsorb onto an oil-water interface. Multiphase materials such as emulsions, rag layers and sludge become magnetically responsive after addition of interfacially active magnetic particles. The interfacially active magnetic particles adsorb on the oil-water interface and imparts magnetic susceptibility to various multiphase mixtures and would therefore enable magnetic separation of difficult multiphase wastes.

Chapter 8 provides a general summary of the investigations completed and described in preceding chapters. Composite responsive particles can be prepared by combining the properties of various materials using a suitable synthetic method. The method of synthesis has a direct effect on the properties of the resulting particles, and therefore must be carefully considered. Three methods of preparing composite particles are presented including chemical functionalization, emulsion droplet dehydration and sequential adsorption.⁷⁻⁹ The properties of the resulting responsive particles can be tuned to meet specific challenges encountered by the oil and gas industry, including separation of multiphase wastes. By tailoring the properties of the responsive particles and the type of response, separation processes can be simplified. For example, triggered aggregation of particles can significantly increase the effective particles size and, consequently, the rate of sedimentation under gravity. Further accelerated separation can be achieved under a magnetic field by making particles magnetically susceptible through incorporation of magnetic material within the structure of composite particles. Future work includes improving the water-absorbent capacity of composite absorbent particles by using super-absorbent polymers. Furthermore, responsive absorbent materials may be incorporated to make regeneration of composite absorbent particles more energy efficient. Moreover, the surface of the composite absorbent particles can be more specific to allow or reject select

materials such as dissolved ions. Future work also expectantly extends the benefits of different responsive composite particles to *in-situ* production methods. This includes triggered bottom blocking agents for improving conformance or altering reservoir properties. In the proposed scheme, a latex is injected into the reservoir followed by a triggering mechanism. Triggered aggregation is possible by covering dispersed particles with chemical moieties that are sensitive to changes in environmental conditions (*e.g.*, pH). The trigger causes aggregation of latex inside pores, reducing the formation permeability in the regions affected in order to improve conformance and improve production in regions with high bitumen content. In addition, triggered polymer degradation can be useful in both bitumen extraction and *in-situ* production. Triggered degradation may be possible by incorporating chemical moieties that are sensitive to radiation (*e.g.*, UV and gamma) in the backbone structure of polymers. Chemical additives added for a specific purpose can be degraded once their purpose is fulfilled and no longer desirable.

Appendix A provides a general background, scientific principles, and engineering concepts relevant to the technical problems related to oil sands extraction addressed in this dissertation as well as particle engineering. Oil sands are an unconsolidated mixture of sand, clay and bitumen. Shallow deposits are recovered by surface mining while deeper deposits are recovered from specialized wells. The bitumen extraction process is complex, involving many concurrent and inter-related processes, making it difficult to apply simple remedies. Bitumen is an extremely heavy petroleum product due to its advanced level of biodegradation, which preferentially consumes the lighter fraction of the original oil.

1.1 References

1. *Oils Sands Technology Roadmap Unlocking the Potential*, Alberta Chamber of Resources, **2004**.
2. Canada. National Energy Board., *Canada's energy future infrastructure changes and challenges to 2020*, National Energy Board, Calgary, AB, **2009**.

3. Canada. National Energy Board., Canada's energy future energy supply and demand projections to 2035, National Energy Board, Calgary, AB, **2011**.
4. J. J. Heron and E. K. Spady, *Annu. Rev. Energy*, 1983, **8**, 137–163.
5. Lines in the Sands: Oil Sands Sector Benchmarking, Northwest and Ethical Investments, **2009**.
6. Sustainability Perspectives Unconventional Risks An investor response to Canada's Oil Sands, The Ethical Funds Company, **2008**.
7. C. Liang, Q. Liu and Z. Xu, *ACS Appl. Mater. Interfaces*, 2014, **6**, 6898–6904.
8. C. Liang, Q. Liu and Z. Xu, *ACS Appl. Mater. Interfaces*, 2015, **7**, 20631–20639.
9. C. Liang, Q. Liu and Z. Xu, *Energy Fuels*, 2016, **30**, 5253–5258.

Chapter 2. Problem Description

Chapter 2.1: Particle-Stabilized Emulsions. A version of this section has been published as D. Harbottle, C. Liang, N. El-Thaher, Q. Liu, J. Masliyah and Z. Xu “CHAPTER 11: Particle-Stabilized Emulsions in Heavy Oil Processing” in Particle-Stabilized Emulsions and Colloids: Formation and Application by the Royal Society of Chemistry with DOI:10.1039/9781782620143-00283.

The sustainable development of bitumen, as a unique Canadian resource, requires a more holistic approach to problem solving. Many technical challenges and opportunities associated with the bitumen extraction process remain. These challenges must be addressed in order to improve the efficiency of processes in both present economic terms and reducing the legacy impact of bitumen extraction. Multiphase mixtures are unavoidable in bitumen production as water is both integral to the recovery process and present in the formation. Although together immiscible, bitumen and water are emulsified when exposed to mechanical agitation and intensive mixing. The presence of indigenous surfactants in bitumen and solid particle fines in the oil sands ore provides extended stability to bitumen emulsions. The role of solids in stabilizing emulsions is specifically addressed in **Chapter 2.1**. Efficient separation of dispersed multiphase mixtures is a major challenge to bitumen extraction by both surface mining and *in-situ* production methods. Specific problems associated with separation of multiphase waste generated by the bitumen extraction process have been identified and are further described in the **Chapter 2.2**.

2.1 Particle-Stabilized Emulsions

2.1.1 Introduction

The landscape of oil production is shifting, with non-conventional oil resources seen as a credible option to meet the ever-growing demand for oil. The 2013 ExxonMobil report: “The Outlook for Energy: A View to 2040” projected a rise in the total liquid fossil fuel demand to 113 million of oil-equivalent barrels per day in 2040.¹ A vast proportion of this demand is expected to be addressed through developments in heavy oil, oil sands, tight oil and deepwater oil. A common challenge in oil production from various oil resources is the formation of stable

emulsions. The formed emulsions can be: (i) water-in-oil (W/O), (ii) oil-in-water (O/W) or even (iii) complex multiple (W/O/W, O/W/O) emulsions, creating numerous operational challenges. Oil-water separation can often become the ‘bottleneck’ in production processes without the ability to effectively destabilize emulsions. The challenge in oil-water separation is magnified in non-conventional oil production, where the high oil density and the entrainment of fine particles (*e.g.*, clays) favour the production of stable emulsions that are relatively more difficult to destabilize. The stable emulsions of intermediate density accumulate between oil and water phases to form so-called ‘dense-packed layers’ or ‘rag layers’ consisting of complex emulsions (W/O, O/W, W/O/W, O/W/O). These emulsions are stabilized by surface active species that partition at the oil-water interface. The rag layer represents a pseudo-filter, hindering water dropout (W/O) or oil droplet creaming (O/W) and therefore reducing oil-water separation efficiency and oil production. The carry-over of micron-sized water droplets often leads to long-term corrosion issues and catalyst poisoning in downstream crude oil processing and refining. Chemical demulsifiers are frequently added to prevent rag layer formation and hence enable more efficient oil-water separation. Common commercial demulsifiers are polymers based on ethylene oxide (EO) and propylene oxide (PO) chemistry with the EO portion more water-soluble and PO portion more oil-soluble. Their surface activity enables interfacial partitioning to disrupt the protective interfacial film and promote fruitful coalescence upon direct contact of neighboring droplets. The objective of this chapter is to address the key surface properties of solid particles that promote the formation of solid-stabilized petroleum emulsions, assess the properties of interfacial materials, and finally illustrate the mechanisms by which chemicals successfully disrupt interfaces and promote demulsification.

2.1.2 Theory of Particle-Stabilized Emulsions

For over a century,^{2,3} solids-stabilized emulsions have been the subject of considerable scientific interest, with recent advancements focused on microscopic and theoretical understanding. The term ‘Pickering emulsion’ has been widely used to describe solids-stabilized emulsions after the inaugural work by Pickering, who observed in 1907 the interfacial partitioning of water-wetted particles and formation of stable oil-in-water emulsions.³ The critical role of particle wettability on emulsion type and stability was further investigated by Schulman and

Leja.⁴ By controlling the contact angle of barium sulfate particles these authors observed formation of stable oil-in-water emulsions by particles with a contact angle $< 90^\circ$ and water-in-oil emulsions by particles with a contact angle $> 90^\circ$, as schematically shown in **Figure 2-1**. The stability of emulsions was observed to decrease with increasing particle hydrophilicity or hydrophobicity away from 90° , demonstrating that the particles with a contact angle close to 90° would form the most stable emulsions.

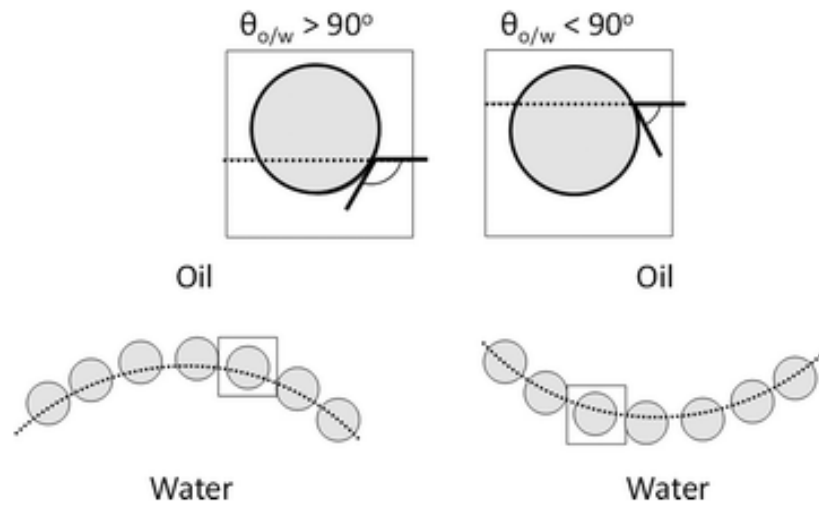


Figure 2-1. Preferential particle location at the oil-water interface governed by particle wettability. Modified figure from Aveyard *et. al.*⁷

To understand the relationship between particle wettability and emulsion stability we can consider a simple case of two droplets coalescing to form one larger droplet of reduced total surface area. The total Gibbs free energy change due to a coalescence event is given by:⁵

$$\Delta G = \gamma_{o/w} \times \Delta A - W_d \times \Delta_n \quad (2.1)$$

where $\gamma_{o/w}$ is the oil-water interfacial tension, ΔA is the change in interfacial area, Δ_n is the number of particles detached from the interface, and W_d given by Equation 2.2 is the work needed to detach a particle from a planar oil-water interface.^{5,6}

$$W_d = \pi r^2 \gamma_{o/w} (1 \mp \cos \theta)^2 \quad (2.2)$$

In Equation 2.2, θ represents the contact angle of particles, and \mp sign describes particle detachment into the oil phase (positive) or water phase (negative). The particle radius, r , is

considered to be sub-micron such that the gravity contribution is negligible. **Figure 2-2** shows the scaled energy of particle detachment into the oil phase (solid line) as a function of particle contact angle from 0° to 180° . For an extremely low contact angle ($\theta \rightarrow 0^\circ$), the energy required to detach a strongly hydrophilic particle into a hydrophobic solvent approaches the maximum. With an increasing affinity for the particle to reside in the oil phase (reduced particle surface area in the water phase), the energy of particle detachment from the interface to the oil phase decreases to eventually reach zero when $\theta = 180^\circ$. A second curve (broken line) considers the energy of particle detachment from the interface into water as a function of particle contact angle. With a uniform wettability the two curves are symmetrical around $\theta = 90^\circ$ where $W_d/\pi r^2 \gamma_{o/w} = 1$. Hence for a particle partitioned at the oil-water interface, the maximum detachment energy into either the water or oil phases is observed at $\theta = 90^\circ$. At this condition, solids-stabilized emulsions exhibit the greatest stability, which results from steric hindrance to compensate for the work of detachment.

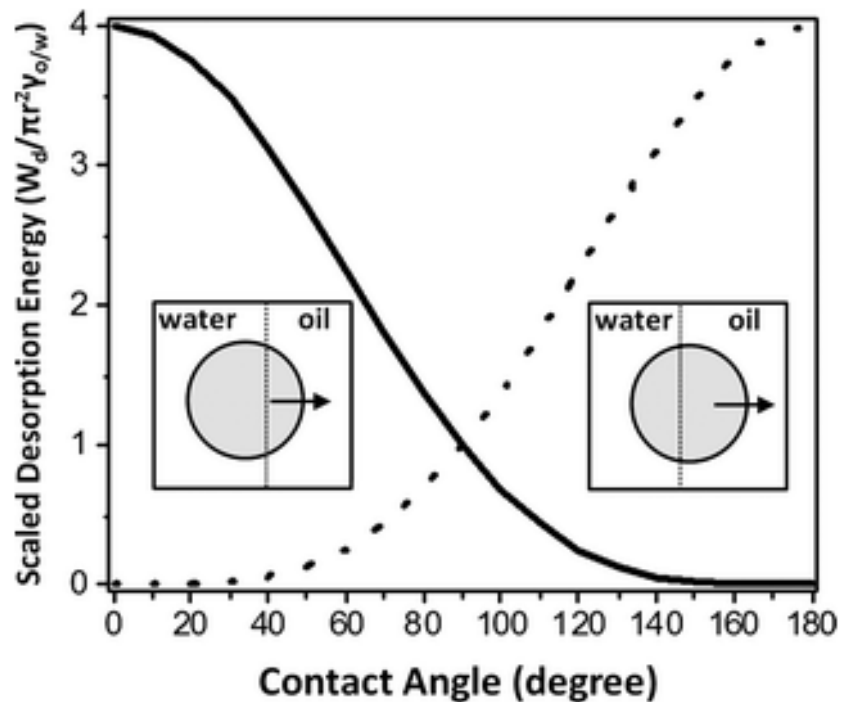


Figure 2-2. Scaled energy of particle detachment from the equilibrium position at the oil-water interface into the oil phase (solid line) or water phase (dashed line) as a function of the particle contact angle.

Whilst assuming uniform particle wettability is often sufficient to describe the stability of many particle-stabilized emulsion systems, particles encountered during petroleum processing are often heterogeneous in chemistry and hence in surface wettability. Contamination of clays and heavy minerals by organic matter results in a patchy particle of hydrophilic and hydrophobic segments.⁸ These particles can be considered Janus-like with two distinct surface properties. Binks and Fletcher⁹ provided a theoretical assessment of the detachment energy of Janus particles from an oil-water interface to a bulk oil or water phase by considering a particle geometry as shown in **Figure 2-3**. With polar and apolar patches the particle displays some similarity to a surfactant molecule and can be considered a colloidal surfactant.¹⁰ Similar to the hydrophilic-lipophilic balance (HLB) of surfactants, the Janus balance (J) describes the energy needed to detach the particle from its equilibrium position into the oil phase, normalized by the energy needed to transfer the particle from its equilibrium into the water phase.¹¹

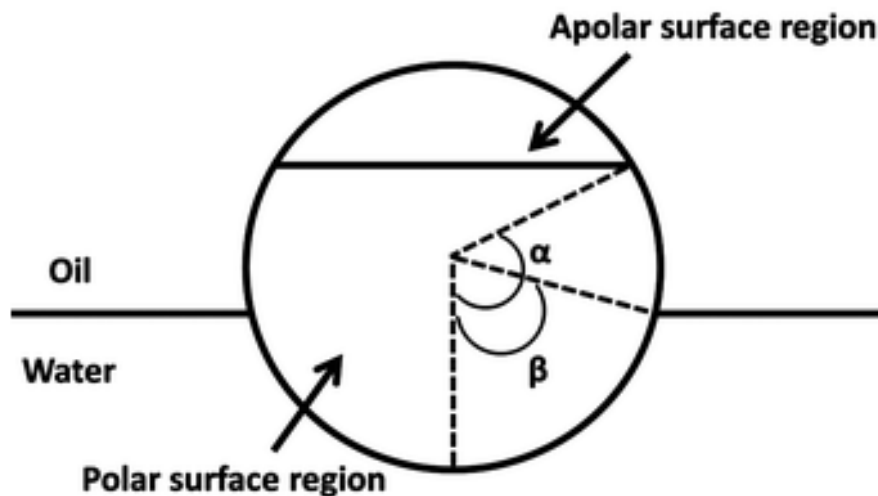


Figure 2-3. Geometry of a Janus particle partitioning at the oil-water interface. The parameters α and β describe the position of the surface boundary between the apolar and polar patches, and the immersion depth of the particle in the oil-water interface, respectively. Binks and Fletcher⁹

The particle contact angle is dependent on the contact angle of the polar (θ_P) and apolar (θ_A) patches, and the relative areas occupied by these patches. The overall (or average) contact angle of this type of particles is given by:

$$\theta_{ave} = \frac{\theta_A(1 + \cos\alpha) + \theta_P(1 - \cos\alpha)}{2} \quad (2.3)$$

with the particle amphiphilicity characterized by:

$$\Delta\theta = \frac{\theta_P - \theta_A}{2} \quad (2.4)$$

for a homogeneous particle, $\Delta\theta = 0^\circ$ and $\Delta\theta = 90^\circ$ represent the maximum possible particle amphiphilicity. Similar to the example shown in **Figure 2-2**, the total surface free energy (E) for a Janus particle located at the planar oil-water interface is dependent on the immersion depth, β , and can be expressed as:

For $\beta \leq \alpha$:

$$E(\beta) = 2\pi r^2 \left[\gamma(\text{AO})(1 + \cos\alpha) + \gamma(\text{PO})(\cos\beta - \cos\alpha) \right. \\ \left. + \gamma(\text{PW})(1 - \cos\beta) - \frac{1}{2}\gamma(\text{OW})(\sin^2\beta) \right] \quad (2.5)$$

For $\beta \geq \alpha$:

$$E(\beta) = 2\pi r^2 \left[\gamma(\text{AO})(1 + \cos\beta) + \gamma(\text{AW})(\cos\alpha - \cos\beta) \right. \\ \left. + \gamma(\text{PW})(1 - \cos\alpha) - \frac{1}{2}\gamma(\text{OW})(\sin^2\beta) \right] \quad (2.6)$$

where γ is the interfacial tension between phases with A = apolar, P = polar, O = oil and W = water. Calculating the Janus particle detachment energy as a function of the particle amphiphilicity (**Figure 2-4**), Binks and Fletcher demonstrated a three-fold increase in detachment energy as $\Delta\theta$ increased from 0° to 90° .⁹ The high detachment energy exhibited by Janus particles as calculated over a wide range of θ_{ave} , dissimilar to the narrow range of stability exhibited by homogeneous particles. Readers who are interested in more details on the detachment energy of Janus particles from oil-water interface into bulk oil or water phase are referred to finding more details elsewhere.^{9,11}

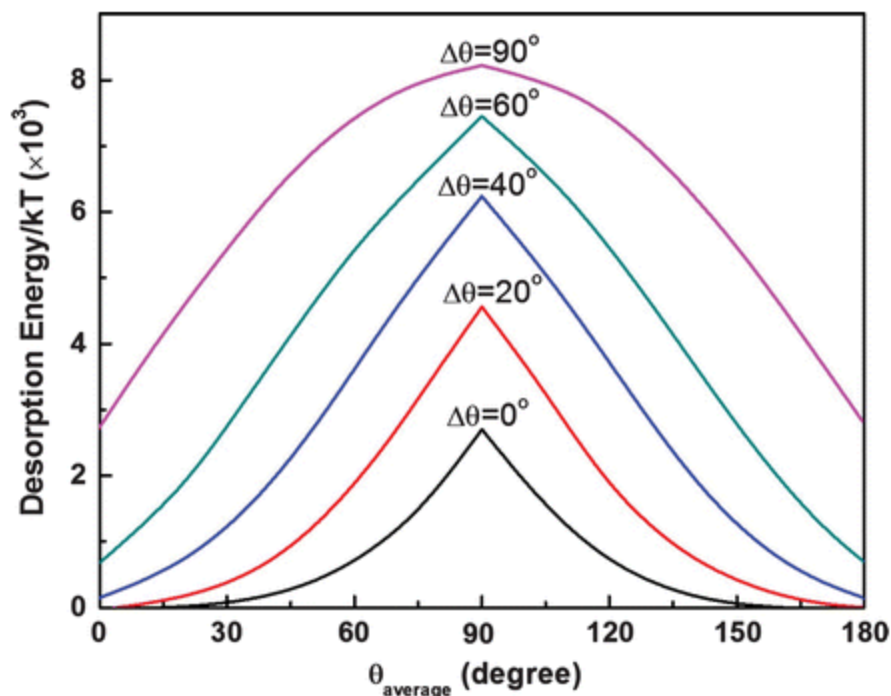


Figure 2-4. Variation of particle detachment energy with area-weighted average contact angle for particles of radius 10 nm and $\alpha = 90^\circ$. Binks and Fletcher.⁹

2.1.3 Asphaltenes

Asphaltenes, as the heavy components of crude oil and bitumen are often blamed for causing emulsion stability in petroleum emulsions. Asphaltenes are commonly defined as a solubility class: soluble in aromatic solvents (toluene) and insoluble in n-alkanes (heptane, hexane, pentane). With hundreds of thousands of chemically distinct molecules acting as the building blocks of asphaltenes, this generalized definition of asphaltenes has often limited our understanding of asphaltene systems. Over the last decade or more, a renaissance in asphaltene research has seen advancement in the understanding of asphaltene molecular and colloidal structures. While there is no clear analogue for asphaltenes, their behavior has been shown to provide similarities to both polymer and particle systems, although such science does not completely describe asphaltenes. Depending on the physical and chemical properties, asphaltenes are shown to exhibit different states of molecules from monomer (single unit) to nanoaggregates (several units) and colloidal clusters (multiple nanoaggregates), forming nanoparticles in the size range of nanometers to tens of nanometers. Their partial polarity

renders them interfacially active, readily partitioning at the liquid-liquid interface. Accumulation of asphaltene particles and their potential to associate and reorganize at the oil-water interface lead to the formation of an interfacial film. The presence of such films hinders the rapid and efficient separation of water-in-oil emulsions which are often unavoidably formed during crude oil production and processing.

2.1.3.1 Molecular Structure of Asphaltenes

Elemental composition analysis indicates that asphaltenes consist of carbon, hydrogen, nitrogen, sulfur and oxygen, with trace amounts of vanadium and nickel. The aromaticity of asphaltenes is typically on the order of 0.5 with the remaining carbon being aliphatic.¹² The molecular structure of asphaltenes has been the subject of strong debate in recent years, with different molecular structures proposed to account for the observed varying physicochemical properties of asphaltenes. The first molecular structure of asphaltenes is described by the Yen-Mullins model^{13,14} (modified Yen model) and is an extension of the Yen model proposed in 1967.¹⁵ The basic feature of the Yen–Mullins model indicates a most probable island-like structure with a single polyaromatic core consisting of seven condensed aromatic rings and several alkyl and naphthenic side chains, as shown in **Figure 2-5a**. This structure is consistent with an asphaltene molecular weight around 750 Da.¹⁴ With increasing asphaltene concentration the monomer units interact to form nanoaggregates at the critical nanoaggregate concentration (CNAC) of $\sim 100 \text{ mg L}^{-1}$ and larger clusters beyond the critical cluster concentration (CCC) of $\sim 3 \text{ g L}^{-1}$.¹³

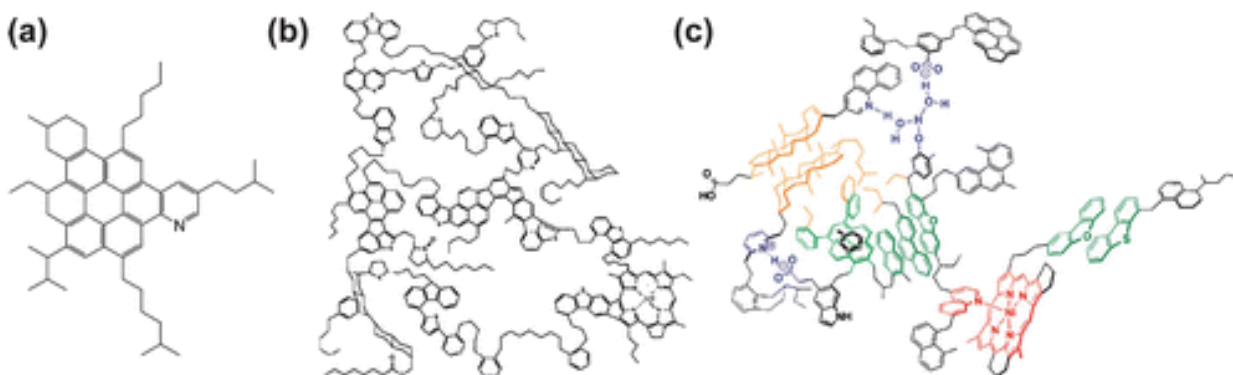


Figure 2-5. Proposed molecular architecture of asphaltenes: (a) island-like model, (b) archipelago model and (c) supramolecular model. Mullins,¹⁴ Strausz *et. al.*¹⁶ and Gray *et. al.*¹⁷

Based on the Yen–Mullins model, nanoaggregates are formed by π – π stacking of aromatic cores with the aggregate growth limited by steric repulsion from aliphatic side chains. The disordered structure of the central backbone allows for entrained solvent and limits the aggregation number to less than 10, with a nanoaggregate size of approximately 2 nm. Subsequent aggregation of nanoaggregates under favourable conditions produces 5 nm asphaltene clusters, with the structure entropy limiting the aggregation number to less than 10.¹⁴ An alternative molecular structure was proposed by Strausz *et. al.*,¹⁶ who presented the archipelago model describing several different polyaromatic ring structures connected via aliphatic chains, as shown in **Figure 2-5b**. The inclusion of multiple active sites (functional groups) is supported by the recent three-dimensional aggregation model of asphaltenes, arising from supramolecular assembly.¹⁷ The approach seeks to address inconsistencies that cannot be satisfied by an architecture dominated by a single aromatic backbone.

The supramolecular assembly model, on the other hand, broadens the basis for intermolecular interactions to include: (i) acid–base interactions, (ii) hydrogen bonding, (iii) metal coordination complexes, (iv) van der Waals interactions between apolar, cycloalkyl and alkyl groups and (v) aromatic π – π stacking. Characteristics of host molecules, guest molecules and solvent(s) are identified, with the host molecules viewed as having two or more active sites, guest molecules consisting of a range of small and large alkyl aromatics, and solvents (low molecular weight species) to act as assembly terminators. By increasing the number of interaction mechanisms, the size and shape of aggregates can be highly variable, exhibiting polydispersity in the population (**Figure 2-5c**).¹⁷ The polydispersed nature of asphaltene aggregates has been confirmed by the round-robin study on the size distribution of self-associated asphaltenes.¹⁸ Analyzing the same sample of asphaltenes with different analytical techniques (supported by co-contributors), 90% of the asphaltenes were identified as self-associating, forming loose, open and disc-like nanoaggregates spanning one order of magnitude in physical dimensions (2–20 nm).

2.1.3.2 Interfacial Activity

The mechanism of asphaltene transport from the bulk to the interface (liquid-liquid, liquid–solid) and subsequent association at the interface (interfacial aging) has been studied using a number of experimental techniques, including tensiometry,¹⁹ light absorption,²⁰ UV

spectrometry,²¹ interferometry,²² quartz crystal microbalance,²³ ellipsometry²⁴ and surface force apparatus.²⁵ Despite continued effort, there remains uncertainty in areas related to the physical and mechanical properties of the adsorbed layer. **Figure 2-6a** shows the dynamic interfacial tension curves for different mass fractions of asphaltenes dispersed in a model oil containing 15 wt% toluene and 85 wt% aliphatic base oil.¹⁹ For all mass fractions of asphaltenes studied, the interfacial tension is observed to decrease rapidly at short times, followed by a progressive reduction of the decay rate. A short time approximation for dynamic interfacial tension is given by a coupled Gibbs–Duhem and diffusion equation as:

$$\gamma(t) = \gamma_0 - 2RTC\sqrt{\frac{Dt}{\pi}} \quad (2.7)$$

where γ is the dynamic interfacial tension; γ_0 , the pure solvent–water interfacial tension; R , the universal gas constant; T , the temperature; C , the bulk asphaltene concentration; D , the diffusion coefficient; and t , the time. For diffusion-limited adsorption, Equation 2-7 states that the change in the interfacial tension scales linearly with $t^{-1/2}$. As shown in **Figure 2-6b**, the interfacial tension decreases linearly with $t^{-1/2}$ for all mass fractions considered in the study, especially over a short adsorption time. The slope increases with increasing mass fraction of asphaltenes in solution. While diffusion is accepted as rate-determining of asphaltene adsorption at short time intervals, the adsorption kinetics over an extended period has been viewed differently. The deviation of asphaltene adsorption from diffusion-controlled linearity at high asphaltene concentration has been discussed in terms of: (i) energy barrier-controlled kinetics as a result of hindrance due to already adsorbed species, which causes a delay to the rate of adsorption by an energy barrier;¹⁹ and (ii) slow evolution with time of relaxation and reorganization of the interfacial network constructed of asphaltene particles, as supported by pressure relaxation and interfacial shear rheology studies.^{26,27}

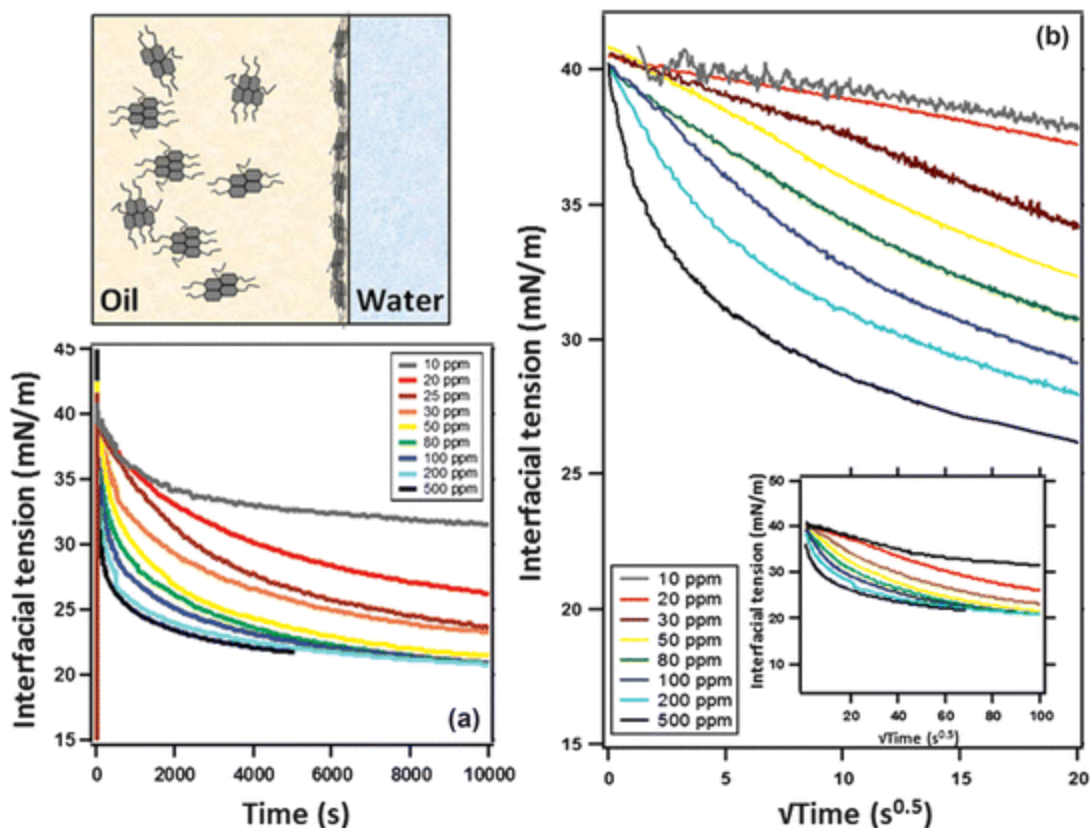


Figure 2-6. Dynamic interfacial tension for asphaltene mass fractions 10 to 500 ppm in model oil, (a) function of time, (b) function of square root time (inset – complete experimental time). Upper-left schematic shows the experimental configuration and illustration of the adsorption process of asphaltenes from the oil phase to the water-oil interface. Rane *et. al.*¹⁹

2.1.3.3 Asphaltene 'Skins'

The adsorption of asphaltenes and/or their nano-aggregates with subsequent formation of an interfacial film contributes significantly to the stability of water-in-crude oil emulsions. Direct observation of these films and their inherent stability was demonstrated using the micro-pipette technique.^{28,29} The technique involves generating a micron-sized water droplet in heavy crude (diluted bitumen) and aging of the droplet (adsorption of surface active species) before controlled water withdrawal and reduction in droplet size (and hence surface area). **Figure 2-7a₁** shows a 15–20 μm spherical water droplet formed in 0.1 wt% bitumen diluted in heptol 1:1 (heptane to toluene at equivalent volumes). As the droplet is deflated and the interfacial area compressed, the surface of the droplet crumpled (**Figure 2-7a₂**), revealing a rigid interfacial film

that is resistant to in-plane shear and hence providing a steric barrier to droplet-droplet coalescence.²⁸ The nature of the interfacial 'skin' is highly dependent on petroleum chemistry, with saturate, aromatic, resin and asphaltene (SARA) analysis providing a means to characterize chemistry of the oil through its constituent fractions. The resin and asphaltene fractions are often discussed as the problematic components influencing droplet stability, with their interplay both in the bulk and at the interface impacting the physical properties of the interfacial skin. Wu³⁰ designed an elegant experiment to isolate and characterize accumulated material residing at the interface of a water-in-diluted bitumen emulsion with increasing bitumen concentrations from 0.1 to 10 wt% in 1:1 heptol. At low bitumen concentration (0.1 wt%) the micro-pipette study confirmed the formation of rigid interfacial film (as shown in **Figure 2-7a₂**), while at high bitumen concentration (10 wt%) the micron-sized droplet was observed to remain spherical as the interfacial area was compressed, leading to spontaneous emulsification of the water droplet as its size was further decreased. To study the properties of interfacial materials, a 3 wt% heavy water-in-diluted bitumen emulsion was prepared. The 'clean' interfacial material on stable heavy water droplets was isolated after washing by allowing the emulsified heavy water droplets passing through a clean oil phase and a planar oil-water interface, and then settling through clean water phase. After drying of the settled heavy water droplets, the H/C atomic ratio of the accumulated material was determined by elemental analysis. The data in **Figure 2-7b** indicates a step-change in H/C ratio for the recovered material from the heavy water emulsion droplets prepared in 3–5 wt% bitumen-in 1:1 heptol solutions. At lower bitumen concentrations an H/C ratio of ~1.15 suggests an interfacial material of asphaltene character (H/C ~1.16). At higher bitumen concentrations an H/C ratio of ~1.32 indicates an interfacial material containing other crude oil components, perhaps naphthenates, mixed in with a proportional amount of asphaltenes in the original crude.

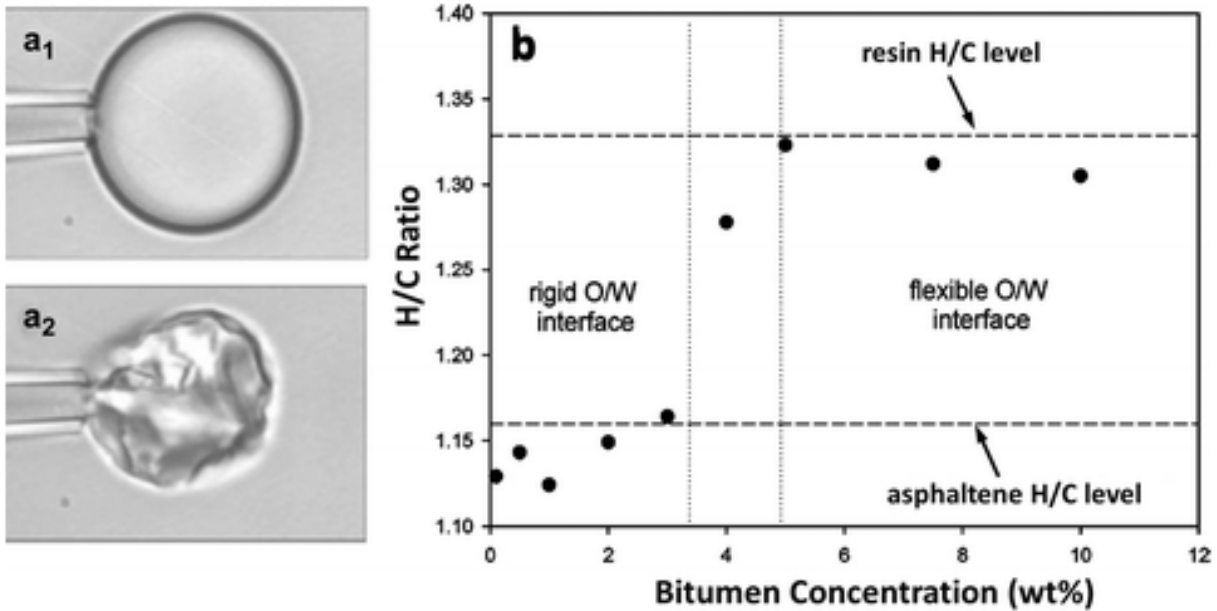


Figure 2-7. (a₁) Water droplet-in-diluted bitumen (0.1 wt% bitumen in 1:1 heptol), (a₂) interfacial crumpling observed during controlled droplet volume reduction and (b) H/C atomic ratio of the interfacial material extracted from emulsions of water-in-diluted bitumen. Yeung *et. al.*,²⁸ Wu,³⁰ and Czarnecki and Moran³¹

Gao *et. al.*³² examined the crumpling ratio ($CR = \frac{A_f}{A_i}$, where A_i is the initial projected area of the droplet and A_f is the projected area of the droplet at the onset of crumpling) of micron-sized water droplets prepared in heptol solutions containing: (i) asphaltene (10^{-6} to 10^0 wt%) and (ii) asphaltene (10^{-6} to 10^0 wt%)+0.1 wt% sodium naphthenate. Naphthenic acids are a complex mixture of surface active cyclic carboxylic acids that can compete for the interfacial area. In both cases, at low asphaltene concentrations (10^{-6} to 10^{-5} wt% asphaltenes) droplet crumpling was not observed due to very little adsorption of asphaltene nanoaggregates. For asphaltenes at higher asphaltene concentrations (10^{-4} to 10^1 wt% asphaltenes) the crumpling ratio 'jumped' to ~ 0.6 with consecutive increases to ~ 0.8 , confirming the formation of a rigid interfacial layer. With co-addition of sodium naphthenates the crumpling was significantly depressed, reducing the maximum crumpling ratio to ~ 0.3 .³² The mechanism by which rigid and non-rigid films form has been postulated by Czarnecki and Moran.³¹ The model considers the competitive adsorption between a sub-fraction of asphaltenes and low molecular weight surfactants, with the surface

competition dependent on the adsorption rate and reversibility, rather than the adsorption energy. The model assumes that: (i) asphaltenes adsorb slowly and irreversibly; (ii) low molecular weight surfactants adsorb quickly through a reversible process to reach an equilibrium state; and (iii) interfacial affinity of asphaltenes is lower than surfactants. To allow the slow diffusing asphaltene particles adsorb at the interface, the surfactant concentration should be sufficiently low so that the interface is not crowded by surfactant molecules. Under this scenario the asphaltene nanoaggregates can attach to the free interface and begin to interact with each other to form larger aggregates. As the asphaltene network begins to occupy large fractions of the interfacial area, the surfactant molecules which obey equilibrium are pushed out of the interface. With sufficient interfacial aging, the irreversible adsorption of asphaltene aggregates can span the droplet interface to form a thick, rigid film. At high concentrations of surface active species, rapid partition of the low molecular weight surfactants exhausts any available interfacial area for asphaltene aggregates to adsorb. Displacement of surfactant molecules by asphaltene particles cannot happen due to differences in their adsorption energies. As a result, the interface remains completely dominated by the surfactant molecules, which provide no shear resistance under interfacial area compression, and hence flexible.

2.1.3.4 Interfacial Film Rheology

Interfacial rheology is a technique that has been used to characterize the evolution of asphaltene 'skins'. Dilatational and shear are two common approaches to measure film rheology, with the latter receiving substantial attention in recent years.^{27,33,34} Dilatational rheology considers the viscoelastic properties of the interfacial layer through harmonic oscillation of the interfacial area, while shear rheology describes the material deformation by shear at constant interfacial area.³⁵ Rheology measured by dilatation illustrates the rapid formation (typically < 15 min, depending on asphaltene concentration and solvent type) of an elastic dominant interfacial film [G' (elastic) > G'' (viscous)] that remains almost insensitive to film aging (see **Figure 2-8**). In general, the link between dilatational rheology and emulsion stability is at best qualitative, with a reasonable agreement between increasing dilatational elasticity and emulsion stability being observed. In recent years we studied the relationship between interfacial shear rheology and droplet-droplet coalescence using the double wall ring (DWR) geometry (shear rheology) and in-

house built integrated thin film drainage apparatus (ITFDA) (coalescence), respectively. Readers are referred to other references for detailed discussion on instrument techniques.^{34,36,37} The film properties as assessed by dilatational rheology are in contrast to the time evolution of interfacial shear properties. Under shear the viscoelasticity (G' and G'') exhibits greater sensitivity to film growth, with elastic and viscous properties showing substantial development with film aging (see **Figure 2-8**). At short aging time, the interfacial asphaltene film is shown to be dominant by viscous character. At long aging time, the elastic contribution develops and eventually exceeds the viscous contribution, resulting in an elastic dominated film (**Figure 2-9a**). For an equivalent system (0.4 g L^{-1} asphaltene in toluene), the coalescence times (square symbols in **Figure 2-9a**) for two water droplets aged between 0.5 and 4.0 hours were measured from the bimorph trace using the ITFDA (**Figure 2-9b**).

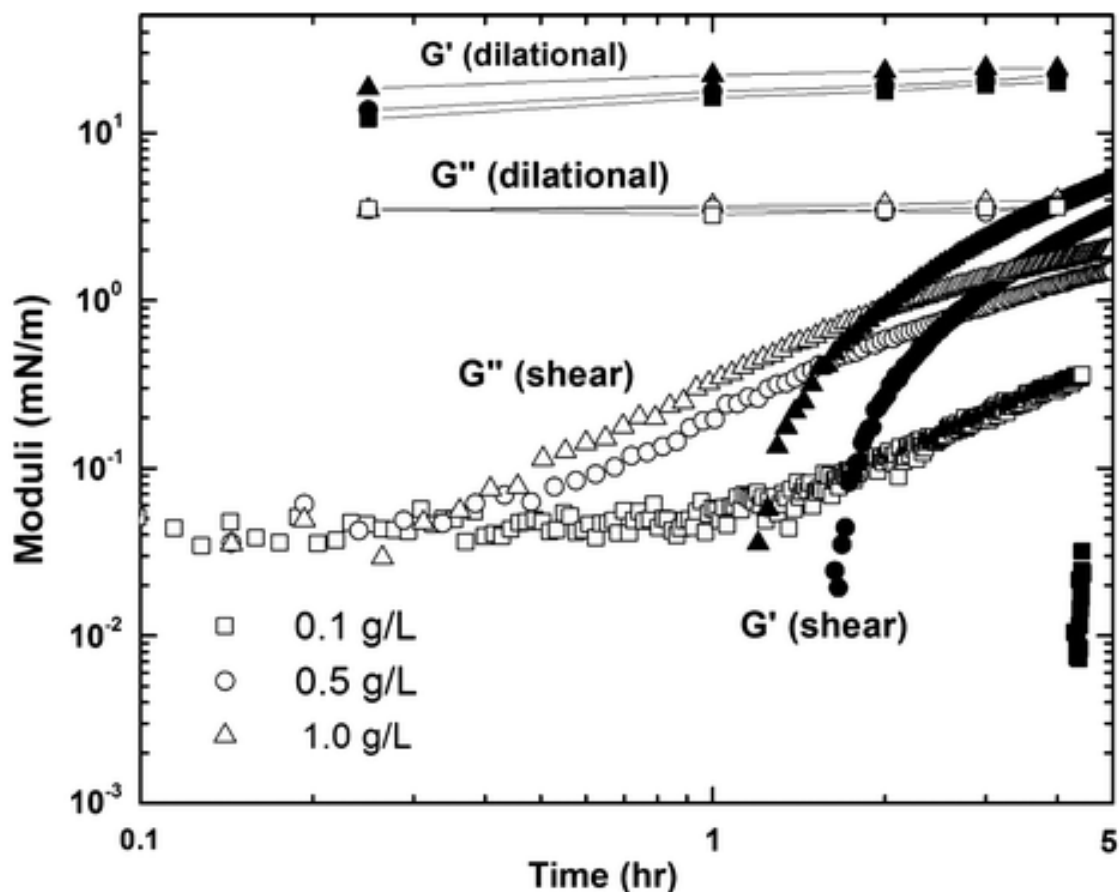


Figure 2-8. Comparison of asphaltene layers measured by dilatational and shear rheology (g L^{-1} – initial bulk concentration of asphaltenes in toluene). Harbottle *et. al.*³⁴

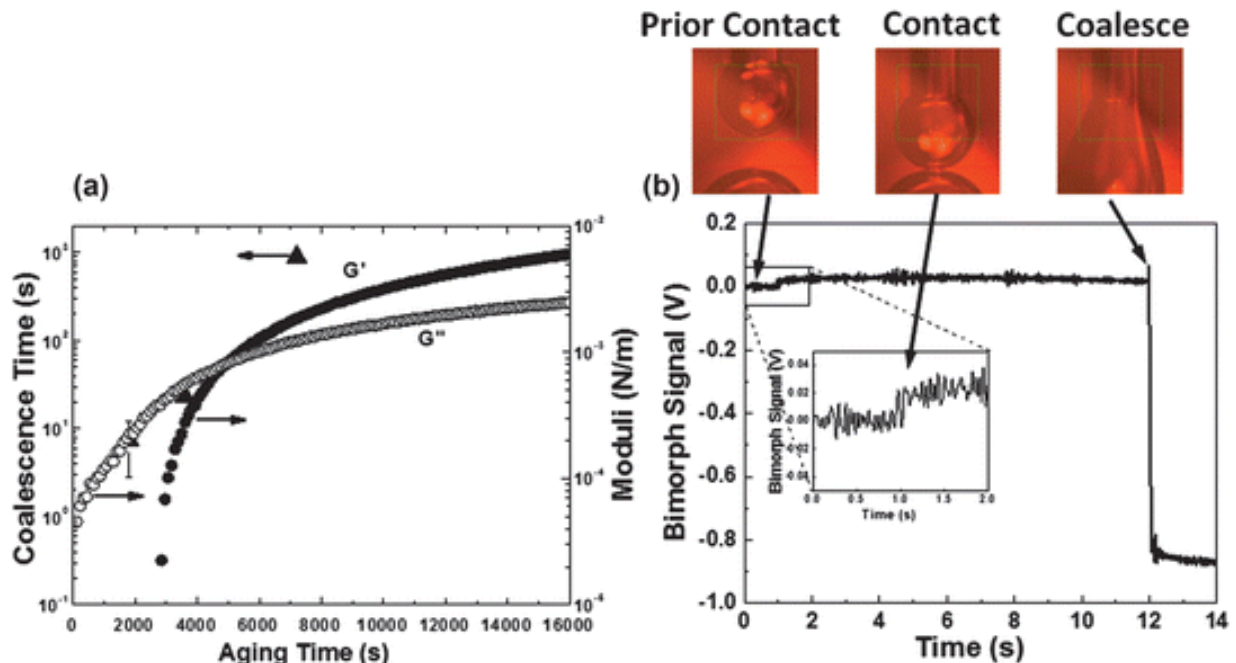


Figure 2-9. (a) Shear viscoelastic properties of an aging asphaltene film (initial bulk concentration 0.4 g L⁻¹ asphaltene in 1:1 heptol) and (b) direct comparison with droplet-droplet coalescence time as measured by the bimorph trace of ITFDA. Harbottle *et. al.*³⁴

With the two techniques providing nearly equivalent surface area to volume ratios and interfacial aging governed by diffusion-controlled adsorption in the absence of advection diffusion, it is reasonable to relate both properties (shear rheology and droplet coalescence) to infer important physical parameters that govern droplet stability. With a viscous dominant film ($G'' > G' = 0$), droplet coalescence is of the order of a few seconds. As the film develops and the elastic contribution impacts the film ($G'' > G'$), the droplet coalescence time increases to tens of seconds. Finally, as the elasticity dominates the film ($G' > G''$) the droplets remain stable for 15 min and are considered to be non-coalescing. The characteristic behaviour has been observed for different asphaltene concentrations and solvent aromaticity.³⁴ It is interesting to note that the development of shear properties appears to be more sensitive when tracking changes in droplet stability as compared with dilatational properties. The transition to the condition $G' > G''$ could provide an insight into the physical mechanism that resists film rupture and droplet-droplet coalescence.

2.1.3.5 Thin Liquid Film Drainage

As two droplets approach one another an approximately flat thin oil film is formed between them. Drainage of the thin oil film to a critical film thickness and possible coalescence are governed by fluid and interfacial forces. The thin liquid film technique has been used to study drainage of water droplets in crude oil to elucidate the mechanism of droplet stabilization. A schematic of the thin liquid film apparatus is shown in **Figure 2-10**. The technique is based on a micro-interferometric method using a Scheludko-Exerowa measuring cell. The film holder is made from a porous glass plate with a 0.8 mm diameter hole drilled in the centre. The plate is soaked in the oil of interest and then immersed in the water-filled measuring cell. The thin liquid oil film is formed when liquid is withdrawn through the capillary by decreasing the pressure (P_r) in the capillary or by increasing the pressure (P_g) in the measuring cell. Drained films are observed in reflected light with the intensity used to calculate the film thickness.

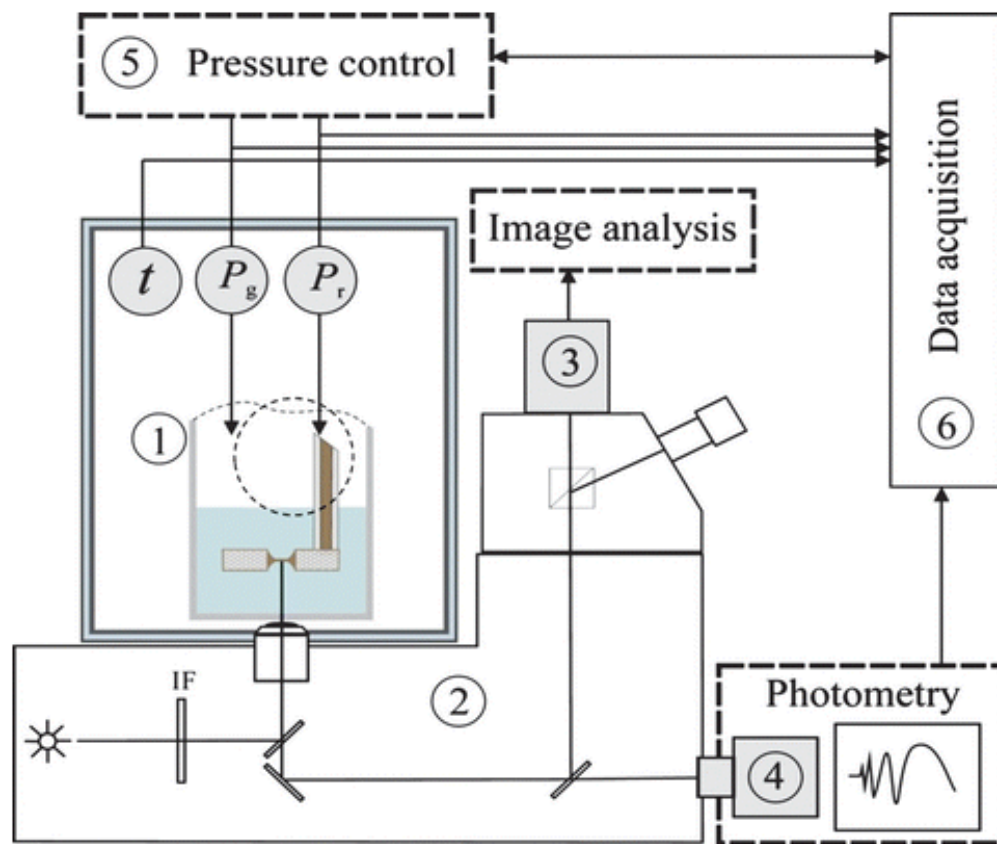


Figure 2-10. Thin liquid film apparatus: (1) thermostatted chamber, (2) inverted microscope, (3) CCD camera, (4) photodiode, (5) pressure control unit and (6) data acquisition. Tchoukov *et. al.*³⁸

The work of Czarnecki and co-contributors^{38–40} elucidated characteristics of petroleum films that feature flexible and rigid interfacial ‘skins’ as shown in **Figure 2-11a, b** and **Figure 2-11c, d**, respectively. For flexible films (50 wt% bitumen in 80:20 vol/vol heptol), shortly after film formation a thick dimple develops and rapidly drains to the meniscus in one or several points. After several minutes the film reaches a critical film thickness (~ 30 nm for the highlighted example). The kinetics of the film thinning can be suitably modelled using Reynolds equation,⁴¹ indicating similar characteristics of emulsion films stabilized by surfactants. At lower bitumen concentration (10 wt% in 80:20 heptol) rigid films formed affect both the drainage kinetics and film thickness. **Figure 2-11c, d** shows snapshots of the film after 15 min and 2.5 hours of interfacial aging, respectively. Similar to a flexible film, a thick dimple is initially formed. However, unlike a flexible film, the dimple in this case does not drain into the meniscus.

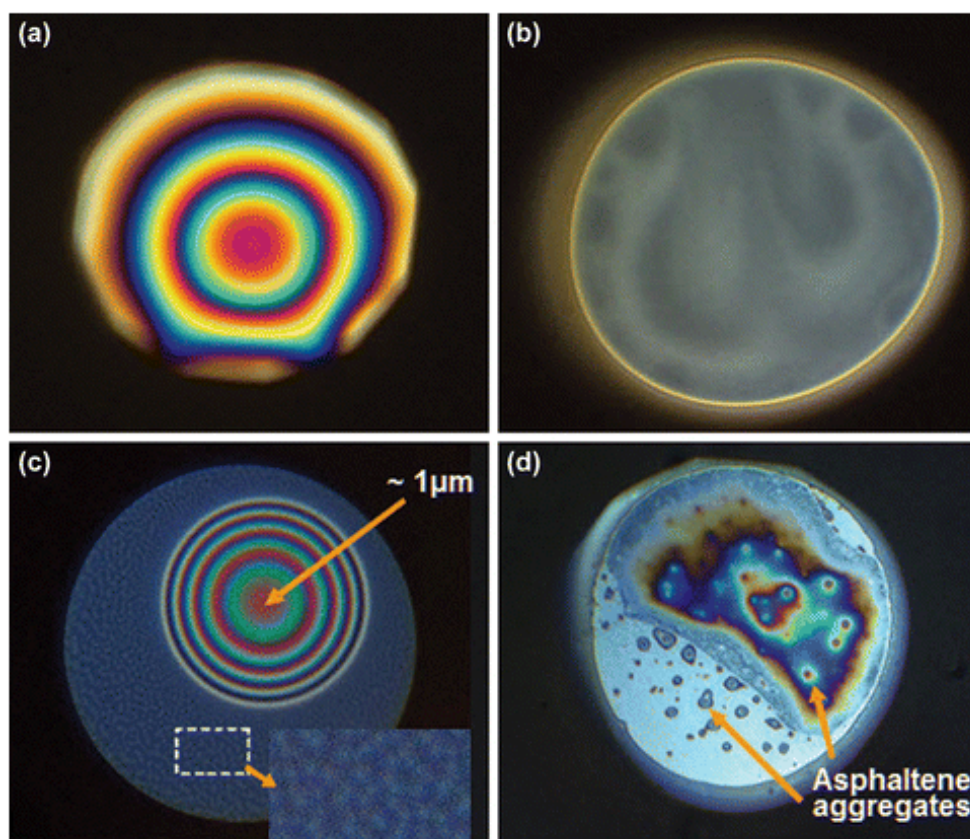


Figure 2-11. Thin film drainage: (a, b) 50 wt% bitumen in 80:20 heptol at time intervals 20 s (a) and 7 min (b); (c, d) 10 wt% bitumen in 80:20 heptol at time intervals 15 min (c) and 2.5 hours (d). Tchoukov *et. al.*³⁸

Examining the darker film area around the dimple, a large number of small lighter spots (inset **Figure 2-11c**) were visible, which the authors attributed to the formation of small asphaltene aggregates in the film. On further aging the film thickness became more heterogeneous with several lenses (thicker areas in the film) observed, indicating the formation of larger asphaltene aggregates. These aggregates are estimated to be ~ 300 nm. The research on thin liquid film identified the formation of multilayer structures that can resist coalescence. The authors introduced, for the first time, the critical importance of film yield stress that must be exceeded to destabilize the film.^{39,40}

To determine the strength of asphaltene films, a continuous oscillation stress ramp can be applied to measure the critical stress for film rupture and fragmentation. Using the DWR technique, apparent (conversion by length) yield stresses up to 10^4 N m⁻² are readily measured for aged films that satisfy the condition $G' > G''$.³⁴ These high shear yield stress values indicate that interaction stresses upon droplet-droplet collision in dynamic environments are not sufficient to break the films to attain coalescence. Alternative approaches for film 'softening' are highly desired and need to be applied.

2.1.4 Particles

2.1.4.1 Asphaltene Nanoaggregates as Emulsion Stabilizers

As indicated above, asphaltenes are considered as a major component in stabilizing water-in-crude oil emulsions. Asphaltenes defined by a molecular class soluble in toluene but insoluble in heptane or pentane represent the heaviest class of molecules in crude oil. The content of asphaltenes increases as the crude becomes heavier, typically much less than 1 wt% for conventional oil and could be as high as 20 wt% for heavy bitumen. Asphaltenes are known to aggregate even at very low concentrations in a highly aromatic solvent such as toluene.⁴² The aggregation of asphaltenes is enhanced at the oil-water interface, forming a three-dimensional network of asphaltene nanoaggregates. Extensive molecular dynamic simulations confirmed molecular aggregation through π - π stacking.⁴³ These nanosized molecular aggregates, as shown schematically in **Figure 2-12**, have been blamed for stabilizing W/O petroleum emulsions.⁴⁴ With variable amounts of heteroatoms distributed within asphaltene molecules and hence their nanoaggregates, these molecular aggregates can be considered as Janus-like particles with their

heteroatoms and fused aromatic rings creating hydrophilic patches in contact with the aqueous phase and the hydrophobic aliphatic side chains protruding into the oil phase to stabilize emulsions. The only difference between conventional Pickering and asphaltene-stabilized emulsions would be the special colloidal interactions between asphaltene nanoaggregates at the oil-water interface that lead to the formation of a three-dimensional protective interfacial film through intermolecular bridging or interdigitation.^{44,45} These interfacial layers make the emulsion extremely stable and difficult to break.

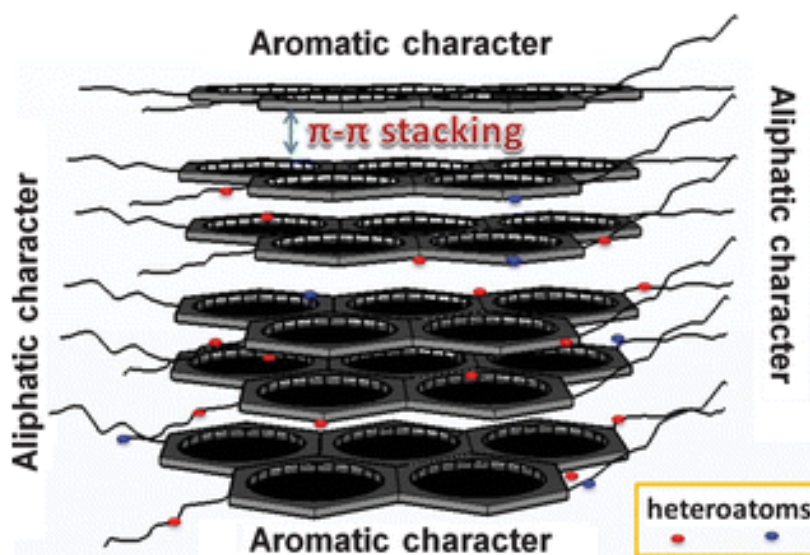


Figure 2-12. Schematic view of asphaltene nanoaggregates exhibiting anisotropic surfaces with aromatic planes preferring aqueous phase and aliphatic side surfaces preferring oil phase or lateral linkage/association. Courtesy of Dr. Robel Teklebrhan of the University of Alberta, Edmonton, Canada.

2.1.4.2 Mineral Particles as Emulsion Stabilizers

In petroleum production various types of inorganic solids such as sand, heavy metal minerals (pyrite, siderite, rutile, zircon, etc.) and clays are recovered with the oil. Depending on the particle surface chemistry these particles can act as emulsion stabilizers, creating substantial above-ground processing challenges. Typically, the heavy metals and clays are naturally hydrophilic but become contaminated by indigenous compounds of crude, making them biwettable and hence increasing their potency to stabilize W/O and O/W emulsions.

Clay particles with distinct basal planes and edges are more surface active due to their small size ($< 2 \mu\text{m}$) and surface anisotropy. The surface anisotropy leads to a variety of possible interactions between clays and indigenous components of crudes. A typical kaolinite clay particle is shown schematically in **Figure 2-13**, exhibiting three types of surfaces: a tetrahedron silica (T-) basal plane, an octahedron aluminum oxyhydroxyl (O-) basal plane and an aluminum-silicates edge (E-) surface. In an aqueous solution of neutral pH, the T-basal plane carries a net negative surface charge, while the O-basal plane and E-surface carry a net positive surface charge. The magnitude of the charge on each basal plane depends on the degree of isomorphous substitution of clay lattice ions.

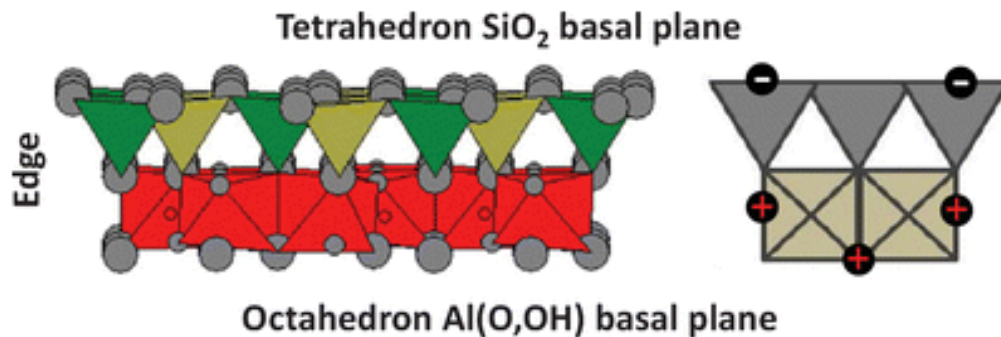


Figure 2-13. Structure of kaolinite clays exhibiting three different surface characteristics: a tetrahedron silica basal plane of pH-independent negative surface charges, an octahedron aluminum oxy-hydroxyl basal plane of weak-pH dependent surface charges, and two sides of edge surfaces of strong pH-dependent surface charge characteristics. Each surface exhibits different responses to the adsorption of a given solution species such as surfactant, rendering them to different surface hydrophobicities and hence Janus type of particle behaviour.

Clay particles are known to interact with crude oil due to their anisotropic nature of basal planes and edge surfaces, as shown in **Figure 2-13**. This characteristic allows clay minerals to become biwettable or even Janus-like due to their interactions with other natural compounds in crude oil. For example, the highly ionic nature of clay edge surfaces would interact with natural surfactant more favourably than the basal planes. The edge surfaces at neutral pH often carry positive charges which attract anionic surface active molecules, while the basal plane featuring permanent deficiency of positive charges would attract cationic surfactants. Depending on the

abundance of cationic and anionic surfactants in crude oil and the type of clays, the clay surfaces could be preferentially modified by natural surfactant to exhibit Janus-like properties.

The chemical nature of toluene-insoluble organic carbon (TIOC), which contaminates clay surfaces, remains poorly understood. In an attempt to determine the chemistry of the organic contaminants that modify clay surfaces, Fu *et al.*⁴⁶ extracted the solids from crude with toluene, separated residual organic matter under supercritical conditions with methanol as the solvent, characterized the methanol extracts by various methods and compared the results with the SARA fractions. The properties of the methanol extracts closely resembled those of the resins fraction. The organic matter extracted by methanol under supercritical conditions was also found to be soluble in toluene after extraction. These findings indicate the challenge of breaking emulsions due to the strong affinity of contaminated heterogeneous clay particles to the oil-water interfaces. However, Osacky *et al.*⁴⁷ proposed that the TIOC consists mainly of humic matter and asphaltene-like compounds rather than resins. Their study showed that the presence of ultra-thin illite correlated quite well with the amount of residual organic matter extracted by methanol at supercritical conditions. Pyridines were also found in the residual organic matter in high concentrations. The association of pyridines with illite is well known to alter the wettability of clays. Konan *et al.*⁴⁸ studied pyridine adsorption on illite and kaolinite minerals. Their results showed that pyridine mainly adsorbs on Lewis acid sites of clays, which accept the lone pair electrons of the pyridine nitrogen. The authors quantified Lewis acid sites on clay surfaces as a function of pretreatment temperature. Kaolinite was shown to feature very few Lewis acid sites whereas illite had significantly more sites, which decreased at higher pretreatment conditions due to the removal of surface water. Lewis acid sites on clay increase the affinity of polar hydrocarbons.⁴⁹ The removal of surface water by thermal treatment of illite at high temperatures was demonstrated to reduce the affinity of alkenes and aromatics on illite, but not on kaolinite. On the other hand, the affinity of alkanes to illite and kaolinite was found to be unaffected by the thermal treatment of increasing temperature.⁵⁰ The presence of water appears to enhance the adsorption of resins and polar organic compounds on illite, thereby enhancing their biwettability.

Humic matter containing both hydrophilic and hydrophobic moieties can adsorb on clay minerals and make them biwettable.⁵¹ Humic matter consists of humic and fulvic acids and

humic acid is soluble only at high pH, fulvic acid is soluble at high and low pH, whereas humin is completely insoluble in the aqueous phase. Fulvic acids are small, polar molecules with simple sugar and amino acid-related structures.⁵² These characteristics make fulvic acids soluble in water and are therefore readily displaced by the larger, less polar humic acids on the surfaces of minerals.⁵³ Because of the chemistry of fulvic acids and humin, biwettability of clay minerals is therefore not expected to be greatly affected by their presence.

Humic acids are organic macromolecular polyelectrolytes. Soluble in both acid and base solutions, humic acids have the highest affinity to mineral surfaces and their interactions with clay have the greatest contribution to the biwettability of minerals. Because of their highly variable molecular structures, the adsorption of humic acids is difficult to understand. The adsorption isotherms of humic acids on clays depend on the history of clay surfaces and surface-area-to-volume ratio of clays.⁵⁴ Individual humic acid molecules of 2–5 nm radius can aggregate to form hydrogen bonded supramolecules of a few hundred nm in diameter. Humic acids are also known to form complexes with metal cations. Combined with hydrogen bonding, humic acids show strong adsorption on various clay minerals.⁵⁵

Collectively there are six mechanisms which explain humic acid adsorption on clay minerals: (i) cation bridges; (ii) anion/cation exchange; (iii) hydrogen bonding; (iv) van der Waals interactions; (v) hydrophobic interactions; and (vi) ligand exchange on a charged clay–water interface. The type of clay influences the adsorption mechanism. Ligand exchange and hydrogen bonding are the two most dominant driving forces for humic acid adsorption on clay edge surfaces which contain hydrolyzed ferric, aluminum, calcium and magnesium cations. The presence of multivalent cations promotes adsorption of humic acids through cation bridges. Polysaccharides tend to adsorb strongly on kaolinite whereas aromatic compounds bind more favourably to smectite. Adsorption of humic acids on a clay surface is also enhanced with increased ionic strength or decreased pH due to poorer solvation of humic acid molecules by water. The molecular weight of humic acids also plays a role, with smectite minerals adsorbing lower molecular weight compounds than kaolinite.⁵⁶ Vermeer *et. al.*⁵⁷ noted charge compensation and specific interactions as the driving force for humic acid adsorption, while the lateral electrostatic repulsion and loss of entropy hinder the adsorption. Positive charges on clay

surfaces attract anionic moieties on the humic acid molecules. As a result, humic acid adsorption increases with increasing positive surface charges by multivalent cation activation. As more anionic sites from the humic acids form complexes with cations in the solution, lateral electrostatic repulsion is decreased, leading to an increase in humic acid adsorption on clay surfaces.

2.1.5 Rag Layers

These particle-stabilized emulsions exhibit a density intermediate to the two immiscible liquids. As a result, the emulsion partitions the oil and water phases by forming a layer that hinders creaming of oil droplets and settling of water droplets. The build-up of dispersed droplets leads to the formation of a complex multiphase layer, commonly referred to as a rag layer, composed of water and oil droplets stabilized by fine solids, asphaltenes and surfactants. Over time its presence eventually impacts separation performance. Despite the major operational challenge posed by rag layers, the nature and formation mechanism of rag layers remain poorly understood.⁵⁸ A recent study on an industrial sample revealed that rag layers are very stable complex oil-continuous emulsions of typically high solids content.⁸ Rag layer formation is commonly encountered in oil sands processing and the extraction of bitumen where asphaltene precipitation coupled with the presence of biwettable fine solids prevents droplet coalescence and phase separation. Although low-quality oil sands contain a high fines fraction which is frequently shown to promote the formation of stable liquid-liquid interfaces, the role of fines in rag layer formation is less clear. There are at least two possible mechanisms postulated to describe the formation of rag layers: (i) slow coalescence rate of water droplets compared with the accumulation rate; and (ii) the formation of a solid barrier to settling materials due to the accumulation of biwettable fines at the oil-water interface.⁵⁹

To elucidate the mechanism of rag layer formation, a novel rag layer generator (**Figure 2-14**) was designed to form well-controlled laboratory samples through washing of solids-free naphtha-diluted bitumen froth.⁶⁰ Despite the absence of inorganic solids, an ample amount of rag layer was formed from naphtha-diluted bitumen froth. After fractionation of rag layer materials into chloroform-insoluble, heptane-insoluble and heptane-soluble fractions, it was determined by detailed characterization using elemental analysis, FTIR characterization and TGA

that the rag layer consists of 27 wt% dry rag materials, 29.4 wt% naphtha and 43 wt% water. Among the dry rag materials, chloroform-insoluble accounts for 45–49 wt%, while the asphaltene content ranges from 23 to 56 wt% of the chloroform-soluble fractions, depending on the naphtha to bitumen ratio used for rag layer production. The heteroatom concentration of asphaltenes isolated from the rag layer was found to be twice as high as that from crude. The chloroform-soluble components and asphaltenes from the rag layer exhibited the greatest interfacial stability.

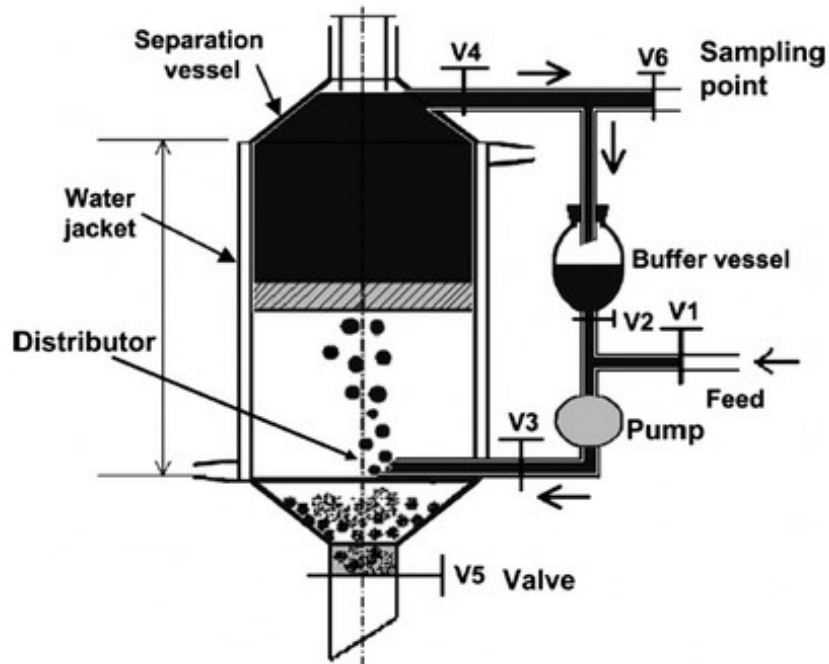


Figure 2-14. A schematic diagram of the vessel for generation of petroleum rag layer materials. Gu *et. al.*⁶⁰

With repeated centrifugation of water-in-diluted bitumen froth emulsions, Czarnecki *et. al.*⁵⁸ showed that the rag layer is a mixture of clay particle-mediated multiple emulsions. Saadatmand *et. al.*⁵⁹ prepared rag layer samples by diluting bitumen froth (with mixtures of heptane and toluene) obtained from oil sands extraction using the Denver flotation cell. The diluted froth was then centrifuged to assess possible mechanisms for rag layer stability. The type of solvent and its effect on asphaltene solubility were shown to govern rag layer formation. During the centrifugation, a mechanical barrier was speculated to accumulate at the oil-water interface due

to the presence of oil-wet materials. The small size water droplets are known to be stabilized by oil-wet fine solids and asphaltene nanoaggregates. Slow coalescence of these emulsified water droplets results in their accumulation at the oil-water interface, forming a barrier that prevents water and fine solid particles passing through the interface and hence promotes the formation of rag layers. Such mechanical barrier was absent in a 50:50 heptane to toluene mixture, in which asphaltenes are highly soluble.

Addition of poor solvent is known to increase asphaltene precipitation, which promotes rag layer formation. A similar observation was made in a recent study by Kiran *et. al.*⁶¹ In the presence of water, poor solvents such as 80:20 heptol allowed asphaltenes to partition at the liquid-liquid interface, thereby increasing emulsion stability. In contrast, the addition of good solvents such as 50:50 heptol reduced rag layer formation. Good solvents are known to lower the affinity of asphaltenes to partition at the oil-water interface, exhibiting less potency for rag layer formation. The study by Saadatmand *et. al.*⁵⁹ concluded that crude containing a greater amount of fine clays leads to the formation of significantly thicker rag layers. Accumulation of fine solids at the oil-water interface, which stabilizes water-in-crude emulsions, was found to be responsible for the greater rag layer formation. Jiang *et. al.*⁶² revealed the formation of a persistent rag layer when clays are present. Although the natural clays are considered hydrophilic (water-wettable), the clays in contact with crude oil contain toluene-soluble organic content, making them biwettable and hence promoting rag layer formation through the stabilization of multiple emulsions. Sodium silicate addition was found to make clay solids in a crude system more water-wettable, decreasing the volume of rag layers during a given crude-water separation.⁶²

In a recent study, focus was placed on characterizing solids from a rag layer sample taken from the secondary cyclone overflow of a naphthenic bitumen froth treatment plant.⁸ The received rag layer was found to be fragile and easily destroyed by handling. However, a thick rag layer as much as 40 vol% of the total sample could be reformed even after vigorous mechanical agitation and then left undisturbed at room temperature for 14 days. The rag layer had a density of 960-980 kg m⁻³, intermediate to the density of the oil phase and the water phase of 860 kg m⁻³ and 1000 kg m⁻³, respectively. The rag layer contained 23-29 wt% water and 15 wt% solids. Solids recovered from the rag layer were found to be more hydrophobic than the solids recovered

from the water layer, indicating the critical importance of particle wettability in stabilizing emulsions and hence inducing rag layer formation. The solids from the water layer consisted mostly of kaolinite and illite. In contrast, an elevated level of siderite and pyrite was measured in the solids isolated from the rag layer. The solids recovered from the rag layer appeared to be more severely contaminated with organic matter, exhibiting a stronger hydrophobicity. Chemical binding of carboxylic acid groups in heavy oil with metallic sites on clays and iron-containing siderite appeared to be the cause of severe contamination and significant wettability alteration. These biwetable fine particles attached strongly to the oil-water interface. Collectively with asphaltene nanoaggregates, the presence of hydrophobic particles contributed to rag layer formation and stabilization. Understanding the formation mechanism and role of particle wettability in promoting rag layer formation provides directions on mitigating rag layer formation.

To summarize, the contact of clay particles with petroleum leads to adsorption of indigenous components of petroleum such as asphaltenes, resins and humic acids. Subsequent contamination renders the clay particles highly biwetable. The particle-stabilized emulsions in petroleum are most likely a result of collective actions from contaminated biwetable clay particles and asphaltene nanoaggregates in the presence of resins. The emulsions formed through such complex mechanisms lead to great difficulties in petroleum processing and handling, as a result of the formation of so-called rag layers as described below.

2.1.6 Demulsification

The accumulation of asphaltene nanoaggregates and biwetable fine particles at the oil-water interface generates emulsions of extreme stability. These emulsions will remain stable for prolonged periods (longer than separator residence times) with little or no separation. To enhance the driving force for separation it is desirable to increase the droplet size either by: (i) droplet-droplet flocculation; and/or (ii) droplet-droplet coalescence. With a squared dependence on droplet diameter, the free-settling Stokes' equation indicates that the settling velocity increases four-fold as the droplet diameter doubles. To promote fruitful droplet interactions, the armoured films surrounding droplets have to be disrupted by molecules that are interfacially active and can compete for available liquid-liquid interfacial area. These molecules are referred

to as demulsifiers and are frequently added into the process to minimize the formation and break-up of problematic emulsions and rag layers.

2.1.6.1 PO/EO Demulsifiers

The commonly used demulsifiers in petroleum processing include copolymers of PO (propylene oxide) and EO (ethylene oxide). Xu *et. al.*⁶³ studied this category of demulsifier by grafting PO/EO copolymers onto DETA (diethylenetriamine) as shown in **Figure 2-15**. The copolymers with dendrimer structures of an intermediate molecular weight (i.e., 7500–15,000 Da) were found effective at breaking W/O emulsions. These authors investigated demulsification performance of the copolymer by changing the EO:PO ratio. For PO \gg EO, demulsification performance was shown to be poor at low demulsifier concentrations and effective at high demulsifier concentrations. For PO \ll EO, the demulsifier was shown to be effective at low concentrations but overdosed at high concentrations to produce a stable middle-phase emulsion. For PO \approx EO, effective emulsion separation was observed at low demulsifier concentrations with no concerns of overdosing and no formation of a stable middle-phase emulsion at high demulsifier concentrations. The authors concluded that the demulsifiers of balanced PO/EO number provided optimum demulsification performance.

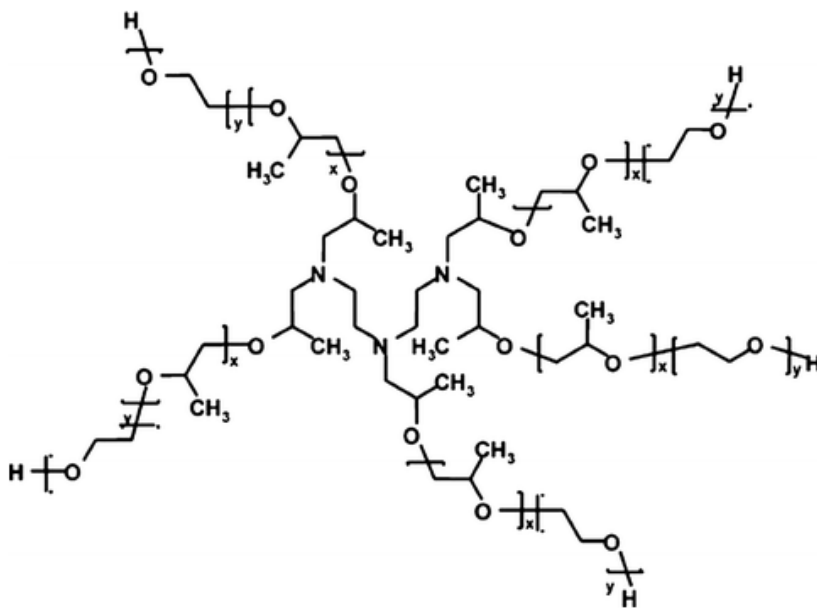


Figure 2-15. Chemical structure of DETA-based block copolymer with EO/PO units. Xu *et. al.*⁶³

The hydrophilic and hydrophobic nature of the EO/PO copolymer promotes solubility in both liquid phases and hence a capability to partition at the liquid-liquid interface. The hydrophilic lipophilic balance (HLB) describes the potential of the surfactant to control the emulsion type. For demulsification, the HLB value of the surfactant should be in the region of 7 to 9. Due to the definition of the HLB concept, it is not easy to measure the HLB value of demulsifier molecules due to lack of exact structure of the molecules. Alternatively, relative solubility numbers (RSNs) can be used to represent the hydrophobicity of large molecules such as PO/EO demulsifiers. The RSN values of the demulsifiers are measured using ethylene glycol dimethyl ether and toluene as titration solvents. In this method, 1 g of demulsifier is dissolved in 30 mL of solvent consisting of toluene and ethylene glycol dimethyl ether. The resultant solution is titrated with deionized water until the solution becomes turbid. The volume of water (mL) titrated is recorded as the RSN.

For an equivalent PO number in an EO/PO copolymer of increasing EO content, the interfacial activity of the copolymer increases, further decreasing the water-oil interfacial tension with increasing RSN. Xu *et. al.*⁶³ reported that the demulsification performance of EO/PO copolymers increased with a decrease in the bitumen–water interfacial tension. Hence a good demulsifier should reduce the interfacial tension by partitioning at the oil-water interface. However, it is important to note that the magnitude by which the interfacial tension decreases is not the sole guide for demulsification performance. Other parameters such as interfacial rheology, film pressure and film structure also need to be considered.

2.1.6.2 Demulsification Mechanism

In several recent studies, ethylcellulose (EC) has been identified as a suitable biodegradable demulsifier for bitumen froth.^{64,65} EC is a polymeric material produced by treating alkali cellulose with chloroethanol, resulting in a cellulose ester. In a typical EC molecule, the hydroxyl and oxyethyl side chains are either equatorial or axial, located on both sides of the ring as shown in **Figure 2-16**. The structure of EC makes it distinguishable from conventional linear or star-like EO/PO copolymer demulsifiers. Various grades of EC have been synthesized with different molecular weights and degrees of substitution. By controlling the cellulose/sodium

hydroxide/iodoethane molar ratio in the etherification reaction, EC polymers of varying molecular weight and hydroxyl content can be synthesized.⁶⁶

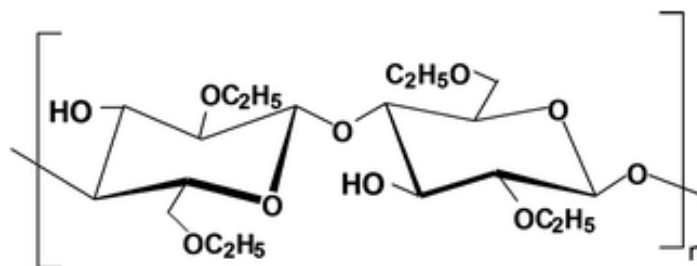


Figure 2-16. Structure of EC with a degree of substitution of 2. Feng *et. al.*⁶⁴

EC is miscible with organic solvent and is interfacially active. The interfacial activity of EC is attributed to the amphiphilic nature of its molecular structure of hydrophilic cellulose backbone and the side chain of hydrophobic ethyl substituents. On the basis of the monomer unit of EC and Davies formula,⁶⁷ the HLB value of EC was estimated to be around 8, which is within the range of effective W/O demulsifiers. Feng *et. al.*⁶⁴ studied the interfacial tension between naphtha and water in the presence and absence of 60 wt% bitumen in naphtha solution as a function of EC concentration, as shown in **Figure 2-17a**. Clearly, EC is more efficient at reducing the naphtha–water interfacial tension than reducing naphtha-diluted bitumen (naphtha/bitumen mass ratio = 0.6)-water interfacial tension, indicating that EC molecules have to compete with the indigenous surface active species in bitumen to lower the naphtha-diluted bitumen-water interfacial tension. At an appropriate demulsifier dosage EC is able to coalesce water droplets (**Figure 2-17b₂**) causing a 5- to 10-fold increase in the droplet diameter than the case without EC addition (**Figure 2-17b₁**), and thus promote a rapid decrease in water content.

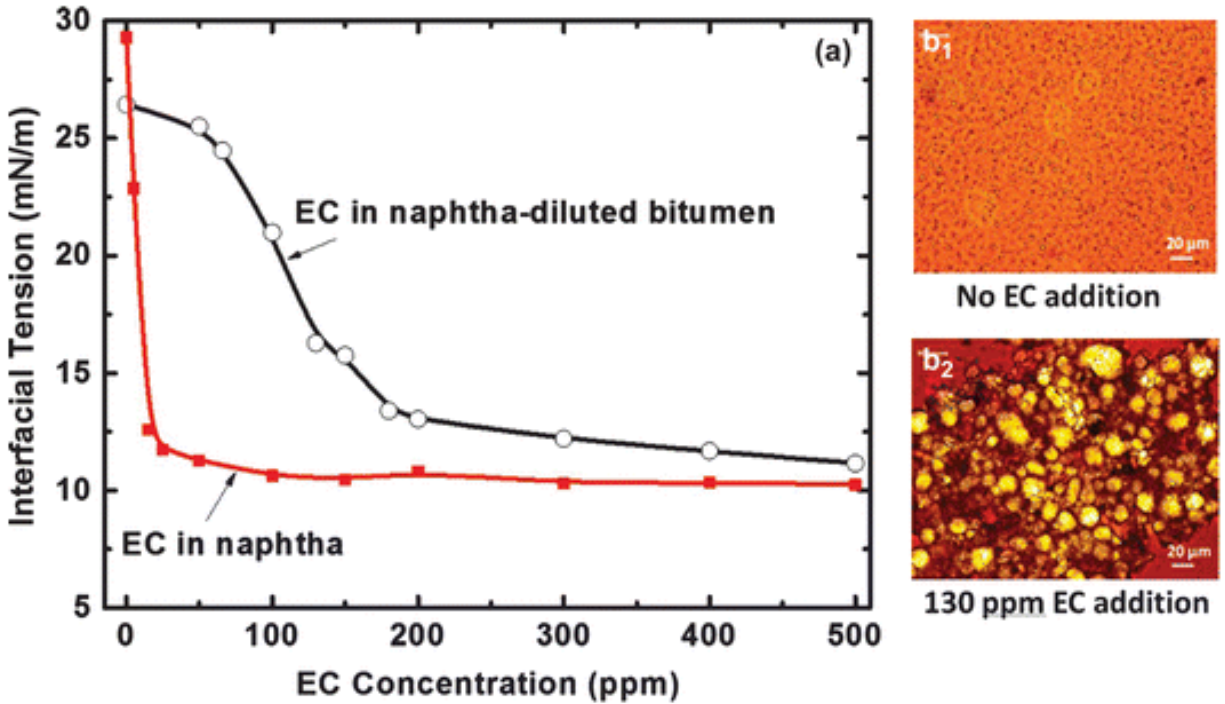


Figure 2-17. (a) Interfacial tension between naphtha and water in the presence and absence of 60 wt% bitumen as a function of EC concentration at 20 °C. (b) Micrographs of emulsions without demulsifier addition and 130 ppm EC addition. Samples were taken at 6.5 cm from the emulsion surface (bottom of the test tube). Feng *et. al.*⁶⁴

To understand the role of molecular structure on demulsification performance, Feng *et. al.*⁶⁶ synthesized six different EC demulsifiers of different molecular weights and degrees of hydroxyl substitution (DHS). The demulsification performance of EC was shown to depend on both the hydroxyl content and molecular weight. For an equivalent molecular weight (EC3, EC4, EC5 = 143,000 Da), greater water removal was measured with increasing degrees of hydroxyl substitution (EC5, DHS = 1.33; EC4, DHS = 1.70; EC3, DHS = 2.14). The dependence on hydroxyl substitution was evaluated at high demulsifier concentrations (290 ppm). The observed dewatering performance is reasonable because higher DHS increases the interfacial activities of EC due to the decreased hydroxyl content. However, excessive hydroxyl substitution (EC1 = 45,000 Da, DHS = 2.79) increases the solubility of the EC molecules in the oil phase and reduces the effectiveness of the demulsifier to partition the oil-water interface. Such drop-off in performance is highlighted by comparing the performance of EC1 and EC2 (EC2 = 45,000 Da, DHS

= 2.40) demulsifiers (**Figure 2-18**). Comparing performance on the basis of molar concentration (data shown in inset of **Figure 2-18**), EC demulsifiers of similar hydroxyl content and higher molecular weight (EC3 = 143,000 Da and EC6 = 177,000 Da) were shown to provide the best demulsification performance. EC1 with the lowest hydroxyl content and lowest molecular weight was shown to be the worst demulsifier.

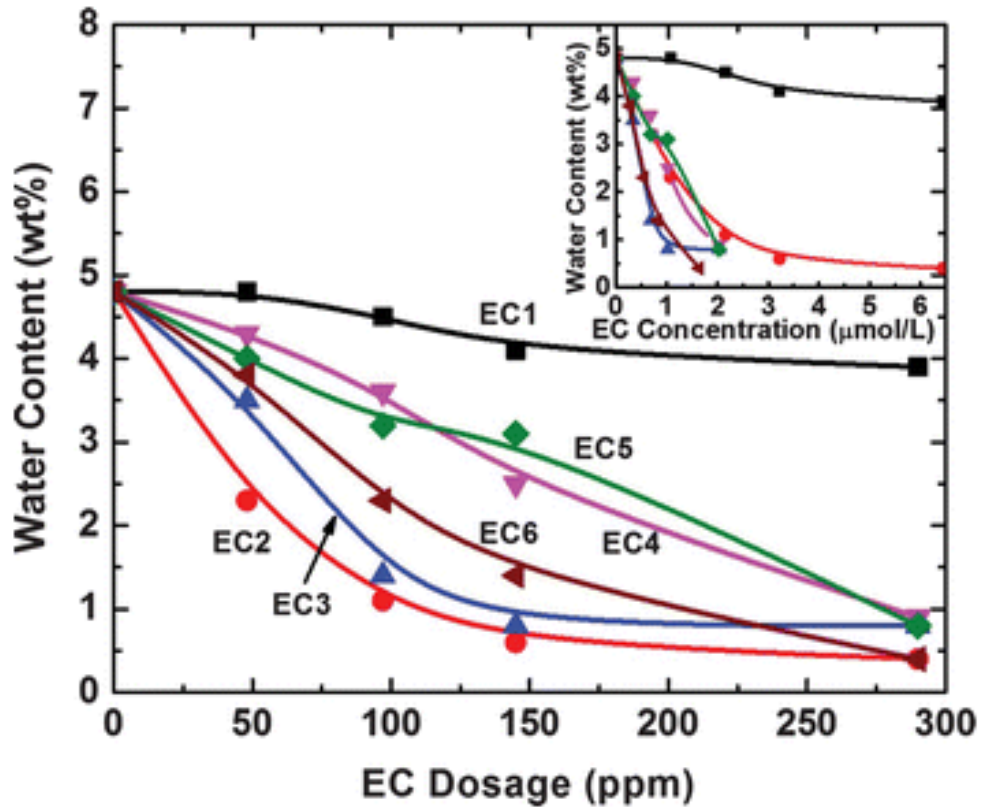


Figure 2-18. Water content at 2.5 cm from the top of the emulsion surface as a function of EC dosage for six EC demulsifiers. Feng *et. al.*⁶⁶

To better understand the demulsification performance based on molecular weight and hydroxyl substitution, the authors measured the water-diluted bitumen interfacial tension as a function of EC concentration (data not shown). On a molar basis, in general, the demulsifiers of high molecular weight were shown to be more effective in reducing interfacial tensions. However, no clear correlation could be established between interfacial tension and dewatering performance. The lack of correlation was attributed to the hydroxyl content that governs the

molecular conformation of the EC molecule and its ability to flocculate water droplets. Higher hydroxyl content would lead to stronger intra- and intermolecular interactions between cellulose molecules, causing the molecule to self-coil, thus decreasing its ability of bridging flocculation.

To further elucidate the demulsification mechanism by EC molecules, droplet-droplet interactions were visualized in situ using the micropipette technique.⁶⁴ **Figure 2-19** shows sequential still images of two micron-sized water droplets in naphtha-diluted bitumen with and without EC addition. In the absence of EC, two micron-sized water droplets were brought in contact for a few minutes under a given applied compression force and did not coalesce. Upon release of the compression force the two droplets separated and returned to their original spherical shape with no visible droplet deformation under contact or retraction (**Figure 2-19A1** and **A2**). The characteristic nature by which the droplets reside in contact and remain spherical upon retraction indicates that there was no attractive force (coagulation) between the two droplets. The lack of interaction between the two droplets is a result of a steric barrier surrounding the water droplets. Wang *et. al.*⁶⁸ reported strong steric repulsive forces between two asphaltene-coated surfaces in toluene and heptane/toluene mixtures, measured by atomic force microscopy (AFM). The repulsion was attributed to the asphaltene brush-like layers resisting adhesion unless a critical compressive force is exceeded.²⁵

Figure 2-19B1 and **B2** shows the interaction between two water droplets in the presence of 35 ppm EC. Applying a compressional force the two droplets remained stable and did not coalesce (**Figure 2-19B1**). However, when the compressional force was removed the water droplets adhered to each other and stretched substantially before final separation (**Figure 2-19B2**). The strong adhesion confirms flocculation of the two droplets in the presence of EC without coalescence. By increasing the concentration of EC further to 130 ppm, the two water droplets flocculated immediately upon contact (**Figure 2-19C1**) and coalesced shortly to one larger droplet (**Figure 2-19C2**). The coalescence time occurred over several seconds, with the coalescence rate increasing with higher demulsifier concentration.

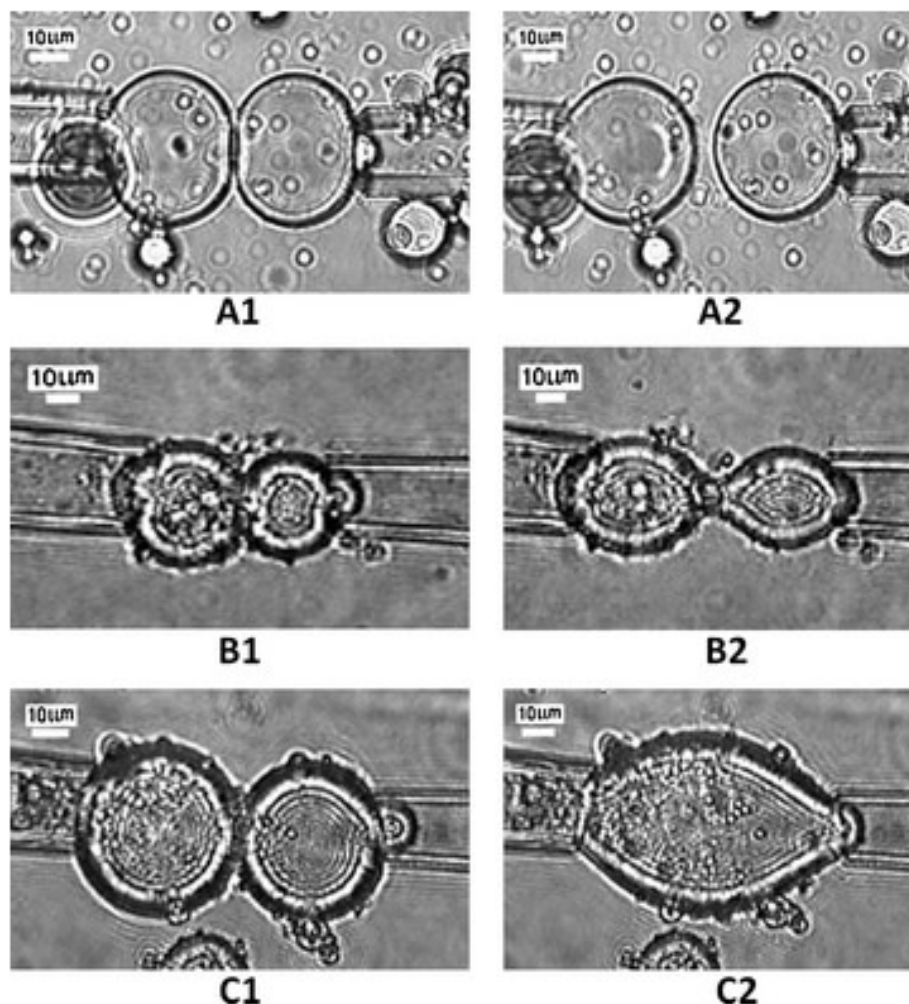


Figure 2-19. Interactions of water droplets visualized by the micropipette technique. Water droplets were present in 0.1 wt% naphtha-diluted bitumen emulsion. (A) no demulsifier addition, (B) 35 ppm EC addition and (C) 130 ppm EC addition. Feng *et. al.*⁶⁴

From the micropipette study it was hypothesized that the concentration dependence on flocculation and coalescence behaviour was closely related to the degree of interfacial material substitution by EC molecules. Wang *et. al.*⁶⁹ considered the interaction between adsorbed asphaltenes and EC molecules in solution by quartz crystal microbalance with dissipation monitoring (QCM-D) and AFM. From their QCM-D studies the authors noted the positive interaction between EC molecules and the asphaltene layer coated on a silica substrate, gradually transforming the adsorbed layer over several hours. Washing of the newly formed film resulted in no mass loss, indicating that the new layer was irreversibly adsorbed. With limited structural

information the authors supplemented their findings with AFM imaging of adsorbed asphaltene layers soaked in EC solutions for up to 7 hours. **Figure 2-20** AE-0 (t = 0 hours) shows the topographical features of asphaltenes adsorbed on hydrophilic silica. The asphaltenes are randomly distributed in the form of close-packed colloid-like nanoaggregates with a mean square roughness of ~ 1 nm. With increasing soaking time (**Figure 2-20** AE-6, t = 6 hours) in the EC solution the topography of the asphaltene film shows two distinct changes: some aggregates grew in size while the discrete flat areas expanded on the surface. Those discrete flat areas are considered as a result of adsorption of EC molecules on silica (data not shown). After 7 hours of soaking (**Figure 2-20** AE-7, t = 7 hours) the changes in film properties become even more apparent, showing higher rough domains (larger aggregates) and much expanded flat open areas.

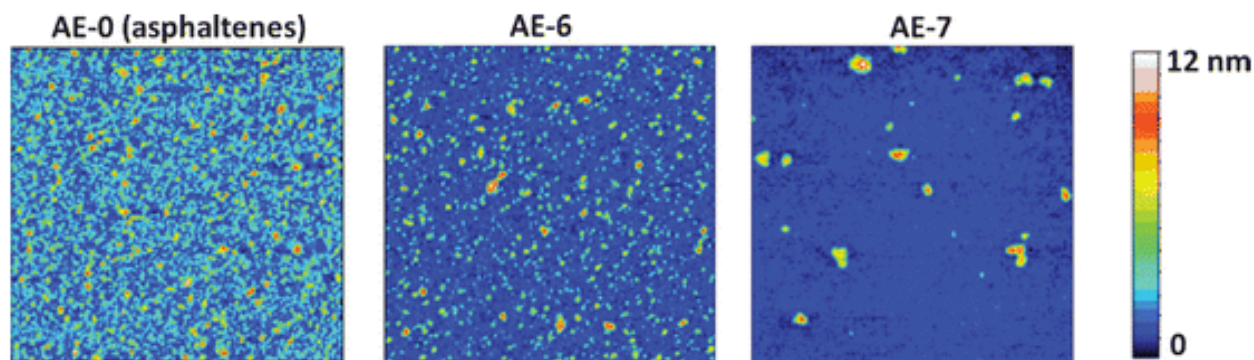


Figure 2-20. AFM topography images of asphaltene-coated sample surfaces soaked in EC-in-toluene solution for 0 – 7 hours. Wang *et. al.*⁶⁹

The process of EC displacing asphaltenes from a silica surface is illustrated in **Figure 2-21**. Initially, the more surface active EC molecules adsorb on the silica surface at the defects of the asphaltene layer. The distribution of polar groups on asphaltenes is neither dense nor uniform, hence the asphaltene layer cannot occupy all the binding sites on a substrate. As such, opportunity is provided for sequential adsorption of EC molecules. This initial EC adsorption is rapid. Compared with asphaltenes, the polar binding groups on EC molecules are more uniformly distributed along the polymeric chains and of higher density. As a result, each EC molecule can form multiple binding sites with the substrate. Because the EC molecules interact more strongly

with the substrate, the EC molecules gradually expand, displacing the asphaltene layer and weakening the binding between asphaltenes–asphaltenes and asphaltenes–substrate. The driving force for EC to displace the adsorbed asphaltenes is attributed to its higher number of stronger hydrogen bonding sites toward the hydroxyl groups on the hydrophilic substrate. This process gradually squeezes the asphaltene aggregates into small areas of larger size domains of significantly greater thickness. Once these voids are created in the film, there is an opportunity for water to connect and hence promote droplet coalescence. Although the mechanism for asphaltene displacement by EC molecules has been demonstrated at the solid–liquid interface, the system is a good analogue for the liquid-liquid system. Asphaltene displacement and the formation of voids in the film has also been confirmed by imaging (AFM) Langmuir–Blodgett films transferred from the liquid-liquid interface after EC addition.^{64,70}

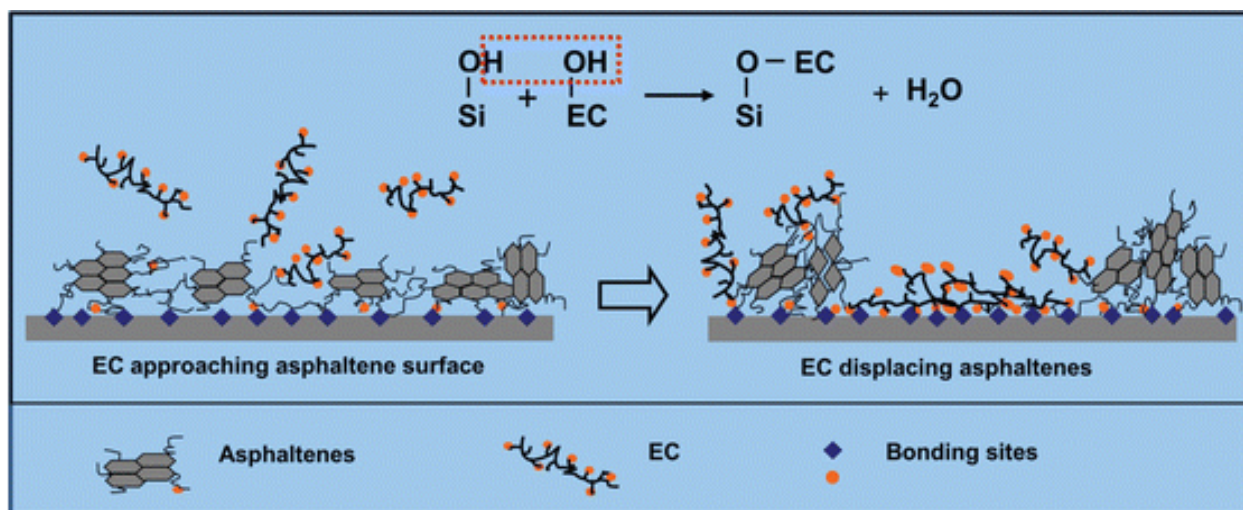


Figure 2-21. Schematics of asphaltene displacement by EC on a hydrophilic solid surface. Reprinted with permission from Wang *et. al.*⁶⁹

2.1.6.3 Magnetic Responsive EC Demulsifier (M-EC)

One drawback from chemical demulsification is the continual supply of demulsifier to treat the petroleum emulsion. Recently, a novel approach for chemical demulsification has been demonstrated through the synthesis of a magnetically responsive demulsifier that can be manipulated under a magnetic field and hence recovered for reuse.^{71,72} The concept of synthesizing magnetic-ethylcellulose (M-EC) nanoparticles is illustrated in **Figure 2-22**. Firstly,

magnetite (Fe_3O_4) nanoparticles are coated with a thin layer of silica using a dense liquid silica coating method to protect the magnetic particle and make the surface amenable for further functionalization. The silica-coated magnetic nanoparticles are then modified by a silane coupling agent, 3-aminopropyltriethoxysilane (3-APTES), to render the surface of amine functionality. EC molecules are modified through an esterification reaction of acryl halide ($\text{O}=\text{C}-\text{Br}$) with hydroxyl ($-\text{OH}$) to replace some hydroxyl groups of EC with 2-bromoisobutyryl bromide, forming bromoesterified EC, or EC-Br. The modified EC interacts through the chemical reaction between $-\text{NH}_2$ groups on the $\text{Fe}_3\text{O}_4\text{-SiO}_2\text{-NH}_2$ surface and bromine on EC-Br, chemically anchoring onto the amine-functionalized Fe_3O_4 nanoparticle ($\text{Fe}_3\text{O}_4\text{-SiO}_2\text{-NH}_2$) surface to form a polymer EC layer, leading to the formation of M-EC. As prepared, M-EC nanoparticles possess a strong magnetic core with an interfacially active organic EC layer on the surface.⁷²

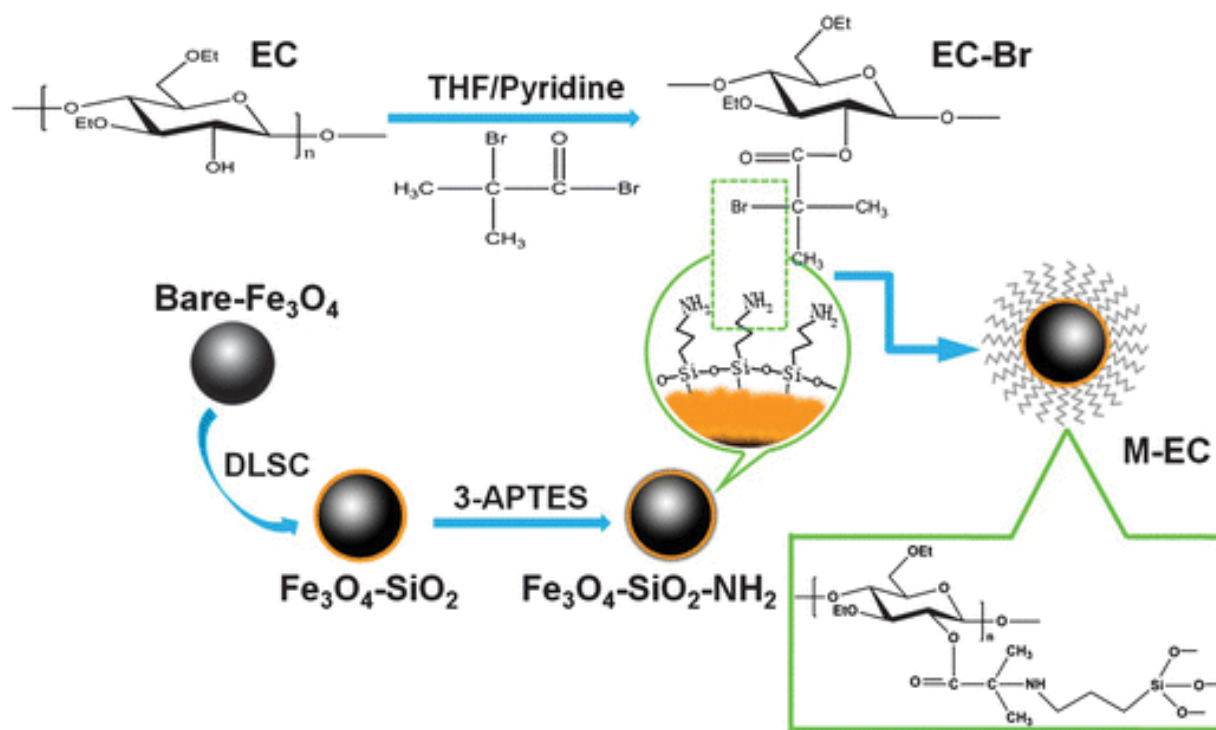


Figure 2-22. Schematic illustration of the synthesis of magnetic ethylcellulose-grafted nanoparticles (M-EC). Peng *et. al.*⁷²

Figure 2-23a compares demulsification performance of a 5 wt% water-in-naphtha-diluted bitumen emulsion (naphtha/bitumen mass ratio = 0.65) by M-EC and conventional chemical EC at 130 ppm. The control experiment (blank without demulsifiers) shows a negligible difference in the water content along the test tube after 1 hour of settling, remaining at around 4.7 wt%. This observation indicates a very stable W/O emulsion without noticeable water separation under gravity alone. In contrast, the addition of 1.5 wt% M-EC with magnetic separation reduced the water content of the emulsion to less than 0.4 wt% at a location of 6 cm below the emulsion surface. Thereafter, the water content increased sharply to well above 20 wt%. The results clearly show that more than 90% of the water in the original emulsion settled under magnetic forces to less than 14% of the original emulsion volume. In comparison to a water content of 18.5 wt% at the depth of 6 cm for the case with EC addition, the addition of M-EC clearly shows a better water separation into a much smaller volume of sludge and less oil loss because of the enhanced separation of M-EC tagged water droplets by magnetic forces. The rate of M-EC water separation was of the order of seconds rather than minutes or hours. A further study showed the potential regeneration and reuse of M-EC (**Figure 2-23b**) by effective (~90%) water removal from a water-in-diluted bitumen emulsion over 10 consecutive cycles. With improved demulsification efficiency and kinetics, the reusable M-EC demulsifier is also economically attractive for continuous operations. Preliminary studies showed that the demulsification performance could be extended to industrial bitumen froths, with the original water content in the froth reduced to below 0.5 wt% in 5 minutes at room temperature.⁷¹

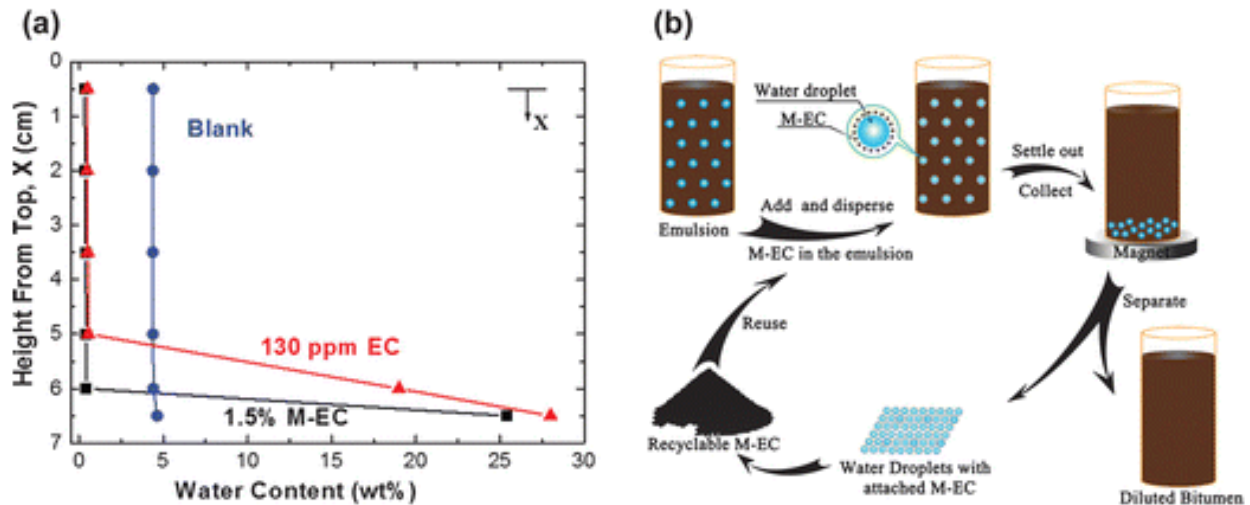


Figure 2-23. (a) Water content at different depths of diluted bitumen emulsions treated with 1.5 wt% M-EC or 130 ppm EC after settling on a hand magnet for 1 hour at 80 °C. (b) Schematic illustration of the demulsification process and recycling tests using M-EC as demulsifiers. Peng *et al.*⁷¹

2.1.7 Summary

In petroleum production there are many operational challenges that have galvanized a research community over several decades. One of the greatest challenges is to achieve rapid and efficient separation of problematic emulsions that form due to the accumulation of surface active species (indigenous oil compounds and fine biwetttable particles) which stabilize liquid-liquid interfaces and prevent fruitful droplet-droplet interactions. To enhance separation, chemical demulsifiers are added to compete for available interfacial sites and disrupt the rigid interfacial networks. It is important to note that this chapter is by no means exhaustive and is not meant to cover all aspects of the emulsification and demulsification problems facing the petroleum industry. Work has been selected to provide an overview of the key fundamental mechanisms that contribute to the formation and break-up of emulsions and provide scientific directions. It is our intention to clearly illustrate the importance of understanding basic science in emulsion stabilization before tackling the technology for effective demulsification.

2.2 Problem Statement and Objective

The objective of this thesis project is to design and test composite responsive materials useful in the treatment of biphasic wastes, including bitumen emulsions, encountered throughout the bitumen extraction process.

The bitumen extraction process presents numerous examples of dispersed mixtures comprising immiscible phases (*e.g.*, oil and water). One of the most commonly encountered multiphase mixtures are emulsions stabilized by surfactants and fine particles (*e.g.*, clay). Dispersed materials are much more difficult to process and phase separation is often challenging for well-stabilized systems. Left alone, well-stabilized emulsified droplets can take months, even years, to completely separate. Different types of chemicals are used by the petroleum industry to treat various mixtures of oil, water and solids. Because of the complex nature of the bitumen extraction process, most chemical additives are not suitable or compatible with the entire process. Certain chemical compounds, although beneficial to one step or unit operation within a complex process, can be very detrimental to a later step in the process. Therefore, supplemental mitigating steps (*i.e.*, separation or treatment) must usually be added to a multistep process when diametrically opposing conditions must be met at different points in the process. However, many treatment protocols have limitations. For instance, calcium salts are added to aggregate tailings solids but high calcium concentration in process water severely reduces bitumen recovery. Substances detrimental to bitumen recovery must be removed or treated before process water can be reused. Before process water can be recycled back into the extraction process, excess calcium ions are precipitated as calcium carbonate. However, this strategy requires a large supply of additives and continuously raises ionic strength. Although effective separation of various materials including dissolved salts is possible, high-efficiency separation processes require additional capital and incur continued operating costs. Without an adequate removal process, continuous addition of process aids is not possible and requires addition of fresh water to maintain proper water chemistry. When an effective separation is not possible or economical, a compromise must be made, which leads to sub-optimal process conditions. Responsive materials are sensitive to a specific stimulus which induces a significant change in one or more properties once applied. For example, the gain or loss of charge in a chemical compound

is usually sufficient to significantly influence properties such as solubility. Uncharged species are often soluble in low polarity organic solvents, while ionic species are generally insoluble in such solvents. Furthermore, certain chemical functionalities will undergo other transformations under specific conditions (*i.e.*, pH, electrical potential, irradiation and numerous others). The induced change in properties may be reversible or irreversible, depending on the nature of the applied stimulus. Thoughtful incorporation of responsive materials is a powerful methodology used to design process aids that are capable of adapting to the specifications of more than one step in a complex process. Responsive materials are useful in chemical processes and manufacturing processes, as complex multi-step processes often have diverse ideal requirements for each individual step and responsive materials are capable of adopting more than one state.

2.2.1 Preparing Composite Particles

Composite materials are made by combining different materials together. Thus, a variety of chemical or physical properties may be combined within a single particle by using the appropriate materials and preparative method. The structure of the composite material must be carefully considered in order to promote advantageous properties. Furthermore, responsive behaviour can be imparted to a composite particle by incorporating a responsive element. Composite responsive particles can be tailored to deliver a specific function or to facilitate subsequent separation. Therefore, developing composite responsive particles tailored for the bitumen extraction process is of great interest.

Particles are three-dimensional structures and, for composite particles, the spatial arrangement of the incorporated materials has an important impact on their overall effectiveness. Very different structures can be made from only two different materials, as shown in **Figure 2-24**. Ideally, the morphology of a composite particle should complement or supplement its intended function. The structure of a particle is determined by the physicochemical conditions at the time of preparation. The type of physicochemical processes involved in the preparation of solid particles can have a marked impact on its structure and function. In order to effectively treat multiphase mixtures, solid particles must enter and move through the continuous phase in order to reach the non-continuous phase. Therefore, the particle wettability must be suitable for the type of continuous phase encountered.

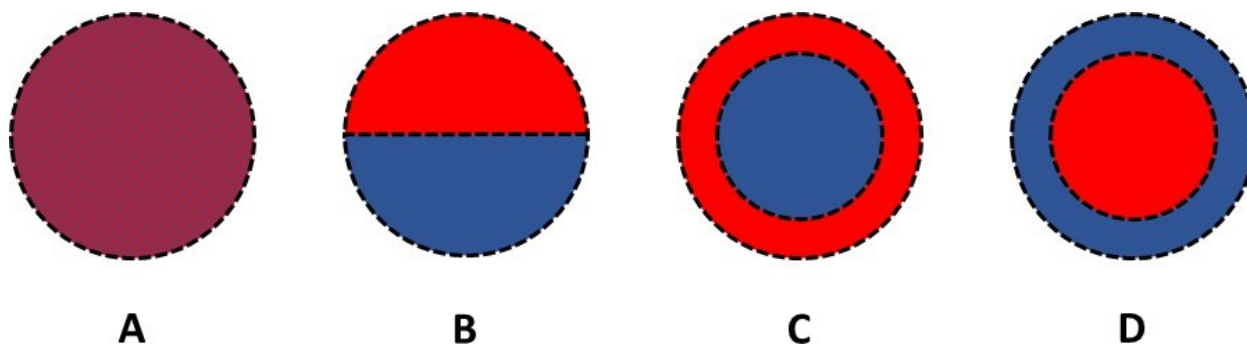


Figure 2-24. Illustration of composite particles, consisting of two different materials, with contrasting structures. Constituent materials can be well-mixed [A]. Alternatively, constituent materials can be entirely segregated [B]. Furthermore, when two materials are segregated, one constituent material may completely envelope the other [C and D].

In addition to surfactants, particles are also capable of stabilizing emulsions. A stabilizer particle is positioned at the interface between immiscible phases, lowering the energy of an emulsified mixture. A particle-stabilized emulsion is most stable when the stabilizer particles are biwettable, with contact angle approaching 90° . The wettability of a surface or particle depends on the nature of the material but can be modified by altering the surface properties through chemical functionalization with hydrophobic or hydrophilic substances. Particles can stabilize emulsions but are distinct from surfactants with important differences. The ability of a surfactant to stabilize an emulsion is linked to its relative solubility in each phase. Any change to the chemical structure of a surfactant has significant impact on its solubility and therefore its performance. In contrast, solid particles have extremely limited solubility. Emulsion-stabilizing particles attach irreversibly to the oil-water interface while surfactants are concentrated at the oil-water interface in a dynamic equilibrium with the bulk phase. The ability to tune performance independently of solubility, by adjusting surface coverage of both switchable and non-switchable surface moieties, is an important distinction of solid particle emulsion stabilizers and a clear advantage over molecular surfactants. The effect of CO_2 on emulsion stabilizer particles functionalized with different responsive surface groups is further explored in **Chapter 4**.

Insoluble particles are much easier to separate compared to dissolved solutes. Dissolved solutes are typically separated based on a change in physical state. For example, low boiling point

compounds can be removed by evaporation. Separation of dissolved species is much easier if precipitation can be induced, for various types of high-efficiency solid-liquid separation techniques are available. In general, sedimentation processes are favoured in large scale processes due to the low cost of operation but are limited by the slow rate of sedimentation under gravity, which can take many years for very small well-stabilized particles. Filtration and screening processes can rapidly remove solids from liquid streams but are limited by the surface area and efficiency of the filter or screen. High pressure differential can develop during filtration as a result of filter clogging or membrane fouling. Maintenance in filtration processes can be especially high and replacement of filters or membranes can be very costly. High-performance centrifuges and cyclones separate even very fine solids but require high upfront capital cost and are relatively expensive to operate.

A composite particle can be made to have both organic material and inorganic material. For example, the chemical properties of an organic molecule can be combined with the magnetic susceptibility of an inorganic solid. Depending on the desired function of the composite particle, the structure can either suppress the effect of a constituent material or enhance its effect. For example, only the material on the outermost surface can affect colloidal properties. On the other hand, magnetic susceptibility of a composite particle is less affected by the location of the magnetically responsive material. In order to treat bitumen emulsions, the composite particle should have intermediate wettability to allow composite particles to be dispersed in the non-aqueous continuous phase and promote attachment on the oil-water interface. A robust method of preparing composite particles is presented in **Chapter 5**. This simple method provides the flexibility required to produce composite materials capable of handling a variety of dispersed mixtures.

Magnetic separation can be applied to a variety of different materials including scrap iron as well as magnetically-labelled biological material. Under a magnetic field, magnetically-responsive materials can be selectively attracted or repelled. Magnetic separation of non-magnetic material such as cells requires an adjunct magnetic particle that is capable of specifically attaching to the target material. It is possible to combine the properties of an organic polymer with the strong magnetic susceptibility of iron oxide (Fe_3O_4). Fe_3O_4 nanoparticles are superparamagnetic and lose

their magnetization once removed from an applied magnetic field. Manipulation of functionalized solids under a magnetic field can both enhance its function as well as facilitate separation. Magnetic Fe₃O₄ particles are often coated with silica in order to prevent further oxidation. Silica also provides a suitable shell onto which further functionalization with organic moieties is possible. In previous investigations,^{1,2} a chemical demulsifier, ethylcellulose (EC), was successfully grafted onto magnetically responsive silica-coated Fe₃O₄ nanoparticles by first functionalizing silica-coated Fe₃O₄ particles with 3-aminopropyltriethoxysilane (3-APTES) [H₂N(CH₂)₃Si(OC₂H₅)₃] and subsequently reacting with EC (previously activated using 2-bromopropionyl bromide [CH₃CHBrCOBr] in dry tetrahydrofuran). Once the appropriate surface is applied, interfacially active particles are made. EC-grafted magnetic particles performed well in demulsification of water-in-oil emulsion droplets. Following magnetic separation, EC-grafted magnetic particles could be treated and recycled.

2.2.2 Multiphase Waste

A major objective in froth treatment is the removal of emulsified water droplets. Water and dissolved salts are undesirable as they lower the value of the product and contribute to operational problems such as corrosion and deactivation of refinery catalysts. Unfortunately, water is integral to the extraction process and emulsification is inevitable during transport through pipelines and intensive mixing processes. Water-in-oil emulsions are typically formed at various stages of oil production and can lead to many downstream issues (*e.g.*, accelerated corrosion, fouling, plugging and catalyst poisoning).^{1,2} Consequently, the feed entering a bitumen upgrader should ideally contain less than 0.5 wt% water and solids. Stabilized bitumen emulsion droplets behave differently when diluted with a solvent mixture containing varying ratios of aromatics (*e.g.*, toluene) and saturates (*e.g.*, heptane).³ Bitumen asphaltenes exhibit poor solubility and precipitate when diluted with a sufficient amount of non-solvent. Precipitated asphaltenes flocculate along with emulsified water droplets, leaving bitumen with relatively low water content and nearly free of solids. However, a large amount of non-solvent diluent is required to induce asphaltene precipitation.

Alternatively, following dilution with a good solvent, emulsified droplets are separated using inclined plate settlers, hydrocyclones and centrifuges. The majority of water is removed using a

combination of heating, dilution with low density solvent, mechanical separation equipment and chemical process aids. However, due to stability of emulsified droplets and the relatively small difference in density between the continuous and dispersed phases, phase separation is incomplete. Up to 5 wt% of fine water droplets ($< 5 \mu\text{m}$) remain emulsified, as shown in **Figure 2-25**, and are disproportionately difficult to remove, due to the presence of indigenous surfactants and other stabilizing material. Chemical demulsifiers are often required in addition to oil-water separation equipment (*i.e.*, sedimentation ponds, cyclones and centrifuges) to achieve an acceptable level of separation. Chemical demulsifiers must be capable of migrating to the oil-water interface in order to destabilize the interfacial film and/or modify the wettability of stabilizing solids.⁴⁻¹⁰

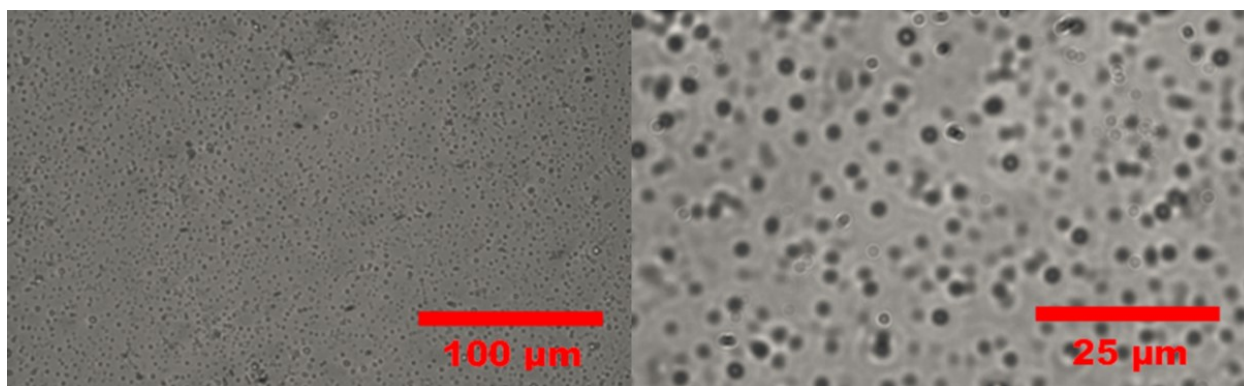


Figure 2-25. Magnified images of emulsified water droplets in bitumen diluted with heavy naphtha. Emulsified droplets are very small due to the presence of indigenous surfactants.

Chemical demulsifiers include various classes of polymers. One of the most studied demulsifier compounds are block copolymer of polyethylene oxide (PEO) and polypropylene oxide (PPO).^{4,11-14} The HLB or RSN of this type of polymer is adjusted by increasing polymer molecular weight, by changing the PEO:PPO ratio and by using different branch structure. The properties of many resins can be similarly adjusted by grafting polymer chains consisting of PEO and PPO. Many chemical demulsifiers only function within a narrow concentration range. Simply increasing the demulsifier concentration does not necessarily result in faster or more complete phase separation. To the contrary, chemical demulsifiers often increase emulsion stability at high dosage, in a phenomenon known as overdosing. A major difficulty encountered in chemical

treatment of emulsions is the inability to predict changes to demulsification efficacy resulting from changes to the feed, environmental conditions, process chemistry or unplanned maintenance. The need for better separation methods is always present when well-stabilized emulsions are encountered. Smart composite materials constructed with responsive materials should provide enhanced separation of emulsified water.

Petroleum is stored at various stages of production in large storage tanks. Multiphase mixtures such as diluted-bitumen froth contain emulsified water droplets and continue to separate inside storage tanks. Eventually, denser materials settle to the bottom and form sludge. Storage tanks and other vessels containing accumulated sludge must ultimately be emptied. Similarly, a rag layer (see **Figure 2-26**) sometimes forms inside separation vessels, especially when the concentration of solids is high.¹⁵⁻¹⁷ The rag layer consists of multiple emulsions and is difficult to characterize. This complex mixture of oil, water and solids is very stable and causes numerous operational issues. Separated rag layers are treated with compounds that promote flocculation and coalescence. There is no effective method for breaking or separating rag layers as they are formed. Accumulation of the rag layer, if left unchecked, can result in overflow into adjacent process equipment. Rag layer build-up must be manually removed by an operator, leading to additional process downtime.



Figure 2-26. High viscosity persistent rag layer formed inside separator. Rag layer accumulates and must be removed by an operator eventually leading to additional process downtime.

2.3 Multiphase Separation in Surface Mining

2.3.1 Surface Wettability Response

One of the major challenges in petroleum production is the formation of undesirable emulsions, leading to an increased cost for downstream operations. This problem is exacerbated for bitumen, which contains a greater fraction of interfacially active materials known to stabilize small emulsified water droplets that are extremely difficult to separate. To accelerate separation of emulsified water droplets from bitumen, chemical demulsifiers are extensively used to modify interfacial properties, promote droplet flocculation and facilitate coalescence of the emulsified droplets. However, the use of chemical demulsifiers is rather system-specific as a result of the overdosing phenomenon. As an alternative to chemical demulsification, composite absorbent particles, prepared by dehydrating well-designed water-in-oil emulsion droplets, were proposed to promote dewatering of water-in-diluted bitumen emulsions. The composite particles were composed of nanosized magnetic particles dispersed in an absorbent matrix coated with an interfacially active material. The composite structure combines the absorptive capacity of sodium carboxymethyl cellulose (CMC) for water with the interfacial activity of ethylcellulose (EC) while retaining the magnetic responsiveness of dispersed Fe_3O_4 nanoparticles. Using composite absorbent particles, nearly complete dewatering of water-in-diluted bitumen emulsions was achieved by increasing the dosage of absorbent particles. The dewatering rate was improved using smaller particles of greater specific surface area or increasing mixing intensity to promote contact between absorbent particles and emulsified water droplets. Although the surface of composite absorbent particles was initially suitable for dispersing in non-aqueous media, the subsequent change in wettability upon absorption of water (hydration) caused hydrated absorbent particles to aggregate. This provided an opportunity for regeneration/reuse of hydrated particles by first separating particles from diluted bitumen through gravity separation or a simple filtration process.

A smart material responds to a change in process conditions, leading to pre-determined response in its behaviour. Responsive particles are useful in treating some of the various dispersed multiphase mixtures encountered throughout the bitumen extraction process. During

the extraction process, bitumen is separated from oil sands ore. However, the process also generates various dispersed mixtures including water-in-oil emulsions and complex multiphase mixtures of oil, water and solids (*e.g.*, rag layers and sludge). Timely and efficient separation of solids, oil and water from such complex mixtures is possible with the assistance of specialty particles engineered with the required combination of properties and responsive behaviour.

The properties of composite absorbent particles, prepared by dehydrating emulsion droplets, are ideally-suited for dewatering bitumen emulsions, due to their unique combination of properties. The process used to prepare composite absorbent particles produces particles with distinctive properties. The composite absorbent particles initially dispersed well in non-aqueous solvents due to its outermost surface of intermediate wettability. Upon absorbing water through its water-permeable surface, the surface becomes more hydrophilic and composite particles lose their colloidal stability. The dewatering process using composite absorbent particles is illustrated in **Figure 2-27**. The surface of composite absorbent particles is responsive to water-absorption and composite absorbent particles lose colloidal stability after absorbing emulsified water.

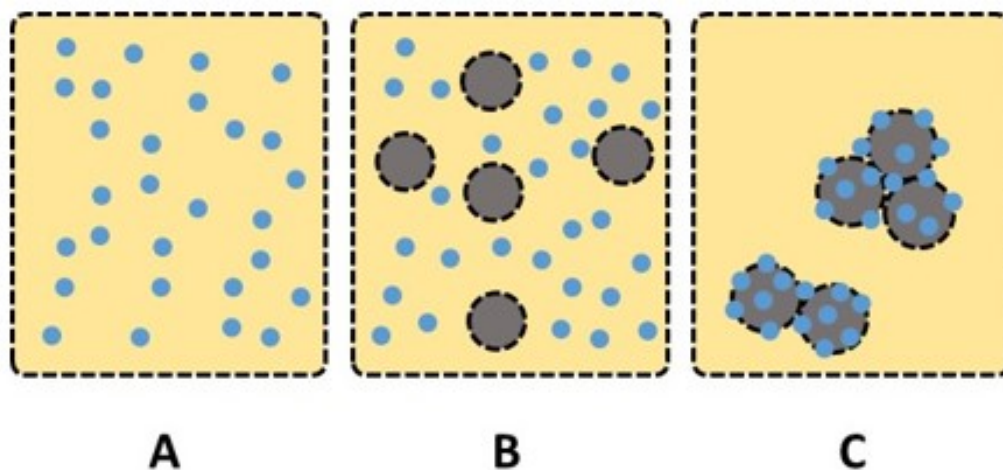


Figure 2-27. Illustration of emulsion dewatering using responsive composite absorbent particles. Water droplets emulsified in a non-aqueous continuous phase [A]. Composite absorbent particles of intermediate wettability are well-dispersed in the non-aqueous continuous phase [B], which improves contact with dispersed water droplets. A change in wettability after absorbing water causes hydrated absorbent particles to aggregate, which facilitates separation [C].

Droplet settling can also have a negative impact on phase separation if it is not accompanied by an adequate rate of droplet coalescence. A rag layer is eventually formed inside oil-water separators, as emulsion droplets accumulate at the bulk oil-water interface. The rag layer hinders further phase separation by acting as a high viscosity physical barrier. The volume of the rag layer reduces the residence time inside gravity settling tanks and must eventually be removed. Sludge often forms in storage tanks as droplets continue to settle and accumulate inside different vessels along with solids that also continue to settle. Eventually, the tank must be emptied and any accumulated sludge is removed by an operator. The rag layer and sludge are both complex mixtures of oil, water and solids.

2.3.2 Magnetically Response

Powerful electromagnets are commonly found in industrial machinery and can run using either direct current or alternating current. Magnetic separation technology is commercially available for separation of magnetic material from ores and for recycling of iron from metal scraps. Magnetic separation is an effective means of recovering dispersed magnetic particles. Smart composite materials constructed with responsive materials should provide enhanced separation of rag layers and sludge using magnetic separation technology. Once tagged with interfacially active magnetic particles, the oil-water interface within dispersed multiphase mixtures are also magnetically responsive. Interfacially active particles preferentially adsorb on the oil-water interface and do not readily detach without experiencing a sufficient change in its wettability. Emulsions stabilized by magnetic interfacially active particles remain magnetically responsive and could therefore be manipulated using a magnet. An engineered particle with the right properties and the appropriate morphology would effectively attach to the oil-water interface. Suitable composite particles may be prepared by combining the magnetic property of an inorganic material (*i.e.*, magnetic iron oxide particles) and the interfacial properties of an organic material (*i.e.*, ethylcellulose). The ability to manipulate multiphase material would be desirable as an effective method of removing any accumulation of emulsified wastes (*i.e.*, sludge and rag layers). Magnetic separation of multiphase material of different specific gravity is illustrated in **Figure 2-28** and **Figure 2-29**.

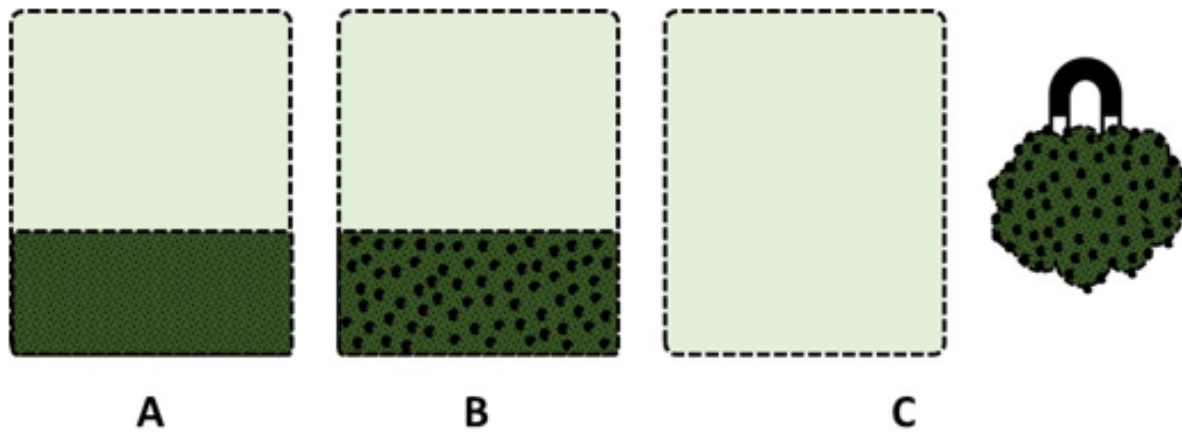


Figure 2-28. Illustration of magnetic removal of sludge tagged with interfacially active magnetic particles. High-density sludge settles at the bottom of a storage vessel [A]. Interfacially active magnetic particles adsorb on the sludge consisting of a complex mixture of oil, water and solids [B]. Sludge tagged with magnetic particles is removed under a magnetic field [C].

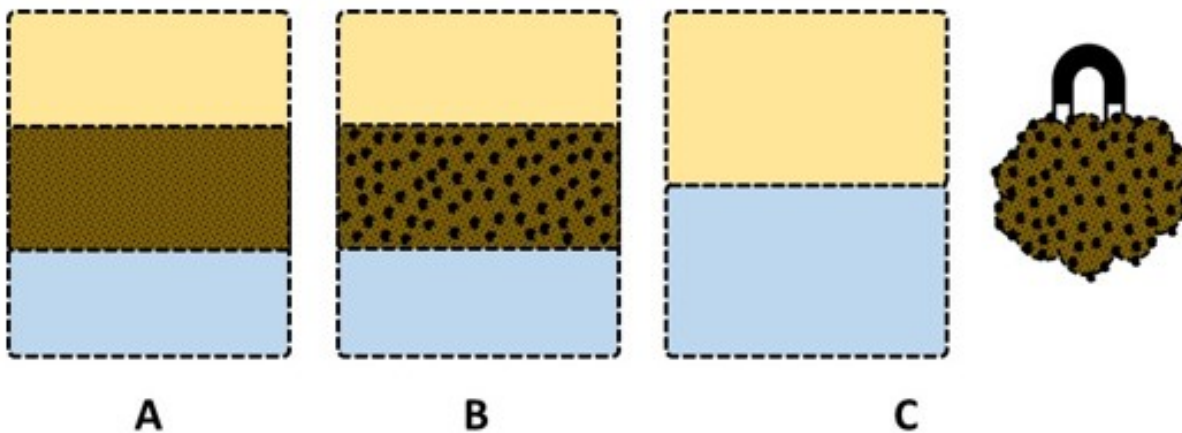


Figure 2-29. Illustration of magnetic removal of rag layer tagged with interfacially active magnetic particles. Rag layer forms in separation vessel between the lighter phase and the denser phase [A]. Interfacially active magnetic particles adsorb on the rag layer consisting of a complex mixture of oil, water and solids [B]. Rag layer tagged with magnetic particles is removed under a magnetic field [C].

2.4 References

Chapter 2.1

1. ExxonMobil, *The Outlook for Energy: A View to 2040*, Exxon Mobil Corporation, Irving, TX, **2013**.
2. W. Ramsden, *Proc. R. Chem. Soc.*, 1903, **72**, 156–164.
3. U. Pickering, *J. Chem. Soc. Trans.*, 1907, **91**, 2001–2021.
4. J. H. Schulman and J. Leja, *Trans. Faraday Soc.*, 1954, **50**, 598–605.
5. R. J. G. Lopetinsky, J. H. Masliyah and Z. Xu, in *Colloidal Particles at Liquid Interfaces*, ed. B. P. Binks, Cambridge University Press, New York, **2006**.
6. D. E. Tambe and M. M. Sharma, *Adv. Colloid Interface Sci.*, 1994, **52**, 1–63.
7. R. Aveyard, B. P. Binks and J. H. Clint, *Adv. Colloid Interface Sci.*, 2003, **100**, 503–546.
8. M. M. Kupai, F. Yang, D. Harbottle, K. Moran, J. Masliyah and Z. Xu, *Can. J. Chem. Eng.*, 2013, **91**, 1395–1401.
9. B. P. Binks and P. D. I. Fletcher, *Langmuir*, 2001, **17**, 4708–4710.
10. A. Kumar, B. J. Park, F. Tu and D. Lee, *Soft Matter*, 2013, **9**, 6604–6617.
11. S. Jiang and S. Granick, *J. Chem. Phys.*, 2007, **127**, 161102.
12. R. I. Rueda-Velásquez, H. Freund, K. Qian, W. N. Olmstead and M. R. Gray, *Energy Fuels*, 2013, **27**, 1817–1829.
13. O. C. Mullins, H. Sabbah, J. Eyssautier, A. E. Pomerantz, L. Barré, A. B. Andrews, Y. Ruiz-Morales, F. Mostowfi, R. McFarlane, L. Goual, R. Lepkowicz, T. Cooper, J. Orbulescu, R. M. Leblanc, J. Edwards and R. N. Zare, *Energy Fuels*, 2012, **26**, 3986–4003.
14. O. C. Mullins, *Energy Fuels*, 2010, **24**, 2179–2207.

15. J. P. Dickie and T. F. Yen, *Anal. Chem.*, 1967, **39**, 1847–1852.
16. O. P. Strausz, T. W. Mojelsky and E. M. Lown, *Fuel*, 1992, **71**, 1355–1363.
17. M. R. Gray, R. R. Tykwinski, J. M. Stryker and X. Tan, *Energy Fuels*, 2011, **25**, 3125–3134.
18. H. W. Yarranton, D. P. Ortiz, D. M. Barrera, E. N. Baydak, L. Barre, D. Frot, J. Eyssautier, H. Zeng, Z. Xu, G. Dechaine, M. Becerra, J. M. Shaw, A. M. McKenna, M. M. Mapolelo, C. Bohne, Z. Yang and J. Oake, *Energy Fuels*, 2013, **27**, 5083–5106
19. J. P. Rane, D. Harbottle, V. Pauchard, A. Couzis and S. Banerjee, *Langmuir*, 2012, **28**, 9986–9995.
20. S. Acevedo, M. A. Ranaudo, C. García, J. Castillo and A. Fernández, *Energy Fuels*, 2003, **17**, 257–261.
21. A. W. Marczewski and M. Szymula, *Colloids Surf. Physicochem. Eng. Asp.*, 2002, **208**, 259–266.
22. J. Castillo, M. A. Ranaudo, A. Fernández, V. Piscitelli, M. Maza and A. Navarro, *Colloids Surf. Physicochem. Eng. Asp.*, 2013, **427**, 41–46.
23. K. Xie and K. Karan, *Energy Fuels*, 2005, **19**, 1252–1260.
24. H. Labrador, Y. Fernández, J. Tovar, R. Muñoz and J. C. Pereira, *Energy Fuels*, 2007, **21**, 1226–1230.
25. A. Natarajan, J. Xie, S. Wang, J. Masliyah, H. Zeng and Z. Xu, *J. Phys. Chem. C*, 2011, **115**, 16043–16051.
26. E. M. Freer and C. J. Radke, *J. Adhes.*, 2004, **80**, 481–496.
27. P. M. Spiecker and P. K. Kilpatrick, *Langmuir*, 2004, **20**, 4022–4032.

28. A. Yeung, T. Dabros, J. Masliyah and J. Czarnecki, *Colloids Surf. Physicochem. Eng. Asp.*, 2000, **174**, 169–181.
29. A. Yeung, T. Dabros, J. Czarnecki and J. Masliyah, *Proc. R. Soc. Math. Phys. Eng. Sci.*, 1999, **455**, 3709–3723.
30. X. Wu, *Energy Fuels*, 2003, **17**, 179–190.
31. J. Czarnecki and K. Moran, *Energy Fuels*, 2005, **19**, 2074–2079.
32. S. Gao, K. Moran, Z. Xu and J. Masliyah, *J. Phys. Chem. B*, 2010, **114**, 7710–7718.
33. Y. Fan, S. Simon and J. Sjöblom, *Colloids Surf. Physicochem. Eng. Asp.*, 2010, **366**, 120–128.
34. D. Harbottle, K. Moorthy, L. Wang, Q. Chen, S. Xu, Q. Lu, J. Sjöblom and Z. Xu, *Langmuir*, 2014, **30**, 6730–6738.
35. P. Erni, *Soft Matter*, 2011, **7**, 7586–7600.
36. L. Wang, D. Sharp, J. Masliyah and Z. Xu, *Langmuir*, 2013, **29**, 3594–3603.
37. L. Wang, Z. Xu and J. H. Masliyah, *J. Phys. Chem. C*, 2013, **117**, 8799–8805.
38. P. Tchoukov, J. Czarnecki and T. Dabros, *Colloids Surf. Physicochem. Eng. Asp.*, 2010, **372**, 15–21.
39. J. Czarnecki, P. Tchoukov, T. Dabros and Z. Xu, *Can. J. Chem. Eng.*, 2013, **91**, 1365–1371.
40. J. Czarnecki, P. Tchoukov and T. Dabros, *Energy Fuels*, 2012, **26**, 5782–5786.
41. B. Ivanov and D. T. Dimitrova, in *Thin Liquid Films Fundamentals and Applications*, eds I. B. Ivanov and D. T. Dimitrova, Marcel Dekker Inc., New York, **1988**.
42. A. M. McKenna, L. J. Donald, J. E. Fitzsimmons, P. Juyal, V. Spicer, K. G. Standing, A. G. Marshall and R. P. Rodgers, *Energy Fuels*, 2013, **27**, 1246–1256.

43. R. B. Teklebrhan, L. Ge, S. Bhattacharjee, Z. Xu and J. Sjöblom, *J. Phys. Chem. B*, 2014, **118**, 1040–1051.
44. P. Tchoukov, F. Yang, Z. Xu, T. Dabros, J. Czarnecki and J. Sjöblom, *Langmuir*, 2014, **30**, 3024–3033.
45. A. Natarajan, N. Kuznicki, D. Harbottle, J. Masliyah, H. Zeng, and Z. Xu, *Langmuir*, 2014, **30**, 9370–9377.
46. D. Fu, J. R. Woods, J. Kung, D. M. Kingston, L. S. Kotlyar, B. D. Sparks, P. H. J. Mercier, T. McCracken and S. Ng, *Energy Fuels*, 2010, **24**, 2249–2256.
47. M. Osacky, M. Geramian, D. G. Ivey, Q. Liu and T. H. Etsell, *Fuel*, 2013, **113**, 148–157.
48. L. Konan, C. Peyratout, J.-P. Bonnet, A. Smith, A. Jacquet, P. Magnoux and P. Ayrault, *J. Colloid Interface Sci.*, 2007, **307**, 101–108.
49. T. J. Bandoz, J. Jagiełło, B. Andersen and J. A. Schwarz, *Clays Clay Miner.*, 1992, **40**, 306–310.
50. N. El-Thaher and P. Choi, *Ind. Eng. Chem. Res.*, 2012, **51**, 7022–7027.
51. A. M. Shaker, Z. R. Komi, S. E. M. Heggi and M. E. A. El-Sayed, *J. Phys. Chem. A*, 2012, **116**, 10889–10896.
52. R. Baigorri, M. Fuentes, G. González-Gaitano, J. M. García-Mina, G. Almendros and F. J. González-Vila, *J. Agric. Food Chem.*, 2009, **57**, 3266–3272.
53. A. W. P. Vermeer and L. K. Koopal, *Langmuir*, 1998, **14**, 4210–4216.
54. Q. Zhou, P. A. Maurice and S. E. Cabaniss, *Geochim. Cosmochim. Acta*, 2001, **65**, 803–812.
55. Z. R. Komi, A. M. Shaker, S. E. M. Heggi and M. E. A. El-Sayed, *Chemosphere*, 2014, **99**, 117–124.

56. X. Feng, A. J. Simpson and M. J. Simpson, *Org. Geochem.*, 2005, **36**, 1553–1566.
57. A. W. P. Vermeer, W. H. van Riemsdijk and L. K. Koopal, *Langmuir*, 1998, **14**, 2810–2819.
58. Czarnecki, K. Moran and X. Yang, *Can. J. Chem. Eng.*, 2007, **85**, 748–755.
59. Saadatmand, H. W. Yarranton and K. Moran, *Ind. Eng. Chem. Res.*, 2008, **47**, 8828–8839.
60. G. Gu, L. Zhang, Z. Xu and J. Masliyah, *Energy Fuels*, 2007, **21**, 3462–3468.
61. S. K. Kiran, E. J. Acosta and K. Moran, *Energy Fuels*, 2009, **23**, 3139–3149.
62. T. Jiang, G. J. Hirasaki, C. A. Miller and S. Ng, *Energy Fuels*, 2011, **25**, 545–554.
63. Y. Xu, J. Wu, T. Dabros, H. Hamza and J. Venter, *Energy Fuels*, 2005, **19**, 916–921.
64. X. Feng, P. Mussone, S. Gao, S. Wang, S.-Y. Wu, J. H. Masliyah and Z. Xu, *Langmuir*, 2010, **26**, 3050–3057.
65. X. Feng, Z. Xu and J. Masliyah, *Energy Fuels*, 2009, **23**, 451–456.
66. X. Feng, S. Wang, J. Hou, L. Wang, C. Cepuch, J. Masliyah and Z. Xu, *Ind. Eng. Chem. Res.*, 2011, **50**, 6347–6354.
67. J. T. Davies, A quantitative kinetic theory of emulsion type. 1. Physical chemistry of the emulsifying agent. In: *Gas/Liquid and Liquid/Liquid Interfaces*, Proceedings of 2nd International Congress Surface Activity, Butterworths, London, **1957**, vol. 1, 426–438.
68. S. Wang, J. Liu, L. Zhang, J. Masliyah and Z. Xu, *Langmuir*, 2010, **26**, 183–190.
69. S. Wang, N. Segin, K. Wang, J. H. Masliyah and Z. Xu, *J. Phys. Chem. C*, 2011, **115**, 10576–10587.
70. J. Hou, X. Feng, J. Masliyah and Z. Xu, *Energy Fuels*, 2012, **26**, 1740–1745.
71. J. Peng, Q. Liu, Z. Xu and J. Masliyah, *Energy Fuels*, 2012, **26**, 2705–2710.
72. J. Peng, Q. Liu, Z. Xu and J. Masliyah, *Adv. Funct. Mater.*, 2012, **22**, 1732–1740.

Chapter 2.2

1. C. Angle, in *Encyclopedic Handbook of Emulsion Technology*, ed. J. Sjöblom, CRC Press, 2001, 541–594.
2. K. A. Clark and D. S. Pasternack, *Ind. Eng. Chem.*, 1932, **24**, 1410–1416.
3. J. D. McLean and P. K. Kilpatrick, *J. Colloid Interface Sci.*, 1997, **189**, 242–253.
4. Y. Xu, J. Wu, T. Dabros, H. Hamza and J. Venter, *Energy Fuels*, 2005, **19**, 916–921.
5. Y. Xu, J. Wu, T. Dabros, H. Hamza, S. Wang, M. Bidal, J. Venter and T. Tran, *Can. J. Chem. Eng.*, 2008, **82**, 829–835.
6. R. A. Mohammed, A. I. Bailey, P. F. Luckham and S. E. Taylor, *Colloids Surf. Physicochem. Eng. Asp.*, 1993, **80**, 223–235.
7. Y. Wang, L. Zhang, T. Sun, S. Zhao and J. Yu, *J. Colloid Interface Sci.*, 2004, **270**, 163–170.
8. Y. H. Kim and D. T. Wasan, *Ind. Eng. Chem. Res.*, 1996, **35**, 1141–1149.
9. J. Wu, Y. Xu, T. Dabros and H. Hamza, *Energy Fuels*, 2003, **17**, 1554–1559.
10. T. Sun, L. Zhang, Y. Wang, S. Zhao, B. Peng, M. Li and J. Yu, *J. Colloid Interface Sci.*, 2002, **255**, 241–247.
11. A. M. Atta, A. A. Fadda, A. A.-H. Abdel-Rahman, H. S. Ismail and R. R. Fouad, *J. Dispers. Sci. Technol.*, 2012, **33**, 775–785.
12. P. Alexandridis and T. Alan Hatton, *Colloids Surf. Physicochem. Eng. Asp.*, 1995, **96**, 1–46.
13. N. N. Zaki, M. E. Abdel-Raouf and A.-A. A. Abdel-Azim, *Monatshefte Für Chem. Chem. Mon.*, 1996, **127**, 621–629.
14. I. Kailey and X. Feng, *Ind. Eng. Chem. Res.*, 2013, **52**, 785–793.
15. J. Czarnecki, K. Moran and X. Yang, *Can. J. Chem. Eng.*, 2008, **85**, 748–755.

16. M. Saadatmand, H. W. Yarranton and K. Moran, *Ind. Eng. Chem. Res.*, 2008, **47**, 8828–8839.
17. S. K. Kiran, E. J. Acosta and K. Moran, *Energy Fuels*, 2009, **23**, 3139–3149.

Chapter 3. Experimental

3.1 Materials

3.1.1 Chemical Reagents

Chemical compounds, reagents and other material used throughout the course of the investigation are listed in **Table 3-1**. Unless otherwise noted, chemical reagents were used as received without further purification. Deionized water, with conductivity of 18.2 MW/cm and total organic content below 5 ppb, was supplied from a Thermo Fisher Barnstead Nanopure® ultrapure water purification system and used, unless otherwise specified.

Table 3-1. Chemical compounds and reagents used during the course of the investigation.

Compound	Supplier	Notes
Hydrochloric acid	Fisher Scientific	ACS grade
Sulfuric acid	Fisher Scientific	ACS grade
Hydrogen peroxide solution	Fisher Scientific	30 wt% solution
Toluene	Fisher Scientific	ACS grade
Toluene	Fisher Scientific	HPLC grade
Ethanol	Commercial Alcohols	99 %
Methanol	Fisher Scientific	ACS grade
Ethyl acetate	Fisher Scientific	ACS grade
Butyl acetate	Fisher Scientific	ACS grade
Acetone	Fisher Scientific	ACS grade
Tetrahydrofuran	Fisher Scientific	Stabilized with butylated hydroxytoluene
Heavy Naphtha	Champion Technology	Petroleum reformat
Biodiesel	Alberta Innovates Technology Futures	From waste oil

Cellulose is one of the most abundant natural substance produced by plants as structural component of cells. Cellulose is a polysaccharide made of linear chains of glucose; each glucose unit has three hydroxyl groups available for substitution. Cellulose ethers are made by activating cellulose using a strongly alkaline solution and subsequently treating with appropriate chemical reagent. The structure of cellulose ethers is shown in **Figure 3-1**. Cellulose ethers are derived from renewable resources and are biodegradable.¹ Ethylcellulose (EC) is made by reacting alkali cellulose with ethyl chloride. Sodium carboxymethyl cellulose (CMC) is made by reacting alkali cellulose with sodium chloroacetic acid. Industrially produced cellulose ethers are often heterogeneously substituted along the polymer chain, due to non-ideal mixing during the chemical reaction. Non-substituted cellulose would have a degree substitution of zero while complete substitution of cellulose would result in a degree substitution of three. The solubility of both modified polymers depends on the degree of substitution. CMC with a sufficient degree of substitution is soluble in water. EC with sufficient ethoxy content is soluble in organic solvents such as toluene, methylene chloride and butyl acetate.

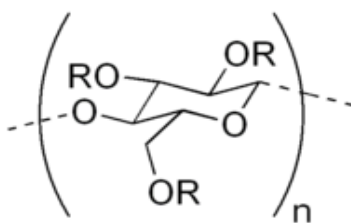


Figure 3-1. The general chemical structure of cellulose ethers. Unmodified cellulose is a polysaccharide containing repeating glucose units ($R = H$). Ethylcellulose (EC) is a cellulose derivative with a portion of hydroxyl groups substituted with ethoxy groups ($R = CH_2CH_3$). Sodium carboxymethyl cellulose (CMC) is a cellulose derivative with a portion of hydroxyl groups substituted with carboxymethyl groups ($R = CH_2COONa$).

EC is a surfactant and an effective stabilizer for water-in-oil (W/O) emulsions.² EC enhances phase separation in water-in-diluted bitumen emulsions.^{3,4} EC is an effective demulsifier capable of promoting water droplet coalescence by irreversibly displacing surface active components of bitumen at the oil-water interface as well as modifying the wettability of hydrophilic surfaces coated with bitumen.⁵⁻⁷ The absorbent properties of CMC are well-known. Water absorption of

CMC increases with degree of substitution and decreases with amount of cross-linking.⁸ When preparing absorbents, an insolubilisation treatment is typically applied, due to the water-solubility of CMC with degree substitution greater than approximately 0.7. CMC solubility can be inhibited by chemical cross-linking, thermal treatment or conversion to free acid.⁸ Cellulose derivatives used are listed in **Table 3-2**.

Table 3-2. Cellulose derivatives used during the course of the investigation.

Cellulose Ether	Supplier	Notes **
Sodium carboxymethyl cellulose	Sigma-Aldrich	MW: 250000 g/mol DS: 0.7
Sodium carboxymethyl cellulose	Sigma-Aldrich	MW: 250000 g/mol DS: 0.9
Sodium carboxymethyl cellulose	Sigma-Aldrich	MW: 250000 g/mol DS: 1.2
Ethylcellulose	Sigma-Aldrich	VISC: 10 cP EC: 48 wt%
Ethylcellulose	Sigma-Aldrich	VISC: 46 cP EC: 48 wt%
Ethylcellulose	Sigma-Aldrich	VISC: 100 cP EC: 48 wt%

** DS = degree substitution; MW = molecular weight; VISC = viscosity of 5 wt% solution in toluene/ethanol (80:20); EC = ethoxy content

3.1.2 Bitumen Samples

Oil sands ore, bitumen froth and bitumen samples were kindly provided by Syncrude Canada Ltd. and Teck Resources Ltd. Oil sands ore was stored in a freezer prior to use. Selected physical and chemical properties of different oil sands ores are provided in **Table 3-3**.

Table 3-3. Selected chemical and physical properties of different typical oil sands ore samples.

Ore grade	Water (wt%)	Bitumen (wt%)	Solids (wt%)	Fines (wt%)
GOOD	3.7	11.6	84.7	20.0
MEDIUM	6.2	10.1	83.7	30.1
POOR	2.2	9.8	88.0	39.3

3.1.3 Process Water Samples

Recycled process water was kindly provided by Syncrude Canada Ltd. The recycled water is slightly basic (pH = 8 -9) and contains a variety of different dissolved species listed in **Table 3-4**.

Table 3-4. The typical chemical composition of process water sample.

Dissolved Ion	Concentration (mg/L)
Ca ²⁺	25 – 30
Mg ²⁺	13 – 17
Na ⁺	650 – 700
K ⁺	20 – 25
Cl ⁻	340 – 725
NO ₃ ⁻	3 – 7
SO ₄ ²⁻	400 – 500

3.2 Instrumentation

Various analytical instruments were employed over the course of the investigation. A brief description of the instrument's operation is also provided. For more information, please see relevant references or the instrument's instruction manual or a general analytical reference handbook.⁹

3.2.1 Physical Properties

Microscopy techniques use diffraction, reflection, refraction and even scattering of electromagnetic radiation or particles to resolve different structures. Optical microscopes function by passing visible light through a series of different magnifying lenses. The resolution of optical microscopes is limited by the wavelength of light, which is approximately 0.5 μm. The resolution of electron microscopes is much lower depending on its mode of operation. Electron microscopes achieve greater resolution when compared to optical microscope by using electrons instead of light. Electron microscopes use electromagnetic lenses to control the path of electrons. A Hitachi scanning electron microscope (SEM) and a JOEL transmission electron microscope (TEM) were used to observe extremely small particles.

The Malvern Mastersizer 2000 and Malvern Mastersizer 3000 instruments were used to determine hydrodynamic particle size distributions with an effective detection range between approximately 100 nm to 3 mm. The Mastersizer 3000 instrument was equipped with the Hydro EV dispersion unit, which features an ultrasonic probe. The Malvern Zetasizer Nano instrument, with an effective detection range between approximately 10 nm and 100 μm , was used to determine size of smaller particles. The Malvern Zetasizer Nano instrument uses static and dynamic light scattering to determine the particle size and the electrophoretic mobility of dispersed particles. The relationship for light scattered by a particle is given by the Rayleigh equation or the Mie equation, depending on the size of the particles. Light scattered by very small particles is considered to have originated from point sources and modelled based on the Rayleigh model. Scattered light from larger particles produces constructive and destructive interference patterns based on their size and position. Moving particles disrupt light through reflection and diffraction of incident radiation. The velocity of moving particles is tracked using the diffraction of light. The electrophoretic mobility is determined by measuring particle motion under an applied voltage.

Contact angle was measured using the Krüss DSA10 or Attension T200 Theta instrument. Both instruments consist of an adjustable stage, light source and digital camera. A small droplet of approximately 3 - 4 mm in diameter was gently placed in contact with a particular surface or injected into another immiscible liquid. A digital image was taken with the camera and the contact angle was evaluated using built-in software that analyses the shape of the droplet.

A TA Instruments Q500 thermogravimetric analyzer was used for thermogravimetric analysis (TGA). A small sample was placed in a platinum pan suspended from a sensitive microbalance inside a well-insulated chamber. The temperature of the chamber was raised according to a specific program while the mass of the sample was accurately tracked. Chemical reactions (*e.g.*, decomposition or oxidation) or physical transitions (*e.g.*, Curie temperature) of substances at different temperature can be used to estimate composition of different mixtures.

3.2.2 Chemical Properties

Fourier-transform infrared spectroscopy (FTIR) was performed on a BioRad FTS 6000 instrument or an Agilent Technologies Cary 670 instrument. A sample is placed under infrared

radiation (*i.e.*, wavenumber between 14 000 – 20 cm^{-1}). The frequency of the infrared radiation matches the rotational and vibrational frequency of molecules. Absorption of infrared radiation occurs from changes to the rotational or vibrational mode of a molecular bond. The oscillating dielectric moments of the rotational or vibrational motion interact with the electric field of the radiation. The numerous rotational and vibrational modes associated with complex molecular motion are captured by the infrared adsorption spectrum, which is characteristic to its constituent functional groups and general structure. A photodetector inside the instrument monitors the radiation after it has interacted with the sample. The FTIR spectrometer uses a Michelson interferometer to form an interferogram, captured by the detector and later converted into the frequency domain using computer algorithms. The FTIR spectrometer monitors all wavelengths simultaneously and is much faster than dispersive spectrometers. Liquid samples were prepared in appropriate solvent and placed between clear windows made from potassium bromide (KBr). Solid samples were prepared in powder form by grinding a small amount (*i.e.*, approximately 0.05 g) with KBr powder and analyzed using a diffuse reflectance accessory. Incident light is directed towards the solid powder sample and scattered by the particles. The scattered light is captured using specialized optics and reflected back to the detector.

Ultraviolet-visible light spectroscopy (UV-VIS) was performed on a Shimadzu UV-3000 instrument. Certain molecules are capable of absorbing visible and/or ultraviolet radiation (*i.e.*, wavelengths of 180 – 2500 nm). UV-VIS spectroscopy can be used to identify structural features (*e.g.*, aromatic and conjugated molecules). A sample is illuminated with ultraviolet and visible light radiation from various sources. A photo-detector inside the instrument monitors the amount of transmitted radiation from the sample. Structural information can be gathered relating to aromatic and unsaturated moieties that strongly absorb UV-VIS. Qualitative analysis of compounds using UV-VIS is possible as absorption is described by the Beer-Lambert law. Adsorption of UV-VIS can be used to estimate the concentration of dilute solution.

Photoelectrons are emitted after high-energy radiation (*e.g.*, X-ray) or particles (*e.g.*, electrons) interact with an atom. The characteristics of the emitted photoelectrons create a spectrum with different energy levels associated with different specific atomic transitions.

Electron dispersion spectroscopy (EDS) is a common accessory available for SEMs. The energy of the electron is sufficient to penetrate many atomic layers. The energy of the ejected photoelectron provides information in regards to its composition. Auger electrons are ejected when an inner-shell vacancy is filled and are more indicative of the surface of a material.

3.3 Procedures

A brief description of various experimental techniques and preparative methods used through the course of the investigation is provided in the following section along with non-constraining illustrative examples. The various associated risks and hazards should be considered before attempting any of following procedures. Evaluation of potential risk for chemicals should include examination of the appropriate Material Safety Data Sheet (MSDS).

3.3.1 Diluted-Bitumen Emulsion

Model emulsions were prepared using bitumen diluted with heavy naphtha and process water. A sample of vacuum distillation feed bitumen was diluted with a known quantity of heavy naphtha. The mass ratio between bitumen and heavy naphtha was between 0.65 – 0.70. The diluted-bitumen mixture was shaken overnight using a reciprocating mechanical shaker. Process water was added to the diluted bitumen and mixed using a high-speed homogenizer to produce process water-in-diluted emulsion with approximately 5.0 wt% water content. The final water concentration was determined by Coulometric Karl-Fischer titration. The type of emulsion was confirmed using the drop test wherein a drop of the emulsion was added to water or solvent. The drop will disperse in water if the continuous phase is aqueous and, conversely, the drop will disperse in solvent if the continuous phase is organic.

A small container of bitumen was heated in a water bath at 70 °C. Bitumen (150.0 g) was charged into a glass jar sealed with a Teflon cap. Heavy naphtha (100.0 g) was added to the bitumen and the diluted bitumen mixture was placed in a mechanical shaker overnight. Process water was filtered through a glass fibre filter. A small beaker was charged with diluted-bitumen (50.0 g). Filtered process water (2.6 g) was added to the diluted-bitumen. Diluted-bitumen and water mixture were emulsified using a high-speed homogenizer at 30000 rpm for 120 s.

3.3.2 Silica-Coating

Different materials such as iron oxide can be coated with silica by dense-liquid coating. Reagents used for coating process are summarized in **Table 3-5**. Silica-coated particles are subsequently functionalized with different chemical reagents. A sample of iron oxide is first dispersed in acetone using an ultrasonic bath. Magnetic particles are recovered using a strong magnetic or centrifuge and washed again in deionized water.

Table 3-5. Materials and chemical reagents used for silica coating of magnetic particles.

Compound	Supplier	Notes
Iron oxide	Sigma-Aldrich	< 20 nm (TEM)
Iron oxide	Sigma-Aldrich	< 50 nm (TEM)
Sodium meta-silicate nonahydrate	Sigma-Aldrich	98%

A saturated solution of sodium meta-silicate and a dilute solution of sulfuric acid were prepared. The dispersion of iron oxide was transferred to a beaker equipped with baffles and well-mixed using a four-blade impeller attached to an overhead mixer and heated to approximately 90 – 95°C in a water bath. Sodium meta-silicate solution was slowly added dropwise until the pH reached approximately 9.5. Dilute sulfuric acid was then added intermittently, as needed, to maintain the pH close to 9.5. The dispersion was allowed to cool to ambient temperature after addition of sodium meta-silicate solution. Magnetic particles were separated using a strong hand magnet, rinsed liberally with deionized water and dried in an oven.

3.3.3 Silica-Functionalization

The surface of silica can be functionalized with different silane coupling reagents. Silane coupling reagents are effective in producing silica particle and surfaces with different wettability. Reagents used for coating process are summarized in **Table 3-6**. Numerous trialkoxysilane reagents are available commercially and can be used to attach different functional groups (*e.g.*, aminopropyl, phenyl, chloro and alkyl chains of different length) to the surface of silica. The reaction of trialkoxysilanes is sensitive to water and therefore rigorous control of water content is necessary to produce consistent coatings.

Table 3-6. Materials and chemical reagents used for chemical functionalization of silica.

Compound	Supplier	Notes
Silica	Sigma-Aldrich	Fumed silica
Silica gel	Sigma-Aldrich	
Silicon wafer	Silicon Materials Inc.	Prime <100>
N,N-dimethylacetamide-dimethylacetal	Sigma-Aldrich	Stabilized in 15% methanol
3-aminopropyltriethoxysilane	Sigma-Aldrich	99%
3-aminopropyltrimethoxysilane	Sigma-Aldrich	99%
3-propyltriethoxysilane	Sigma-Aldrich	99%
3-phenyltriethoxysilane	Sigma-Aldrich	99%

A suspension of silica particles is prepared in a suitable solvent containing a silane coupling agent with an amine functional group. Silica particles (1.0 g) were dispersed in water adjusted to a pH of 9.5 – 10.0 using an ultrasonic bath for 300 s. Aqueous silica suspension was placed in a mechanical shaker for 3 h. Particles were recovered by filtration or using a high-speed centrifuge. Separated particles were dried in a vacuum oven at 85°C under reduced pressure and stored in a desiccator. Silica particles were dispersed in a mixture of toluene (100 ml) and ethanol (20 ml) using an ultrasonic bath for 300 s. The silica dispersion was charged into a round bottom flask flushed with nitrogen gas. A silane coupling agent (*e.g.*, 1.0 ml 3-aminopropyltrimethoxysilane) was added dropwise into the reaction mixture. The reaction mixture was stirred for 10 h at ambient temperature. The reaction mixture was heated to 50°C for 1 h. After cooling, silica particles were recovered by filtration or by using a high-speed centrifuge. Separated silica particles were washed with ethanol. Particles were placed in an oven at 105°C for 24 h, cooled to ambient temperature and stored in a desiccator.

The silica-functionalization reaction may be alternatively carried out by chemical vapour deposition. Chemical vapour deposition was more effective in producing uniform monolayer coatings on flat surfaces. A silica surface was cleaned using freshly prepared Piranha solution (*i.e.*, a mixture of HCl, H₂SO₄, H₂O₂) and dried using N₂. A small scintillation vial with silane coupling agent was placed next to the silica wafer surface and placed in a fumed hood overnight. The

coated silica wafer was placed in an oven at 105°C for 24 h. The functionalized silica wafer was washed with ethanol and dried.

3.3.4 Emulsion Dehydration

Emulsion dehydration is a convenient method of preparing particles. An aqueous phase was prepared containing dissolved materials (*e.g.*, salts) or dispersed materials (*e.g.*, hydrophilic particles). A separate organic phase (*e.g.*, toluene) was prepared containing a suitable emulsifier (*e.g.*, ethylcellulose). An emulsion was prepared by dispersing the aqueous phase into the organic phase using a high-speed homogenizer. The emulsion was transferred to a round-bottom flask equipped with a magnetic stirrer and a Dean-Stark trap. The emulsion was heated to a gentle reflux to remove water, which was collected by the trap. After dehydration of emulsion droplets, a suspension of solid particles was produced.

An aqueous solution was prepared by dissolving CMC (2.0 g) in 100 g of deionized water. An organic solution was prepared by dissolving EC (2.0 g) in 100 g of toluene. A beaker was charged with 40 g organic EC solution and 40 g aqueous CMC solution. The mixture was preheated to about 70°C and emulsified using a high speed homogenizer for 120 s. The emulsified mixture was transferred to a round bottom flask equipped with magnetic stir bar, a Dean-Stark apparatus and a reflux condenser. The emulsion was heated to reflux until all water was collected in the trap. After cooling to ambient temperature, the suspension was transferred to centrifuge tubes and separated using a centrifuge. Separated particles were washed by dispersing in toluene in ultrasonic bath and subsequently recovered using the centrifuge. The process was repeated with ethanol. Washed particles were placed in a vacuum oven at 85°C under reduced pressure to remove remaining solvent and later stored in a desiccator.

Emulsion dehydration is a robust method of preparing particles. Alternate solvents such as ethyl acetate, butyl acetate and methylene chloride can also be used. In a similar manner, an aqueous solution was prepared by dissolving CMC (2.0 g) and dispersing titanium oxide nanoparticles (2.0 g) in 100 g of deionized water. An organic solution was prepared by dissolving EC (2.0 g) in 100 g of butyl acetate. A beaker was charged with 40 g organic solution and 40 g aqueous solution. The mixture was preheated to about 70°C and emulsified using a high speed homogenizer for 120 s. The emulsified mixture was transferred to a round bottom flask equipped

with magnetic stir bar, a Dean-Stark apparatus and a reflux condenser. The emulsion was heated to reflux until all water was collected in the Dean-Stark trap. After cooling to ambient temperature, the suspension was transferred to centrifuge tubes and separated using a centrifuge. Separated particles were washed by dispersing in toluene in ultrasonic bath and subsequently recovered using the centrifuge. The process was repeated with ethanol. Washed particles were placed in a vacuum oven at 85°C under reduced pressure to remove remaining solvent and later stored in a desiccator.

Emulsion dehydration may be used to prepare residue particles that contain dispersed solids. An aqueous solution was prepared by dissolving CMC (2.0 g) and dispersing titanium oxide nanoparticles (2.0 g) in 100 g of deionized water. An organic solution was prepared by dissolving EC (2.0 g) in 100 g of toluene. A beaker was charged with 40 g organic solution and 40 g aqueous solution. The mixture was preheated to about 70°C and emulsified using a high speed homogenizer for 120 s. The emulsified mixture was transferred to a round bottom flask equipped with magnetic stir bar, a Dean-Stark apparatus and a reflux condenser. The emulsion was heated to reflux until all water was collected in the Dean-Stark trap. After cooling to ambient temperature, the suspension was transferred to centrifuge tubes and separated using a centrifuge. Separated particles were washed by dispersing in toluene in ultrasonic bath and subsequently recovered using the centrifuge. The process was repeated with ethanol. Washed particles were placed in a vacuum oven at 85°C under reduced pressure to remove remaining solvent and later stored in a desiccator

3.4 Environmental Health and Safety

Disposal of any waste material should be in accordance to local laws and regulations. Proper disposal practices and methods for specific substances can typically be found in the Workplace Hazardous Materials Information System (MSDS) information sheets provided by the supplier. In general, waste materials should be separated whenever possible. Emulsified waste should ideally be separated into aqueous and non-aqueous phases. Dispersed solids should be removed firstly by filtration or electrolyte-induced coagulation. Halogenated compounds and solvents should also be kept separately from non-halogenated materials.

Various physical and chemical hazards are encountered in chemical processes. Such risks must be mitigated using appropriate layers of administrative and engineering controls. Proper personal protective equipment should be donned, but must be considered the last line of defence in case all administrative and engineering controls fail. Examples of controls include: i) proper planning and design of chemical experiments; ii) regular housekeeping in order to reduce the chances for an accident and minimize the effects if an accident does occur; iii) performing operations that involve toxic substances at night when only minimum staff is present and iv) restricting access to areas involving hazards such as lasers, energized electrical equipment or excessive noise. The following descriptions are not exhaustive and meant only to outline some of the specific risks encountered by the author.

Ingestion and inhalation are major entry points into the human body. Ingestion of any material in the vicinity of any chemicals should be avoided in case of contamination. Volatile substances should only be handled inside functioning fumed hoods. Small particulates can remain suspended in air and cause irritation, if inhaled. More serious problems such as silicosis can occur as a result of prolonged exposure to crystalline silica. For specific inhalation hazards please consult the MSDS information sheet of suspect material. Properly fitting and rated (NIOHS N95 or P95) respirators are effective in removing fine particulates. Direct contact with chemical substances should be avoided by using the appropriate glove ware. Compatibility charts are typically available from manufacturers for different types of materials. Breakthrough time provides a suitable guideline for selection, as no glove is indefinitely impermeable to all solvents. Specifically, latex gloves are not recommended for work with organic solvents as the latex material is very quickly degraded. Certain solvents such as dimethylsulfoxide (DMSO) can make skin more permeable to organic compounds.

Asphyxiation occurs when an insufficient supply of oxygen is available to the body. Even non-toxic and inert gases can cause asphyxiation by displacing any available oxygen. Liquefied gases are especially hazardous towards asphyxiation, as their volume greatly expands if vaporized. A change in the physical state of a substance can be caused by an increase in temperature or by a reduction in pressure. In addition, large amounts of gas are generated by certain types of chemical reactions, especially combustion processes. This risk is exacerbated in confined spaces

(e.g., elevators), where air supply is limited, access is restricted and escape is more difficult. Work should never be performed inside confined spaces alone or without proper supervision.

Inflammable substances pose a significant fire hazard. The risk of fire is further exacerbated for volatile substances, which form a flammable vapour with explosive potential. Therefore, it is imperative that precautions are followed in order to minimize any flammability hazards. This includes reducing the volume of flammable substances, proper storage and containment of flammable substances, proper handling procedures and emergency planning. Flammability is assessed using a variety of metrics. Flashpoint is the minimum temperature at which a substance's vapour will ignite. The auto-ignition point is the minimum temperature at which a substance will combust without an ignition source. WHMIS arbitrarily defines flammable liquids as having a flashpoint below 37.8°C (100°F) and combustible liquids as having a flashpoint between 37.8 – 93.3°C (100 – 200°F). The lower explosive limit and the upper explosive limit express the concentration range at which an explosive mixture is formed. Vapours are especially dangerous as they easily mix with air. Dry solid particles are also prone to explosive combustion due to their ability to mix with air.

Sulphur compounds are present in petroleum and are anaerobically degraded by microbes into hydrogen sulfide (H₂S). H₂S is a colourless gas at ambient conditions but is heavier than air and will accumulate near the ground in poorly ventilated spaces. H₂S has a pungent rotten odour and is highly flammable and toxic. Very low levels of H₂S (< 0.5 ppb) are detectable due to its strong odour. However, at higher concentration (> 100 ppm), olfactory nerves are paralyzed and H₂S can no longer be identified by smell. H₂S also causes eye irritation at low concentration (10 ppm). When inhaled, even a relatively low concentration of H₂S can cause unconsciousness in humans. At higher concentration, H₂S causes damage to the respiratory and central nervous systems. H₂S is partially soluble in both water and non-polar solvents. Changes in environmental conditions can cause H₂S to be released from a solution. Released H₂S gas can accumulate within sealed containers. Therefore, containers suspected of holding H₂S should only be opened in a well-ventilated area in a safe manner. Typical cartridge-type respirators are NOT effective against H₂S, as filter cartridges are very quickly saturated or ineffective altogether.

Chemical oxidizing and reducing agents are very reactive. Oxidizing agents and reducing agents will react violently with each other, as well as with many organic compounds. Thus, oxidizing agents and reducing agents should be stored away from each other. Strong acid and bases are also very reactive. Acids will react violently with bases and thus should be stored away from each other. Whenever possible, concentrated solutions should be carefully diluted. Diluting concentrated acids and bases can generate large amounts of heat. Certain chemical reactions generate a waste material. Hydrolysis of chemical compounds (*e.g.*, silane coupling agents) can produce reactive by-products in the form of strong acids or bases.

3.5 References

1. D. Klemm, B. Heublein, H.-P. Fink and A. Bohn, *Angew. Chem. Int. Ed.*, 2005, **44**, 3358–3393.
2. E. Melzer, J. Kreuter and R. Daniels, *Eur. J. Pharm. Biopharm.*, 2003, **56**, 23–27.
3. X. Feng, Z. Xu and J. Masliyah, *Energy Fuels*, 2009, **23**, 451–456.
4. X. Feng, S. Wang, J. Hou, L. Wang, C. Cepuch, J. Masliyah and Z. Xu, *Ind. Eng. Chem. Res.*, 2011, **50**, 6347–6354.
5. X. Feng, P. Mussone, S. Gao, S. Wang, S.-Y. Wu, J. H. Masliyah and Z. Xu, *Langmuir*, 2010, **26**, 3050–3057.
6. S. Wang, N. Segin, K. Wang, J. H. Masliyah and Z. Xu, *J. Phys. Chem. C*, 2011, **115**, 10576–10587.
7. J. Hou, X. Feng, J. Masliyah and Z. Xu, *Energy Fuels*, 2012, **26**, 1740–1745.
8. R. A. Young, in *Textile Science and Technology*, Elsevier, **2002**, vol. 13, 233–281.
9. J. A. Dean and P. Patnaik, in *Dean's analytical chemistry handbook*, McGraw-Hill, New York, **2004**.

Chapter 4. CO₂-Responsive Stabilizing Particles

Chapter 4. : *CO₂-Responsive Stabilizing Particles*. A version of this section has been published as C. Liang, Q. Liu and Z. Xu “Surfactant-Free Switchable Emulsions Using CO₂-Responsive Particles” in Volume 6, Issue 9 of *ACS Applied Materials & Interfaces* by the American Chemical Society with DOI:10.1021/am5007113.

Surfactant-free emulsions are prepared using biwetting particles which occupy the oil-water interface to effectively reduce the oil-water interfacial area. The equilibrium position of the particle at the interface is determined by its wettability. CO₂-responsive chemical functional groups are grafted onto the surface of silica particles. Particles with only CO₂-switchable functional groups are capable of stabilizing oil-in-water emulsions. Particles prepared with both CO₂-responsive and hydrophobic chemical functional groups on its surface are capable of stabilizing water-in-oil emulsions. Emulsion stability is disturbed when the wettability of the stabilizing particle is altered by introducing CO₂ gas to the biphasic mixture, leading to phase separation of emulsions prepared using the functionalized particles. The emulsion stability can be re-established by the removal of CO₂ through air sparging. The presence of CO₂ imposes positive surface charge to the responsive particles, increasing wettability and, consequently, the ability of the particles to destabilize emulsions.

4.1 Introduction

Emulsions are commonly encountered in chemical processes where both organic and aqueous phases coexist. In some cases, stable emulsions are desirable as the high specific interfacial surface area benefits mass transfer in extraction processes; also, the lower viscosity of oil-in-water emulsions facilitates transport of very viscous material. In other cases, however, stable emulsions are undesirable, as most unit operations do not tolerate multiphase mixtures. Stable emulsions must therefore be broken if generated during an intermediate process step. Unfortunately, well-stabilized emulsions may persist for months, even years. Breaking these stable emulsions by physical methods requires capital and energy intensive equipment such as

centrifuges. The use of chemical methods requires continuous addition of demulsifiers and other additives.

Surfactants stabilize emulsions by their accumulation at the oil-water interface, effectively reducing the interfacial tension. Droplet coalescence in surfactant-stabilized emulsions is retarded by either electrostatic repulsion for ionic surfactants or by steric hindrance for polymeric surfactants adsorbed/accumulated at the oil-water interface. Emulsions with controllable and switchable stability are prepared using responsive surfactants. Various types of responsive surfactants are available including compounds sensitive to pH,¹⁻⁵ temperature,^{3,6-9} electrical potential,¹⁰⁻¹² irradiation,¹³⁻¹⁷ carbon dioxide (CO₂),^{18,19} and other stimuli.²⁰⁻²⁵ CO₂ is unique and forms a chemical equilibrium with carbonic acid in aqueous solutions. Unlike most acids, dissolved CO₂ can be removed by sparging the solution with nitrogen or air which contains very little CO₂ (400 ppm). The addition or removal of CO₂ is therefore reversible without requiring very specialized equipment. CO₂ has other attractive attributes such as low cost, wide availability and is generally benign to humans and the environment.

In addition to surfactants, particles are also capable of stabilizing emulsions by irreversibly occupying the oil-water interface, effectively decreasing the oil-water interfacial area.²⁶⁻²⁸ Wettability is a critical physical property for emulsions stabilized by solid particles, as the equilibrium immersion depth of a particle is controlled by the wettability of stabilizer particles (see **Figure 4-1**).²⁹⁻³⁶ The energy required to displace a small spherical particle from the oil-water interface into the bulk liquid is given by the equation as the insert of **Figure 4-1**, which reaches a maximum when the contact angle is 90°. ³⁰ Hydrophobic particles with a contact angle greater than 90° will be mostly immersed in the oil phase and preferentially stabilize water-in-oil (W/O) emulsions. Hydrophilic particles with a contact angle lesser than 90° will be mostly immersed in the aqueous phase and preferentially stabilize oil-in-water (O/W) emulsions. Biwetting particles with a contact angle close to 90° are the most effective emulsion stabilizers. More hydrophilic biwetting particles will preferentially stabilize a water-continuous emulsion while more lipophilic biwetting particles will preferentially stabilize oil-continuous emulsions. In contrast, particles with either very hydrophilic surface (much lesser than 90°) or very hydrophobic surface (much greater than 90°) are both poor emulsion stabilizers.

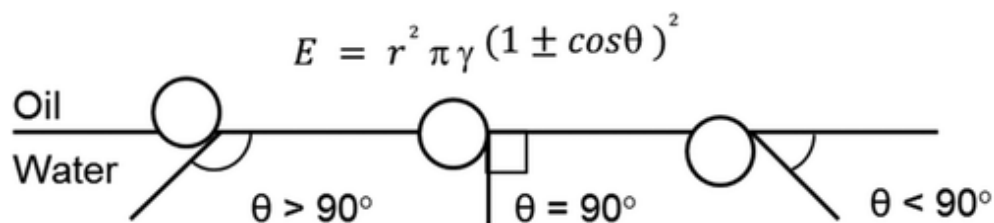


Figure 4-1. Illustration of spherical particles with different wettability at an oil-water interface.

4.2 Concept of Switchable Particle

We propose CO₂-responsive particles of variable initial wettability that are capable of controlling the stability of surfactant-free emulsions by applying an appropriate trigger to induce changes in emulsion properties. As shown in **Figure 4-2**, for CO₂-responsive particles with original contact angle around 90°, the addition of CO₂ gas or its removal from the system by sparging the system with air may be sufficient to induce substantial changes in emulsion stability.

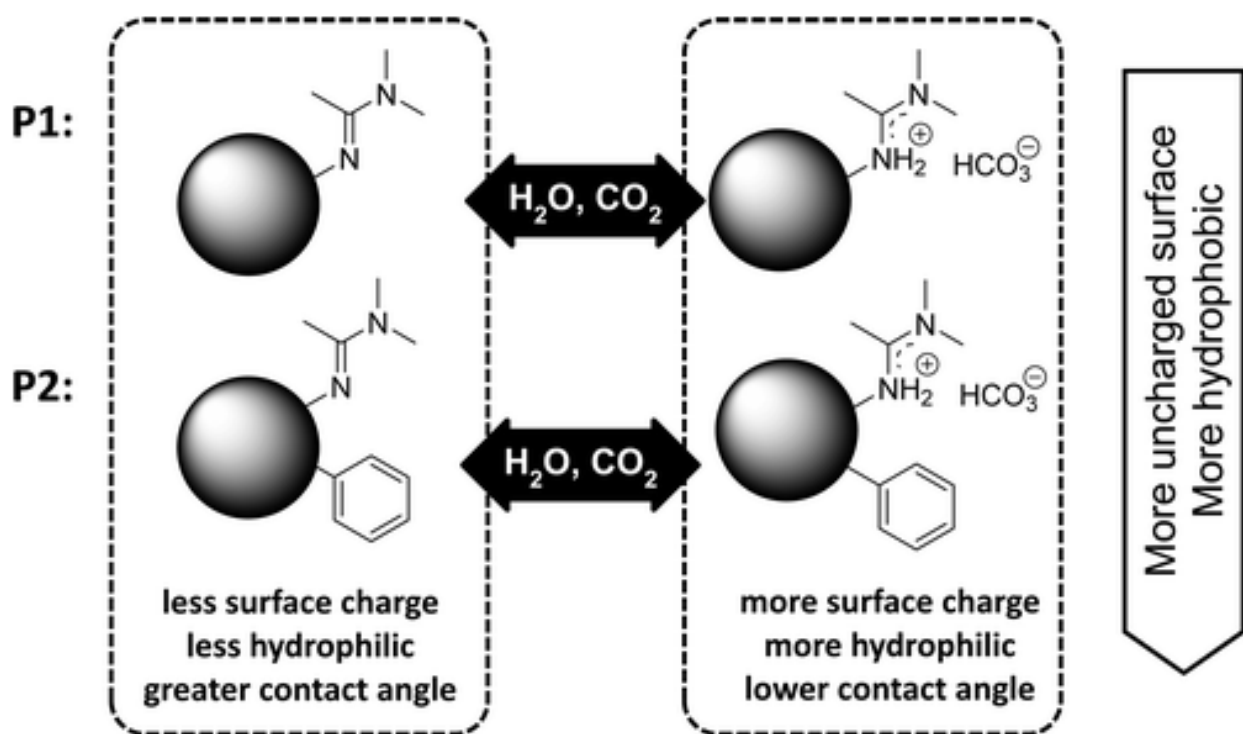


Figure 4-2. Illustration of switchable particles (**P1** and **P2**) functionalized with CO₂-responsive surface groups. Both **P1** and **P2** become more ionic in the presence of CO₂, leading to a decreased hydrophobicity and lower contact angle.

To this end, the surface properties of particles functionalized with CO₂-responsive surface groups (**P1** and **P2**) are modified in the presence of CO₂, which causes functionalized particles to become more hydrophilic by increasing the density of ionic moieties on its surface. Particles with different initial wettability, capable of stabilizing O/W and W/O emulsions, are prepared by surface functionalization with a combination of responsive hydrophilic groups and non-responsive hydrophobic surface groups. **P1** particles are less hydrophobic as compared to **P2** particles which contain additional non-responsive hydrophobic aromatic moieties on its surface. We put forward a control mechanism for emulsion stability by an *in situ* change in the surface properties of stabilizer particles. Particles with tunable wettability are capable of stabilizing emulsions in one specific state and destabilizing the emulsion in another, thus providing a viable mechanism for triggering phase separation.

4.3 Experimental

Unless otherwise indicated, all chemicals were used as received without further purification. CO₂ gas (Praxair, medical grade) and N₂ gas (Praxair, 99.998%) were used as received. Air was supplied by in-house compressors. CO₂ or air was injected continuously into the emulsion samples through an 18-gauge blunt-tip syringe at a continuous flow rate of approximately 0.5 L/min. Deionized water was used throughout and supplied from a Thermo Fisher Barnstead Nanopure ultrapure water purification system.

For particle functionalization, 3.1 g of fumed silica particles (Sigma-Aldrich) was charged into a round-bottom flask equipped with magnetic stirrer and well-dispersed in approximately 100 mL of toluene (ACS grade, Fisher Scientific). Ten milliliters of ethanol (99%, Commercial Alcohols) along with 3.0 mL (13.5 mmol) of 3-aminopropyltriethoxysilane (3-APTES, 99%, Sigma-Aldrich) and/or 3.0 mL (12.5 mmol) of triethoxy(phenyl)silane (PTES, 95%, Sigma-Aldrich) were added to the mixture. After the mixture was stirred at ambient temperature for 24 h, functionalized particles were recovered using a Hettich Rotanta 460R high-speed centrifuge and washed with excess toluene and ethanol. Recovered particles were charged into a round-bottom flask equipped with magnetic stirrer, dispersed in approximately 70 mL of methanol (ACS grade, Fisher Scientific), and treated with 2.0 mL of *N,N*-dimethylacetamide dimethylacetal (DMA-DMA) (90%,

Sigma-Aldrich). After the mixture was stirred at ambient temperature for 10 h, particles were recovered, washed with ethanol, and dried in an oven at 70 °C under reduced pressure. In the form of a white solid, 3.0 g of **P1** and 2.9 g of **P2** were recovered, crushed into a free-flowing powder, and stored inside a desiccator. Functionalized particles dispersed in potassium bromide (KBr) were characterized using a BioRad 2000 Fourier transform infrared spectroscopy instrument by diffuse reflectance infrared Fourier-transform spectroscopy (DRIFTS) method. **P1** (KBr): 797 cm⁻¹ (s), 1093 cm⁻¹ (s), 1652 cm⁻¹ (s), 2863 cm⁻¹ (w), 2922 cm⁻¹ (w), 3621 cm⁻¹ (w). **P2** (KBr): 696 cm⁻¹ (w), 795 cm⁻¹ (s), 1089 cm⁻¹ (s), 1430 cm⁻¹ (w), 1644 cm⁻¹ (s), 2858 cm⁻¹ (w), 2920 cm⁻¹ (w), 3052 cm⁻¹ (w), 3054 cm⁻¹ (w), 3613 cm⁻¹ (w). The degree of particle functionalization was determined using a TA Instruments Q500 thermogravimetric analyzer (TGA) by tracking the mass loss during heating to 900 °C.

The zeta-potential of particles was measured using a Malvern Nano-Zetasizer instrument. Particle samples (50 mg) were well-dispersed into a small amount of methanol and diluted into 30 mL of deionized water. Dispersions were treated with either compressed air or CO₂ gas from a gas cylinder for 30 s. Particle partitioning was determined gravimetrically. Equal amounts of particles were, separately, well-dispersed into water and organic solvent using an ultrasonic bath. The two immiscible phases were combined, and the mixture was homogenized using a vortex mixer for 30 s. Emulsion was broken using a low-speed centrifuge. After phase separation, the quantity of particles in the aqueous phase, toluene phase, and interfacial region was subsequently determined, after solvent was removed by evaporation under reduced pressure, from aliquots taken from each phase.

Silica wafers (NanoFab; University of Alberta) were cut into small pieces and pre-conditioned by immersing in Piranha solution comprising: one-part aqueous hydrogen peroxide and one-part concentrated sulfuric acid. (**Caution:** Piranha solution is aggressive and explosive. Never mix piranha waste with solvents. Check the safety precautions before using it.) Clean wafers were subsequently rinsed with water and dried using N₂ gas. In one instance, silica wafers were functionalized by chemical vapor deposition of 3-APTES under ambient conditions for 3 h. Silica wafers were also functionalized, in a similar manner as **P1** and **P2** particles, using solutions of 3-APTES and/or PTES in toluene. Amino-functionalized silica wafers were washed with ethanol,

dried with N₂ gas, and treated with a solution of 3 vol % DMA-DMA in methanol. Contact angle was measured by Sessile drop method using Krüss DSA10. A small drop of water was placed in contact with a surface in either air or toluene using a syringe. To investigate the effect of surface switching on surface wettability, the functionalized silica wafers were placed in a beaker with water while a stream of CO₂ or N₂ gas was bubbled directly into the beaker for 60 s.

Emulsions were prepared by first dispersing the stabilizer particles in either the aqueous or organic phase using an ultrasonic bath. To facilitate visualization, a water-soluble green dye was added to the aqueous phase. Biphasic mixtures were emulsified using a Fisher Scientific PowerGen high-speed homogenizer. The continuous phase of the emulsion was determined by placing small droplets of the emulsion into Petri dishes containing either water or organic solvent. Emulsion micrographs were taken using a Zeiss Axioskop 40 optical microscope after emulsification. Functionalized **P1** (top) or **P2** (bottom) silica particles were added to biphasic mixtures (4 mL) of toluene and water (1:1), emulsified for 20 s using high-speed homogenizer, and left under ambient conditions for 30 min.

4.4 Results and Discussion

Two types of silica-based switchable particles were prepared by grafting CO₂-responsive functionalities onto particle surfaces using appropriate reagents (see **Figure 4-3**). Particle size and morphology of silica particles were observed by transmission electron microscopy (TEM). The TEM micrograph shown in **Figure 4-4** indicates primary silica particles of irregular shapes and average diameter ranging from 30 to 40 nm. Silica particles were functionalized by hydrolysis of 3-aminopropyltriethoxysilane (3-APTES) and/or triethoxy(phenyl)silane (PTES).^{37,38} Using dilute *N,N*-dimethylacetamide dimethylacetal, primary amino functionality was converted to *N,N*-dimethylacetamide in methanol.^{39,40} Particles functionalized solely with 3-APTES were referred to as **P1**. In contrast, more hydrophobic **P2** particles, functionalized with both 3-APTES and PTES, contain additional aromatic surface functional groups. Functionalized particles were characterized using Fourier transform infrared spectroscopy. Spectra in **Figure 4-5a** obtained for both **P1** and **P2** particles show broad peaks at 3621 cm⁻¹, 1093 cm⁻¹ and 797 cm⁻¹, assigned to Si–O–Si vibrations. The functionalization of **P1** particles leads to the bands at 2863 cm⁻¹ and 2922

cm^{-1} due to aliphatic C—H stretching, and a band at 1652 cm^{-1} due to C=N stretching. As anticipated and shown in **Figure 4-5a**, **P2** particles show additional aromatic bands at 3054 cm^{-1} , 3052 cm^{-1} , 1430 cm^{-1} and 696 cm^{-1} , attributed to arene C—H vibrations.

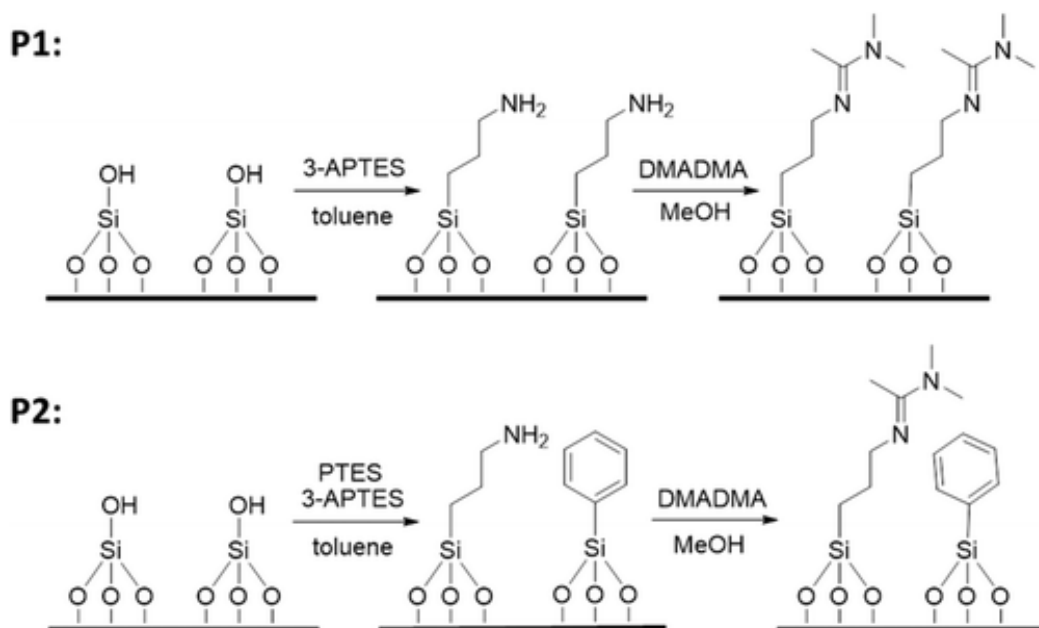


Figure 4-3. Modifying the surface of CO_2 -responsive particles. Silica particles with different wettability are prepared by functionalizing silica particles using 3-APTES (**P1**) or in combination with PTES (**P2**) in toluene, and subsequent treatment with dilute DMA-DMA in methanol.

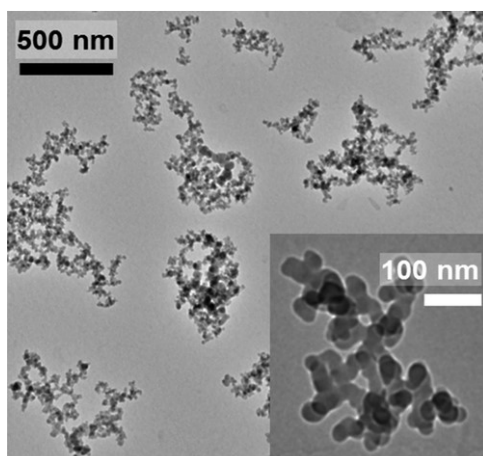


Figure 4-4. TEM micrograph of silica particles before functionalization showing irregular shapes and average primary particle diameter ranging from 20 to 30 nm. Similar TEM micrographs were obtained for functionalized **P1** and **P2** particles, which are not shown here.

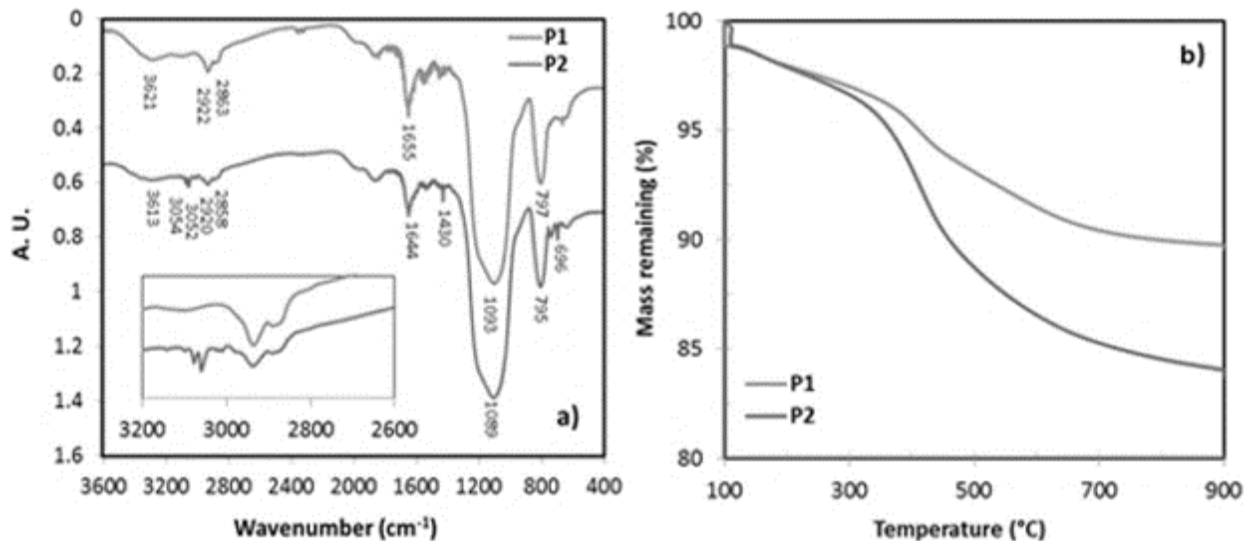


Figure 4-5. (a) Fourier-transform infrared spectra of functionalized silica particles in KBr; and (b) thermogravimetric analysis.

To quantify the degree of functionalization of **P1** and **P2** particles, thermogravimetric analysis was applied. The results in **Figure 4-5b** show a 10 wt% loss of **P1** particles after decomposition at 900 °C, indicating the presence of 10 wt% of switchable organic compounds functionalized on silica particles. In contrast, a 16 wt% weight loss was observed for **P2** particles, indicating an additional 6 wt% weight loss organic materials loaded on **P2** particles, most likely as triethoxy(phenyl) silane, which contributed to an increased contact angle of particles to around 90°. The molar ratio of triethoxy(phenyl) silane to acetamidined *N,N*-dimethylacetamide dimethylacetal on **P2** particles was estimated to be 1:1.3.

The zeta-potential of functionalized particles, which is indicative of particle surface charge, was measured; and the results are given in **Table 4-1**. As anticipated, fumed silica particles, which were negatively-charged initially, became positively-charged after functionalization with 3-APTES. The particles became more positively charged after reaction with DMA-DMA as the product amidine is more basic than analogous amines. In order to show the switchable nature of the particles, the response of **P1** and **P2** particles to CO₂ was investigated after directly bubbling CO₂ gas into particle dispersions prepared in water. Addition of CO₂ increased the surface charge of both **P1** and **P2** particles to 34 ± 2 mV; an increase of 12 ± 4 mV for **P1** particles and 25 ± 2 mV for **P2** particles. The original surface charge was restored after subsequent removal of dissolved

CO₂ by sparging dispersion with air, which does not contain a significant concentration of CO₂. The change in surface charge of functionalized silica particles in response to CO₂ exposure was found to be reversible.

For a given material with reversible surface charge, the maximum contact angle occurs at the point of zero charge and the presence of surface charge renders the material more hydrophilic.³⁴ The contact angle is also strongly dependent on the concentration of surface ions and electrolytes.^{35,36} CO₂ in aqueous solutions generates carbonic acid and produces bicarbonate ions when a suitable base, such as organic compounds with amidine moieties, is present.^{18,19,41-43} Increasing the concentration of charged groups on the particle surface by ionizing surface functional groups renders the surface more hydrated by polar water molecules, as indicated by the lower contact angle upon exposure to CO₂ gas of wafers functionalized using procedures for preparation of **P1** and **P2** particles.

Table 4-1. Zeta-potential of **P1** and **P2** silica particles functionalized with CO₂-responsive surface groups.

Step	Description	Zeta Potential (mV)	
		P1	P2
1	unmodified SiO ₂	-13 ± 1	
2	treatment with silane agent ^a	+14 ± 2	+9 ± 2
3	further treatment with DMA-DMA	+21 ± 3	+13 ± 4
4	purging with CO ₂ ^b	+33 ± 1	+34 ± 1
5	subsequent purging with air ^b	+20 ± 3	+9 ± 1
6	subsequent purging with CO ₂ ^b	+34 ± 1	+34 ± 1
7	subsequent purging with air ^b	+22 ± 3	+8 ± 1

^a **P1** particles treated solely with 3-APTES; **P2** particles treated with both 3-APTES and PTES. ^b The dispersion was prepared and subjected to a stream of CO₂ or air purging, as indicated.

The effect of CO₂ on reversible tuning of particle wettability was verified by preparing a silica wafer with CO₂-responsive surface groups by chemical vapor deposition (CVD) of 3-APTES, followed by conversion of primary amine groups into CO₂-responsive groups using DMA-DMA. Typically, CVD produces a more uniform coating. As shown by the results in **Table 4-2**, the contact angle, measured using sessile drop method in air, of the functionalized wafer was responsive to CO₂ gas. The wafer, with initial contact angle of water in air of 48 ± 3°, became more hydrophilic after subjecting to CO₂ gas in water, as indicated by a significant depression in contact angle to 38 ± 2°. Upon treating the solution with nitrogen gas (N₂) to remove dissolved CO₂, the depressed contact angle returned to its original value, restoring to the initial wettability. As shown in **Table 4-2**, reversible switching between different wettability states was possible using non-toxic gases. Our results are consistent with the results from other studies wherein primary and secondary amines on silicon wafers were transformed into carbamates species in the presence of CO₂, leading to a corresponding decrease in contact angle of approximately 10°. ⁴⁴

Table 4-2. Contact angle of a silica wafer functionalized with CO₂-responsive surface groups measured in air.

Cycle	Treatment ^c	Contact Angle (°) ^d
0	none	51 ± 3
1	CO ₂	39 ± 2
2	N ₂	49 ± 2
3	CO ₂	38 ± 1
4	N ₂	47 ± 3

^c Dissolved CO₂ gas was removed from solution by purging the water with N₂ gas. ^d Contact angle of water droplet on functionalized surface measured in air.

Silica particles, as received, did not stabilize emulsions. However, after introducing CO₂-responsive and/or hydrophobic aromatic groups, functionalized silica particles (**P1** and **P2**) are capable of stabilizing different types of emulsions, as shown in **Figure 4-6**. As designed, oil-in-water (O/W) and water-in-oil (W/O) emulsions could be stabilized by particles with different wettability. Emulsions (O/W or W/O) were prepared with 10 mg of functionalized particles (**P1**

or **P2**), 2.0 mL of water and 2.0 mL of toluene using a high-speed homogenizer. It should be noted that the mechanical force generated by the bubbling of air through the **P1** and **P2** particle-stabilized emulsions showed a negligible effect on the stability of the emulsions. To facilitate visualization of emulsions, a water-soluble green dye was added to the aqueous phase. The continuous phase of the emulsion was determined by adding a few emulsion droplets into water or toluene. In the absence of CO₂, the more hydrophilic switchable particles with contact angle around 66° (**P1**) stabilized a toluene-in-water emulsion. The more hydrophobic switchable particles with contact angle around 89° (**P2**) stabilized a water-in-toluene emulsion. The emulsions prepared using **P2** particles were of smaller droplet sizes and more stable as compared with the emulsions prepared using **P1** particles. The type and stability of an emulsion stabilized by particles can be wholly tuned by adjusting the coverage of different types of surface functional groups. This is an important advantage over switchable emulsifiers,^{18,45-47} which typically experience significant changes to inherent physicochemical properties such as solubility when additional functional groups are incorporated into its structure. Without greatly modifying the structure of the emulsifier such as increasing the molecular weight of emulsifier, only limited engineering of switchable emulsion is possible. Particles as emulsion stabilizers are much more versatile, as additional properties such as magnetic susceptibility are readily imparted to the particles independently of its surface wettability.

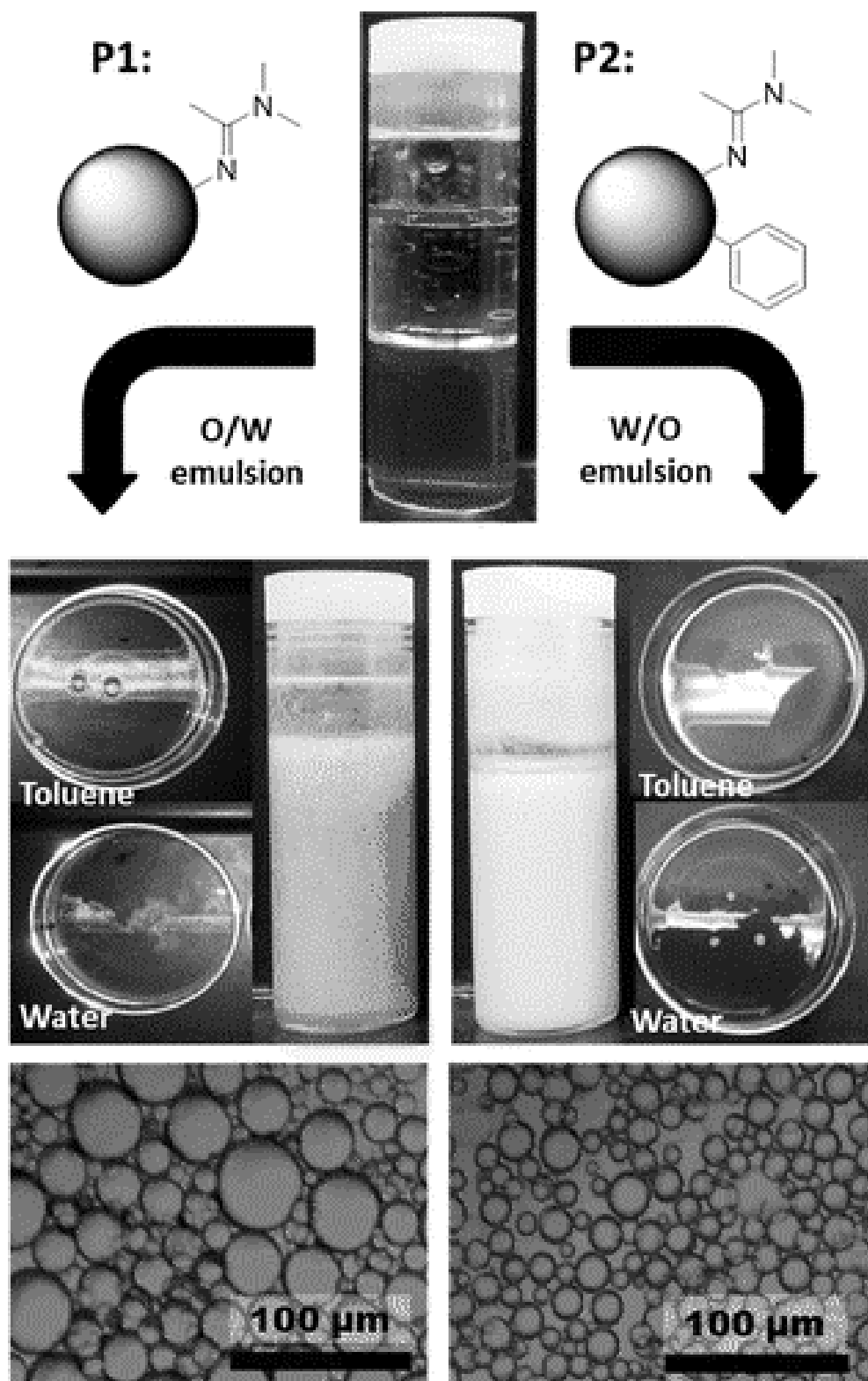


Figure 4-6. Images of different types of emulsions stabilized by more hydrophilic **P1** particles (left) and more hydrophobic **P2** particles (right).

Figure 4-1 shows the basic requirement of forming stable W/O and O/W emulsions by particles of contact angle greater and smaller than, but close to 90° , respectively. More hydrophobic **P2** particles stabilized W/O emulsions, while more hydrophilic **P1** particles stabilized O/W emulsions. W/O emulsions stabilized by **P2** particles of contact angle around 90° become destabilized when the contact angle of the particles is reduced to 79° by CO_2 purging. In contrast, for the O/W emulsions formed by **P1** particles, the stability of the emulsion decreased by decreasing the contact angle of the particles from 66° to 56° upon CO_2 purging. The stability of emulsions is greatest when stabilized by particles of contact angle close to but less than 90° .

Switchable surface groups grafted onto functionalized particles are ionized when CO_2 is present, as indicated by the corresponding increase in measured zeta-potential. Ionization of surface groups on stabilizer particles lowered wettability of particles and reduced emulsion stability but may additionally contribute to electrostatic repulsion between both dispersed particles and particle-stabilized droplets. This additional electrostatic stabilization upon addition of CO_2 was insufficient to overcome the destabilizing effect of CO_2 on emulsion stability due to reducing wettability of **P1** and **P2** particles. The electrostatic stability imparted by increasing surface ionization is more significant for particles with elevated surface charges. However, electrostatic interactions are less predominant in low polarity, non-aqueous environments such as water-in-oil emulsions.

In the absence of CO_2 , functionalized **P1** and **P2** particles stabilized O/W and W/O emulsions, respectively. The bubbling of air to stable emulsion samples stabilized with **P1** or **P2** particles showed a negligible effect on emulsion stability. However, the wettability of both **P1** and **P2** particles is depressed in the presence of CO_2 , making them more hydrophilic. The change in wettability of the stabilizer particles, a decrease in contact angle by 10° , has an effect on emulsion stability. As shown in **Figure 4-7**, the stability of emulsions prepared using **P1** and **P2** particles was responsive to CO_2 gas. Emulsions stabilized by both **P1** and **P2** particles were destabilized after purging the emulsions directly with CO_2 gas for 30 s, leading to phase separation. Upon removal of CO_2 from the mixture by purging with the air for 60 s, stable emulsions were formed again by re-emulsifying the mixture using the high-speed homogenizer without adding additional stabilizer particles. Successive stabilization–destabilization cycles were possible by the addition

or removal of dissolved CO₂ from the biphasic mixture through alternate sparging of CO₂ gas and air.

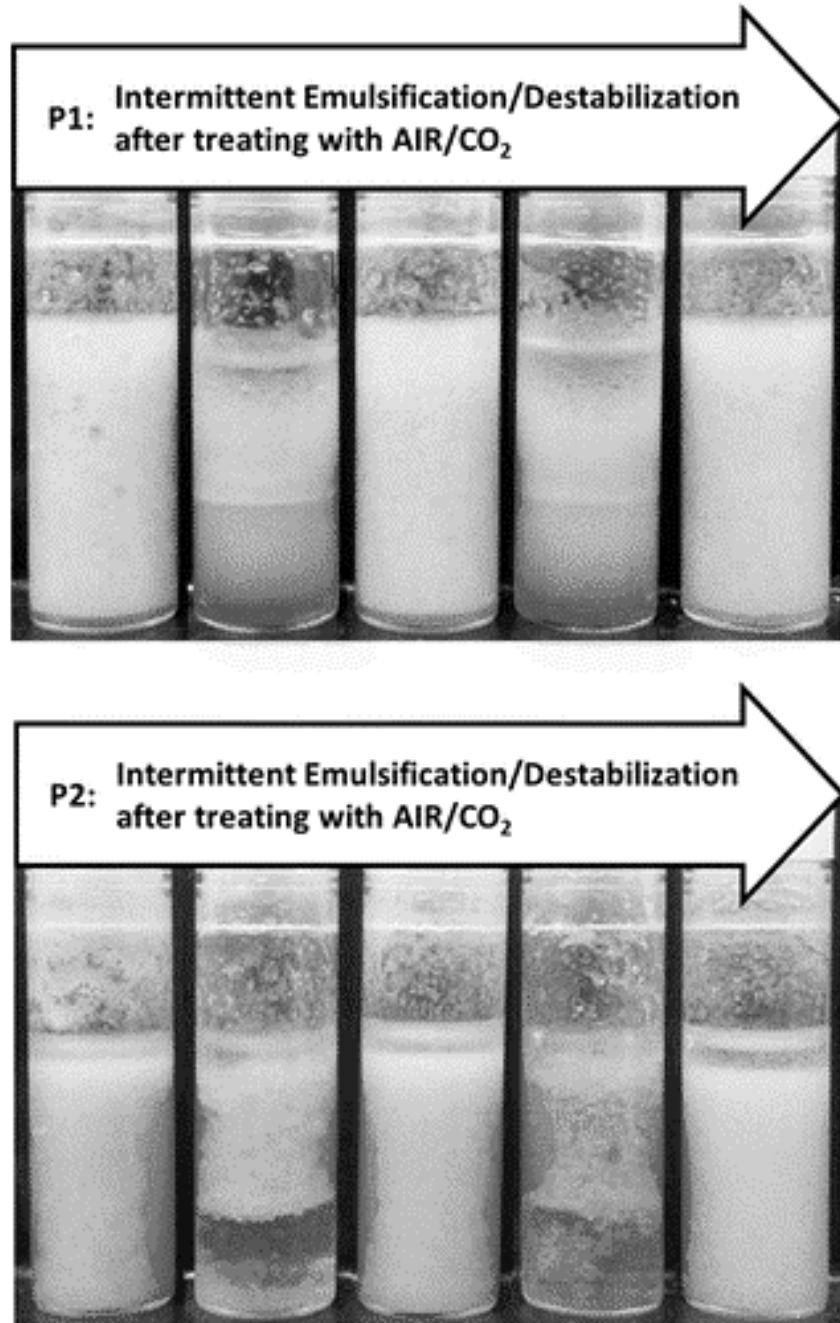


Figure 4-7. Images of emulsion samples stabilized using more hydrophilic **P1** particles (top) and more hydrophobic **P2** particles (bottom). Emulsion stability was affected by change in particle wettability as result of treating the emulsion with air and CO₂ in order to control the ionization of the surface.

4.5 Conclusions

CO₂-responsive particles were synthesized to control stability of surfactant-free emulsions. Switching particle-stabilized emulsions was demonstrated by the addition of CO₂ gas and removal of dissolved CO₂ by sparging with air. Triggered phase separation of particle-stabilized emulsions was possible due in part to the reversible change in wettability of stabilizing particles. This hypothesis was verified by monitoring the zeta-potential of stabilizing particles and the contact angle of silica wafer as model surfaces after direct addition of CO₂ gas and the removal of CO₂ by sparging with air or N₂. Our study demonstrates that both O/W and W/O surfactant-free emulsions of tunable responses can be developed by engineering particles with appropriate responsive and non-responsive surface groups.

4.6 References

1. Y. Jiang, Z. Wang, X. Yu, F. Shi, H. Xu, X. Zhang, M. Smet and W. Dehaen, *Langmuir*, 2005, **21**, 1986–1990.
2. X. Yu, Z. Wang, Y. Jiang, F. Shi and X. Zhang, *Adv. Mater.*, 2005, **17**, 1289–1293.
3. F. Xia, L. Feng, S. Wang, T. Sun, W. Song, W. Jiang and L. Jiang, *Adv. Mater.*, 2006, **18**, 432–436.
4. J. Wang, J. Hu, Y. Wen, Y. Song and L. Jiang, *Chem. Mater.*, 2006, **18**, 4984–4986.
5. L. Tan, L. Cao, M. Yang, G. Wang and D. Sun, *Polymer*, 2011, **52**, 4770–4776.
6. K. Senshu, S. Yamashita, H. Mori, M. Ito, A. Hirao and S. Nakahama, *Langmuir*, 1999, **15**, 1754–1762.
7. T. Sun, G. Wang, L. Feng, B. Liu, Y. Ma, L. Jiang and D. Zhu, *Angew. Chem. Int. Ed.*, 2004, **43**, 357–360.

8. N. J. Shirtcliffe, G. McHale, M. I. Newton, C. C. Perry and P. Roach, *Chem. Commun.*, 2005, 3135.
9. Q. Yu, X. Li, Y. Zhang, L. Yuan, T. Zhao and H. Chen, *RSC Adv.*, 2011, **1**, 262.
10. J. Lahann, *Science*, 2003, **299**, 371–374.
11. L. Xu, W. Chen, A. Mulchandani and Y. Yan, *Angew. Chem. Int. Ed.*, 2005, **44**, 6009–6012.
12. A. K. Sinha, M. Basu, M. Pradhan, S. Sarkar, Y. Negishi and T. Pal, *Langmuir*, 2011, **27**, 11629–11635.
13. R. Wang, K. Hashimoto, A. Fujishima, M. Chikuni, A. Kitamura, M. Shimohigoshi and T. Watanabe, *Nature*, 1997, 431–432.
14. K. Ichimura, *Science*, 2000, **288**, 1624–1626.
15. P. F. Driscoll, N. Purohit, N. Wanichacheva, C. R. Lambert and W. G. McGimpsey, *Langmuir*, 2007, **23**, 13181–13187.
16. H. S. Lim, D. Kwak, D. Y. Lee, S. G. Lee and K. Cho, *J. Am. Chem. Soc.*, 2007, **129**, 4128–4129.
17. J. Wang, B. Mao, J. L. Gole and C. Burda, *Nanoscale*, 2010, **2**, 2257.
18. Y. Liu, *Science*, 2006, **313**, 958–960.
19. Liang, J. R. Harjani, T. Robert, E. Rogel, D. Kuehne, C. Ovalles, V. Sampath and P. G. Jessop, *Energy Fuels*, 2012, **26**, 488–494.
20. Julthongpiput, Y.-H. Lin, J. Teng, E. R. Zubarev and V. V. Tsukruk, *Langmuir*, 2003, **19**, 7832–7836.
21. M. Motornov, S. Minko, K.-J. Eichhorn, M. Nitschke, F. Simon and M. Stamm, *Langmuir*, 2003, **19**, 8077–8085.

22. P. Uhlmann, L. Ionov, N. Houbenov, M. Nitschke, K. Grundke, M. Motornov, S. Minko and M. Stamm, *Prog. Org. Coat.*, 2006, **55**, 168–174.
23. P.-C. Lin and S. Yang, *Soft Matter*, 2009, **5**, 1011.
24. J. Yang, Z. Zhang, X. Men, X. Xu, X. Zhu, X. Zhou and Q. Xue, *J. Colloid Interface Sci.*, 2012, **366**, 191–195.
25. P. Brown, A. Bushmelev, C. P. Butts, J. Cheng, J. Eastoe, I. Grillo, R. K. Heenan and A. M. Schmidt, *Angew. Chem. Int. Ed.*, 2012, **51**, 2414–2416.
26. B. P. Binks, *Curr. Opin. Colloid Interface Sci.*, 2002, **7**, 21–41.
27. R. Aveyard, B. P. Binks and J. H. Clint, *Adv. Colloid Interface Sci.*, 2003, **100-102**, 503–546.
28. R. J. G. Lopetinsky, J. H. Masliyah and Z. Xu, in *Colloidal Particles at Liquid Interfaces*, eds. B. P. Binks, T. S. Horozov, B. P. Binks and T. S. Horozov, Cambridge University Press, Cambridge, 186–224.
29. B. P. Binks and S. O. Lumsdon, *Langmuir*, 2001, **17**, 4540–4547.
30. B. P. Binks and S. O. Lumsdon, *Langmuir*, 2000, **16**, 8622–8631.
31. B. P. Binks and S. O. Lumsdon, *Langmuir*, 2000, **16**, 3748–3756.
32. B. P. Binks and S. O. Lumsdon, *Langmuir*, 2000, **16**, 2539–2547.
33. L. G. J. Fokkink and J. Ralston, *Colloids Surf.*, 1989, **36**, 69–76.
34. S. Moya, O. Azzaroni, T. Farhan, V. L. Osborne and W. T. S. Huck, *Angew. Chem. Int. Ed.*, 2005, **44**, 4578–4581.
35. N. Stevens, C. I. Priest, R. Sedev and J. Ralston, *Langmuir*, 2003, **19**, 3272–3275.
36. S. Abbott, J. Ralston, G. Reynolds and R. Hayes, *Langmuir*, 1999, **15**, 8923–8928.

37. Y. Shiraishi, G. Nishimura, T. Hirai and I. Komasaawa, *Ind. Eng. Chem. Res.*, 2002, **41**, 5065–5070.
38. Z. Xu, Q. Liu and J. A. Finch, *Appl. Surf. Sci.*, 1997, **120**, 269–278.
39. J. Oszczapowicz and E. Raczyska, *J. Chem. Soc. Perkin Trans. 2*, **1984**, 1643.
40. J. R. Harjani, C. Liang and P. G. Jessop, *J. Org. Chem.*, 2011, **76**, 1683–1691.
41. J. Heldebrant, P. K. Koech, M. T. C. Ang, C. Liang, J. E. Rainbolt, C. R. Yonker and P. G. Jessop, *Green Chem.*, 2010, **12**, 713.
42. L. Phan, D. Chiu, D. J. Heldebrant, H. Huttenhower, E. John, X. Li, P. Pollet, R. Wang, C. A. Eckert, C. L. Liotta and P. G. Jessop, *Ind. Eng. Chem. Res.*, 2008, **47**, 539–545.
43. P. G. Jessop, L. Phan, A. Carrier, S. Robinson, C. J. Dürr and J. R. Harjani, *Green Chem.*, 2010, **12**, 809.
44. F. S. Mohammed, S. Wuttigul, C. L. Kitchens, *Ind. Eng. Chem. Res.* 2011, **50**, 8034.
45. C. I. Fowler, P. G. Jessop, M. F. Cunningham, *Macromolecules* 2010, **45**, 2955.
46. X. Su, C. I. Fowler, C. O'Neill, J. Pinaud, E. Kowal, P. G. Jessop, M. F. Cunningham, *Macromol. Symp.* 2013, **333**, 93.
47. Z. G. Cui, C. F. Cui, Y. Zhu, B. P. Binks, *Langmuir* 2012, **28**, 314.

Chapter 5. Emulsion Droplet Dehydration

Chapter 5. : *Dehydration of Emulsion Droplets. A version of this section has been published as C. Liang, Q. Liu and Z. Xu “Synthesis of Surface-Responsive Composite Particles by Dehydration of Water-in-Oil Emulsions” in Volume 7, Issue 37 of ACS Applied Materials & Interfaces by the American Chemical Society with DOI:10.1021/acsami.5b05093.*

5.1 Introduction

Particles are finite units of matter, defined not only by their composition, but also by their structure. Engineering particles with a high-order organization, from one or more materials, can impart beneficial properties that would otherwise be unattainable from a single material. The method for preparing composite particles has a critical effect on the physicochemical properties of the resulting product. Solid particles are prepared through physical processes (*e.g.*, precipitation, condensation and evaporation) or chemical reactions (*e.g.*, chemical vapor deposition, polymerization and pyrolysis). The mechanism of particle formation is complex for the majority of preparation methods and involves numerous and interconnected physicochemical processes.^{1,2} Preparation of particles having various degrees of complexity and organization is possible by either controlling conditions during particle formation or subsequently transforming previously formed particles (*e.g.*, surface coating, chemical functionalization, annealing, sintering, *etc.*). Specific methods, such as spray drying^{3,4} and emulsion polymerization,⁵⁻⁷ produce particles with characteristic properties corresponding to the nature of the particle formation processes. Depending on the application, desirable characteristics of particles may include: controlled narrow particle size distribution and low toxicity for pharmaceutical formulations; specific molecular structure and composition for engineering polymers; and extended stability and shelf life for latex coatings. A process for preparing composite materials should ideally provide the desired functions (*e.g.*, dewatering of a water-in-oil emulsion) by combining various materials with desirable attributes in a predefined configuration using a minimal number of preparation steps while simultaneously meeting as

many ancillary specifications as possible (*e.g.*, optimal particle size, suitable composition, desired surface properties and preferred structure).

Particle size is a basic but important physical property that can have a dramatic impact on the physicochemical properties of a given material. The disproportionate change in specific volume and surface area with decreasing particle size is a major issue in both macroscopic terms (*i.e.*, transport phenomena in chemical engineering) and microscopic terms (*i.e.*, nanomaterials and nanotechnology). Although the rate of an absorptive process is greater for smaller particles because of greater specific surface area, microscopic particles are more difficult to prepare and more difficult to remove from complex multiphase mixtures. Particle size reduction to micron or submicron sizes through physical means is challenging due to excessive deformation and difficulties in adequate dissipation of heat generated by friction. Unlike fluids, solids are rigid and resistant to flow. High-intensity cryogenic milling was reported to produce solid particles down to approximately 1 - 10 μm .⁸⁻¹⁰ Liquids, on the other hand, are readily deformable when sufficient shear is applied. Despite the larger amount of energy required to produce very small droplets (*i.e.*, less than approximately 1 μm) due to the increase in interfacial surface area, the energy required for emulsification remains less than a fraction of the energy required to reduce solid particles to the similar sizes. However, emulsified droplets are prone to rapid coalescence unless stabilizing chemicals are used. With adequate shear and stabilization, emulsions with droplet sizes of approximately 0.1 μm are routinely prepared.¹¹

Particle composition has an obvious influence on the properties and functions of the particles. Unfortunately, not all materials can be readily combined, and their properties are not always additive. For example, phase separation is problematic when extruding incompatible polymer blends.^{12,13} In this case, compatible additives with intermediate properties must be added to mediate the interactions between the two incompatible components to achieve a microscopically or macroscopically uniform mixture. In addition to composition, the structure of a particle is another important feature that can be controlled to yield novel and interesting materials. For example, the surface of a Janus particle consists of at least two distinct regions with contrasting wetting properties,¹⁴ which make them excellent stabilizers for Pickering emulsions when one portion is hydrophilic and the other is lipophilic.¹⁵⁻¹⁷ Alternatively, particles

made from two different materials can also be arranged in a structured configuration as such that one material is exposed to the surface while the other occupies the interior. Core-shell particles are a typical example of this type of particle and are widely used in providing diagnostic labels or targeted therapy,¹⁸⁻²² and in medical applications wherein the outer layer acts as an enteric coating (*i.e.*, to suppress taste, control release rate, retard degradation, *etc.*).²³⁻²⁷ Other possible structural configurations for a composite particle made from two different materials include dumbbell-, acorn-, snowman- and raspberry-shaped particles.^{28,29}

The outermost layer of a particle is critical in determining its stability in colloidal systems, as the compatibility with dispersing media is largely controlled by surface wettability. A hydrophobic particle with water contact angle greater than 90° prefers non-aqueous media, while a hydrophilic particle with water contact angle smaller than 90° exhibits a stronger affinity for aqueous media.³⁰ When particles are dispersed in a liquid, they either remain individually suspended or aggregate to form larger masses, depending on the properties of the particle surface and type of media. Aggregation may be suppressed by providing an electrostatic or steric energy barrier between the particles. Conversely, aggregation is promoted by neutralizing surface charge or by introducing specific chemicals (*e.g.*, high molecular weight polymers) to induce flocculation. Latex paint, for example, must possess sufficient stability to last from time of manufacture to application by the end-user. In medical and environmental applications, it is essential that the surface coating is both nontoxic and biocompatible. Although an impermeable coating is useful in reducing the toxicity of a core substance, permeability is desirable in applications where a substance must be expelled from the particle (*i.e.*, controlled drug delivery) or a foreign substance must enter into the particle (*i.e.*, absorption).

In this study, we present an innovative yet simple method, as schematically illustrated in **Figure 5-1**, to produce organic composite particles through dehydration of emulsion droplets. The process takes advantage of the liquid phase, wherein droplets are readily emulsified in the presence of an interfacially active polymer. The interfacially active polymer acts both as an emulsifier for liquid droplets, before removal of the dispersed phase, and as a stabilizer for the residual solid particles to be highly dispersed in organic media, after removal of the dispersed aqueous phase. Material, initially dissolved or dispersed inside the droplets, solidifies after the

dehydration of emulsion droplets and forms the interior of composite particles. To realize this simple method, the selection of continuous phase is paramount. For the desired synthesis, we selected ethylcellulose (EC)-containing toluene as the organic phase to form carboxymethyl cellulose (CMC)-containing water-in-oil emulsions. Toluene forms an azeotrope with water to feature a boiling point of 84 °C. The toluene-water vapour azeotrope contains 80 wt% toluene which separates into two phases after condensation and thus allows for dehydration of the emulsified water droplets by distillation using a simple Dean-Stark trap.³¹ During the distillation process, emulsified water must diffuse into the continuous phase, as only water in the continuous phase is vaporized along with the solvent as an azeotropic mixture. Upon condensation of the vapor phase, the water-rich phase is removed in the Dean-Stark trap, while the solvent-rich phase is returned. This process leaves oil-insoluble CMC as the central feature of the resultant particles and interfacially active EC on the surface of resultant particles. The lipophilic EC on the surface of synthesized particles imparts colloidal stability to composite particles in an organic continuous phase. This well-thought preparation method is capable of incorporating a number of hydrophilic materials into the interior of the composite particles, while at the same time, coating the particles with an interfacially active material of desired functionality, all without the need for chemical derivatization reactions.

The composite particles prepared according to **Figure 5-1** could have many important applications, including the separation of emulsified water from petroleum emulsions by absorption. In downstream petroleum processing, for example, the presence of water can lead to accelerated corrosion, increased scale build-up and catalyst poisoning; all of which adversely affect process performance. Although emulsions are known to lack thermodynamic stability, coalescence and phase separation in well-stabilized emulsions are often extremely slow. The enhanced kinetic stability of emulsion droplets is provided by interfacial materials such as surfactants and biwetable fine particles, which present an electrostatic or steric barrier. Both electrostatic and steric barriers prevent intimate contact between droplets and reduce the rate of droplet coalescence. Separation of water from emulsions is further delayed when the difference in density between the continuous phase and the dispersed phase is minute or when the continuous phase is extremely viscous. Emulsified water may be separated using absorbent

materials, which are typically very hydrophilic. However, hydrophilic materials are generally poorly compatible with a non-aqueous continuous phases, leading to rapid aggregation of dispersed particles and poor contact with emulsified water droplets. This shortcoming can be addressed by producing a composite absorbent particle from two distinct materials of contrasting properties in a particular structural arrangement (*i.e.*, a particle with CMC in its interior coated with a permeable outer layer of EC).

The method described in this study is well suited for preparing such composite absorbent particles for removal of emulsified water, as illustrated in **Figure 5-2**. CMC and EC are both cellulosic polymers produced from renewable resources and share structural similarity. The solubility behavior of both EC and CMC is closely related to the degree of substitution in the polymer chains. EC with sufficient ethoxy content is soluble in a variety of organic solvents (*e.g.*, ethanol, ethyl acetate, chloroform and toluene) and is used as enteric coating for many pharmaceutical products.³²⁻³⁶ CMC with sufficient carboxymethyl content, on the other hand, is water-soluble and commonly used as a viscosity modifier and water absorbent.³⁷ The absorbent portion of the composite particle made of CMC is capable of absorbing water, while the permeable interfacial coating made of EC allows effective dispersion of the composite particles into organic solvents and further promotes effective attachment of the particles onto emulsified water droplets.

EC is an effective demulsifier for water-in-diluted bitumen emulsions and functions by displacing indigenous emulsion-stabilizing materials (*e.g.*, asphaltenes) from the oil-water interface of stabilized water droplets.³⁸ Coating an absorbent substance, which is generally prepared from hydrophilic material (*i.e.*, CMC), with a substance of intermediate wettability (*i.e.*, EC) should increase its performance in biphasic systems, such as diluted-bitumen emulsions wherein stabilized water droplets are dispersed in a non-aqueous continuous phase. Because of this unique combination of properties, CMC-EC composite particles were expected to perform effectively as absorbents for removing emulsified water. The purpose of this study is to synthesize and characterize interfacially active composite water-absorbent particles using the approach illustrated in **Figure 5-1**. As potential application, the synthesized particles were evaluated as dewatering agents for water-in-oil-type emulsions.

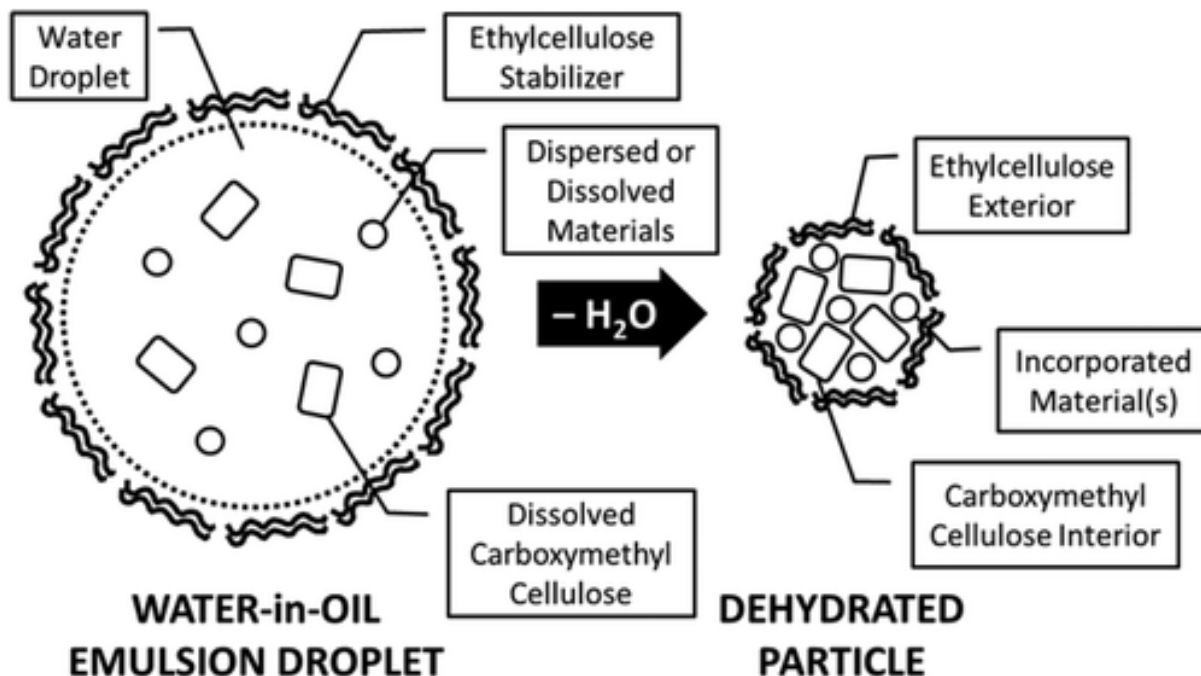


Figure 5-1. Composite particle produced after removal of water from a water-in-oil emulsion droplet comprising CMC dissolved in the aqueous phase and interfacially active EC dissolved in the organic phase. Other desirable substances such as magnetic nanoparticles can additionally be incorporated in the particle interior, if needed.

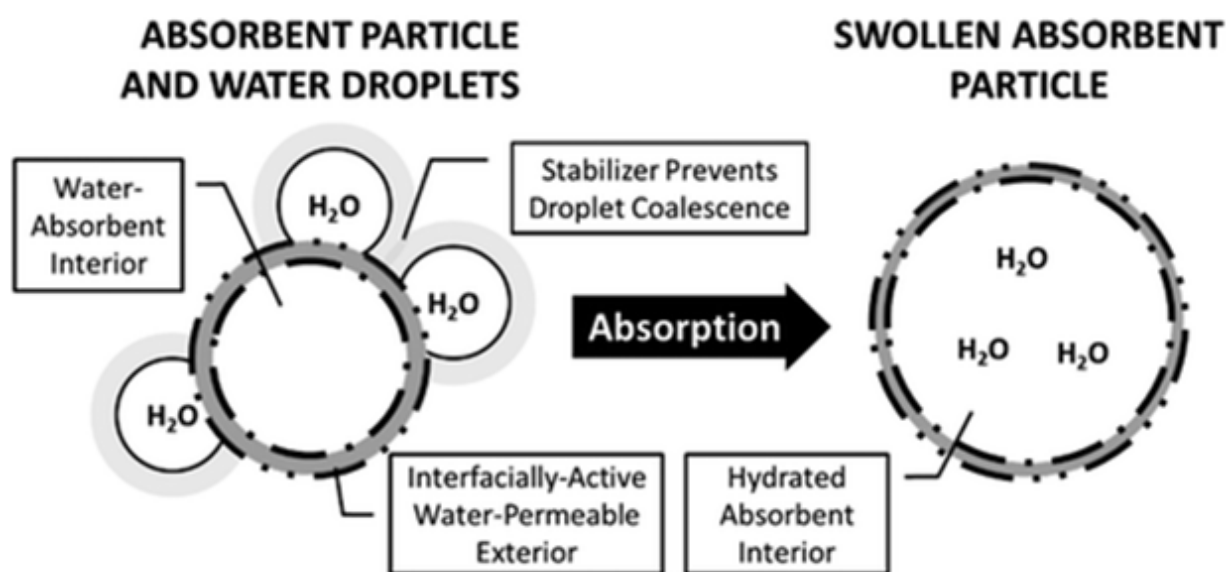


Figure 5-2. Composite absorbent particles, comprising an absorbent interior and an interfacially active exterior, ideally suited for removing emulsified water by water absorption mechanism.

5.2 Experimental

Sodium carboxymethyl cellulose (Acros Organics; average MW 250 000 g/mol; degree of substitution = 0.7), ethyl cellulose (Sigma-Aldrich; 48% ethoxyl content), iron oxide nanoparticles (Sigma-Aldrich, < 50 nm diameter), toluene (Fisher Chemical; HPLC grade), ethanol (Commercial Alcohols; 99%), ethyl acetate (Fisher Chemical; ACS grade), butyl acetate (Fisher Chemical; ACS grade), Pluronic P123 (BASF) and Span 80 (Sigma-Aldrich) were used as received without further purification. Deionized water (> 18.0 M Ω -cm) was produced from Thermo Fisher Barnstead Nanopure ultrapure water purification system.

Optical diameters were obtained using Malvern Mastersizer 2000 with a small volume dispersion accessory or using Malvern Mastersizer 3000 with an extended volume dispersion accessory. Thermal properties were investigated using a TA Instruments Q200 thermogravimetric analyzer. BioRad 2000 Fourier transform infrared spectrometry with diffuse reflectance accessory was used to acquire IR spectra. Micrographs were acquired using a Hitachi S-2700 scanning electron microscope.

An aqueous solution of CMC was prepared by slowly dissolving CMC powder in deionized water (*e.g.*, 2.0 g of CMC dissolved in 98.0 g of water). Optionally, superparamagnetic Fe₃O₄ nanoparticles were dispersed into the prepared CMC aqueous solution. The pH of the 2.0 wt% CMC aqueous solution was determined to be approximately 8.5. An organic solution of EC was prepared by dissolving EC powder in toluene (*e.g.*, 1.0 g of EC dissolved in 99.0 g of toluene). The prepared CMC aqueous solution was emulsified into the EC solution using Fisher Scientific PowerGen hand-held homogenizer for 60 s. The resulting water-in-toluene emulsion was transferred to a round-bottom flask equipped with a magnetic stirrer on a Dean-Stark apparatus. Alternatively, the round-bottom flask was equipped with a Fisher Scientific Model 500 ultrasonic dismembrator. The dehydration was performed at approximately 84 °C, which is the boiling point of the azeotrope formed by toluene and water. Under typical distillation conditions, water was removed from emulsion at a rate of 20 mL/h. For example, dehydrating a 60 g emulsion containing 20 g of emulsified water required approximately 1 h. After cooling to ambient temperature, the mixture was transferred into a centrifuge tube and the solids were separated by centrifugation at 1500 g-force. Particles were washed several times with toluene and ethanol.

Recovered particles were placed in a vacuum oven at 120 °C for 72 h. After drying, a white solid was recovered, crushed into a free-flowing white powder, and stored in a desiccator. The water absorbency of the synthesized particles was determined by placing 0.1–1.0 g of solid particles into 20–50 mL of deionized water and agitating the mixture using a vortex mixer for 30 s. After an additional 90 s, free water was separated by decantation and gravity filtration.

To confirm the biwettable nature of the synthesized organic composite absorbent particles, the critical surface tension of the particle was determined by conducting film flotation experiments using binary solutions of water and methanol.³⁹ The surface tension of binary water–methanol solutions ranges from 22.5 mN/m for pure methanol to 72.8 mN/m for pure water. To probe particle wettability, a known quantity of solid particles was carefully placed on the top of the solution containing different proportions of methanol and water. After 30 s, any particles remaining on the surface of the solution were physically separated and dried overnight in the vacuum oven at 110 °C. The mass fraction of the particles remaining on the surface was plotted as a function of the liquid surface tension, and the critical surface tension of the particle was estimated as the surface tension of the solution for which one-half of the particles remained on the surface of the solution.

CMC substrates were prepared by evaporation of an aqueous solution containing 2.0 g of CMC in a 100 mm glass dish. Similarly, additional EC substrate was prepared by evaporation of a toluene solution containing 2.0 g of EC. To prepare CMC–EC substrate, the CMC substrate prepared above was placed in a vacuum oven at 70 °C to remove remaining water. Ten milliliters of 2 wt% EC in toluene solution was then placed on the top of dried CMC substrates and left to evaporate the solvent. Excess EC was washed away with an ample amount of toluene. Variable amounts (0.20, 0.10 and 0.05 g) of EC were deposited in such a manner onto the CMC substrates. The mass of the initial EC coating layer was determined gravimetrically.

The static contact angle of water droplets, placed directly onto CMC substrates covered with variable amount of EC, was measured using Krüss DSA instrument. Small water droplets (3–4 mm) suspended from the tip of the needle point were brought carefully in contact with the substrate, upon which the water droplet detached from the needle and spread on the substrate. The contact angle of the water droplet on the substrate was measured immediately after the

three phase contact line stopped moving, roughly within 10–15 s of contact. The contact angle measured as such represents the advancing equilibrium contact angle or static contact angle.⁴⁰ Considering the penetration and absorption of water by underlying CMC film, the reproducible measurement of advancing and receding contact angle was difficult if not impossible for the CMC-EC composite films on glass substrates. For this reason, the measurement of advancing and receding contact angle was not attempted in this study.

A water-in-mineral oil emulsion was prepared by emulsifying approximately 3.6 g of deionized water using a high-speed homogenizer into 57.0 g of mineral oil (Acros Organics) with 0.4 g of SPAN 80 as emulsifier. Initial water content of mineral oil emulsion was determined accurately to be 5.9 wt%. Small aliquots of emulsion were taken using a syringe at the midway point depth. The amount of remaining water was determined by Coulometric Karl-Fischer titration.

5.3 Results and Discussion

The CMC-EC composite particles were prepared by dehydration of a water-in-toluene emulsion. Because of its surface active nature, EC adsorbs at the toluene–water droplet interface to stabilize the emulsion. As shown in **Figure 5-3**, the opacity of the emulsion, consisting of emulsified CMC-containing water droplets, diminished during dehydration as a result of decreasing the size of dispersed droplets, which eventually become smaller dehydrated CMC particles. The surface active nature and contrasting solubility of EC from CMC ensure that EC remains on the surface of the CMC solid particles after dehydration, forming the desired composite particle structure with biwetttable surface characteristics.

CMC-EC composite particles produced using the emulsion dehydration method were characterized using infrared spectroscopy. As shown in **Figure 5-4**, the DRIFTS (diffuse reflectance infrared Fourier transform spectroscopy) spectra of CMC-EC composite particles taken in KBr matrix encompass all characteristic peaks of CMC and EC, including a broad peak at 3352 cm^{-1} due to stretching vibration of hydrogen-bonded -OH groups, multiple peaks between 2914 cm^{-1} and 2874 cm^{-1} assigned to C–H stretching, strong peaks at 1616 cm^{-1} , 1419 cm^{-1} and 1325 cm^{-1} as a result of -COO^- vibration, strong peaks between 1062 cm^{-1} and 1111 cm^{-1} from ring

stretching, and a peak at 911 cm^{-1} due to CH_3 vibrations. It is interesting to note the shift of $-\text{COO}^-$ stretching vibration band from 1646 cm^{-1} and 1456 cm^{-1} for CMC (**Figure 5-4B**) to 1616 cm^{-1} and 1419 cm^{-1} for CMC-EC composite absorbent particles (**Figure 5-4D**), indicating the binding of carboxylate groups of CMC with EC molecules. To further confirm the binding of CMC with EC, the spectra were further analyzed by calculating the arithmetic spectra of CMC and EC mixture and comparing the resultant arithmetic spectra with measured spectra of CMC-EC mixture and CMC-EC composite absorbent particles.

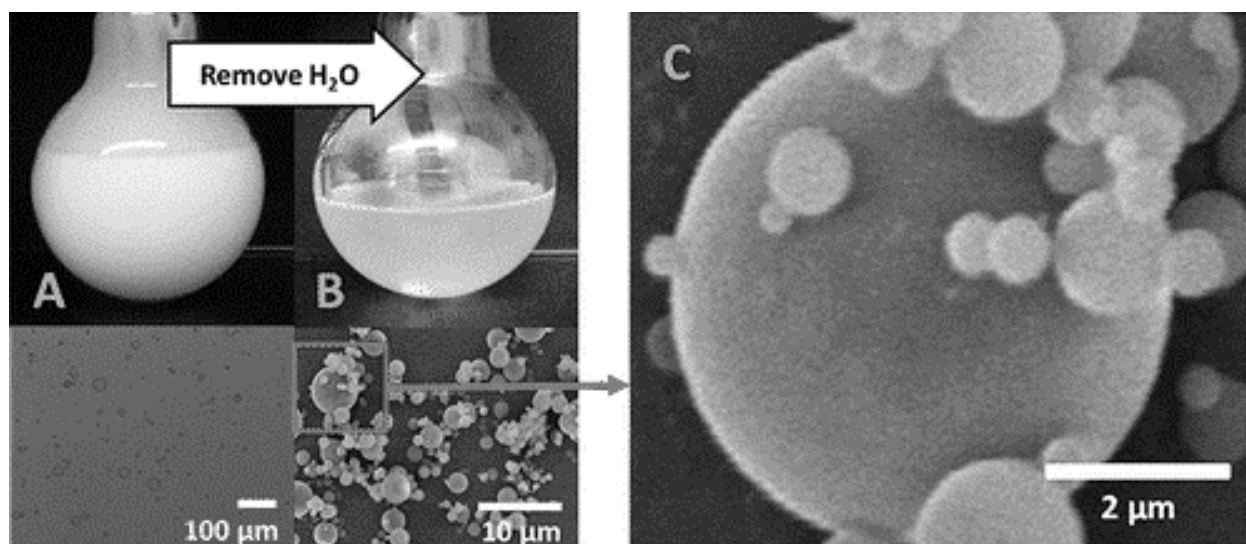


Figure 5-3. Preparation of CMC-EC composite particles by emulsion dehydration showing transition from an emulsion containing emulsified water droplets (A) to a dispersion containing dispersed CMC-EC composite particles (B). The enlarged micrograph (C) shows the spherical shape and polydispersed nature of the synthesized particles in the box from panel B.

The EC content of the synthesized CMC-EC composite particles was estimated by thermogravimetric analysis performed using a constant heating rate of $5^\circ\text{C}/\text{min}$. The results in **Figure 5-5** show the onset temperature of EC decomposition at 317°C and complete decomposition at 450°C . The onset temperature for CMC decomposition was 264°C , and approximately 45 wt% of CMC remained after being heated to 450°C . The decomposition of the CMC-EC composite particles started at 246°C with only a single decomposition event below 300°C . The decrease in the onset temperature for thermal decomposition of the CMC-EC

composite particles along with the lack of the decomposition event for EC at 317°C suggests the complexation of EC with CMC, most likely on the surface of the composite particles. The thermal decomposition characteristics of the CMC-EC composite particles was distinctively different from that of a simple physical admixture of CMC and EC, which shows characteristic decomposition peaks of CMC and EC, as anticipated. The finding further confirms the binding of EC with CMC in the synthesized composite particles.

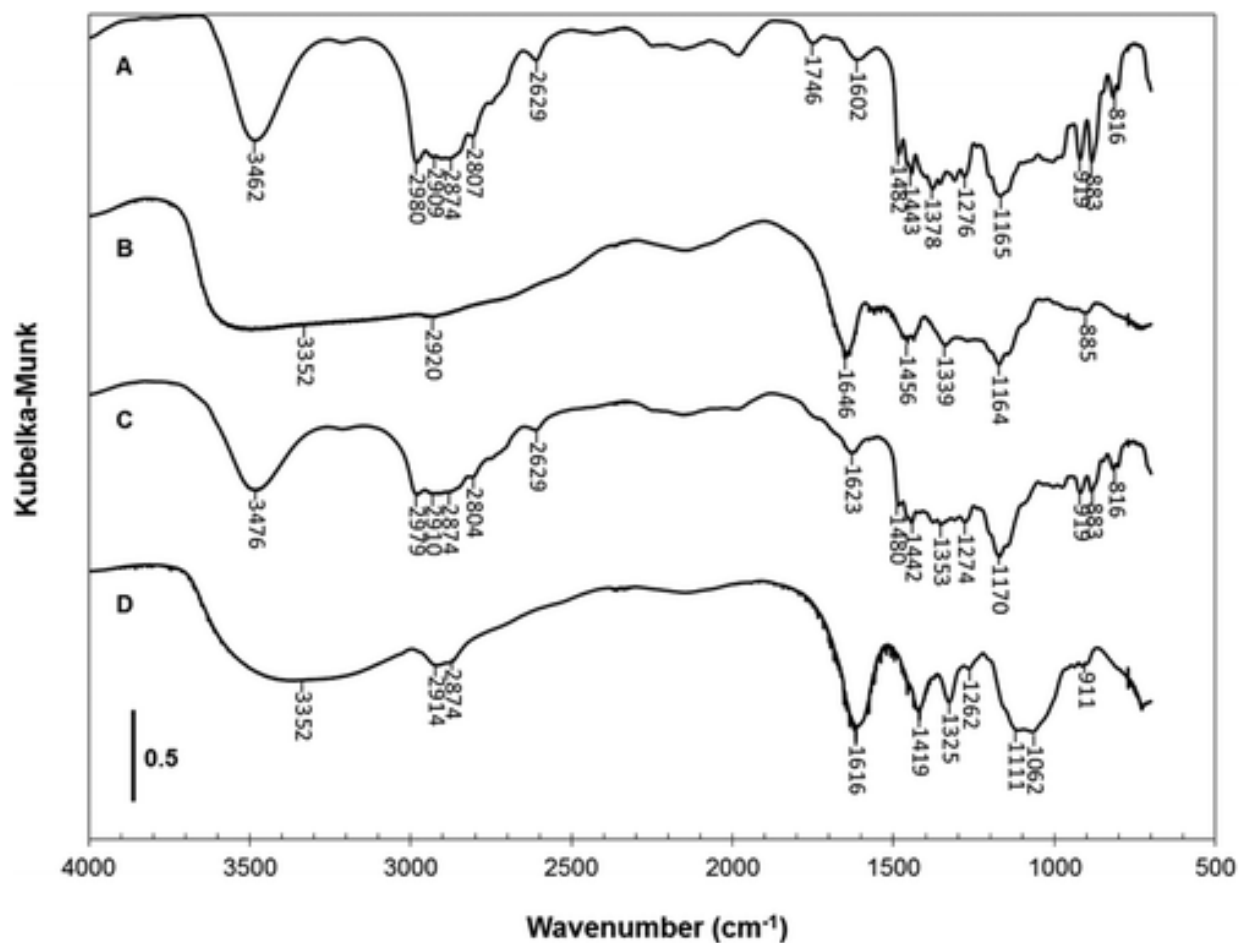


Figure 5-4. Diffuse reflectance infrared Fourier transform spectra of **A:** ethylcellulose (EC); **B:** carboxymethyl cellulose (CMC); **C:** a mixture of CMC and EC and **D:** CMC-EC composite particles. The shift of -COO^- stretching vibrational band from 1646 cm^{-1} and 1456 cm^{-1} for CMC to 1616 cm^{-1} and 1419 cm^{-1} for CMC-EC composite absorbent particles indicates the binding of -COO^- groups with EC molecules.

Water-in-toluene emulsions (1:1 ratio by mass) stabilized by more than 0.5 wt% EC (based on the mass of the organic phase) prepared using a high-speed homogenizer did not show any noticeable phase separation at ambient condition. However, sedimentation was observed with lower EC concentration or when the emulsion was heated. Primary CMC-EC composite particles prepared by the dehydration of the emulsion droplets are spherical in shape and micron in size as revealed in scanning electron microscopy (SEM) micrographs. The lower size limit of CMC-EC composite particles prepared by emulsion-dehydration using a magnetic stirrer during dehydration was approximately 2 μm . However, particles are polydispersed in size, most likely due to the polydispersity of the precursor emulsion water droplets prepared by intermittent simple high-speed mechanical agitation. Continuous coalescence of water droplets during the dehydration process may also contribute to non-uniform size distribution of the resulting particles.

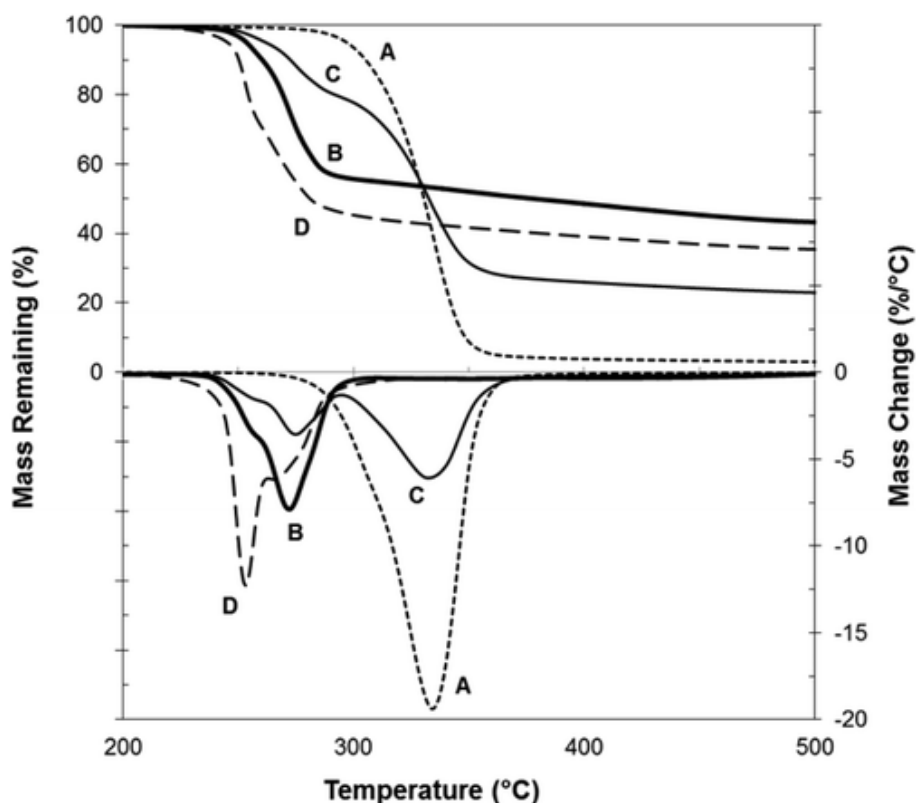


Figure 5-5. Thermogravimetric analysis (top) and derivative thermogravimetric analysis (bottom) curves for (A) ethylcellulose, (B) carboxymethyl cellulose, (C) a mixture of CMC and EC and (D) CMC-EC composite particles.

As shown in **Table 5-1**, the size of CMC-EC composite particles, prepared by dehydrating 2 wt% CMC water droplets emulsified in an equal mass of continuous organic toluene phase, decreases from 76 μm with 0.5 wt% EC in toluene to 35 μm and further to 13 μm with 1.0 and 2.0 wt% EC in toluene, respectively. Increasing the concentration of EC appears to increase the stability of CMC-containing water-in-oil emulsions and hence leads to smaller sizes of CMC-EC composite particles, as shown in **Figure 5-6**. At 2 wt% of EC in toluene as the continuous phase, increasing CMC concentration in the aqueous phase from 1 wt% to 3 wt% did not lead to any significant change in the size of resulting CMC-EC composite particles. The difficulty encountered in controlling monodispersity of particle size by varying EC and CMC concentration highlights the kinetic nature of emulsions. Despite being stabilized by EC, emulsion droplets at high temperature are continuously coalescing during the dehydration of precursor emulsions.^{11,41} Without sufficient emulsification during the dehydration process, dispersed droplets are prone to coalescence, which inevitably leads to the formation of larger particles with a wider particle size distribution.

Table 5-1. Properties of various micron size CMC-EC composite particles.

Sample	Aqueous phase	Organic phase	Particle size (μm)	EC content (wt%)
CMC-EC-I	2.0 wt% CMC	0.5 wt% EC	76	22
CMC-EC-II	2.0 wt% CMC	1.0 wt% EC	35	30
CMC-EC-III	2.0 wt% CMC	2.0 wt% EC	13	38

We further studied the possibility to control the size and size distribution of CMC-EC composite particles by adjusting the intensity of agitation and sonication during the dehydration of emulsions. In this case, emulsions were first prepared by emulsifying an aqueous CMC solution into an equal volume of EC in toluene solutions using a high-speed homogenizer followed by an ultrasonic dismembrator with a micro tip probe (500 W; 20 kHz). The emulsion was then transferred into a round-bottom flask with Dean-Stark apparatus and heated to reflux. Over the course of the dehydration process, intermittent pulses of low-intensity sonication (20–30%

amplitude) were applied to the emulsion in the reaction vessel. The energy supplied by the sonic dismembrator was sufficient to break up emulsion droplets; however, no broken CMC-EC composite particles were seen from SEM micrographs of the resultant particles. As shown in **Figure 5-7**, the resulting CMC-EC composite particles are 580 ± 80 nm in size with a polydispersity index (PDI) of 0.2, which demonstrates the critical importance of continuous agitation during dehydration of emulsions for the synthesis of CMC-EC organic composite particles.

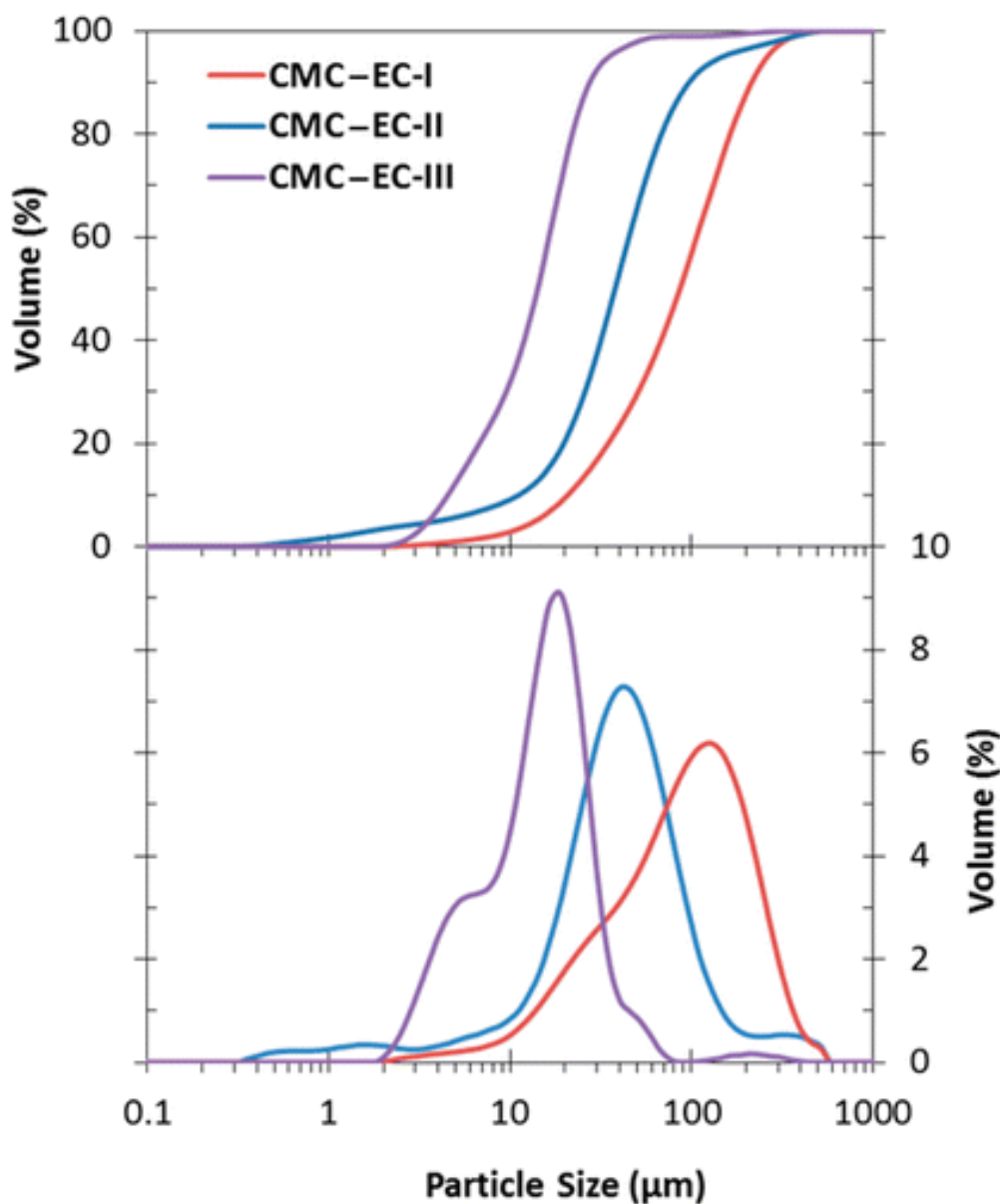


Figure 5-6. Cumulative and differential particle size distribution of CMC-EC composite particles prepared using different concentrations of EC in the continuous phase.

The critical surface tension at which small particles no longer remain attached to the air–liquid interface is indicative of particle wettability. For a high surface tension liquid, hydrophobic particles will remain at the interface, while hydrophilic particles will quickly sink into the liquid. Uncoated CMC powders were completely wetted by pure water (72.8 mN/m), while EC powders were completely wetted only by pure methanol (23 mN/m). The wettability of CMC-EC composite particles was evaluated using critical surface tension measured using binary mixtures of methanol and water, with the surface tension of the liquids being tuned by adjusting mixture composition. CMC-EC particles synthesized with different amount of EC in toluene all exhibited similar critical surface tension of approximately 26 to 28 mN/m. The lower critical surface tension of the synthesized CMC-EC organic composite particles indicates that the surface of these composite particles is more hydrophobic than that of unmodified CMC particles. As a result, the EC-coated CMC composite particles are more compatible with organic solvents and are therefore more suitably dispersed in a continuous oil phase, ensuring effective accessibility to emulsified water droplets. It should be noted however that the hydrated CMC-EC organic composite particles upon contact with emulsified water droplets in silicon oil were completely water-wet, indicating not only absorption of water by CMC-EC organic composite particles, but also the change of CMC-EC composite particles from biwetable to water wet. Once hydrated, the surface properties of the CMC–EC composite particles are more CMC dominant and become more hydrophilic.

Samples of CMC-EC composite particles were placed inside sealed vials with deionized water and agitated using a vortex mixer for 30 s. After an additional 90 s, excess free water was carefully removed by decanting and filtration. As shown in **Table 5-2**, the water absorption capacity of various EC-coated CMC composite particles was dependent on its composition. Samples with greater CMC content were able to absorb more water, as anticipated. Since EC is unable to absorb a significant amount of water, the ability of the synthesized CMC-EC organic composite particles to absorb water confirms that the EC shell is permeable to water, despite its biwetable nature.

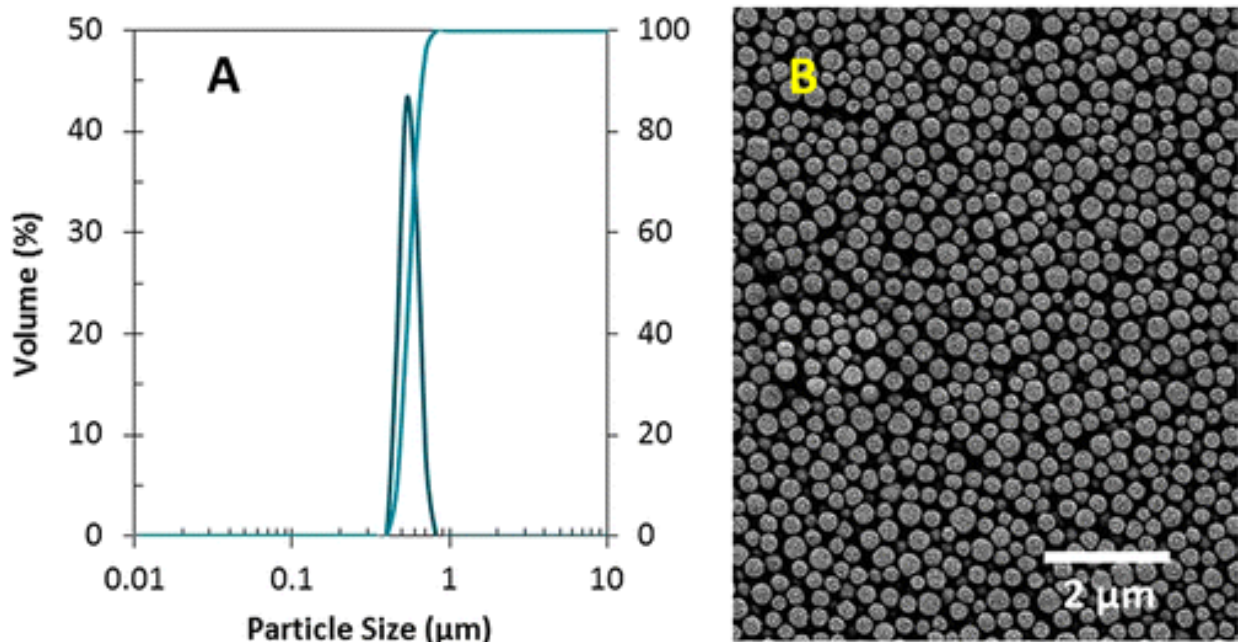


Figure 5-7. Cumulative and differential particle size distribution (A) of CMC-EC organic composite particles prepared under intermittent sonication during dehydration of CMC aqueous emulsion droplets in EC–toluene solutions and SEM micrograph of the resultant particles (B).

Table 5-2. Absorbent properties of micron size CMC-EC composite particles.

Sample	EC content (wt%)	Water absorbency (g/g) ^a	Critical surface tension (mN/m) ^b
CMC	0	7.8 ± 1.0	> 73
EC	100	< 0.01	< 23
CMC-EC-A	15	4.6 ± 1.0	26 ± 2
CMC-EC-B	24	3.8 ± 0.6	30 ± 3
CMC-EC-C	36	2.3 ± 0.4	28 ± 2

^a Amount of deionized water retained by a specific sample of dry solid particles within 2 min. ^b Surface tension of binary mixtures of methanol and water for which particles drop through the interface into the solution.

CMC substrates were prepared by evaporation of aqueous CMC solutions. EC substrate was prepared by evaporation of an organic EC solution prepared using toluene as solvent. A thin coating with variable amounts of EC was deposited onto the CMC substrate by placing toluene

solutions with variable EC concentration on the CMC substrate and removing solvent by evaporation. Substrates were then placed in a vacuum oven at 70 °C under reduced pressure to remove remaining toluene. The initial contact angle of water on the CMC substrates with a variable amount of EC was measured in air.

The results summarized in **Table 5-3** show that CMC substrate is weakly hydrophilic, as indicated by a contact angle value of $54 \pm 9^\circ$, while EC is weakly hydrophobic as indicated by a contact angle of $82 \pm 4^\circ$.³⁰ Oh and Luner reported similar contact angle values between $83.5 - 86.6^\circ$ for EC films prepared from solutions of different solvents and EC concentrations with or without annealing of the film.⁴² As expected, all the composite EC films on CMC coatings were initially weakly hydrophobic with the measured contact angle value of $90 \pm 16^\circ$, a value similar to the contact angle values measured on EC films.⁴² The surface of CMC-EC composite was responsive to water-absorption; initially more hydrophobic-like EC (before absorbing water) but becoming more hydrophilic-like CMC after absorbing water. Measurement of contact angle on composite surfaces after being hydrated became more variable, usually between $10 - 40^\circ$. The rate of water absorption for CMC, cast in glass molds and coated with EC, was influenced by the amount of EC and excessive coating of CMC with EC hindered water absorption.

Table 5-3. Properties of substrates prepared with CMC and EC.

Substrate	EC coverage (mg/m ²)	Contact angle (°) ^a	Water flux (g/s/m ²) ^b
CMC	n/a ^e	54 ± 9	3.0
EC	n/a	82 ± 4	< 0.01
<u>CMC-EC</u> ^c	1.6	52 ± 7	n/a
<u>CMC-EC</u> ^d	1.6	89 ± 5	n/a
CMC-EC-1	8.0	88 ± 5	0.4
CMC-EC-2	14.5	91 ± 6	0.2

^a Initial contact angle of a water droplet placed directly onto substrate surface; ^b time required for substrate to completely absorb a 500 μ L water droplet in air; ^c contact angle was measured on the CMC layer of the composite CMC-EC film; ^d contact angle was measured on the EC layer of the composite CMC-EC film.

To test the interfacial activity of the synthesized CMC-EC composite particles, EC, CMC and CMC-EC samples were carefully placed on an immiscible mixture of toluene and water (1:1 by volume). As shown in **Figure 5-8**, EC powder were hydrophobic and did not cross through the interface. EC remained essentially in the organic phase, where they slowly began to dissolve. CMC powder absorbed water after reaching the oil-water interface and quickly penetrated into the aqueous phase where they also began to dissolve. In contrast, the synthesized CMC-EC composite particles remained attached to the toluene-water interface, clearly demonstrating the biwettable nature of the particles. As a result, the CMC-EC composite particles were readily dispersed in toluene. However, colloidal stability of the synthesized CMC-EC composite particles in toluene was lost after water addition to toluene.

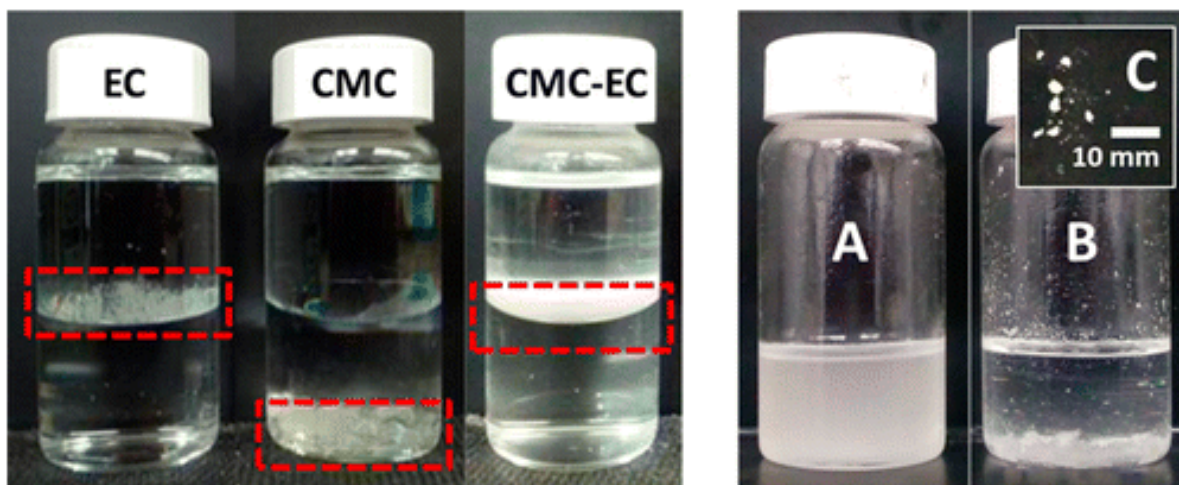


Figure 5-8. Interfacial and colloidal properties of composite particles. EC particles are hydrophobic and remain in the non-aqueous phase; CMC particles are hydrophilic and reside in the aqueous phase; CMC-EC composite particles are biwettable or interfacially active and attach to the toluene-water interface. The original CMC-EC composite particles are highly dispersed in toluene before absorbing water (**A**), but aggregate together (**B**) to form larger aggregates after absorbing water (**C**).

The responsive nature of the CMC-EC composite particles was most evident when attempting to stabilize emulsions. The CMC-EC composite particles, as synthesized, are interfacially active and could provide sufficient stability to prevent immediate phase separation

of a water-in-mineral oil emulsion, as shown in **Figure 5-9**. The synthesized CMC-EC composite particles experienced a drastic change in wettability after absorbing water. Before water absorption, the surface of CMC-EC composite particles with a contact angle of approximately 89° was similar to that of EC. The particle with this hydrophobicity was capable of stabilizing water-in-oil emulsions, as shown in **Figure 5-9A**. Upon absorbing water, the surface of CMC-EC composite particles become more like CMC, which has a contact angle of approximately 52° . As a result, they aggregated in the non-aqueous phase and hence lose their ability to stabilize any type of emulsions. For this reason, the stability of the water-in-mineral oil emulsion stabilized by CMC-EC composite particles was lost, as shown in **Figure 5-9B**. The responsive surface of the CMC-EC composite particles ensured that absorbent particles have only finite colloidal stability, which is lost upon absorbing water and eventually leads to the formation of large aggregates of hydrated absorbent particles. The increased size of absorbent aggregates facilitated separation of hydrated CMC-EC composite particles from emulsions for the purpose of water removal and sorbent particle regeneration.



Figure 5-9. Change in interfacial properties of composite absorbent particles after water-absorption. (A) Water-in-mineral oil emulsion stabilized by 2.5 wt% CMC-EC composite particles with initial contact angle of approximately 89° (before absorbing water) and (B) phase separation of the emulsion after 24 h as the particles absorb water and become increasingly hydrophilic with contact angle of approximately 52° .

Given their initial biwettability, interfacial activity and water absorptivity, the synthesized CMC-EC composite particles were ideally suited for removing water from emulsions through absorption. Removal of water from water-in-mineral oil emulsions stabilized by a nonionic

surfactant (0.75 wt% SPAN 80) was enhanced using both nonmagnetic (CMC-EC) and magnetic (CMC-EC/MAG) composite absorbent particles. Magnetic CMC-EC composite absorbent particles were prepared by dispersing superparamagnetic Fe_3O_4 nanoparticles into the aqueous CMC solution prior to emulsification. After dehydration, magnetic Fe_3O_4 particles were incorporated into the interior of the CMC-EC composite absorbent particles, leading to magnetically responsive particles. The amount of emulsified water that remained at the midway point of samples treated by various types of particles is shown in **Figure 5-10**.

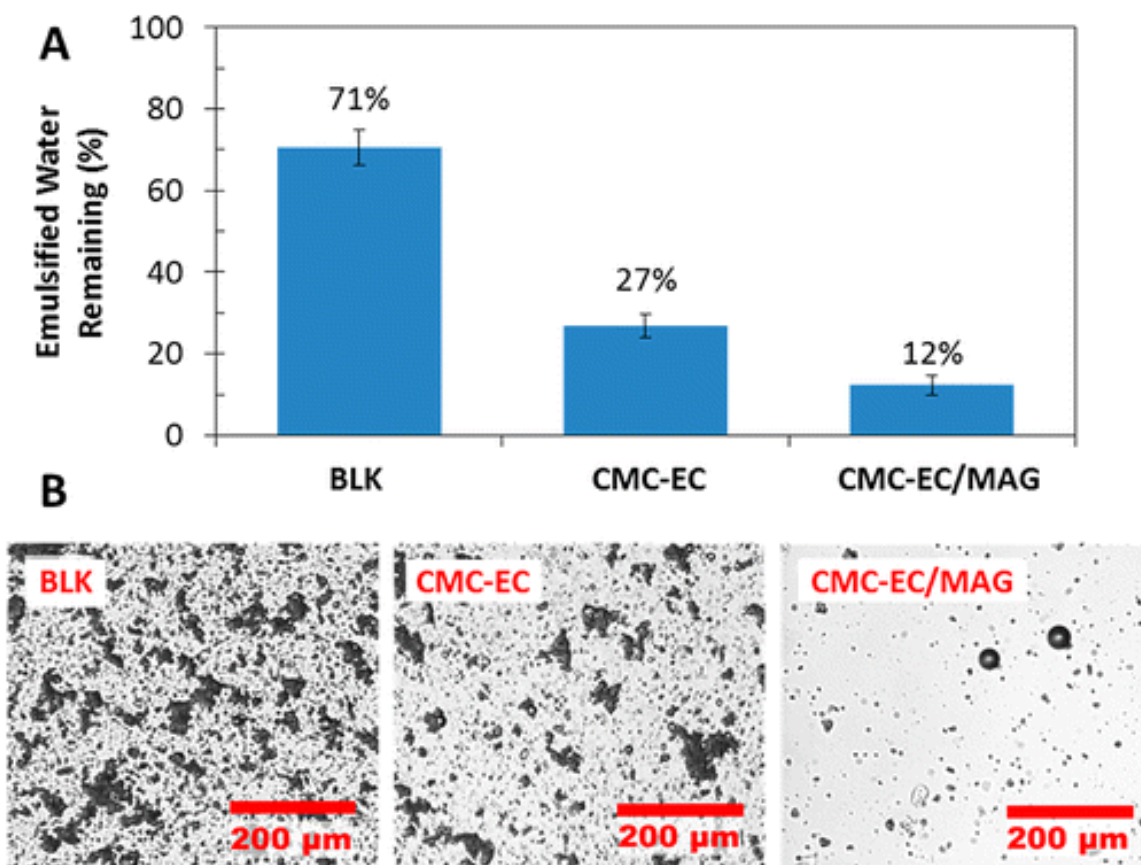


Figure 5-10. Dewatering of mineral oil emulsion using composite absorbent particles. (A) Amount of water emulsified in a mineral oil emulsion lowered after samples treated with either CMC-EC composite absorbent particles or magnetic CMC-EC composite absorbent particles and (B) micrographs of emulsion samples taken at the midway point show the reduction in amount of emulsified water droplets in treated samples. Initial water content of emulsion was 5.9 wt%.

Untreated emulsion samples exhibited poor phase separation with over 70% of emulsified water remaining after 12 h of mechanical agitation followed by 1 h of gravity settling. By adding 2.5 wt% CMC-EC composite absorbent particles, water content at midway point of treated emulsion (following 12 h of mechanical agitation and 1 h of gravity settling) was reduced to less than 30% of the original emulsified sample. Following 12 h of mechanical agitation and separation of spent magnetic CMC-EC composite absorbent particles using a hand magnet, emulsions treated with 2.5 wt% magnetic CMC-EC composite absorbent particles exhibited reduced water content at the midway point corresponding to less than 12% of the originally emulsified water. The additional magnetic force further accelerated dewatering of water-in-mineral oil emulsion.

5.4 Conclusions

Interfacially active organic CMC-EC composite water-sorbent particles were successfully synthesized by dehydration of water-in-toluene emulsions, wherein CMC was dissolved in the aqueous phase and EC was dissolved in the organic phase. The size of CMC-EC composite particles could be tuned by increasing EC concentration in the continuous phase or continuous emulsification during dehydration of the emulsions. The proposed synthesis of CMC-EC composite particles did not require chemical derivatization and generated no chemical waste. EC-coated water absorbent particles possessed a greater compatibility with hydrophobic media and were readily dispersed in organic solvents. Composite absorbent particles were prepared by evaporating water from water droplets dispersed in toluene by vaporizing the water-toluene azeotrope. Thus, the surface of CMC-EC composite particles remained permeable and the resulting composite absorbent particles were capable of absorbing water. Because of the absorptive properties of CMC and the interfacial activity of EC, the CMC-EC composite absorbent particles were effective in removing water from water-in-oil emulsions by absorption. By using a similar procedure with Fe_3O_4 nanoparticles dispersed within CMC-containing emulsion water droplets, magnetic CMC-EC composite absorbent particles were also prepared and showed superior performance in removing water from similar stable water-in-mineral oil emulsions.

5.5 References

1. S.-D. Yeo and E. Kiran, *J. Supercrit. Fluids*, 2005, **34**, 287–308.
2. M. T. Swihart, *Curr. Opin. Colloid Interface Sci.*, 2003, **8**, 127–133.
3. R. Vehring, *Pharm. Res.*, 2008, **25**, 999–1022.
4. R. Vehring, W. R. Foss and D. Lechuga-Ballesteros, *J. Aerosol Sci.*, 2007, **38**, 728–746.
5. R. Arshady, *Colloid Polym. Sci.*, 1992, **270**, 717–732.
6. Guyot and K. Tauer, in *Polymer Synthesis*, Springer Berlin Heidelberg, **1994**, 43–65.
7. S. A. F. Bon, M. Bosveld, B. Klumperman and A. L. German, *Macromolecules*, 1997, **30**, 324–326.
8. L. Peltonen and J. Hirvonen, *J. Pharm. Pharmacol.*, 2010, **62**, 1569–1579.
9. Martín and M. J. Cocero, *Adv. Drug Deliv. Rev.*, 2008, **60**, 339–350.
10. N. Rasenack and B. W. Müller, *Pharm. Dev. Technol.*, 2004, **9**, 1–13.
11. R. Heusch, in *Ullmann's Encyclopedia of Industrial Chemistry*, ed. Wiley-VCH Verlag GmbH & Co. KGaA, Wiley-VCH Verlag GmbH & Co. KGaA, Weinheim, Germany, **2000**.
12. J. W. Barlow and D. R. Paul, *Polym. Eng. Sci.*, 1981, **21**, 985–996.
13. Liu, H. Qin and P. T. Mather, *J. Mater. Chem.*, 2007, **17**, 1543–1558.
14. S. Jiang and S. Granick, *Janus particle synthesis, self assembly and applications*, Royal Society of Chemistry, Cambridge, U.K., **2012**.
15. P. Binks and P. D. I. Fletcher, *Langmuir*, 2001, **17**, 4708–4710.
16. S. Jiang and S. Granick, *J. Chem. Phys.*, 2007, **127**, 161102.
17. Kumar, B. J. Park, F. Tu and D. Lee, *Soft Matter*, 2013, **9**, 6604.

18. M. Linares, A. Formiga, L. T. Kubota, F. Galembeck and S. Thalhammer, *J. Mater. Chem. B*, 2013, **1**, 2236–2244.
19. H. Hu, L. Xiong, J. Zhou, F. Li, T. Cao and C. Huang, *Chem. – Eur. J.*, 2009, **15**, 3577–3584.
20. K. S. Soppimath, L.-H. Liu, W. Y. Seow, S.-Q. Liu, R. Powell, P. Chan and Y. Y. Yang, *Adv. Funct. Mater.*, 2007, **17**, 355–362.
21. J. Peng, Q. Liu, Z. Xu and J. Masliyah, *Energy Fuels*, 2012, **26**, 2705–2710.
22. W.-C. Law, K.-T. Yong, I. Roy, H. Ding, R. Hu, W. Zhao and P. N. Prasad, *Small*, 2009, **5**, 1302–1310.
23. T. Cole, R. A. Scott, A. L. Connor, I. R. Wilding, H.-U. Petereit, C. Schminke, T. Beckert and D. Cadé, *Int. J. Pharm.*, 2002, **231**, 83–95.
24. S. Leopold, *Pharm. Sci. Technol. Today*, 1999, **2**, 197–204.
25. T. Higuchi and A. Aguiar, *J. Am. Pharm. Assoc.*, 1959, **48**, 574–583.
26. J. Malm, J. Emerson and G. D. Hiait, *J. Am. Pharm. Assoc.*, 1951, **40**, 520–525.
27. Y. Kane, J. Rambaud, H. Maillols, J. P. Laget, D. Gaudy and H. Delonca, *Drug Dev. Ind. Pharm.*, 1993, **19**, 2011–2020.
28. Loxley and B. Vincent, *J. Colloid Interface Sci.*, 1998, **208**, 49–62.
29. S. Fujii, D. P. Randall and S. P. Armes, *Langmuir*, 2004, **20**, 11329–11335.
30. J. Drelich, A. Marmur, *Surfaces and Coatings Surf. Innovations* 2014, **2**, 211– 227.
31. W. Dean and D. D. Stark, *J. Ind. Eng. Chem.*, 1920, **12**, 486–490.
32. Melzer, J. Kreuter and R. Daniels, *Eur. J. Pharm. Biopharm.*, 2003, **56**, 23–27.
33. S. Obara, N. Maruyama, Y. Nishiyama and H. Kokubo, *Eur. J. Pharm. Biopharm.*, 1999, **47**, 51–59.

34. Martinac, J. Filipović-Grčić, D. Voinovich, B. Perissutti and E. Franceschinis, *Int. J. Pharm.*, 2005, **291**, 69–77.
35. M. G. Moldenhauer and J. G. Nairn, *J. Controlled Release*, 1992, **22**, 205–218.
36. T. L. Rogers and D. Wallick, *Drug Dev. Ind. Pharm.*, 2012, **38**, 129–157.
37. R. A. Young, in *Textile Science and Technology*, Elsevier, **2002**, vol. 13, 233–281.
38. X. Feng, P. Mussone, S. Gao, S. Wang, S. Y. Wu, J. H. Masliyah and Z. Xu, *Langmuir*, 2010, **26**, 3050–2057.
39. D. W. Fuerstenau, M. C. Williams, *Colloids Surf.* 1987, **22**, 87–91.
40. J. Drelich, *Surf. Innovations* 2013, **1**, 248–254.
41. J. Briscoe, C. J. Lawrence and W. G. P. Mietus, *Adv. Colloid Interface Sci.*, 1999, **81**, 1–17
42. E. Oh, P. E. Luner, *Int. J. Pharm.* 1999, **188**, 203–219.

Chapter 6. Absorptive Emulsion Dewatering

Chapter 6. : *Absorptive Emulsion Dewatering*. A version of this section has been published as C. Liang, Q. Liu and Z. Xu “Dewatering Bitumen Emulsions using Interfacially Active Organic Composite Absorbent Particles” in *Energy & Fuels* by the American Chemical Society with DOI:10.1021/acs.energyfuels.6b00228.

6.1 Introduction

Crude oil emulsions are commonly encountered during the oil extraction process, especially for bitumen which contains a greater fraction of interfacially active compounds.¹⁻³ Emulsions are stabilized by interfacially active materials, including both process aids and indigenous surfactants in the crude oil.⁴⁻⁷ Stabilized emulsions are undesirable because they hinder water-oil separation and consequently reduce the oil production rate. Residual emulsified water containing dissolved salts can cause problems in downstream operations, such as increased corrosion of equipment and catalyst poisoning in refineries.⁸ Therefore, developing a rapid and efficient method to remove the water from emulsions is of great importance to bitumen extraction and petroleum production in general.⁹ To enhance oil-water separation, emulsions are often treated by (i) thermal stimulation (heating), (ii) solvent addition, (iii) electrocoalescence, (iv) centrifugation, or a combination of these methods.¹⁰⁻¹³ Even with combined processing steps, oil-water phase separation is often slow and ineffective for fine water droplets with low gravity settling rate. Chemical demulsifiers are added to treat stable water-in-oil petroleum emulsions by promoting coalescence of emulsified droplets to enhance phase separation.¹⁴⁻¹⁸ Unfortunately, most chemical demulsifiers are sensitive to changes in their environment, prone to overdosing, and often used only once due to lack of a viable separation method. Demulsifier overdosing occurs from time to time because chemical demulsifiers, in order to function properly, are themselves also surface-active molecules. As a result, demulsifier molecules also adsorb at the oil-water interface with the potential of developing a stabilizing film at a high concentration, depending upon the structure of demulsifier molecules.¹⁹ Less effective phase separation occurs beyond a chemical demulsifier’s optimum concentration range. Pensini *et. al.* studied the mechanism of

polymeric ethylene oxide (EO)–propylene oxide (PO) demulsifiers in asphaltene-stabilized water-in-oil (W/O) emulsions.²⁰ A distinct advantage of using responsive particles for dewatering emulsions is that the demulsification process is much less sensitive to overdosing, although adding a minimal amount is highly desirable from a process flexibility and an economic point of view. Therefore, new strategies for promoting phase separation at ambient temperature are highly desirable to reduce the energy requirement associated with bitumen production and lower greenhouse gas emissions. New methods of treating emulsions include the use of aerogels,²¹ nanomaterials,²² and many other materials with special wettability.²³ The use of absorbent particles may prove to be a suitable alternative for dewatering water-in-diluted bitumen emulsions that overcomes shortfalls associated with traditional chemical demulsifiers.

To dewater water-in-diluted bitumen emulsions at ambient conditions, we designed absorbent particles coated with interfacially active materials in an attempt to improve compatibility of the absorbent particles in non-aqueous media. To allow for more effective separation and hence potential recycle of used absorbent particles, magnetically responsive composite absorbent particles were prepared on the basis of the designed principle illustrated in **Figure 6-1**. Magnetically responsive composite absorbent particles combine three different mechanisms of action in one discrete particle for the purpose of dewatering emulsions: (i) displacement of indigenous surfactants by interfacially active particles, (ii) absorption of emulsified water and (iii) magnetic separation of the absorbent particles for reuse. The structure of composite absorbent particles prepared by dehydrating well-designed emulsion droplets is ideally suited for dewatering of water-in-oil emulsions.²⁴ Specifically, the surface of composite absorbent particles is of intermediate wettability but remains water-permeable, with a high specific surface area to allow for more rapid absorption of emulsified water. The dewatering performance of various absorbent particles is examined using stable water-in-heavy naphtha diluted bitumen emulsions.

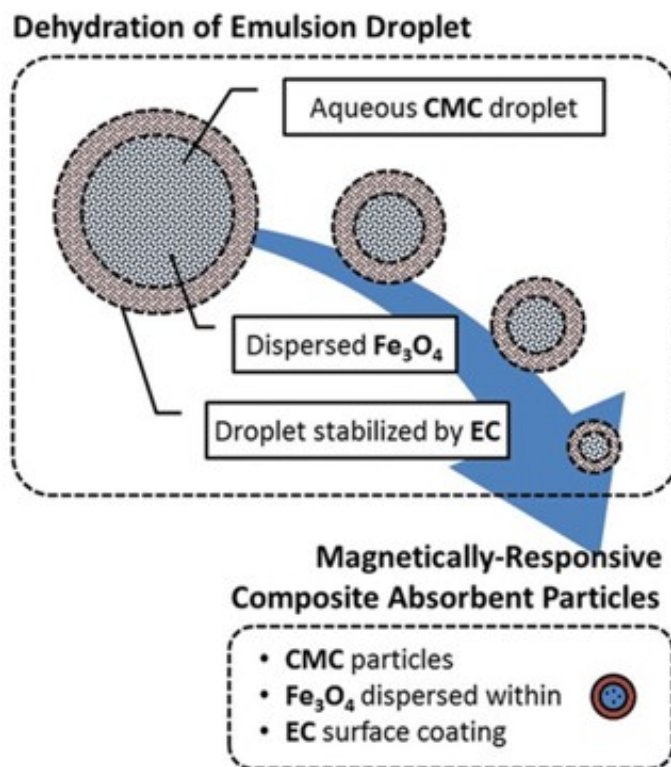


Figure 6-1. Preparation of magnetically responsive composite absorbent particles (M-CMC@EC). An emulsion containing dispersed Fe_3O_4 particles and dissolved CMC in the dispersed phase is prepared. Emulsion droplets stabilized by EC are dehydrated until the formation of Fe_3O_4 -in-CMC solid particles coated with a thin layer of EC.

6.2 Experimental

Sodium carboxymethyl cellulose (CMC, molecular weight of 250 000 g/mol and degree of substitution of 0.7) and ethylcellulose (EC, ethoxy content of 48%) were purchased from Sigma-Aldrich. American Chemical Society (ACS)-grade toluene, acetone and methanol were purchased from Fisher Scientific. All of these chemicals were used as received without further purification. Ethanol from Commercial Alcohols used in this study was of commercial grade (99%). Vacuum distillation feed bitumen was provided by Syncrude Canada, Ltd. Heavy naphtha was supplied by Champion Technologies, Inc. The plant recycled process water was provided by Syncrude Canada, Ltd. and used to prepare water-in-diluted bitumen emulsions, with the pH of the process water being adjusted to 8.9.

CMC@EC particles were prepared from CMC and EC by dehydration of emulsion droplets containing dissolved CMC stabilized by EC in toluene.²⁴ Magnetically responsive, M-CMC@EC particles were prepared using a similar procedure with iron oxide (Fe₃O₄) particles being dispersed in the aqueous CMC solution before emulsification and subsequent dehydration. M-CMC@EC particles were recovered using a strong hand magnet and dried in an oven at 110 °C for 72 h.

To compare the dewatering performance of composite absorbent particles, unmodified CMC absorbent particles were coated with either EC (CMC/EC) or bituminous material (CMC/BIT). CMC particles of 500 – 850 µm were sorted using mesh sieves. Unmodified CMC particles were coated with either EC or bituminous material through adsorption using organic solutions of EC. The sorted CMC particles were dispersed in an EC in toluene solution (1.0 wt%) to allow for EC to adsorb on the CMC particles. The EC-coated absorbent particles (CMC/EC) were separated using a mesh sieve, washed liberally with toluene and ethanol and placed in an oven at 110 °C for 72 h. To coat bituminous materials on CMC particles, the sorted CMC particles were dispersed in a toluene solution of bitumen, followed by slow addition of 2 volume-equivalent heptane. After removal of the supernatant, solids were collected by the mesh sieve and washed with additional toluene. Residual solvent was removed by evaporation under reduced pressure. The CMC content of different absorbent particle samples was estimated using thermogravimetric analysis and the results are summarized in **Table 6-1**.

Table 6-1. Properties of composite absorbent particles prepared using cellulosic materials.

Sample	Particle size range ^a (µm)	CMC content (wt%)	EC content (wt%)
CMC	500 – 850	100	0
CMC/EC	500 – 850	97	3
CMC/BIT	500 – 850	97	0
CMC@EC	3.5 – 144.0	89	11
M-CMC@EC	0.1 – 3.8	65	9

^a The particle size range was taken from the sieve size or measured by light scattering.

To bear practical implications, emulsions were prepared with plant process water and diluted bitumen. Heavy naphtha-diluted bitumen was prepared using a naphtha/bitumen ratio of 0.65, as typically encountered in industrial practices. After dilution, the mixture was shaken in a mechanical shaker overnight at 200 cycles/min. Process water-in-diluted bitumen emulsions were prepared by emulsifying approximately 4 - 5 wt% water using a high-speed homogenizer operating at 30 000 rpm for 3 min. The resulting emulsions were stable with an average drop size typically less than 2 μm , as revealed in optical micrographs. The ability of various particles to remove water was evaluated by titrating the water content of the emulsions using a G.R. Scientific Cou-Lo 2000 automatic Coulometric Karl-Fischer titration. Briefly, various types of particles were added directly to diluted bitumen emulsion samples and mixed using a mechanical shaker or vortex mixer. Emulsion aliquots were taken at the midway point after a specified amount of creaming/settling time for titration to determine the water content.

6.3 Results and Discussion

The dewatering performance of the CMC absorbent coated with different materials (*i.e.*, EC or BIT) was evaluated using water in diluted bitumen emulsions. The water in diluted bitumen emulsions, stabilized solely by indigenous surfactants, contained approximately 4.5 - 5.0 wt% process water and exhibited little phase separation throughout the experiment without any chemical treatment. Emulsion samples inside Teflon tubes were charged with 2.5 wt% absorbent particles (on the basis of total mass of emulsion), and the resulting mixtures were placed in a mechanical shaker at ambient conditions for a specified period of time. Emulsion samples were then removed from the mechanical shaker and left at ambient conditions for 1 h to separate the particles from the emulsion under the force of gravity. The absorbent particles tested (CMC, CMC/EC and CMC/BIT) were relatively large ($> 500 \mu\text{m}$) and settled quickly under gravity without being subjected to continuous agitation. As shown in **Figure 6-2A**, the unmodified CMC particles were able to reduce the water content of the emulsion but are limited by poor mobility and poor colloidal stability in organic solvent environments (*i.e.*, the continuous phase of the diluted bitumen). It took almost 1 h for the water content at the midway point of emulsion samples (*i.e.*, halfway between the bottom and the top of the emulsion sample) to reach half of its original

value when treated with unmodified CMC particles. In comparison to CMC, CMC/BIT was found less effective in removing water from the emulsions and required approximately twice the amount of time (2 h) to achieve the same reduction in the water content as a result of the limited contact of the absorbent material, coated by bituminous material, with water in the emulsified droplet. In comparison to both unmodified absorbent particles (CMC) and bitumen-coated absorbent particles (CMC/BIT), CMC/EC composite particles exhibited an improved dewatering performance. The water content at the midway point of emulsion samples treated with CMC/EC particles was less than half its original value after only 0.5 h in the mechanical shaker. The rate of dewatering for diluted bitumen emulsions treated with CMC/EC was approximately 4 times faster than that with unmodified CMC. The presence of interfacially active EC improved the dispersability of absorbent particles, promoted the attachment of absorbent particles onto the oil-water interface and assisted in displacing indigenous surface-active materials that stabilize water droplets.

Absorption of water from the emulsified water droplets is a mass transfer process, and the rate of water absorption can be further improved using smaller absorbent particles with greater specific surface area. Large particles are prone to settle out from the emulsion. In comparison to larger CMC/EC particles, the rate of emulsion dewatering using smaller size CMC@EC particles is anticipated to be significantly faster. To confirm this hypothesis, emulsion samples with CMC@EC particles were agitated in a vortex mixer for a varying period of time and left for phase separation at ambient conditions under the force of gravity for 1 h. For CMC@EC particles, the mechanical shaker did not provide adequate shear to ensure consistent mixing of the particles in the emulsion. As a result, the results obtained for CMC@EC particles using the mechanical shaker were not consistent. Therefore, only data from the vortex mixer for CMC@EC particles are shown. Results in **Figure 6-2B** show that the water content at the halfway point of emulsion samples treated with CMC@EC was less than half its original value after only 30 s in the vortex mixer. In comparison, the water content at the halfway point of emulsion samples treated with larger absorbent particles (CMC and CMC/EC) was reduced by less than 30% after 90 s in the vortex mixer. While the EC coating of the absorbent particles improved the colloidal stability of CMC@EC absorbent particles in the continuous oil phase as in the case of CMC/EC particles, the

porous nature of EC coatings ensures minimal impedance of water absorption by the CMC@EC particles. In comparison to the smaller sizes of the CMC@EC particles, the observed significant improvement in the rate of water absorption from the emulsified water by the CMC@EC particles is not unexpected.

Dewatering emulsions using a process based on water absorption requires an adequate method of separating the hydrated absorbent particles from the emulsion. This can be an especially difficult challenge for microscopic particles. Although high-efficiency filtration methods exist, separation of small particles suffers from high costs associated with maintaining a high-pressure differential and membrane upkeep. Centrifugation is another effective method for separating small particles and droplets but is also expensive to operate and maintain. In the current application, micrometer-sized CMC@EC particles were added to a diluted bitumen emulsion sample to absorb the water from the emulsified water droplets. After the continuous phase was washed away with toluene, the micrometer-sized hydrated CMC@EC absorbent particles were observed to form large aggregates. It is evident that the absorption of water increased the surface wettability of the originally biwetable CMC@EC particles, reducing the colloidal stability of composite absorbent microparticles as a result of its hydrophilic nature, and hence inducing particle aggregation in the non-aqueous continuous phase. The aggregates formed by hydrated CMC@EC absorbent particles do not redisperse when subjected to low-intensity shear from a magnetic stirrer.

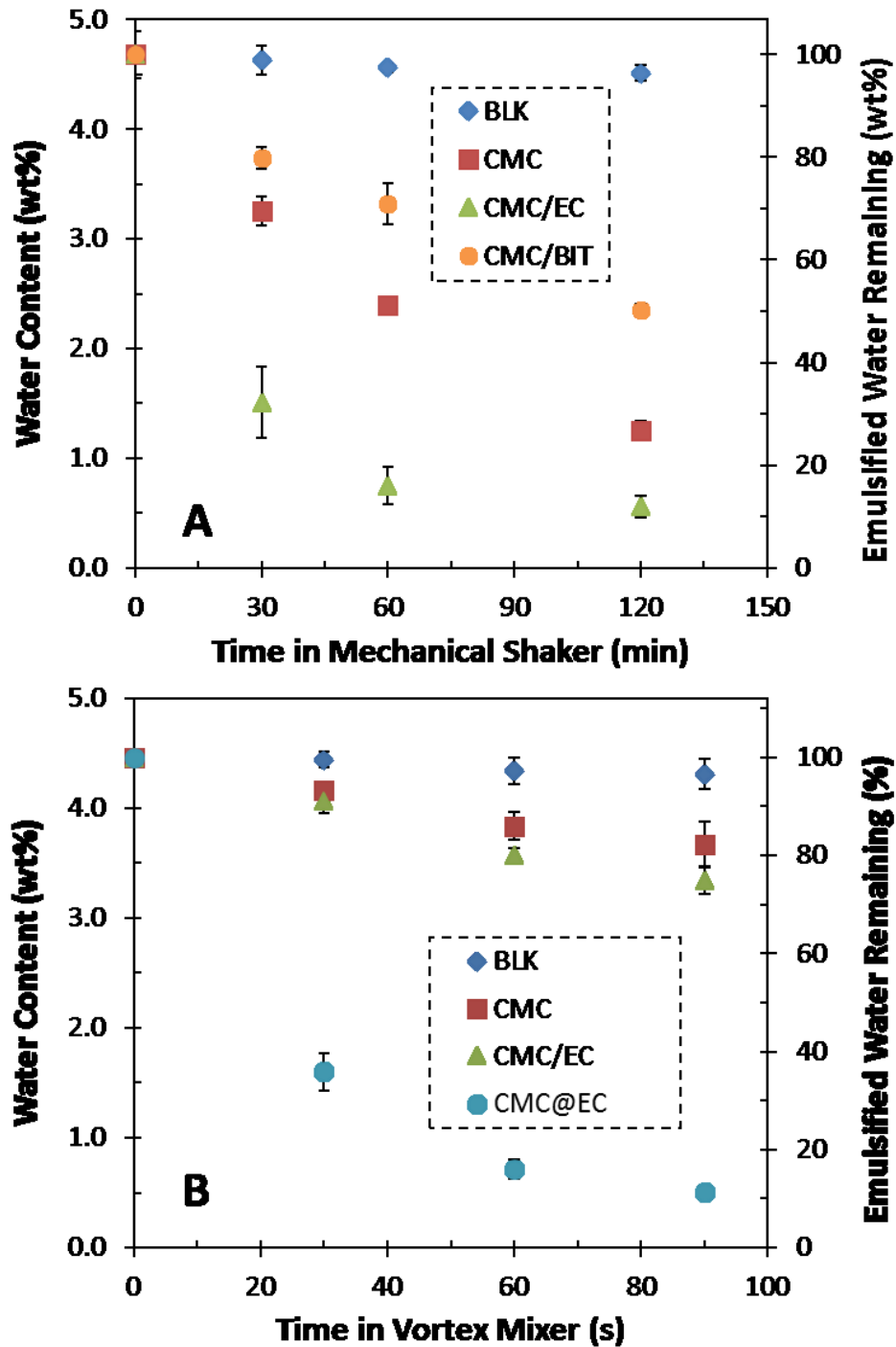


Figure 6-2. Dewatering bitumen emulsion using different absorbent particles. Emulsified water remaining in water in diluted bitumen emulsion samples is reduced after treating with 2.5 wt% absorbent particles coated with interfacially active materials (CMC/EC and CMC@EC) or bituminous materials (CMC/BIT). Absorbent particles were added to the emulsion, mixed using a mechanical shaker (A) or vortex mixer (B), and subsequently left to settle under gravity for 1 h.

In contrast to the original dry CMC@EC particles, which dispersed readily in toluene, as shown in **Figure 6-3A**, the hydrated CMC@EC aggregates formed after absorbing water settled rapidly under gravity, as shown in **Figure 6-3B**. The dispersion of the prepared composite absorbent microparticles in toluene is highly stable as a result of EC coating on the composite absorbent particle surfaces as designed. EC adsorbed/grafted on the particle surfaces in good solvent provides steric stabilization between particles. However, as the composite absorbent particle absorbs a sufficient amount of water to become hydrated, the strong cohesion of water surrounding the hydrated particles causes particles to aggregate in toluene, losing the colloidal stability, which facilitates separation of spent particles with emulsified water from the solvent (*i.e.*, oil) as designed. The hydrated absorbent aggregates formed after dewatering the diluted bitumen emulsions were easily separated by gravity filtration using a simple mesh screen. The responsive nature of increasing the wettability of CMC@EC particles upon absorption of water from the emulsified water droplets allowed us to design micrometer-sized composite absorbent particles for improved dewatering performance by increasing the specific surface area without sacrificing the ability to easily separate the hydrated absorbent particles. Alternatively, it was also possible to recover absorbent particles from stable dispersions by imparting magnetic susceptibility to absorbent microparticles. Even dry magnetically responsive composite absorbent microparticles (M-CMC@EC) dispersed in toluene, as shown in **Figure 6-3**, were easily collected using a hand magnet.

Traditional demulsifiers enhance water separation through promotion of droplet coalescence by either flocculating droplets and/or reducing the energy barrier of droplet coalescence. Phase separation is accelerated because of higher gravity settling velocity of larger droplets and aggregates. However, the use of chemical demulsifiers is prone to overdosing, which can lead to a diminished performance of chemical demulsifiers and unstable operations. Demulsifiers are also interfacially active and, above its effective concentration range, chemical demulsifiers will show reduced effectiveness and may even enhance emulsion stability. In contrast, the rate of an absorptive dewatering process can be accelerated by promoting contact between emulsified water droplets and absorbent particles through either improved mixing (provided that the maximum capacity of the absorbent has not been reached) or by increasing

concentration of absorbent particles. For such systems, rapid water removal is achievable without concerns for overdosing. As shown in **Figure 6-4**, the amount of emulsified water remaining in diluted bitumen emulsions was further reduced by addition of more absorbent particles. It is also important to note that, for optimal dewatering, the composite absorbent micrometer-sized particles must be given sufficient time to absorb the water and form larger aggregates, which settle out rapidly under gravity. Although more than 95 wt% of emulsified water was removed after 2 h in a mechanical shaker followed by 1 h of gravity settling using 3.0 wt% CMC/EC particles, similar results were achieved after only 30 s in a vortex mixer, followed by 1 h of gravity settling or magnetic recovery using CMC@EC or M-CMC@EC. The rate of dewatering was much slower for larger CMC/EC particles at the same concentration, which reduced the water content by only 10 wt% after 30 s in a vortex mixer, followed by 1 h of gravity settling.

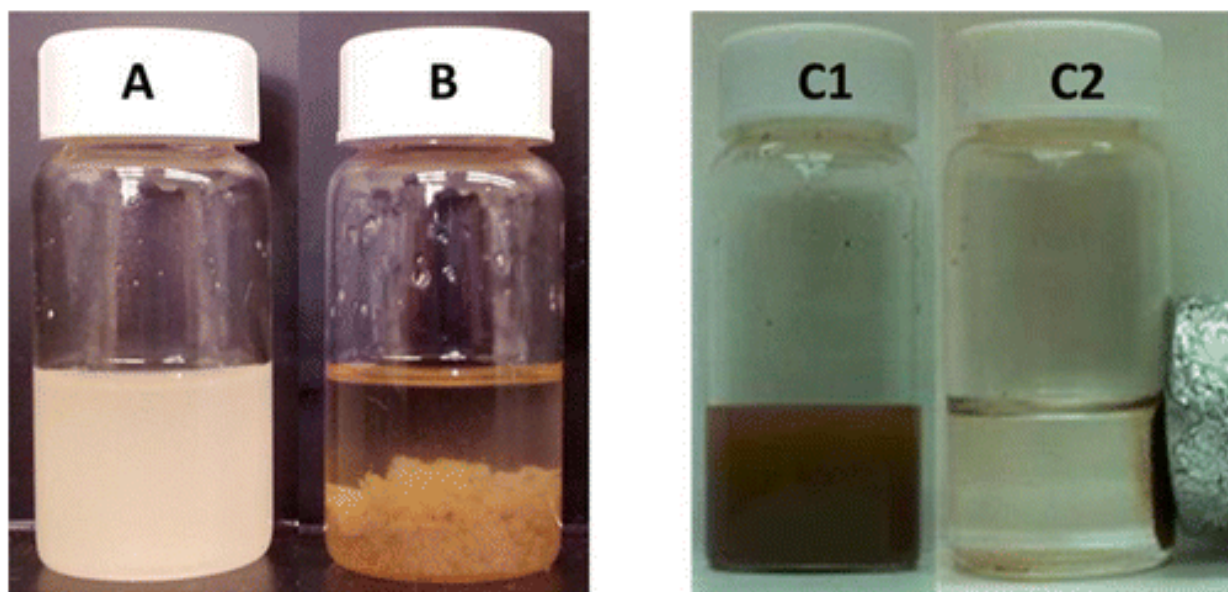


Figure 6-3. Changing colloidal properties of composite absorbent particles. Composite absorbent microparticles (CMC@EC) dispersed well in toluene before absorbing emulsified water (**A**) but formed large aggregates after absorbing emulsified water (**B**). The large aggregates were easily removed by filtration through a simple mesh screen. Alternatively, the dispersed magnetically responsive composite absorbent micrometer-sized particles (M-CMC@EC) were removed using a strong hand magnet (**C2**) from highly dispersed suspensions (**C1**).

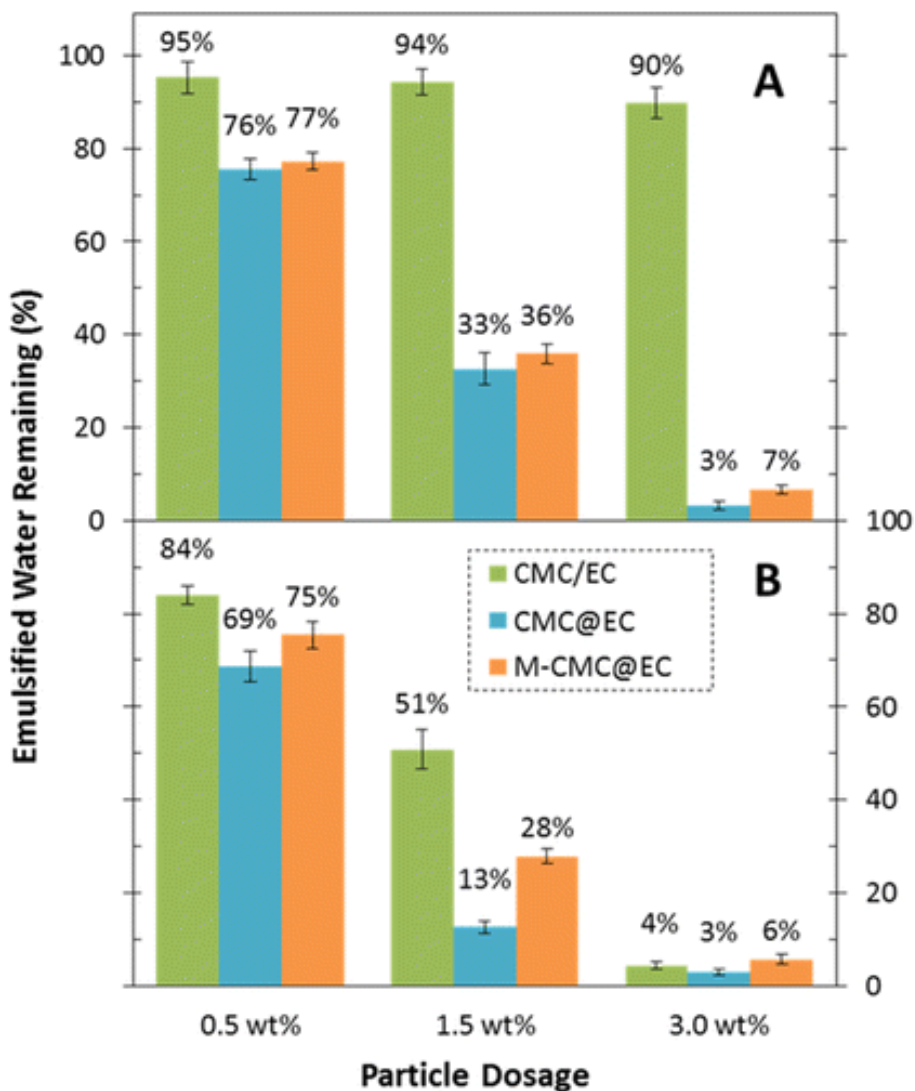


Figure 6-4. Dewatering heavy naphtha-diluted bitumen emulsion samples using various absorbent particles (CMC/EC, CMC@EC and M-CMC@EC). Water remaining in heavy naphtha-diluted bitumen emulsion samples treated with an increasing amount of composite absorbent particles after 90 s in a vortex mixer (**A**) or 2 h in a mechanical shaker (**B**). Non-magnetic particles (CMC/EC and CMC@EC) were separated by gravity settling for 1 h, while magnetic particles (M-CMC@EC) were recovered using a strong magnet.

Composite absorbent particles were prepared by dehydration of emulsion droplets by distillation and regeneration of spent absorbent particles may be possible. To test the reuse potential of spent absorbent particles, micrometer-sized composite absorbent particles

(CMC@EC and M-CMC@EC) along with absorbed water were removed from the emulsion samples by gravity filtration or magnetic separation after particles were immersed in excess diluted bitumen froth samples for 48 h. The hydrated composite absorbent particles were recovered as larger aggregates of hydrated particles. The recovered spent absorbent particle aggregates were soaked and washed liberally with toluene to remove the trapped bitumen. The amount of bitumen within the hydrated absorbent aggregates was determined by evaporating the solvent under the reduced pressure from collecting washing fluid. The washed absorbent aggregates were dried in an oven under the reduced pressure at 70 °C to remove absorbed water. The amount of bitumen and water recovered with the spent micrometer-sized composite absorbent particles is summarized in **Table 6-2**. The hydrated absorbent aggregates recovered by filtration contained up to 6.5 wt% bitumen on the basis of the hydrated absorbent mass. However, after washing the entrained bitumen from hydrated absorbent particle aggregates with toluene, all of the absorbents tested contained less than 0.5 wt% residual bitumen based on dry absorbent mass, as determined using thermogravimetric analysis.

To test the capacity of water absorption, various types of absorbent particles were immersed in either deionized water or process water. Unmodified CMC particles were capable of absorbing approximately 6.8 ± 1.0 and 4.3 ± 0.7 times their dry mass of deionized water and process water, respectively. As anticipated, the presence of dissolved salts and surfactant in the process water appears to hinder the absorption of water by CMC particles. As shown in **Table 6-2**, the capacity of absorbent particles (CMC/EC, CMC@EC and M-CMC@EC) to absorb the process water was lower than the capacity of unmodified CMC particles, which can be attributed to the presence of non-absorbing materials, such as EC and/or Fe_3O_4 , in these composite particles. Although separation, regeneration and reuse of composite absorbent particles is possible, the results in **Figure 6-5** show a gradual decline in water absorption by CMC/EC composite particles, while CMC@EC particles show a larger decrease in water absorption following the first cycle. After composite absorbent particles are recovered, the water absorption capacity for CMC/EC particles was approximately 20% lower, while the water absorption capacity for CMC@EC particles was diminished by approximately half. Irreversible aggregation of smaller particles upon absorption of water may have contributed more significantly to the depressed performance of the CMC@EC

microparticles as a result of less efficient dehydration of particle aggregates than individual particles. The presence of fine mineral solids (*e.g.*, clay) in recovered absorbent particles may present a steric barrier, hindering effective contact between absorbent particles and emulsified water droplets. The presence of any foreign material on the surface of absorbent particles has a detrimental effect on both absorption and regeneration. A further study is underway to investigate the reason for the reduced efficiency of water absorbance in an effort to develop a more effective regeneration method for further enhancing recyclability of the spent absorbent particles.

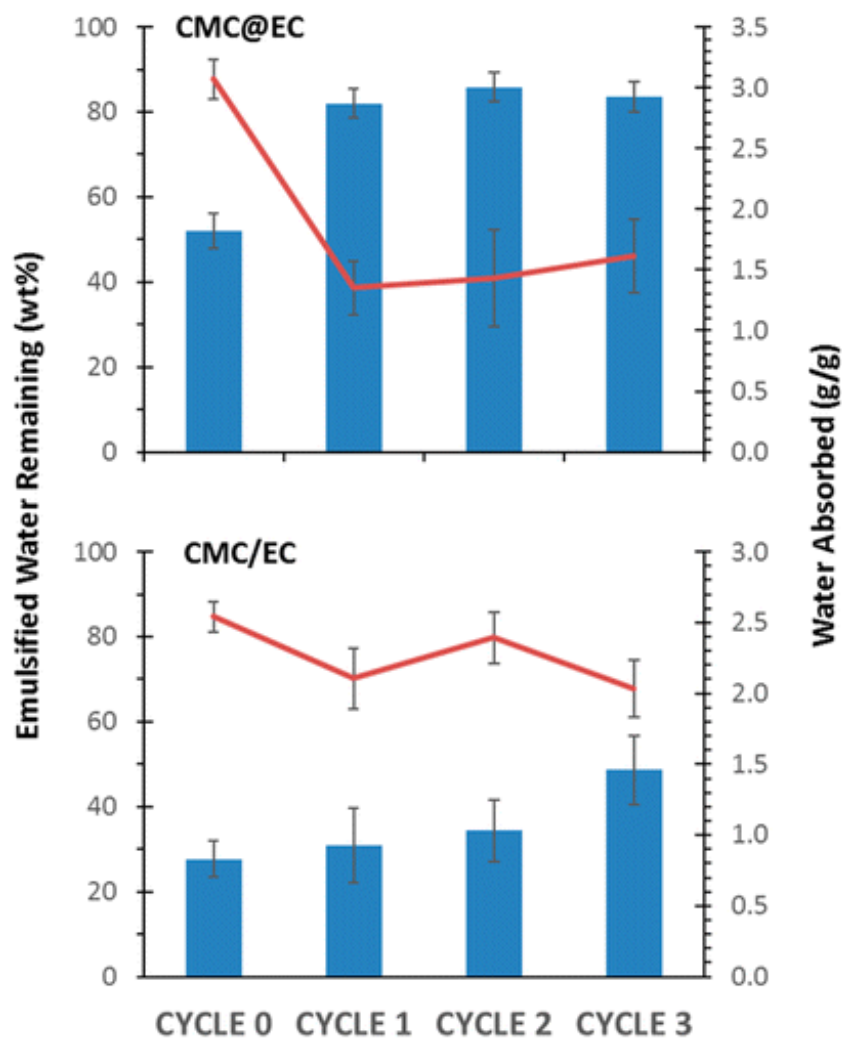


Figure 6-5. Dewatering diluted bitumen emulsions using recycled absorbent particles. The amount of emulsified water remaining in diluted bitumen emulsion samples after treatment with recycled composite absorbent particles (CMC@EC, top; CMC/EC, bottom).

Table 6-2. Properties of hydrated composite absorbent particle aggregates recovered from diluted bitumen froth after absorbing water.

Sample	Deionized water (g/g)	Process water (g/g)	Emulsified water from bitumen froth (g/g)	Trapped bitumen ^a (wt%)
CMC/EC	6.5 ± 1.0	4.0 ± 0.7	3.4 ± 1.0	6.5 ± 1.1
CMC@EC	4.8 ± 0.8	3.5 ± 0.4	3.1 ± 0.8	5.4 ± 1.6
M-CMC@EC	3.7 ± 0.9	2.8 ± 0.5	2.2 ± 0.3	3.8 ± 1.0

^a On the basis of the dry mass of recovered absorbent particle aggregates.

6.4 Conclusions

Magnetically responsive composite absorbent particles with combined advantageous properties of different materials, including the magnetic susceptibility of Fe₃O₄, the water-absorptive capacity of CMC, and the interfacial activity of EC, were shown to be an effective absorbent for emulsified water from stable water-in-diluted bitumen emulsions. The surface wettability of composite absorbent particles was a critical factor in their effectiveness: the interfacially active materials present on the surface of composite particles promote their dispersion in diluted bitumen and attachment to the stabilized water-oil interface. For effective absorption of emulsified water droplets, the biwetable surface layer must remain water-permeable. A layer of hydrophobic bitumen adsorbed on the surface of absorbent particles was detrimental to the rate of water absorption. Smaller size composite absorbent particles (CMC@EC) performed better than larger EC-coated CMC particles (CMC/EC) as a result of an increase in the specific surface area. CMC@EC particles are initially readily dispersed in diluted bitumen but become more hydrophilic after absorbing water, leading to the formation of large aggregates of hydrated absorbent particles. Large hydrated aggregates settled much faster under the force of gravity and are easily separated by simple filtration. The micrometer-sized absorbent particles with imbedded nanosized magnetic particles (M-CMC@EC) can be effectively separated using permanent or electromagnets from multiphase, complex dispersions for potential reuse after regeneration (or simple cleaning). The responsive nature of the composite particles offers

the possibility for enhanced dewatering performance coupled with an effective separation strategy. The use of absorbent particles to remove emulsified water from bitumen emulsions was demonstrated at ambient conditions and may be a viable strategy to lower the energy required for bitumen production.

6.5 References

1. L. A. Stanford, R. P. Rodgers, A. G. Marshall, J. Czarnecki and X. A. Wu, *Energy Fuels*, 2007, **21**, 963–972.
2. A. Goldszal and M. Bourrel, *Ind. Eng. Chem. Res.*, 2000, **39**, 2746–2751.
3. A. M. Al-Sabagh, S. A. Nehal, M. N. Amal and M. M. Gabr, *Polym. Adv. Technol.*, 2002, **13**, 346–352.
4. J. L. Stark and S. Asomaning, *Energy Fuels*, 2005, **19**, 1342–1345.
5. M. Rondón, J. C. Pereira, P. Bouriat, A. Graciaa, J. Lachaise and J.-L. Salager, *Energy Fuels*, 2008, **22**, 702–707.
6. T. Jiang, G. J. Hirasaki, C. A. Miller and S. Ng, *Energy Fuels*, 2011, **25**, 545–554.
7. M. K. Poindexter and S. C. Marsh, *Energy Fuels*, 2009, **23**, 1258–1268.
8. G. Liu, X. Xu and J. Gao, *Energy Fuels*, 2003, **17**, 625–630.
9. M. Fortuny, C. B. Z. Oliveira, R. L. F. V. Melo, M. Nele, R. C. C. Coutinho and A. F. Santos, *Energy Fuels*, 2007, **21**, 1358–1364.
10. J. H. Masliyah, Z. Xu and J. A. Czarnecki, *Handbook on theory and practice of bitumen recovery from Athabasca Oil Sands*, Kingsley Knowledge Pub., Cochrane, AB, **2011**.
11. J. Czarnecki, in *Encyclopedic Handbook of Emulsion Technology*, ed. J. Sjöblom, CRC Press, **2001**, 497–514.

12. U. G. Romanova, H. W. Yarranton, L. L. Schramm and W. E. Shelfantook, *Can. J. Chem. Eng.*, 2008, **82**, 710–721.
13. C. Angle, in *Encyclopedic Handbook of Emulsion Technology*, ed. J. Sjöblom, CRC Press, **2001**, 541–594.
14. M. A. Krawczyk, D. T. Wasan and C. Shetty, *Ind. Eng. Chem. Res.*, 1991, **30**, 367–375.
15. A. A. Peña, G. J. Hirasaki and C. A. Miller, *Ind. Eng. Chem. Res.*, 2005, **44**, 1139–1149.
16. Y. Fan, S. Simon and J. Sjöblom, *Energy Fuels*, 2009, **23**, 4575–4583.
17. A. Pradilla, S. Simon and J. Sjöblom, *Energy Fuels*, 2015, **29**, 5507–5518.
18. I. Kailey and J. Behles, *Ind. Eng. Chem. Res.*, 2015, **54**, 4839–4850.
19. P. Laplante, M. B. Machado, S. Bhattacharya, S. Ng and S. M. Kresta, *Fuel Process. Technol.*, 2015, **138**, 361–367.
20. E. Pensini, D. Harbottle, F. Yang, P. Tchoukov, Z. Li, I. Kailey, J. Behles, J. Masliyah and Z. Xu, *Energy Fuels*, 2014, **28**, 6760–6771.
21. Y. Si, Q. Fu, X. Wang, J. Zhu, J. Yu, G. Sun and B. Ding, *ACS Nano*, 2015, **9**, 3791–3799.
22. J. Liu, X. Li, W. Jia, Z. Li, Y. Zhao and S. Ren, *Energy Fuels*, 2015, **29**, 4644–4653.
23. Q. Ma, H. Cheng, A. G. Fane, R. Wang and H. Zhang, *Small*, 2016, 1–17.
24. C. Liang, Q. Liu and Z. Xu, *ACS Appl. Mater. Interfaces*, 2015, **7**, 20631–20639.

Chapter 7. Interfacially Active Magnetic Particles

Chapter 7. : *Interfacially active Magnetic Particles. A version of this section has been submitted for consideration of publication.*

Magnetically-responsive and interfacially active composite particles, comprising an inner magnetic core and an outer layer of interfacially active material, were prepared by firstly priming the surface of iron oxide (Fe_3O_4) particles with sodium carboxymethyl cellulose (CMC) and subsequently coating primed particles with a surface layer of ethylcellulose (EC). In contrast to previous preparations, the sequential adsorption of contrasting cellulosic material produces magnetically-responsive and interfacially active composite particles in an energy efficient process, without unnecessary derivatization reactions, while generating little waste. The resulting composite particles are biwetttable and thus effectively partition at the interface formed by two immiscible liquids such as oil and water. Once attached on the oil-water interface, magnetically-tagged multiphase materials (including emulsion droplets, rag layers and sludge) are effectively manipulated under an applied magnetic field. CMC functioned to improve colloidal stability of dispersed Fe_3O_4 particles and helped limit aggregation during EC-adsorption. Enhanced phase separation of emulsions, rag layers and sludge was demonstrated using magnetically-responsive and interfacially active composite particles. The composite particles, which are subsequently reused, were regenerated by washing the collected biphasic material with appropriate solvent.

7.1 Introduction

Formation of emulsion droplets, rag layers and sludge is often inevitable during various stages of petroleum production due to the immiscible nature of water introduced and the high levels of shear encountered throughout the process. Petroleum emulsions for example are very difficult to break when surfactants and fine biwetting particles, which are either added as process aids or indigenous to the formation, are present in significant concentrations. Effective strategies for breaking emulsions are required as most industrial processes do not operate optimally when

multiple phases are present. Although numerous techniques have been developed, rapid and effective phase separation remains a challenge for tight emulsions with droplets less than 10 μm . Magnetic separation/breaking of biphasic material is possible using magnetically-responsive and interfacially active particles that readily attach to the interface of two immiscible liquids.^{1,2} The magnetic particles, partitioned at the interface, impart magnetic susceptibility to the tagged dispersion of droplets and/or particles. Emulsified droplets, rag layers and sludge are subsequently concentrated or broken under an applied magnetic field.

Many strategies have been devised for preparation of functionalized magnetic particles. The general approach includes synthesis of magnetic particles followed by their functionalization. Superparamagnetic nanoparticles are prepared by co-precipitation, thermal decomposition, hydrothermal synthesis and from microemulsions.^{3,4} Nanoparticles are typically more reactive than their bulk counterparts due in part to their increased specific surface area, and therefore require either protection or stabilization to prevent unwanted reactions and/or aggregation. Common materials used to coat nanoparticles for this purpose include surfactants, polymers, noble metals, silica and carbon.^{3,4} The type of materials used to coat the surface of magnetic nanoparticles is critical to the scope of the subsequent possible transformations.

Cellulose is a natural polymer, consisting of repeating anhydroglucose units, derived from plant material where it is generally used as a structural component. Cellulose contains numerous polar functional groups and does not dissolve in non-polar solvents such as hydrocarbons. Although cellulose contains a large number of hydroxyl groups (hydrophilic), it is insoluble in water. The abundance of intra- and intermolecular hydrogen bonding is believed to be the main cause for preventing the dissolution of cellulose in water, while the hydrophobic interaction may also be a significant contributor.⁵ To produce materials with unique properties and functionalities, the structure of cellulose is often chemically modified. Each repeating anhydroglucose unit, containing up to three hydroxyl groups, can undergo a variety of chemical reactions to produce derivatives such as cellulose ether and/or cellulose ester. The physicochemical properties of functionalized cellulose including its solubility are influenced by molecular weight, degree substitution and the chemical nature of the substituted functional groups. Cellulose derivatives share a certain degree of structural similarity and can interact with

other cellulose derivatives through intermolecular forces, which form the basis of one of the current approaches of preparing interfacially active and magnetically-responsive composite particles.

The surface of iron oxide particles acquires surface charges in aqueous environment. Functional groups known to bind chemically to the surface of iron oxide particles include phosphates, sulphates and carboxylates.³ Experience from flotation of iron ores demonstrated that sodium oleate is a strong collector for iron oxides.^{6,7} The negatively charged moiety of fatty acid salts is attracted to the positively charged surface of iron-containing minerals such as hematite and magnetite.⁷ Carbohydrates such as starch and dextran are used on the other hand as depressants of hematite in reverse flotation of silica using cationic collectors.⁸ Starch is believed to be attracted to or adsorbed on the surface of hematite through strong hydrogen bonding.⁶ Carboxymethyl cellulose is therefore anticipated to adsorb on iron oxide due to its cellulosic structure and the presence of multiple anionic carboxylate functional groups.

In addition to chemical composition of solid particles, the adsorption of CMC on metal oxide surfaces in solution is also influenced by pH, temperature and electrolyte concentration. CMC was shown to be favourably deposited onto pure cellulose films, while only an insignificant adsorption of CMC on other hydrophilic surfaces such as silicon dioxide and polyvinyl alcohol-coated surfaces was observed.⁹ QCM-D studies revealed the adsorption of CMC on regenerated cellulose.¹⁰ At the same ionic strength, divalent cations (*i.e.*, CaCl₂) were shown to increase the adsorption of CMC more significantly than monovalent cations (*i.e.*, NaCl). The characterization using a combination of surface plasmon resonance (SPR) spectroscopy and QCM-D showed 90 – 95 % water in the CMC layers on cellulose.¹⁰

Interfacially active particles exhibit a strong affinity for the interface formed by two immiscible liquids such as oil and water. The affinity of a solid for a specific phase (*i.e.*, water or solvent) is characterized by its wettability. A hydrophilic material with the contact angle measured through water much less than 90° locates more favorably in aqueous solutions; while a hydrophobic material with contact angle much greater than 90° would be more favorably located in non-aqueous solutions. Biwetting materials with contact angle close to 90° are interfacially active and readily anchored at the oil-water interface. Solid particles anchored at the

oil-water interface of emulsified droplets may provide a physical barrier that can prevent emulsified droplets from contacting one another, leading to stable Pickering emulsions and retarding phase separation.

In a previous study, ethylcellulose (EC) was found to be an effective demulsifier for breaking water-in-diluted bitumen emulsions.¹¹⁻¹³ EC is a derivative of cellulose wherein a portion of hydroxyl groups are substituted with ethoxy groups through a chemical reaction.¹² In solution, EC is capable of adsorbing at the bitumen-water interface and displacing indigenous stabilizers from bitumen. Using EC as a chemical demulsifier, over 90 % of emulsified water was removed by gravity settling from water-in-diluted bitumen emulsions at 70°C.¹⁴ The effectiveness of EC in promoting phase separation was further demonstrated after chemical attachment onto magnetic particles.^{1,2,15,16} Compared to gravity settling, enhanced dewatering provided by the additional magnetic force was possible. EC-grafted magnetic particles prepared by chemical functionalization showed an enhanced dewatering performance by promoting droplet coalescence. Furthermore, EC-grafted magnetic particles could be readily separated from the mixture using a magnet and subsequently reused. However these particles are difficult to prepare, requiring several different chemical reactions in different solvents, as shown in **Figure 7-1A**. Specifically, the preparation of magnetic demulsifier particles in the early studies involved the following steps: i) coating superparamagnetic iron oxide (Fe_3O_4) nanoparticles with silica; ii) modification of silica-coated particles with amino groups using appropriate silane coupling reagent (*e.g.*, 3-aminopropyl triethoxysilane); iii) chemical activation of EC using suitable reagent (*e.g.*, 2-bromopropanoyl bromide); and finally iv) chemical attachment of activated EC onto amino-functionalized silica-coated magnetic particles.¹ A variety of chemical functional groups can be installed onto the surface of silica particles or silica-coated particles using different silane coupling reagents. Further chemical reactions can be used to graft interfacially active substances such as polymeric demulsifiers onto silica-coated particles.²

In this chapter, a simple method of producing magnetically-responsive and interfacially active particles, shown in **Figure 7-1B**, is presented. This method does not require chemical derivatization and generates very little waste. The surface of magnetic Fe_3O_4 particles was first primed with carboxymethyl cellulose (a natural product from plants) and subsequently coated

with ethylcellulose (also a natural product from plants). More importantly, the same cellulosic materials may be used to produce interfacially active composite particles.¹⁶ Interfacially active particles, prepared by coating magnetic particles with cellulosic materials, were effectively employed in magnetic separation of biphasic material such as diluted-bitumen emulsion droplets, dispersed phase in rag layer and sludge from food processing, production of pharmaceuticals and formulation of cosmetics.

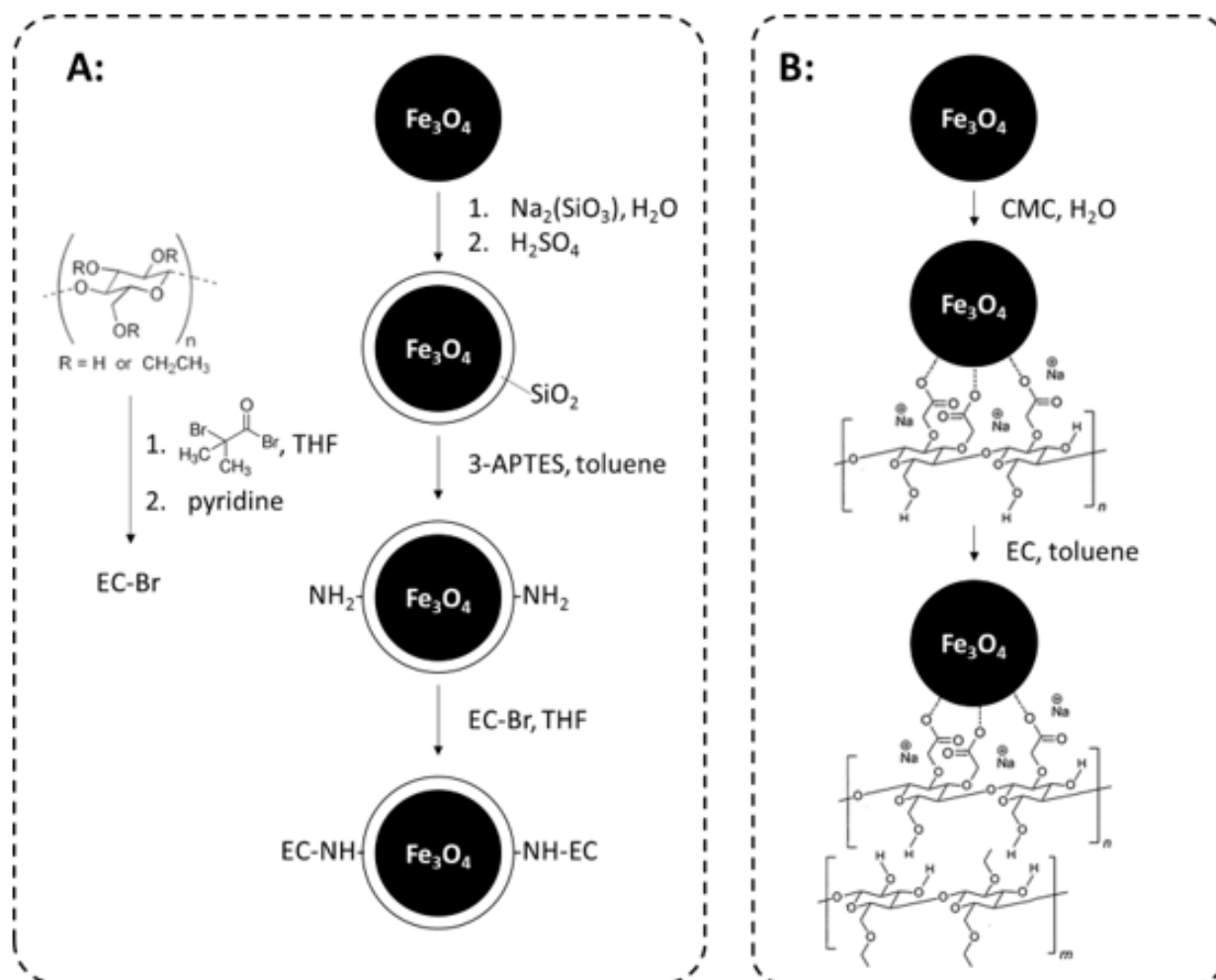


Figure 7-1. Schematic diagram of a magnetically-responsive and interfacially active composite particle prepared from iron oxide (Fe_3O_4) for use in separation of biphasic materials using two different approaches: **A**) chemical functionalization of amine-grafted silica-coated magnetic particles using chemically-activated ethylcellulose (EC); or **B**) sequential adsorption of sodium carboxymethyl cellulose (CMC) and EC onto magnetic particles.

7.2 Experimental

Materials: Sodium carboxymethyl cellulose (Sigma-Aldrich; molecular weight: 250 000 g/mol; degree substitution: 0.7), ethylcellulose (Sigma-Aldrich; ethoxy content: 42%), iron oxide nanoparticles (Fe_3O_4 ; Sigma-Aldrich; < 50 nm), toluene (Fisher Scientific; ACS grade), acetone (Fisher Scientific; ACS grade), methanol (Fisher Scientific; ACS grade), ethanol (Commercial Alcohols; 99%) and 2-propanol (Fisher Scientific; ACS grade) were used as received without further purification. Both vacuum distillation feed bitumen and plant recycle process water were provided by Syncrude Canada Ltd. and used to prepare water-in-diluted bitumen emulsions. The pH of the process water was adjusted to 8.9 prior to emulsification. Deionized water (>18.0 MW/cm) was supplied from Thermo-Fisher Barnstead Nanopure ultrapure water purification system.

Instrumentation: Hydrodynamic diameters of particles and emulsions were obtained using a Malvern Mastersizer 3000 instrument with an extended volume dispersion accessory or Malvern Zetasizer Nano instrument. Zeta-potential of solid particles was measured using a Malvern Zetasizer Nano instrument. In this case, particles were first dispersed in a small amount of methanol and diluted in water prior to taking measurements. Thermal properties of synthesized particles were investigated using a TA Instruments Q200 thermo-gravimetric analyzer to estimate the amount of cellulosic materials coated on solid surfaces. Water content of emulsions was determined by Coulometric Karl-Fischer titration using G.R. Scientific Cou-Lo 2000 automatic titrator.

Preparation of Magnetically-Responsive and Interfacially active Particles: Iron oxide particles were first washed with acetone and dried under nitrogen. Washed particles were well-dispersed in the aqueous solution using a Fisher Scientific Model 500 ultrasonic dismembrator. A dilute 1.0 wt% aqueous CMC solution was prepared and combined with the dispersion of magnetic particles to prime magnetic particles with CMC. The mixture of CMC and magnetic particles was placed in an ultrasonic bath to ensure particles remain dispersed. The CMC-primed magnetic particles were liberally washed three times with deionized water and three times with ethanol. After each washing, nanoparticles were separated using a permanent magnet for 2 h. Magnetic particles primed with CMC were dispersed in toluene, combined with a dilute 1.0 wt% EC solution

prepared in toluene, and the combined mixture was placed in ultrasonic bath. EC-coated magnetic particles were washed three times with toluene and three times with ethanol. After each washing, particles were separated using a permanent magnet. Recovered particles were dried in an oven at 105 °C under reduced pressure. To prepare suspensions of the synthesized particles for characterization or use in separation of biphasic systems, the particles were first wetted by a small amount of methanol and subsequently diluted with deionized water. The dispersion was achieved using an ultrasonic dismembrator followed by an ultrasonic bath for 0.2 h. A small aliquot of the dispersion was transferred to an aqueous 1 mM KCl electrolyte solution and the zeta-potential was measured at ambient temperature.

Critical Surface Tension: To confirm the biwettable nature of the synthesized particles, the critical surface tension of the particle was determined by conducting film flotation experiments using binary solutions of water and methanol. The surface tension of binary water-methanol solutions ranges from 22.5 mN/m for pure methanol to 72.8 mN/m for pure water. In order to probe particle wettability, a known quantity of solid particles was carefully placed on top of the solutions containing different proportions of methanol and water. After 30 s, any particles remaining on the surface of the solution were physically separated and dried overnight in an oven at 105°C under reduced pressure. The mass fraction of the particles remaining on the surface was plotted as a function of the liquid surface tension and the critical surface tension of the particles was estimated as the surface tension of the solution for which one half of the particles remained on the surface of the solution.

Separation of Solids from Oil Sands Ore: A 100 g sample of oil sands ore was defrosted, manually broken up and washed liberally with a mixture of toluene/2-propanol. Mineral particles of sizes greater than approximately 0.5 cm were removed using a screen filter. The remaining under size suspension was placed in an ultrasonic bath for 0.5 h. Solids were separated based on size using mesh sieves and additional 2-propanol. Sorted solids were washed with toluene, separated using a centrifuge, and dried in an oven at 105°C under reduced pressure.

Contact Angle Measurement: The static contact angle of water droplets was measured using Krüss DSA instrument. Small water droplets (3 – 4 mm) suspended from the tip of the needle point were brought carefully in contact with the substrate. Upon contact with the substrate, the

water droplet detached from the needle and spread on the substrate. The contact angle of the water droplet on the substrate was measured immediately after the three phase contact line stopped moving and monitored for 100 s. The contact angle measured as such represents the advancing equilibrium contact angle or static contact angle.

Preparation Biphasic Material: A mineral oil emulsion sample containing 1 wt% solids recovered from oil sands ore with particle size less than 44 μm and 10 wt% process water, was prepared. The mineral emulsion sample was emulsified for 30 s using a high-speed homogenizer at 10 000 rpm. Free water was rejected from the emulsion sample by carefully removing the aqueous layer into a separate beaker. The water content of the mineral oil emulsion stabilized by oil sands ore fine solids was accurately determined by Coulometric Karl-Fischer titration. Another sample was prepared using mineral containing 25 wt% dispersed oil sands ore solids with particle size less than 44 μm and process water. The solids were first dispersed in mineral oil assisted by ultra-sonication in an ultrasonic bath for 300 s.

In addition, various biphasic mixtures were prepared using vacuum feed bitumen diluted with 40 wt% toluene, industrial process water and solids recovered from oil sands ore. The volume ratio of oil to water was kept constant at 1.0. Mixtures were prepared using either low concentration (0.5 wt%) small solids of sizes less than 44 μm or high concentration (5.0 wt%) large solids of sizes between 44 – 90 μm . The oil sands ore solids were first wetted by a small amount of ethanol and dispersed in process water assisted by ultra-sonication in an ultrasonic bath for 300 s. An equal volume of diluted-bitumen was subsequently added to the aqueous dispersion and the biphasic mixture was mechanically agitated for 30 s.

7.3 Results and Discussion

The outermost surface of a particle is known to have a foremost effect on its colloidal stability, especially for nanoparticles which are more susceptible to aggregation due to their high specific surface area. Several factors can influence the colloidal stability of iron oxide particles, including particle concentration, ionic strength of the suspension, pH, and the presence of stabilizers, which work as a result of either electrostatic (*e.g.*, citric acid) or steric (*e.g.*, non-ionic polymers) repulsion. The colloidal stability of iron oxide nanosized particles was inferred by

measuring particle size using light scattering at very low concentration (50 mg/L), as shown in **Figure 7-2**. The unmodified iron oxide nanosized particles (**NP**) formed larger aggregates of approximately 400 nm shortly after dispersing in deionized water by an ultrasonic dismembrator. The surface of iron oxide (Fe_3O_4) has an isoelectric point around 6.5 – 6.8 and therefore has limited charge in neutral aqueous solutions.¹⁷ At high pH of 11, the surface of iron oxide acquired higher charge and exhibited less aggregation, leading to a well-dispersed state with a mean particle size of 44 nm. Similarly, the presence of strong anionic surface charge on iron oxide nanosized particles with adsorbed CMC (**NP-CMC**) reduced the effect of aggregation with mean particles size of 51 nm. Aggregation of magnetic particles in suspensions with high particle concentrations (*e.g.*, 1 g/L) was even more noticeable and sedimentation is clearly evident, as shown in **Figure 7-3**. Even at pH = 11, **NP** particles formed aggregates that sediment within 6 h. In contrast, **NP-CMC** particles exhibited improved colloidal stability and less sedimentation.

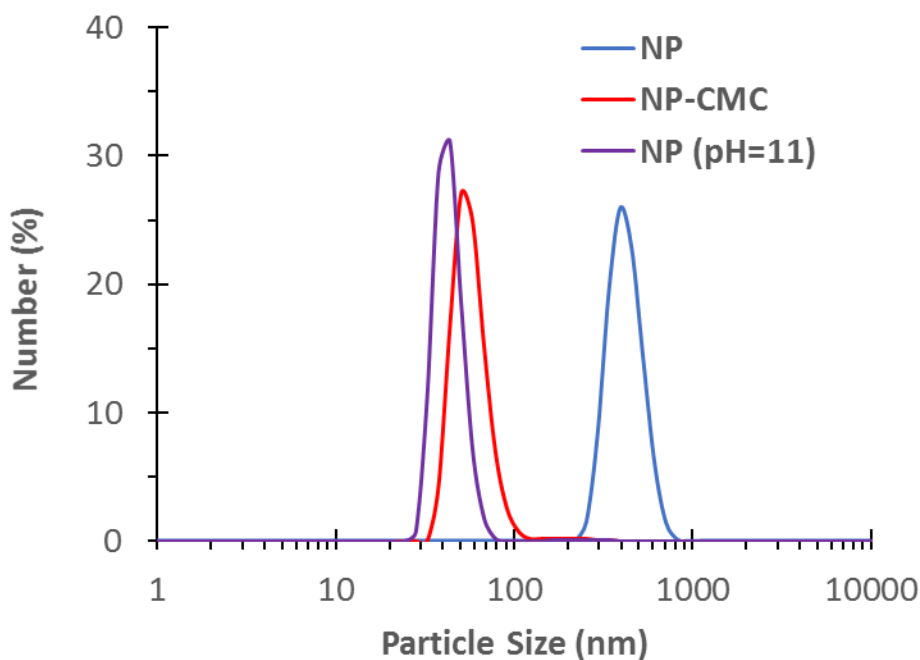


Figure 7-2. The size distribution of iron oxide nanoparticles (**NP**) at neutral pH showed varying levels of aggregation at 50 mg/L. Following an increase in suspension pH to 11 or adsorption of an anionic cellulosic derivative (**NP-CMC**), aggregation was significantly reduced.

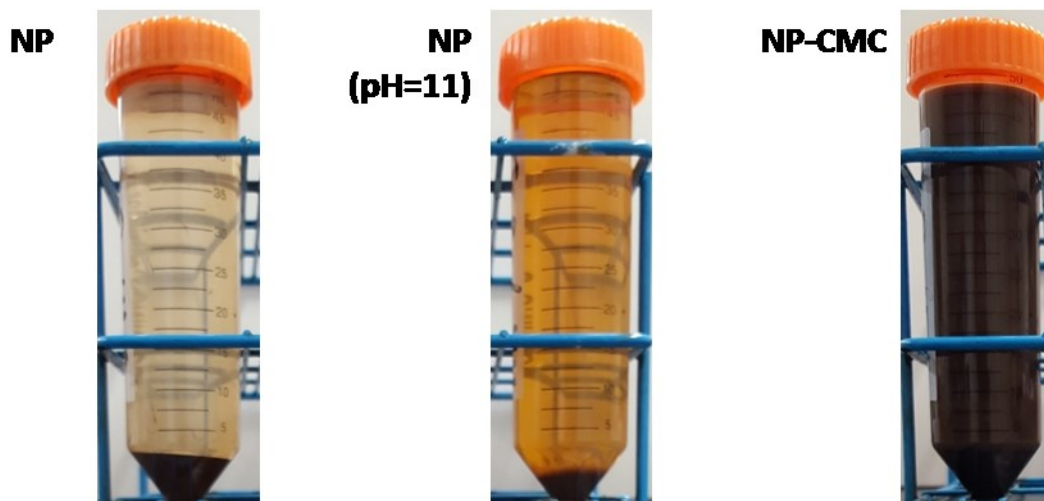


Figure 7-3. Sedimentation of high concentration (1 g/L) iron oxide particle suspensions. Unmodified **NP** particles settle within 6 h at both neutral pH and pH = 11, while particles coated with anionic cellulosic derivative (**NP-CMC**) showed much greater colloidal stability and remained dispersed.

The zeta-potential of magnetic Fe_3O_4 nanoparticles after coating with CMC and EC is shown in **Figure 7-4**. Zeta-potential of uncoated magnetic nanoparticles (**NP**) in a 10 mM KCl solution at pH = 4 was $+ 23.3 \pm 1.7$ mV. Following the absorption of CMC onto surface of Fe_3O_4 particles, the zeta-potential of primed magnetic nanoparticles (**NP-CMC**) in a 10 mM KCl solution at neutral pH was reversed to $- 22.0 \pm 1.0$ mV. CMC is anionic due to the presence of carboxylate functional groups that are capable of interacting with the surface of Fe_3O_4 . The structure of EC lacks charged functional groups and is non-ionic. **NP-CMC** particles were coated with EC by adsorption using very dilute suspensions (*e.g.*, 5 mg/L) to avoid formation of larger aggregates. After further coating with EC, the zeta-potential of magnetic nanoparticles (**NP-CMC-EC**) was reduced to 0.0 ± 0.4 mV, indicating effective surface coverage of **NP-CMC-EC** with uncharged EC. **NP** coated directly with EC produced only large aggregates, even at low concentration.

In order to preserve the magnetic properties of iron oxide nanoparticles, it is important that the individual particles remain well dispersed. Although the high magnetic susceptibilities and superparamagnetic properties of iron oxide nanoparticles are desirable, magnetic collection of submicron size particles is much slower compared to micron-size particles. Therefore, magnetically-responsive and interfacially active particles were prepared by sequential adsorption

of cellulosic derivatives of contrasting properties (*i.e.*, CMC and EC) on the surface of magnetic iron oxide (Fe_3O_4) particles at higher concentration to promote particle aggregation and hence increase the apparent particle sizes. The surface of nanosized iron oxide particles (**NP**) was first primed with a dilute 1.0 wt% aqueous CMC solution at 1 g/L particle concentration. The resulting aggregates of magnetic particles primed with CMC (**MAG-CMC**) were magnetically separated and subsequently coated with interfacially active EC using a 1.0 wt% EC-in toluene solution to produce magnetically-responsive and interfacially active micro-aggregate particles (**MAG-CMC-EC**). **NP** particles were also dispersed directly in 1.0 wt% EC-in toluene solution using the same concentration to produce EC-coated aggregate particles (**MAG-EC**). Direct adsorption of uncharged cellulosic derivative EC on iron oxide surface from organic solutions was possible mainly through hydrogen bonding.

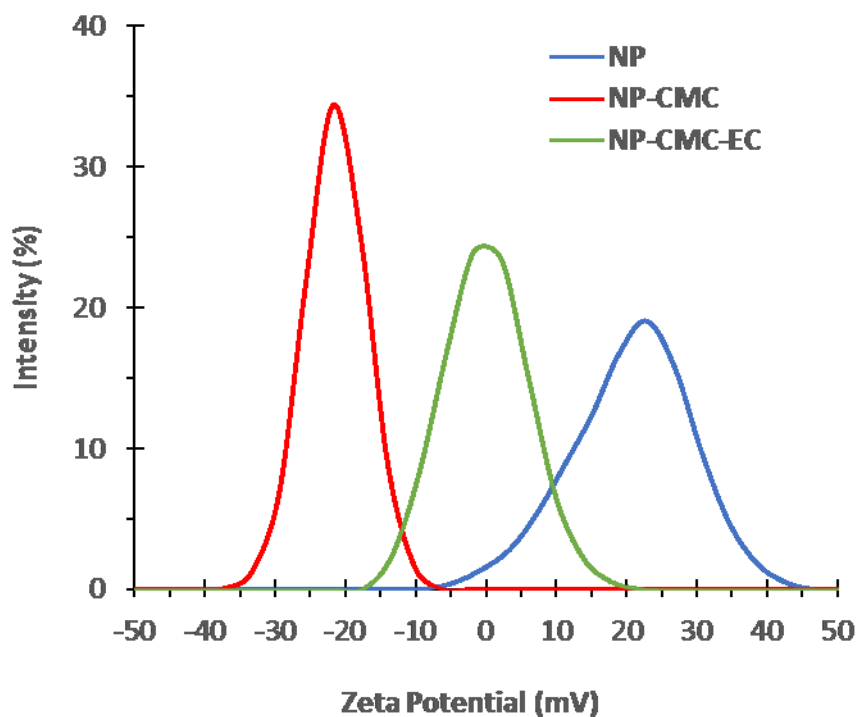


Figure 7-4. Surface charge of well-dispersed iron oxide nanoparticles (**NP**), measured by zeta-potential, changed following the adsorption of different cellulose derivatives including CMC (**NP-CMC**), an anionic cellulosic derivative, and EC (**NP-CMC-EC**), a non-ionic cellulosic derivative.

Particle size distribution of different magnetic particles is shown in **Figure 7-5**. Magnetically collected aggregates (**MAG-CMC**) of 3 μm are much larger compared to individual particles (**NP-CMC**) of approximately 41 nm. Only a very small increase in particle size to 7 μm was observed following EC adsorption (**MAG-CMC-EC**). However, for direct adsorption of EC (**MAG-EC**), particle aggregation without addition of chemical dispersing agent resulted in formation of large aggregates greater than 100 μm that could not be effectively dispersed. The particle size of **MAG-CMC-EC**, as prepared, is well-suited for oil-water separation, as smaller particles are slower to separate under a low-gradient magnetic field and larger particles are more difficult to disperse. The amount of CMC and/or EC adsorbed on **MAG-CMC-EC** and **MAG-EC** was estimated using thermogravimetric analysis and the results are summarized in **Table 7-1**. It is interesting to note only slightly less amount of EC adsorbed on untreated magnetic particles (**MAG-EC**) in comparison to the case of EC on CMC-adsorbed magnetic particles (**MAG-CMC-EC**), although there is a 10-time different in particle sizes, a decrease from 82 μm to 7 μm due to adsorption of CMC that effectively disperses magnetic iron oxide particles.

Table 7-1. Properties of magnetically-responsive particles prepared by adsorption of different cellulosic materials (CMC and/or EC).

Property	NP-CMC	MAG-EC	MAG-CMC-EC
CMC content* (wt%)	3 \pm 1	n/a	3 \pm 1
EC content* (wt%)	n/a	3 \pm 1	4 \pm 1
Mean particle size (μm)**	2.6 \pm 0.2	82 \pm 6	6.7 \pm 0.6
Critical surface tension *** (mN/m)	> 73	42 \pm 5	46 \pm 7

* Estimated using thermogravimetric analysis; ** measured using Malvern Instruments Mastersizer 3000 with Hydro EV accessory; *** measured using binary mixtures of methanol and water.

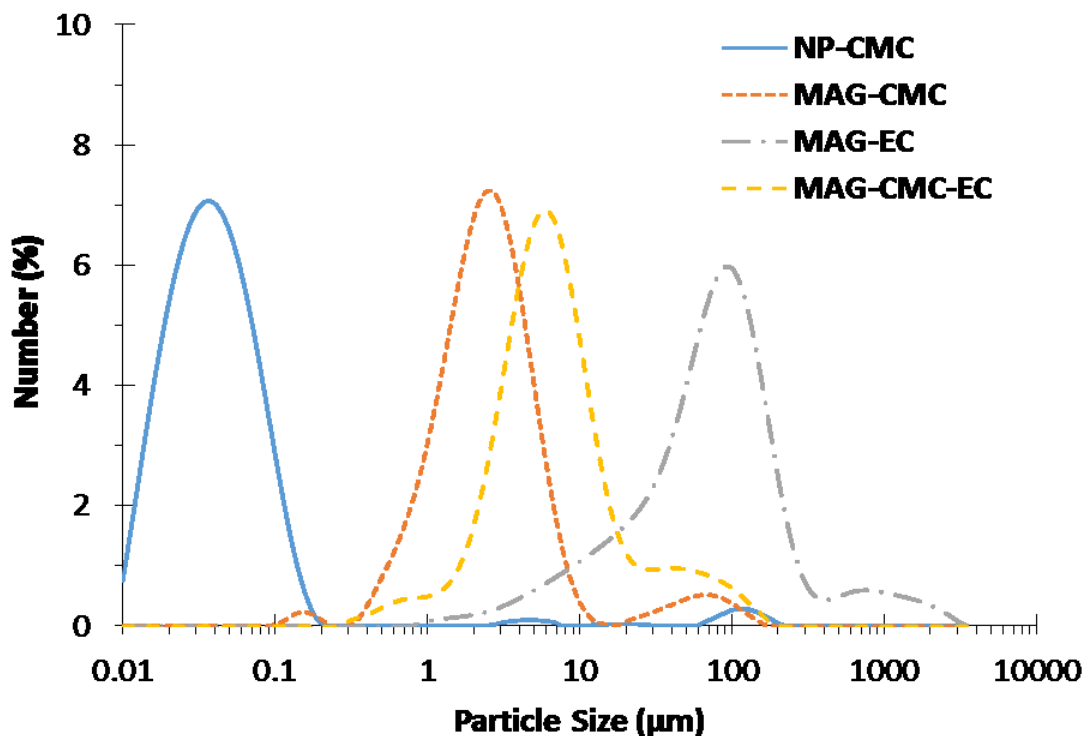


Figure 7-5. Particle size distribution of magnetically-responsive and interfacially active particles (**MAG-CMC-EC** and **MAG-EC**). **MAG-CMC-EC** is prepared by first priming iron oxide (Fe_3O_4) particles with CMC and subsequently adsorbing EC. **MAG-EC** is prepared by directly adsorbing EC on iron oxide. For comparison, the particle size distribution of non-aggregated **NP-CMC** is also shown as well as **MAG-CMC** micro-aggregates used to prepare **MAG-CMC-EC**.







Unmodified iron oxide nanoparticles (**NP**) were completely wet by pure water (73 mN/m). Similarly, CMC-primed magnetic particles (**NP-CMC**) and micro-aggregates (**MAG-CMC**) were also completely wet by pure water. This was expected as particles with polar or ionic species on its surface are generally more hydrophilic. After coating with EC, the critical surface tension, measured by film flotation using binary mixtures of methanol and water, was reduced to 46 ± 7 mN/m for **MAG-CMC-EC**. Similarly, directly coated **MAG-EC** exhibited a slightly lower critical surface tension of 42 ± 5 mN/m. The reduction in critical surface tension is indicative of the corresponding change in wettability as the surface of the magnetic particles become less hydrophilic after coating with non-ionic EC.

Compared with uncoated hydrophilic **NP** particles, EC-coated magnetic particles have lower surface charge (*i.e.*, having a zeta-potential close to zero) and are therefore less hydrophilic (*i.e.*, lack of ionic functional groups). Due to their modified wettability, **MAG-CMC-EC** particles are more effectively dispersed in non-aqueous solvent (*e.g.*, toluene) compared to bare **NP** particles, as shown in **Table 7-2**. In contrast, **MAG-CMC** primed with anionic cellulosic derivative (CMC) do not remain dispersed in toluene and settle rapidly. Furthermore, **MAG-CMC-EC** preferentially adsorbed on the interface formed between water and toluene, indicating that the magnetic particles coated with EC are interfacially active. To illustrate the ability of **MAG-CMC-EC** particles to attach to the oil-water interface, a small amount (approximately 50 mg) of **MAG-CMC-EC** was dispersed in toluene. An equal volume of water was carefully added to the dispersion and shaken gently. After leaving sample overnight at ambient conditions, **MAG-CMC-EC** remained adsorbed on the interface, as shown in **Table 7-2**. All coated magnetic particles remain magnetically-responsive and can be separated under a low-gradient magnetic field generated by a strong hand magnet. Unlike composite absorbent particles made from CMC and EC,¹⁶ water-absorption by magnetically-responsive and interfacially active micro-aggregate particles (**MAG-CMC-EC**) was limited to less than 1 wt%, based on its dry mass, due to the low CMC content on coated particles.

Separation of multiphasic material using magnetically-responsive and interfacially active micro-aggregate particles was demonstrated in different model systems including: 1) a solid-stabilized water-in-mineral oil emulsion and 2) a high-solid content mineral oil sludge. After preparing a water-in-mineral oil emulsion stabilized with fine solids recovered from oil sands ore, a known quantity of **MAG-CMC-EC** was dispersed in a minimal amount of toluene and added to the mixture. The mixture was placed in a vortex mixer for 30 s and left at ambient conditions under a magnetic field generated by a strong permanent magnet. The amount of emulsified water remaining was determined by Coulometric Karl-Fischer titration. The water-in-mineral oil emulsion, stabilized using 1 wt% fine solids (< 44 μm) recovered from oil sands ore, with an initial water content of 5.0 ± 1.1 wt%, was reduced to 1.2 ± 0.1 wt% after 12 h by gravity settling alone. Comparatively, the water content of the mineral oil emulsion treated with 0.3 wt% **MAG-CMC-EC** particles was reduced to 0.4 ± 0.1 wt% after only 3 h of magnetic separation. More rapid and effective dewatering of water-in-mineral oil emulsions was achieved under a magnetic field by

tagging the oil-water interface of emulsified water droplets with magnetically-responsive and interfacially active particles and concentrating tagged droplets under an applied magnetic field.

Table 7-2. Magnetically-responsive and interfacially active micro-aggregate particles (**MAG-CMC-EC**) having a greater colloidal stability in low polarity solvent (toluene) and better interfacial activity compared to both unmodified (**NP**) and CMC-primed (**MAG-CMC**) magnetic particles.

	NP	MAG-CMC	MAG-CMC-EC
Toluene:			
Toluene and Water:			

A mineral oil sample with 25 wt% oil sands ore solids dispersed therein was mixed with process water to prepare a high-solid content mineral oil sludge. Although pure mineral oil has a lower specific gravity than water, the high-solid content of the mineral oil mixture led to sedimentation of the sludge-like material, as shown in **Figure 7-6**. After preparing the mineral oil sludge, 0.3 wt% **MAG-CMC-EC** was added to the mixture. The sample was mixed in a vortex mixer for 30 s to allow **MAG-CMC-EC** particles to adsorb to the oil-water interface. Once tagged with magnetically-responsive and interfacially active particles, high-solid content mineral oil sludge in process water could be separated under a magnetic field, as shown in **Figure 7-6**.

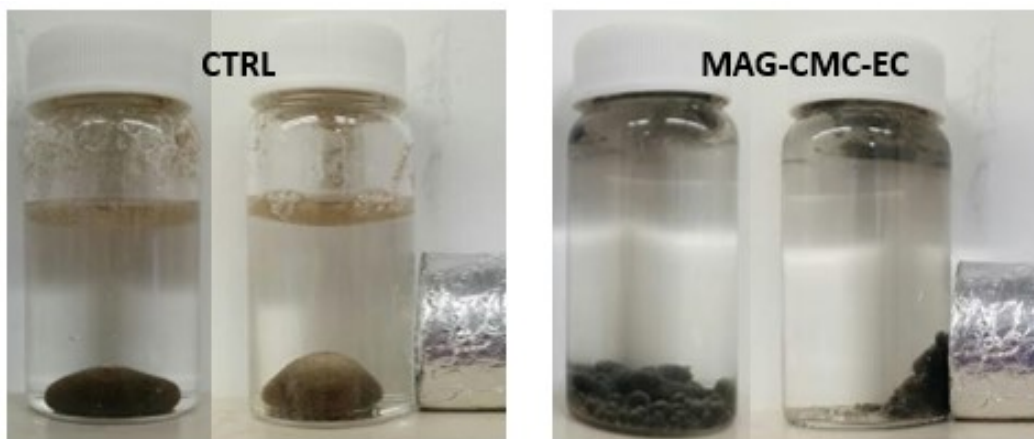



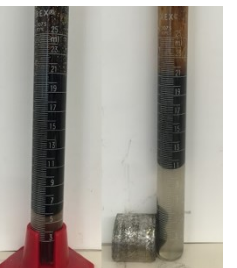


Figure 7-6. Magnetic separation of high-solids content mineral oil sludge in process water. Once tagged with magnetically responsive and interfacially active particles (**MAG-CMC-EC**), sludge is attracted to a permanent magnet. In the absence of **MAG-CMC-EC**, sludge was not responsive to magnetic field generated by permanent magnet.

Phase separation is sometimes hindered by solids which can cause a physical barrier between droplets and prevent both creaming/sedimentation and droplet coalescence. The resulting rag layer formed between the light and heavy phases prevents complete phase separation. Diluted-bitumen emulsions with high solids content were prepared using 5 wt% solids, based on mass of the oil phase, separated from oil sands ore either with particles size between 44 - 90 μm or with particles size less than 44 μm . After two days at ambient temperature, phase separation appeared to reach a standstill. A sludge-like mixture appeared in the lower phase of the emulsion sample containing larger solid particles (44 – 90 μm), as shown in **Figure 7-7A**. Phase separation in the sample containing smaller solid particles (< 44 μm) was extensively hindered by the presence of a thick rag layer, as shown in **Figure 7-7B**. In order to enhance phase separation, 0.3 wt% **MAG-CMC-EC** was added to each biphasic sample containing solids from oil sands ore of different size. The graduated cylinder containing the emulsion was agitated using a vortex mixer for 30 s and manually shaken for another 10 s. No significant changes were immediately observed following the addition of **MAG-CMC-EC** particles. However, solid-stabilized material in both samples was rapidly collapsed within 300 s under the influence of a strong magnet, which allows for a more complete phase separation, as shown in **Figure 7-7**.

A summary of the results of recycling tests of **MAG-CMC-EC** is provided in **Table 7-3**. Over 90 % of **MAG-CMC-EC** was recovered using a strong magnet after each cycle. Thermogravimetric analysis indicated that only a small amount (< 1 wt%) of organic material was coated onto **MAG-CMC-EC** after each use. More importantly, the critical surface tension of recovered **MAG-CMC-EC** remained similar after washing with toluene to remove organic material and 2-propanol to remove water. A slight decrease in the critical surface tension was observed following the third cycle and was likely due to residual organic material that was not completely washed away. However, the critical surface tension of the collected particles returned closer to its initial value in the subsequent fourth cycle. Even after several successive applications, **MAG-CMC-EC** remained interfacially active and effective in promoting separation of biphasic material under an applied magnetic field.

Table 7-3. Recycle of magnetically-responsive and interfacially active micro-aggregate particles (**MAG-CMC-EC**) following magnetic separation of rag layer from biphasic mixture of bitumen and process water.

CYCLE	1	2	3	4
				
Particles added (g)	1.00	0.81	0.60	0.40
Particles recovered (%)	98	95	93	98
Critical surface tension (mN/m)	57 ± 6	51 ± 12	34 ± 21	50 ± 13

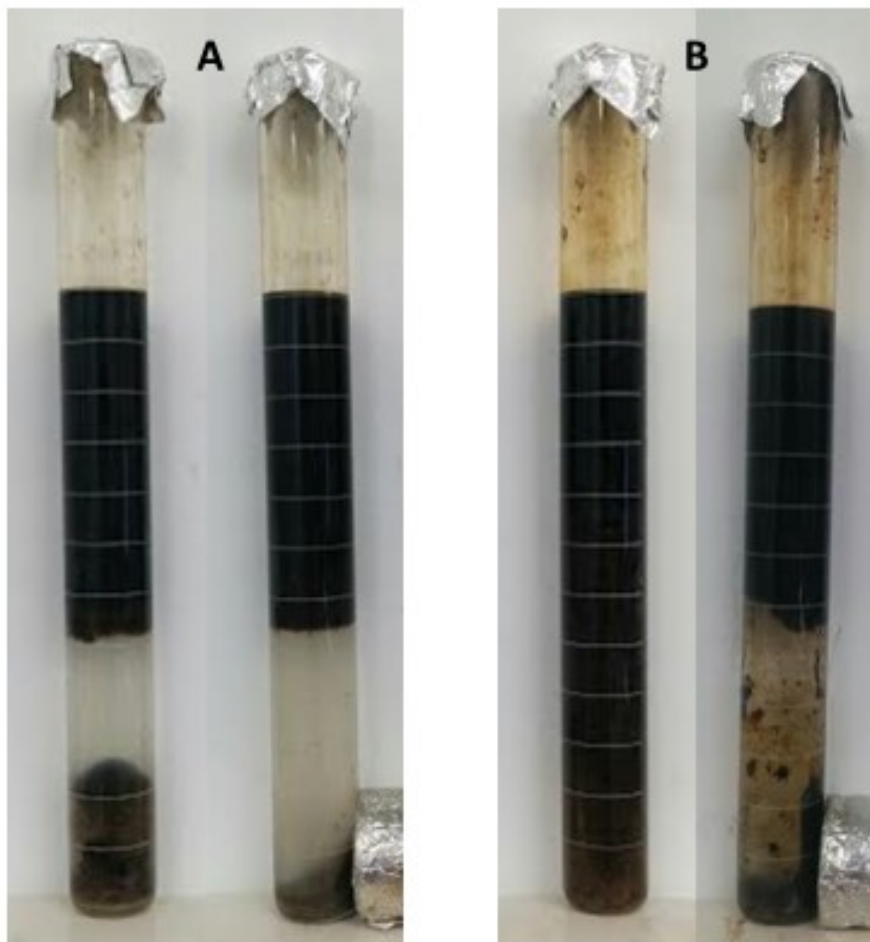


Figure 7-7. Magnetically-assisted phase separation of multiphase mixtures of process water, diluted-bitumen and mineral solids. Samples contain, based on the mass of the oil phase, either 5 wt% solid particles recovered from oil sands ore between 44 – 90 μm (**A**) or less than 44 μm (**B**). Enhanced phase separation of biphasic mixtures was possible under an external magnetic field after tagging with magnetically-responsive and interfacially active micro-aggregate particles (**MAG-CMC-EC**).

7.4 Conclusions

Magnetically-responsive and interfacially active particles (**MAG-CMC-EC**) were prepared by priming the surface of Fe_3O_4 particles with CMC and subsequently coating CMC-primed particles with a layer of EC, both through adsorptive processes in solution. The process combined the magnetic susceptibility of Fe_3O_4 with the interfacial activity of EC without requiring any chemical

derivatization reactions. CMC was used to improve the colloidal stability of Fe₃O₄ nanoparticles and enhanced the adsorption of EC on Fe₃O₄. The adsorption based process is simpler compared to chemical functionalization and generated significantly less chemical waste. The wettability of magnetic particles was altered following adsorption of different cellulosic derivatives, becoming more hydrophilic with CMC and less hydrophilic with EC. Adsorption of ionic CMC increased the amount of surface charge while adsorption of non-ionic EC reduced the amount of surface charge. After sequential adsorption of CMC and EC, the resulting biwetable magnetic particles attach to the interface formed by immiscible phases such as oil and water in either O/W or W/O systems. The oil-water interface of various biphasic wastes tagged with such magnetically-responsive and interfacially active particles becomes magnetically susceptible and allowed for enhanced magnetic separation of mineral oil emulsions, bitumen rag layer and mineral oil sludge. Furthermore, it is possible to recover the interfacially active magnetic particles in order to reuse them after washing the spent particles with a mixture of alcohol and toluene. Magnetic separation of non-magnetic targets, assisted by tagging using the targets with interfacially active magnetic particles, may be suitable as a method of removing biphasic waste from storage tanks and separations vessels without the need for complete shutdown.

7.5 References

1. J. Peng, Q. Liu, Z. Xu and J. Masliyah, *Adv. Funct. Mater.*, 2012, **22**, 1732–1740.
2. J. Peng, Q. Liu, Z. Xu and J. Masliyah, *Energy Fuels*, 2012, **26**, 2705–2710.
3. S. Laurent, D. Forge, M. Port, A. Roch, C. Robic, L. Vander Elst and R. N. Muller, *Chem. Rev.*, 2008, **108**, 2064–2110.
4. M. Mahmoudi, S. Sant, B. Wang, S. Laurent and T. Sen, *Adv. Drug Deliv. Rev.*, 2011, **63**, 24–46.
5. B. Medronho, A. Romano, M. G. Miguel, L. Stigsson and B. Lindman, *Cellulose*, 2012, **19**, 581–587.

6. D. W. Frommer, *J. Am. Oil Chem. Soc.*, 1967, **44**, 270–274.
7. K. Quast, *Miner. Eng.*, 2006, **19**, 582–597.
8. K. Shrimali and J. D. Miller, *Trans. Indian Inst. Met.*, 2016, **69**, 83–95.
9. R. Kargl, T. Mohan, M. Bračič, M. Kulterer, A. Doliška, K. Stana-Kleinschek and V. Ribitsch, *Langmuir*, 2012, **28**, 11440–11447.
10. Z. Liu, H. Choi, P. Gatenholm and A. R. Esker, *Langmuir*, 2011, **27**, 8718–8728.
11. X. Feng, Z. Xu and J. Masliyah, *Energy Fuels*, 2009, **23**, 451–456.
12. X. Feng, P. Mussone, S. Gao, S. Wang, S.-Y. Wu, J. H. Masliyah and Z. Xu, *Langmuir*, 2010, **26**, 3050–3057.
13. J. Hou, X. Feng, J. Masliyah and Z. Xu, *Energy Fuels*, 2012, **26**, 1740–1745.
14. S. Wang, J. Liu, L. Zhang, J. Masliyah and Z. Xu, *Langmuir*, 2010, **26**, 183–190.
15. S. Li, N. Li, S. Yang, F. Liu and J. Zhou, *J Mater Chem A*, 2014, **2**, 94–99.
16. C. Liang, Q. Liu and Z. Xu, *ACS Appl. Mater. Interfaces*, 2015, **7**, 20631–20639.
17. Points of Zero Charge. in *Chemical Properties of Material Surfaces*, CRC Press, **2001**, 731–744.

Chapter 8. Summary and Future Work

The petroleum industry faces a continually changing environment. Growth in developing unconventional petroleum resources should continue as more conventional petroleum resources are depleted. In this regards, technology remains a key determinant due to the more challenging nature of unconventional resources. The multifaceted nature of most recovery processes is a major source of operational problems for separation of bitumen from oil sands ore deposits. Oil sands ore is a complex mixture of bitumen, water and various types of minerals. Although the aqueous extraction process is generally effective in separating bitumen, several difficult dispersed multiphase systems are generated. Various responsive composite particles were designed, synthesized and tested in order to provide new methods of dispersed multiphase systems including bitumen emulsions, rag layers and sludge.

8.1 Summary

In a multistep process wherein the specifications of one step are unsuitable for the others, additional separation steps are required to remove the incompatibility. It is therefore more beneficial if process aids and other additives are capable of performing the desired functions in more than one process step or are designed with a separation method specifically adapted to the process. Composite materials are made in order to enhance or combine various properties. The ability to combine the properties of different materials in a single composite particle is useful in preparing particles with complex behaviour. Responsive particles are prepared by incorporating responsive materials into the composite particle. The design of a smart system is possible using a particle that can undergo a change in its physicochemical properties under specific environmental conditions. The change may be induced by an applied trigger or a physicochemical change associated with the process. Composite particles were prepared using different approaches including chemical functionalization and emulsion droplet dehydration in order to produce particles with responsive behaviour suitable for separation of biphasic wastes.

Enhanced separation of biphasic material (*i.e.*, emulsions, rag layers and sludge) encountered during bituminous sand, oil sand or tar sand extraction was demonstrated using

various original composite particles with responsive behaviour. Various methods of preparing composite particles (*i.e.*, chemical functionalization, emulsion droplet dehydration and sequential adsorption) were used to combine the desirable properties of different materials and incorporate responsive behaviour. The physicochemical properties of responsive composite particles were susceptible to different stimuli including: i) CO₂, ii) water-absorption and iii) an applied magnetic field.

Composite particles were prepared with responsive surface by chemical functionalization. Specifically, the surface of silica particles was modified using silane coupling reagents and subsequent chemical transformations. This method produced particles with basic switchable surface groups that ionize in the presence of CO₂ in aqueous solution, wherein they form a bicarbonate salt. The reaction with carbonic acid in water is reversible and CO₂-responsive functional groups revert back to their basic non-ionic form after sparging the solution with air to remove dissolved CO₂. Silica particles prepared with the different ratios of hydrophilic and hydrophobic surface groups could reversibly stabilize both oil-in-water emulsions and water-in-oil emulsions. Both the colloidal behaviour of CO₂-responsive particles and the stability of emulsions stabilized by CO₂-responsive particles are effectively controlled by applying/removing the appropriate trigger (CO₂). The use of switchable particles to prepare both O/W and W/O emulsions with controlled stability clearly illustrated the effectiveness of responsive particles in controlling behaviour of multiphase dispersed systems.

Furthermore, composite particles consisting of a CMC core coated with EC were prepared by dehydration of specially prepared emulsion droplets. The method of producing composite absorbent particles takes advantage of the contrasting characteristics of CMC and EC. CMC is hydrophilic and soluble in water while EC is hydrophobic, interfacially active and soluble in organic solvents. Following dehydration of water-in-oil droplets, hydrophilic material (CMC) remains within the core while interfacially active material (EC) remains on the surface of the residual particles. The surface of the composite absorbent particles, prepared using this method, was of intermediate wettability and could be dispersed in low-polarity solvents but remained water-permeable. However, following water-absorption, the surface of composite absorbent particles becomes more hydrophilic, which lead to the formation of larger aggregates in non-

aqueous environment. Additionally, composite particles made by emulsion droplet dehydration can incorporate a number of supplemental hydrophilic materials in order to impart additional responsive properties including magnetic susceptibility. Hydrophilic particles such as Fe_3O_4 remain dispersed inside emulsified water droplets undergoing dehydration and are eventually incorporated within the residual solid particles, which become magnetically susceptible and efficiently separated under an applied magnetic field. Emulsion droplet dehydration is an original and robust method of producing composite particles, which can accommodate a variety of materials and incorporate their advantageous properties.

Water is incompatible with certain processes in petroleum production and often causes accelerated corrosion in process equipment. Bitumen recovered from bitumen froth contains emulsified water droplets that require much greater effort to completely remove. Emulsion dewatering by absorption was possible using specially-prepared composite absorbent particles comprising a water-absorbent matrix and an interfacially active surface. Composite absorbent particles were prepared by dehydration of emulsified droplets from specially-prepared emulsions. The properties of the composite absorbent particles were ideally suited for separation of emulsified water droplets. The initial intermediate wettability allowed composite absorbent particles to be effectively dispersed into an oil-continuous emulsion. The initial size of the composite absorbent particles is similar to the size emulsified droplets, which increases contact with emulsified water droplets and increases the rate of absorption. The responsive behaviour of composite absorbent particles facilitated subsequent separation, as larger aggregates settle quicker under gravity and/or may be removed using a simple screen filter. Magnetic composite absorbent particles are readily removed under an applied magnetic field.

Moreover, composite particles were prepared by directly modifying the surface of Fe_3O_4 particles through sequential adsorption of CMC in aqueous solution followed by EC in organic solution. The sequential adsorption method is much simpler and greener compared to the multistep chemical functionalization process, which relied on difficult chemical reactions and generated various chemical wastes. CMC improved colloidal stability of dispersed Fe_3O_4 particles and enhanced adsorption of EC. The surface of the specially-designed interfacially active magnetic particles is biwettable, having similar affinity for both oil and water. Thus, interfacially

active magnetic particles attach and remain at the oil-water interface and impart their magnetic susceptibility to the tagged material.

Complex multiphase mixtures such as rag layers and sludge form inside separation and storage vessels, which can effectively hinder phase separation. Accumulation of rag layer and sludge is an operational issue that requires equipment shutdown if left unmitigated. Magnetic separation of dispersed multiphase mixtures (*e.g.*, emulsions, rag layers and sludge) was possible using interfacially active magnetic particles that effectively attach to the oil-water interface of the dispersed phase within the multiphase mixture. Tagged material can be subsequently separated and collected under an applied magnetic field. The interfacially active magnetic particles could be reused after washing biphasic material with a mixture of solvent and alcohol.

Numerous unit operations involving complex physicochemical processes are used in extraction of bitumen from oil sands ore. Responsive composite particles engineered to match the specifications of complex processes with different operational requirements can provide significant advantages in terms of performance and mitigate the need for difficult separations, with the ultimate goal of reducing the cost and the environmental impact of the extraction process. The properties and behaviour of responsive composite particles is controlled by both their composition (resulting from the materials used to prepare composite particles) as well as their structure (resulting from the process used to prepare composite particles). Colloidal stability and emulsion stability are interfacial properties dominated by the surface of the composite particles and require preparative methods that produce specific surface features. Interfacially active particles were prepared by chemical surface functionalization, surface adsorption and dehydration of emulsified droplets. Additional properties such as magnetic susceptibility and water-absorption can be imparted through incorporation of materials with desired properties within the core of the composite particle structure. Therefore, the design and application of responsive composite particles require careful consideration to the desired properties and/or functions, the materials used and the preparative process.

8.1.1 CO₂-Responsive Stabilizing Particles

The colloidal properties of various types of particles can be made responsive by ensuring its surface is sufficiently covered by a responsive material. The surface of inorganic silica particles

was modified through silica chemistry using silane coupling reagents (*e.g.*, 3-APTES) and subsequent chemical transformations to the amine group. Using this approach, responsive surface groups were installed on the surface of inorganic silica particles. Specifically, the responsive surface group is sensitive to presence of CO₂, whereupon ionization of responsive surface groups into the bicarbonate salt occurs in the presence of water. In CO₂-saturated aqueous solution, CO₂-responsive functional groups, such as secondary amines and amidines, form bicarbonate salts, which are ionic. The reaction with carbonic acid in water is reversible and CO₂-responsive functional groups revert to their basic non-ionic form after sparging the solution with air to remove dissolved CO₂. The contact angle of silica substrate functionalized with CO₂-responsive functional groups exhibited a contact angle of 66° in the absence of CO₂. A change in contact angle of approximately 10° was observed on silica substrate chemically functionalized with CO₂-responsive functional groups. The contact angle of silica substrate functionalized with CO₂-responsive functional and non-responsive hydrophobic groups exhibited a contact angle of 89° in the absence of CO₂.

The surface of silica particles is typically hydrophilic due to presence of acidic silanol groups on its surface, which ionize readily in water. Upon installation of responsive surface groups, the colloidal properties of the responsive particle could be influenced through application of the appropriate trigger (*i.e.*, addition or removal of CO₂ gas from aqueous solution). The switchability of the surface charge of CO₂-responsive particles was confirmed by measuring zeta potential. The surface charge of CO₂-responsive particles was also fine-tuned by installing non-responsive hydrophobic functional groups, which reduced the zeta potential, indicating less charged groups on the surface. Silica particles prepared with CO₂-responsive functional groups exhibited a zeta potential range of 33° – 21°. Silica particles prepared with additional hydrophobic groups exhibited a zeta potential range of 34° – 10°.

Silica particles, prepared with only CO₂-responsive functional groups, stabilized water-continuous (O/w) emulsions. In contrast, CO₂-responsive particles functionalized with additional hydrophobic functional groups effectively stabilized toluene-continuous (W/O) emulsions. Both emulsions were broken upon addition of gaseous CO₂, which appropriately decreased contact angle and lowered emulsion stability sufficiently to induce rapid phase separation. The effect of

CO₂ on particle wettability could be reversed by removing dissolved CO₂; after which, stable emulsions could be prepared once again without additional stabilizer particles. Particles engineered with CO₂-responsive surface groups are more hydrophilic in the presence of CO₂, as indicated by a lower contact angle on functionalized substrate, and more hydrophobic in the absence of CO₂, as indicated by an increase in contact angle.

Colloidal behaviour of particles made with responsive surface is effectively controlled by applying or removing the appropriate trigger. Upon addition or removal of CO₂ from the dispersion, significant changes are induced in particle wettability and colloidal stability. The colloidal behaviour is aptly tuned by controlling the relative proportion of different surface groups (*i.e.*, hydrophilic or lipophilic). The absolute wettability and wettability range of stabilizer particle can be tuned by adjusting the relative coverage of hydrophobic, hydrophilic and responsive surface groups. In terms of responsive behaviour, particles provide a much greater range of possibilities compared to surfactants. The ability of a surfactant to switch is influenced by the molar composition as well as the acidity or basicity of the specific CO₂-responsive group. However, changing molecular composition inherently affects solubility; and it is typically not possible to change the operational pH range of a process. Using particles as emulsion stabilizers has some additional design benefits. The structure of a solid particle has a large effect on its effectiveness. Furthermore, different materials can be incorporated inside individual particles, imparting various additional properties (*e.g.*, magnetic susceptibility) or adjusting properties (*e.g.*, density), without greatly affecting colloidal properties; as only the particle surface is responsible for colloidal properties.

8.1.2 Dehydration of Emulsion Droplets

A method of producing composite absorbent particles was developed by taking advantage of the contrasting characteristics of sodium carboxymethyl cellulose (CMC) and ethylcellulose (EC). CMC is hydrophilic and soluble in water while EC is hydrophobic and soluble in certain organic solvents. An emulsion was prepared with CMC dissolved in the aqueous phase and EC dissolved in the organic phase. Composite particles comprising CMC and EC were prepared by dehydration of emulsion droplets and subsequently separated using a centrifuge. Water is removed from emulsified droplets through azeotropic distillation, leaving a residue consisting of

any hydrophilic material previously dissolved or dispersed within the dispersed aqueous phase, while interfacially active material remains at the interface/surface. Dehydrated droplets initially stabilized by an interfacially active material remained coated by the interfacially active material after dehydration.

The size of particles was affected by the properties of the precursor emulsion. Smaller particles were produced with increasing EC concentration and greater mixing intensity. Using a concentration of 2 wt% CMC in the aqueous phase, the particle size of CMC-EC particles was reduced from 76 μm (using 0.5 wt% EC in the organic phase) to 35 μm (using 1.0 wt% EC in the organic phase) to 13 μm (using 2.0 wt% EC in the organic phase). Smaller particles with greater specific surface area contained more EC. CMC-EC particles were polydispersed, likely due to the coalescence, which occurs during dehydration. Very small uniform CMC-EC particles would be produced with high EC concentration and continuous agitation during the dehydration process.

The dehydration of emulsion droplets was used to prepare microscopic spherical particles consisting of an absorbent material (*i.e.*, CMC) coated with an interfacially active material (*i.e.*, EC). The resulting composite absorbent particles (CMC-EC) were of intermediate wettability and more compatible with non-aqueous solvents. CMC-EC particles are interfacially active and attached to the oil-water interface. The critical surface tension of CMC-EC particles was 28 mN/m and not significantly affected by particle size. The water absorbance was related to the composition of the CMC-EC particles. CMC-EC particle with greater CMC content exhibited greater water absorbency. The water absorbency of CMC-EC particles with 85 wt% CMC was 4.6 g/g while the water absorbency of CMC-EC particles with 64 wt% CMC was reduced to 2.3 g/g.

The presence of EC on CMC films increased the initial contact angle from 52° (for CMC substrate) to 89° (after coating EC on surface of CMC substrate). Despite being coated with EC, the surface of composite absorbent particles remained water-permeable. However, excessive amount of EC on the surface of CMC substrate was observed to reduce water flux. After hydration the contact angle was reduced and become much more variable (between less than 10° to 40°). The surface of CMC-EC particles was responsive to hydration. The interfacial and colloidal properties of CMC-EC particle were altered after absorbing water. Before absorbing water, CMC-EC particles could effectively stabilize W/O emulsions. After absorbing emulsified water, the

emulsion stabilized by CMC-EC broken and an emulsion could no longer be stabilized. Similarly, CMC-EC particles were effectively dispersed in toluene before absorbing water but subsequently formed large aggregates due to the loss of colloidal stability following the change in wettability of the surface after absorbing emulsified water.

Composite particle made by dehydrating emulsified water droplets can include a number of different materials. Supplemental materials can be easily incorporated into dehydrated particles to impart additional responsive properties (*e.g.*, magnetic susceptibility) or to modify other properties (*e.g.*, wettability, density, porosity, *etc.*), as a wide range of materials can be dispersed inside dehydrated particles using the same general approach. Soluble substances dissolved in the dispersed aqueous phase remain within the core of the resulting dehydrated particles. Insoluble particles, initially dispersed within aqueous droplets, also remained dispersed inside particles after dehydrating droplets. To improve colloidal stability, the surface of many oxide solids, including iron oxide (Fe_3O_4), can be coated with an ionic polymer. Following emulsification in the presence of interfacially active stabilizer, the aqueous dispersion of hydrophilic particles formed small emulsified droplets. Hydrophilic particles remain dispersed inside droplets undergoing dehydration and are eventually incorporated within the residual solid mass. Composite absorbent particles, with Fe_3O_4 nanoparticles dispersed within, are susceptible to a manipulation under an applied magnetic field. Thus, magnetically-responsive composite absorbent particles are efficiently separated using a permanent magnet.

Composite absorbent particles, comprising CMC and EC, prepared by dehydration of emulsified droplets were ideally suited for dewatering emulsions. Composite absorbent particles (CMC-EC), produced by emulsion dehydration, were capable of decreasing the amount of water emulsified in a sample of mineral oil by absorption of emulsified water droplets. The absorption process was rapid and effective, even at ambient temperature. Sedimentation of CMC-EC particles after absorption of emulsified water was more effective due to formation of large aggregates. Dewatering of mineral oil emulsion samples containing 5.9 wt% water was evaluated by tracking the water content at the midway point between the top and the bottom of the emulsion. Using 2.5 wt% CMC-EC, the water content of the mineral oil emulsion was reduced to 1.6 wt% while the untreated sample still contained 4.2 wt% emulsified water. Magnetic

separation after adding magnetic CMC-EC/MAG particles to the mineral oil emulsion further reduced the water content at the midway point to 0.7 wt%.

8.1.3 Absorptive Emulsion Dewatering

Dewatering emulsions through absorption was investigated using diluted bitumen emulsions as an alternative to contemporary methods. Absorbents are very different compared to chemical demulsifiers that promote droplet coalescence. Water-absorbent materials are typically hydrophilic materials that are capable of taking in and holding water. Several important properties to absorptive emulsion dewatering were identified by testing performance of different composite absorbents. Successful dewatering by absorption using composite absorbent particles may be a suitable alternative for traditional chemical demulsifiers in certain situations (*e.g.*, atypical operation due to sudden change in ore composition) wherein addition of more chemical demulsifiers may not necessarily lead to better performance (*e.g.*, overdosing).

The surface of an absorbent material is important to its performance. An unsuitable material can result in an impermeable surface that does not allow water to permeate through and prevent absorption. Unmodified CMC particles between 500 – 850 μm were capable of absorbing water from diluted bitumen emulsions but were slower compared to EC-coated CMC (CMC/EC) particles of similar size. CMC/EC absorbent particles were more compatible with non-aqueous environments due to its intermediate wettability. Absorbent particles with an interfacially active surface attach to the oil-water interface, which increased the effectiveness of the absorbent as absorption requires direct contact between the absorbent material and the emulsified droplets. In contrast, bitumen-coated CMC (CMC/BIT) performed poorly compared to both CMC/EC and CMC of similar size. Hydrophobic bituminous material on surface of absorbent particles hindered absorption of emulsified water. It took almost 1 h for the water content at the midway point of emulsion samples (*i.e.*, halfway between the bottom and the top of the emulsion sample) to reach half of its original value when treated with CMC particles. In comparison to CMC, CMC/BIT were found to be less effective in removing water from the emulsions and required approximately twice the amount of time (2 h) to achieve the same reduction in the water content as a result of the limited contact of the absorbent material, coated by bituminous material, with water in the emulsified droplet.

In comparison to both CMC and CMC/BIT, CMC/EC composite absorbent particles, coated with EC, exhibited an improved dewatering performance. The water content at the midway point of emulsion samples treated with CMC/EC particles was less than half its original value after only 0.5 h in the mechanical shaker. The rate of dewatering for diluted bitumen emulsions treated with CMC/EC was approximately 4 times faster compared to CMC. The presence of interfacially active EC improves dispersability of absorbent particles, promotes the attachment of absorbent particles onto the oil-water interface and assists in displacing indigenous surface-active materials that stabilize water droplets.

Absorption is a mass transfer process and water flux is influenced by the surface area in contact between the absorbent and emulsified water droplets. Emulsion droplet dehydration was used to produce composite absorbent microparticles (CMC@EC) comprising a water-absorbent core of CMC and an interfacially-active EC surface with particles size between 4 μm – 144 μm and average CMC content of 89 wt%. Using CMC@EC, dewatering of bitumen emulsions by adsorption was more rapid compared to larger EC-coated CMC (> 500 μm). Additionally, magnetically-responsive composite absorbent particles were also prepared by incorporating a responsive material into the composite particle. Emulsion droplet dehydration is an original and robust method of producing composite particles which can accommodate a variety of materials and incorporate their properties. Well-dispersed composite absorbent microparticles are similar in size as emulsified water droplets and therefore are more likely to collide with emulsified water droplets.

The superior dewatering performance of CMC@EC was most evident with increasing mixing intensity (*i.e.*, vortex mixer instead of reciprocal mechanical shaker), which promotes contact between dispersed CMC@EC absorbent particles and emulsified water droplets. The water content at the halfway point of emulsion samples treated with CMC@EC was less than half its original value after only 30 s in the vortex mixer and 1 h of sedimentation. In comparison, the water content at the halfway point of emulsion samples treated with larger absorbent particles (CMC and CMC/EC) was reduced by less than 30% after 90 s in the vortex mixer and 1 h of sedimentation. The intermediate wettability and size of CMC@EC particles resulted in improved dispersability in low polarity solvents and promoted attachment of particles to the oil-water

interface. Despite the presence of EC, the surface of composite absorbent particles remained water-permeable and permitted emulsified water droplets to be absorbed by the absorbent particle core comprised of CMC. However, absorption of water caused the wettability of CMC@EC to change, making the composite absorbent particle surface more hydrophilic following absorption of emulsified water. Hydrated composite absorbent particles aggregated in non-polar environment and formed larger aggregates, which were much easier to remove by screening and/or sedimentation.

Unlike traditional demulsification, which relies on promoting droplets coalescence or flocculation, the performance of absorptive emulsion dewatering is not disposed to overdosing effects. Improving dewatering rate and dewatering efficacy could be accomplished simply by increasing concentration of CMC@EC particles. Although more than 95 wt% of emulsified water was removed after 2 h in a mechanical shaker followed by 1 h of gravity settling using 3.0 wt% CMC/EC particles, similar results were achieved after only 30 s in a vortex mixer, followed by 1 h of gravity settling or magnetic recovery using CMC@EC or M-CMC@EC. The rate of dewatering was much slower for larger CMC/EC particles at the same concentration, which reduced the water content by only 10 wt% after 30 s in a vortex mixer, followed by 1 h of gravity settling.

8.1.4 Interfacially Active Magnetic Particles

Composite particles were prepared from different materials in order to combine their properties and applied to separation of various dispersed multiphase material encountered in bitumen extraction (*i.e.*, emulsions, rag layers and sludge). The structural complexity of solid particles allows different materials to be combined in different ways, resulting in suppression or enhancement of functional properties. Two different methods were used, including direct adsorption of contrasting materials and emulsion droplet dehydration, in order to produce magnetically responsive composite particles with an interfacially active surface that could promote attachment to the oil-water interface. Direct adsorption was a simpler and greener alternative to chemical functionalization (*e.g.*, silica-coating and chemical grafting) but requires careful choice of materials. Iron oxide particles were first primed with sodium carboxymethyl cellulose (CMC) and ethylcellulose (EC) was subsequently adsorbed onto the surface of primed magnetic particles.

Interfacially active magnetic particles were prepared by sequential adsorption of cellulosic materials (*i.e.*, CMC in water and EC in toluene) instead of chemical functionalization (*i.e.*, silica-coating and chemical grafting). This alternative method is much simpler and produces suitable particles without the need for difficult chemical reactions and generates less waste. CMC showed particular affinity for the surface of iron oxide (Fe_3O_4) particles. In the presence of CMC, enhanced colloidal stability of dispersed Fe_3O_4 particles was observed, although aggregation was still evident at higher suspension concentration. Furthermore, enhanced adsorption of EC on its surface was possible after priming Fe_3O_4 with CMC. Following this method, magnetically-responsive and interfacially active micro-aggregate particles of approximately 7 μm are prepared, which are well-suited for assisting in the magnetic separation of multiphasic mixtures. Without CMC-priming, direct coating of Fe_3O_4 with EC resulted in large aggregates of 83 μm .

Interfacially active magnetic micro-aggregate particles (MAG-CMC-EC) effectively attached to the oil-water interface within dispersed multiphase mixtures (*e.g.*, emulsions, rag layers and sludge). The critical contact angle of EC-coated particles was between 42 - 46 mN/m. The dispersed phase in the multiphasic mixtures is made magnetically-responsive after tagging with magnetic particles. Thus, magnetically-tagged material, including bitumen emulsions, rag layers and sludge, were subsequently separated and collected under an applied magnetic field. After magnetic separation and washing with solvent, it was possible to recycle and reuse magnetically-responsive and interfacially active micro-aggregate particles.

8.2 Future Work: Responsive Composite Particles

The performance of responsive composite particles has been demonstrated with absorptive emulsion dewatering using responsive absorbent particles as well as magnetic separation of biphasic waste using interfacially active magnetically responsive particles. The properties of the composite particles may be further improved in several areas. Various improvements are possible by taking advantage of responsive materials and incorporating them within composite particles in order to tailor their function to complex chemical processes and improve performance.

8.2.1 Composite Absorbent Particles

Future work may improve the water absorbency of composite absorbent particle by using super-absorbent materials such as acrylate and acrylamide polymers and co-polymers. Superabsorbent polymers (SAP) are capable of absorbing extremely large amounts of water and are typically made through various polymerization processes including gel, solution and suspension polymerization. These polymerization processes are compatible with emulsion droplet dehydration and the two processes may be combined together to simplify the production of composite absorbent particles with better performance. The emulsion droplets dehydration method is robust, capable of incorporating a variety of materials. Modification of properties such as density, porosity and other should be possible by addition of appropriate materials. For example, density may be increased by incorporating barium sulphate into composite particles.

The responsive behaviour of composite absorbent particles is currently only associated with the particle surface but can be further extended to the core of the particles to prepare absorbent particles that are capable of expelling absorbed water upon application of a trigger. To this end, polymers which exhibit transitions related to their miscibility with water may provide the appropriate responsive behaviour. Polymers with lower critical solution temperature transition include poly(N-isopropylacrylamide) and methylcellulose. Poly(N-isopropylacrylamide) experiences a reversible coil-to-globule transition at its lower critical solution temperature of approximately 32°C. Methylcellulose is a cellulosic derivative that also exhibits a similar transition. However, the transition poly(N-isopropylacrylamide) and methylcellulose is insufficient to induce a significant change to absorbent performance. Therefore, chemical modification is likely required to develop a suitable material for switchable absorbency.

Another important area of study consists of determining water quality. The fate of dissolved ions after absorptive emulsion dewatering is not yet clear. One possible improvement is related to the permeability of composite absorbent particles. By coating the absorbent particles with a selectively permeable surface, it may be possible to selectively absorb water while rejecting other substances such as dissolved salts. The ability to improve water quality may yield important advantages. In this regard, cellulose acetate and cellulose triacetate are widely used in the manufacture of semi-permeable membranes for reverse osmosis and may be suitable if they can

be incorporated into the structure of the composite absorbent particles. However, swelling of absorbent particles may prevent complete coverage of absorbent particles with a semi-permeable surface.

The responsive behaviour of composite absorbent particles is currently only associated to its surface but can be further extended to the core of the particles to prepare absorbent particles that are capable of expelling absorbed water upon application of a trigger. To this end, polymers which exhibit transitions related to their miscibility with water may provide the appropriate responsive behaviour. Polymers with lower critical solution temperature transition include poly(N-isopropylacrylamide) and methylcellulose. Poly(N-isopropylacrylamide) experiences a reversible coil-to-globule transition at its lower critical solution temperature (LCST) of approximately 32°C. However, the LCST transition for poly(N-isopropylacrylamide) is insufficient to induce a significant change to absorbent performance. Chemical modification of these polymers is likely required to produce a suitable material.

8.2.2 Interfacially Active Magnetic Particles

Future work includes preparing more effective interfacially active magnetic particles with Janus-like structure. Due to their structure, Janus-type particles make excellent emulsion stabilizers when one portion is lyophilic and the other is lyophobic. The attachment energy for particles, wherein one half is hydrophobic while the other half is hydrophilic, to the oil-water interface is greater compared to homogeneously coated particles.

Additional benefits may be possible by investigation the effect of heat generation when interfacially active iron oxide nanoparticles, attached to the oil-water interface, are subjected to an alternating magnetic field.^{1,2} Under an alternating magnetic field, small particles will spin and generate localized heating. This technique has been adapted to treat hypothermia as well to kill cancer cells. Direct input of thermal energy to the oil-water interface may provide a more effective method of breaking emulsions by promoting droplet coalescence. Localized heating is much more energy-efficient compared to heating the entire emulsion. Electromagnetic heating may be applied directly to a separation vessel in order to altogether prevent formation of rag layers. The structure of the interfacially active magnetic iron oxide particles both complements the properties of its constituent materials and enhances the function of the material.

8.3 Future Work: In-Situ Production

Dispersed systems are also commonly encountered during *in-situ* bitumen production. Future work extends the utility of responsive particles to *in-situ* production technologies. The ability of specially-prepared composite particles, made from responsive materials with suitable structure, can be adapted for different purposes. Recovery of bitumen from underground reservoirs is similarly challenging, due in part to the properties of bitumen as well as the geological features of specific reservoirs. The high viscosity of bitumen intensifies conformance problems in heterogeneous reservoirs. Injected fluid (*e.g.*, steam) will travel within the formation through interstitial void spaces (*i.e.*, effective porosity). Bitumen also occupies the void spaces between sand grains. Regions with high bitumen saturation typically also have lower relative porosity because bitumen occupies pore spaces. The amount of injection fluid required could be reduced by directing injection fluid towards specific regions with low porosity and therefore high bitumen saturation, instead of regions with high porosity but low bitumen saturation. High molecular weight polymers have been used to increase viscosity of injection fluids in order to improve conformance. However, the increased viscosity of produced fluid retards phase separation of dispersed oil droplets.

8.3.1 Triggered Blocking Agent

The production rate and ultimate recovery of a well can be increased by injecting a variety of fluids into the formation. Waterflooding is the most commonly employed secondary recovery method.³⁻⁵ Reservoir pressure increases as injected water displaces oil trapped in pores. Movement of a fluid inside a reservoir is governed by its permeability. Injected water can only move through the formation within interconnected open pores. Wettability and pore geometry are the primary determinants for capillary pressure. The mobility of a fluid in porous media depends on both the viscosity of the fluid and relative permeability of the reservoir. The displacement of oil from the reservoir by water is affected by the mobility ratio between water and oil. Recovery efficiency increases as the water-oil mobility ratio decreases. Blocking agents are chemical compounds that direct the injection of a fluid inside the reservoir.

The flow of injected fluid in the reservoir is also affected by the geology and structure of the formation. Shale and anhydrite formations are generally impermeable and are capable of isolating regions within a reservoir. Depending on the conditions during deposition, reservoir permeability may be relatively uniform, highly variable, or directional. Reservoir heterogeneity can exist between different adjacent sedimentary beds or within a single layer. Discontinuous permeability may occur across fractures and fault lines or through biological processes. Conformance problems can arise when the reservoir is heterogeneous. A high-molecular weight polymer is added to increase the viscosity of the injection floodwater. The increased viscosity of the injected water decreases the mobility ratio and increase sweep efficiency. In addition, polymer adsorption on rock surface can also change the wettability of reservoir rocks.

Bitumen is recovered from underground reservoirs using various *in-situ* production methods. Primary bitumen production is not significant due to its low mobility. Steam injection is used in both cyclic steam stimulation (CSS) and steam-assisted gravity drainage (SAGD) in order to heat up underground bitumen and increase its mobility. Due to conditions during deposition and geological history, many bitumen reservoirs are situated within heterogeneous sedimentary formations. Conformance issues and severe losses can result from injection of fluids inside heterogeneous formations or formations with special features (*e.g.*, bottom water). Blocking agents are used to reduce channelling of fluid into regions of high permeability or to isolate regions within a reservoir. However, blocking agents should not be placed in regions where they might prevent production. Successful application of blocking agents can improve production rate and reduce the amount of injection fluids required. Gels are the most common type of blocking agent and typically include a polymer with or without a cross-linker. The polymer and cross-linker react together to form an immobile gel that reduces permeability of all types of formations. Very high resistance is developed if gel formation occurs through most of the aqueous pore network. Increasing viscosity of the injection fluid increases penetration into low-permeability zones. Gel placement is relatively easy in fractured wells where there is a large difference in permeability between the fracture and the formation, but is otherwise difficult.

Particulates have also been used as blocking agent. Smaller particulates form a filter cake from particle accumulation inside porous formation. Larger particulates accumulate at the edge

of a low permeability zone, where particle size is greater than pore opening. The size and size distribution of particulate material is critical to effective placement of blocking agent. A phase change (*e.g.*, precipitation or particle dissolution) can induce a change in permeability. Foams have also been extensively used to direct or to increase the mobility of steam and other gases inside a reservoir. Increasing fluid penetration into low-permeability zones promotes oil displacement and improves sweep efficiency. Foams are less effective as blocking agents.

Dispersed particles with responsive colloidal stability could serve as an intermediate blocking agent, as shown in **Figure 8-1**. Placement of latex in high-permeability zones is favoured due to its low-viscosity. Stability of polymer latex particles prepared by emulsion polymerization can be tuned by using different surfactants during synthesis. Electrostatic stability from charges of pH-sensitive surface groups is suppressed with CO₂ injection. CO₂-responsive particles can be readily aggregated upon addition of CO₂ as very small polymer particles (< 100 nm) form much larger aggregates (> 100 μm) upon exposure to CO₂. Induced aggregation causes a large increase in particle size, which occupies the pore space in the formation. Injection of solvent is a common method of improving recovery and/or lowering the steam ratio. The solubility of polymer is usually limited by high molecular weight and further reduced by crosslinking. Polystyrene will dissolve in aromatic solvents such as toluene, unless crosslinked, but will only swell in non-aromatic solvents such as cyclohexane.

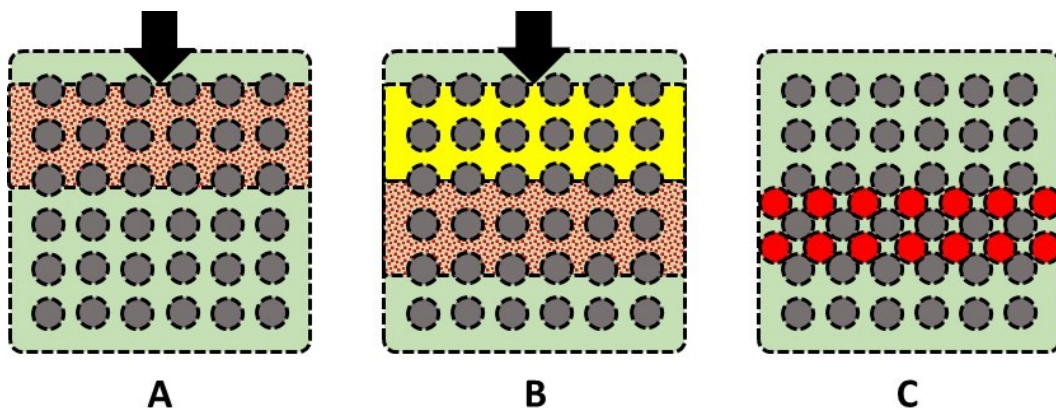


Figure 8-1. A triggered blocking agent suitable for isolation of the upper region of the formation by blocking the lower region of the formation. The blocking agent is injected in its dispersed state [A]. Once the dispersed blocking agent is in place, a trigger is injected [B]. Injection of the trigger causes aggregation of dispersed particles [C].

8.3.2 Triggered Polymer Degradation

Enhanced oil recovery method uses a variety of chemical additives to facilitate transport of petroleum from underground reservoir to the surface. Enhanced oil recovery is required for bitumen as its high viscosity does not allow for significant primary production. Production of bitumen and heavy oil is enhanced by fluid injection to increase reservoir pressure and by heating to increase mobility. Oil produced using secondary or tertiary recovery method inevitably contains water. Both CSS) and SAGD inject a large amount of steam into the reservoir. Emulsification can result from high-shear fields present in surface-injection equipment (*e.g.*, valves, orifices, pumps and tubing), downhole constrictions (*e.g.*, tubing orifices, perforations, or screens) and the formation itself (*e.g.*, reservoir porosity). The energy required for emulsification is lower when indigenous surfactants and process aids lower the interfacial tension.⁵

Produced fluid is a mixture of water, oil and solids. Oil-in-water emulsions are generated as hydrocarbons are carried to the surface along with injection fluid. The presence of high molecular weight polymers in the aqueous phase increases viscosity and reduces mobility ratio. Polymer additives, which enhance displacement of oil, remain in the aqueous phase. Emulsions with a high-viscosity continuous phase are slower to separate. The increase in the viscosity of a solution as a result of changes in molecular weight is described by the Mark-Houwink equation.^a Phase separation can be significantly accelerated by reducing the viscosity of the emulsion, allowing both lighter material to rise quicker, and denser material to settle faster.

High molecular weight co-polymers of acrylic acid and acrylamide are commonly used in *in-situ* production to increase oil recovery by lowering the mobility ratio. The oil-in-water emulsion is viscous due to the effect of high molecular weight polymer on the viscosity of the continuous aqueous phase. The effect of polymer addition on emulsion stability can be lessened by reducing its molecular weight using different methods shown in **Figure 8-2**. A gradual or sudden reduction

^a The Mark-Houwink equation for intrinsic viscosity of a polymer:

$$\eta = KM^\alpha$$

in the molecular weight of a polymer can result from chemical, biological, mechanical and thermal processes. Biological degradation is generally not significant, although certain microorganisms possess the ability to derive energy from breaking down polymers. Biological processes are slow and may be sensitive to environmental conditions. Polymers typically break down under high shear and at elevated temperature. However, excessive shear is undesirable as it further emulsifies the oil.

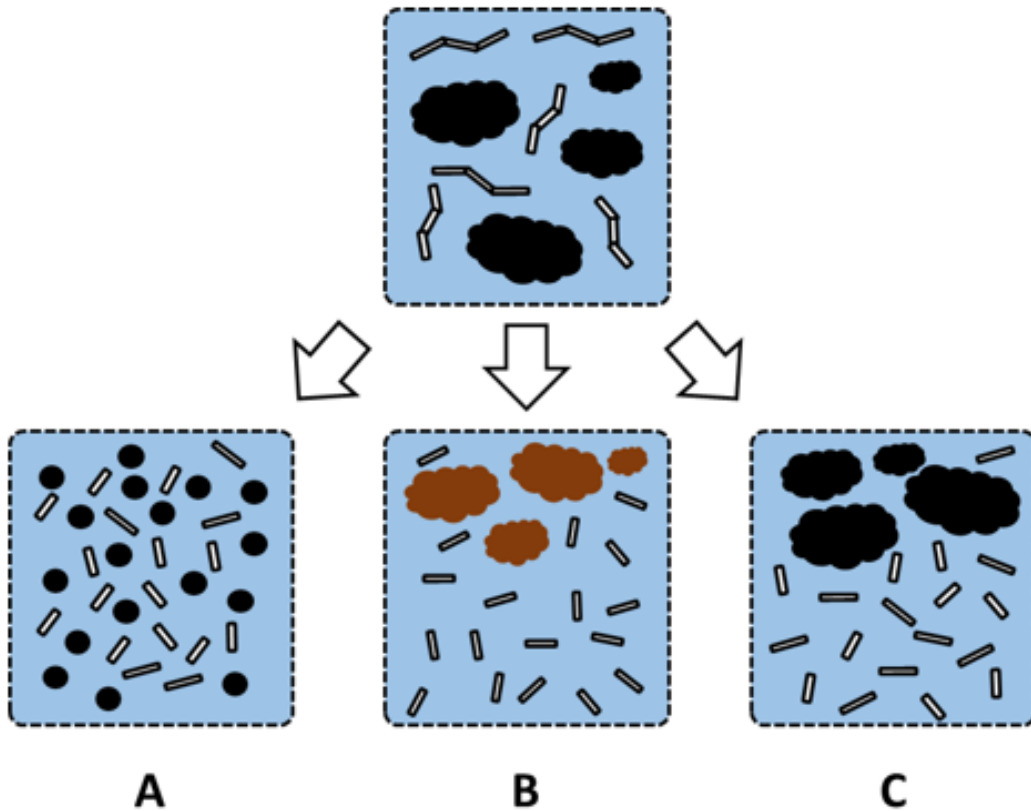


Figure 8-2. Production fluid from *in-situ* operations to recover bitumen consists of an emulsion. The polymer molecular weight can be reduced using shear [A] or chemical oxidants [B]. However, excessive shear can cause further emulsification, while chemical oxidation of polymers reduces molecular weight but can also result in oxidation of bitumen. Alternatively, triggered degradation of the polymer would reduce the viscosity of the emulsion without affecting the emulsified oil [C].

Common oxidants (*e.g.*, sodium hypochlorite, hydrogen peroxide, ammonium peroxide and ozone) generate free radicals that react with polymers and quickly reduce the average molecular

weight of the polymer. Chemical oxidants function on almost all types of polymers used in waterflooding but also react with hydrocarbons. The dispersed oil can be quickly oxidized, reducing the value of the oil. Hydrolysis reactions also degrade polymers but only occur under more specific reaction conditions. Acid- and base-catalysed hydrolysis results in a drop in average molecular weight of polymer chains. Therefore, a method of selectively degrading polymers in the aqueous phase would be desirable.

8.4 References

1. J.-P. Fortin, C. Wilhelm, J. Servais, C. Ménager, J.-C. Bacri and F. Gazeau, *J. Am. Chem. Soc.*, 2007, **129**, 2628–2635.
2. N. Lee, D. Yoo, D. Ling, M. H. Cho, T. Hyeon and J. Cheon, *Chem. Rev.*, 2015, **115**, 10637–10689.
3. G. P. Willhite, *Waterflooding*, Society of Petroleum Engineers, Richardson, TX, **1986**.
4. S. C. Rose, J. F. Buckwalter and R. J. Woodhall, *The Design Engineering Aspects of Waterflooding*, Society of Petroleum Engineers, Richardson, TX, **1989**.
5. F. F. Craig, *The Reservoir Engineering Aspects of Waterflooding* ed. Henry L. Doherty Memorial Fund of AIME, Richardson, Tex, **1993**.
6. G. Gu, Z. Xu, K. Nandakumar and J. H. Masliyah, *Fuel*, 2002, **81**, 1859–1869.

Works Cited

Chapter 1

1. *Oils Sands Technology Roadmap Unlocking the Potential*, Alberta Chamber of Resources, **2004**.
2. Canada. National Energy Board., *Canada's energy future infrastructure changes and challenges to 2020*, National Energy Board, Calgary, AB, **2009**.
3. Canada. National Energy Board., *Canada's energy future energy supply and demand projections to 2035*, National Energy Board, Calgary, AB, **2011**.
4. J. J. Heron and E. K. Spady, *Annu. Rev. Energy*, 1983, **8**, 137–163.
5. *Lines in the Sands: Oil Sands Sector Benchmarking*, Northwest and Ethical Investments, **2009**.
6. *Sustainability Perspectives Unconventional Risks An investor response to Canada's Oil Sands*, The Ethical Funds Company, **2008**.
7. C. Liang, Q. Liu and Z. Xu, *ACS Appl. Mater. Interfaces*, 2014, **6**, 6898–6904.
8. C. Liang, Q. Liu and Z. Xu, *ACS Appl. Mater. Interfaces*, 2015, **7**, 20631–20639.
9. C. Liang, Q. Liu and Z. Xu, *Energy Fuels*, 2016, **30**, 5253–5258.

Chapter 2.1

1. ExxonMobil, *The Outlook for Energy: A View to 2040*, Exxon Mobil Corporation, Irving, TX, **2013**.
2. W. Ramsden, *Proc. R. Chem. Soc.*, 1903, **72**, 156–164.
3. U. Pickering, *J. Chem. Soc. Trans.*, 1907, **91**, 2001–2021.
4. J. H. Schulman and J. Leja, *Trans. Faraday Soc.*, 1954, **50**, 598–605.

5. R. J. G. Lopetinsky, J. H. Masliyah and Z. Xu, in *Colloidal Particles at Liquid Interfaces*, ed. B. P. Binks, Cambridge University Press, New York, **2006**.
6. D. E. Tambe and M. M. Sharma, *Adv. Colloid Interface Sci.*, 1994, **52**, 1–63.
7. R. Aveyard, B. P. Binks and J. H. Clint, *Adv. Colloid Interface Sci.*, 2003, **100**, 503–546.
8. M. M. Kupai, F. Yang, D. Harbottle, K. Moran, J. Masliyah and Z. Xu, *Can. J. Chem. Eng.*, 2013, **91**, 1395–1401.
9. B. P. Binks and P. D. I. Fletcher, *Langmuir*, 2001, **17**, 4708–4710.
10. A. Kumar, B. J. Park, F. Tu and D. Lee, *Soft Matter*, 2013, **9**, 6604–6617.
11. S. Jiang and S. Granick, *J. Chem. Phys.*, 2007, **127**, 161102.
12. R. I. Rueda-Velásquez, H. Freund, K. Qian, W. N. Olmstead and M. R. Gray, *Energy Fuels*, 2013, **27**, 1817–1829.
13. O. C. Mullins, H. Sabbah, J. Eyssautier, A. E. Pomerantz, L. Barré, A. B. Andrews, Y. Ruiz-Morales, F. Mostowfi, R. McFarlane, L. Goual, R. Lepkowicz, T. Cooper, J. Orbulescu, R. M. Leblanc, J. Edwards and R. N. Zare, *Energy Fuels*, 2012, **26**, 3986–4003.
14. O. C. Mullins, *Energy Fuels*, 2010, **24**, 2179–2207.
15. J. P. Dickie and T. F. Yen, *Anal. Chem.*, 1967, **39**, 1847–1852.
16. O. P. Strausz, T. W. Mojelsky and E. M. Lown, *Fuel*, 1992, **71**, 1355–1363.
17. M. R. Gray, R. R. Tykwinski, J. M. Stryker and X. Tan, *Energy Fuels*, 2011, **25**, 3125–3134.
18. H. W. Yarranton, D. P. Ortiz, D. M. Barrera, E. N. Baydak, L. Barre, D. Frot, J. Eyssautier, H. Zeng, Z. Xu, G. Dechaine, M. Becerra, J. M. Shaw, A. M. McKenna, M. M. Mapolelo, C. Bohne, Z. Yang and J. Oake, *Energy Fuels*, 2013, **27**, 5083–5106

19. J. P. Rane, D. Harbottle, V. Pauchard, A. Couzis and S. Banerjee, *Langmuir*, 2012, **28**, 9986–9995.
20. S. Acevedo, M. A. Ranaudo, C. García, J. Castillo and A. Fernández, *Energy Fuels*, 2003, **17**, 257–261.
21. A. W. Marczewski and M. Szymula, *Colloids Surf. Physicochem. Eng. Asp.*, 2002, **208**, 259–266.
22. J. Castillo, M. A. Ranaudo, A. Fernández, V. Piscitelli, M. Maza and A. Navarro, *Colloids Surf. Physicochem. Eng. Asp.*, 2013, **427**, 41–46.
23. K. Xie and K. Karan, *Energy Fuels*, 2005, **19**, 1252–1260.
24. H. Labrador, Y. Fernández, J. Tovar, R. Muñoz and J. C. Pereira, *Energy Fuels*, 2007, **21**, 1226–1230.
25. A. Natarajan, J. Xie, S. Wang, J. Masliyah, H. Zeng and Z. Xu, *J. Phys. Chem. C*, 2011, **115**, 16043–16051.
26. E. M. Freer and C. J. Radke, *J. Adhes.*, 2004, **80**, 481–496.
27. P. M. Spiecker and P. K. Kilpatrick, *Langmuir*, 2004, **20**, 4022–4032.
28. A. Yeung, T. Dabros, J. Masliyah and J. Czarnecki, *Colloids Surf. Physicochem. Eng. Asp.*, 2000, **174**, 169–181.
29. A. Yeung, T. Dabros, J. Czarnecki and J. Masliyah, *Proc. R. Soc. Math. Phys. Eng. Sci.*, 1999, **455**, 3709–3723.
30. X. Wu, *Energy Fuels*, 2003, **17**, 179–190.
31. J. Czarnecki and K. Moran, *Energy Fuels*, 2005, **19**, 2074–2079.
32. S. Gao, K. Moran, Z. Xu and J. Masliyah, *J. Phys. Chem. B*, 2010, **114**, 7710–7718.

33. Y. Fan, S. Simon and J. Sjöblom, *Colloids Surf. Physicochem. Eng. Asp.*, 2010, **366**, 120–128.
34. D. Harbottle, K. Moorthy, L. Wang, Q. Chen, S. Xu, Q. Lu, J. Sjöblom and Z. Xu, *Langmuir*, 2014, **30**, 6730–6738.
35. P. Erni, *Soft Matter*, 2011, **7**, 7586–7600.
36. L. Wang, D. Sharp, J. Masliyah and Z. Xu, *Langmuir*, 2013, **29**, 3594–3603.
37. L. Wang, Z. Xu and J. H. Masliyah, *J. Phys. Chem. C*, 2013, **117**, 8799–8805.
38. P. Tchoukov, J. Czarnecki and T. Dabros, *Colloids Surf. Physicochem. Eng. Asp.*, 2010, **372**, 15–21.
39. J. Czarnecki, P. Tchoukov, T. Dabros and Z. Xu, *Can. J. Chem. Eng.*, 2013, **91**, 1365–1371.
40. J. Czarnecki, P. Tchoukov and T. Dabros, *Energy Fuels*, 2012, **26**, 5782–5786.
41. B. Ivanov and D. T. Dimitrova, in *Thin Liquid Films Fundamentals and Applications*, eds I. B. Ivanov and D. T. Dimitrova, Marcel Dekker Inc., New York, **1988**.
42. A. M. McKenna, L. J. Donald, J. E. Fitzsimmons, P. Juyal, V. Spicer, K. G. Standing, A. G. Marshall and R. P. Rodgers, *Energy Fuels*, 2013, **27**, 1246–1256.
43. R. B. Teklebrhan, L. Ge, S. Bhattacharjee, Z. Xu and J. Sjöblom, *J. Phys. Chem. B*, 2014, **118**, 1040–1051.
44. P. Tchoukov, F. Yang, Z. Xu, T. Dabros, J. Czarnecki and J. Sjöblom, *Langmuir*, 2014, **30**, 3024–3033.
45. A. Natarajan, N. Kuznicki, D. Harbottle, J. Masliyah, H. Zeng, and Z. Xu, *Langmuir*, 2014, **30**, 9370–9377.

46. D. Fu, J. R. Woods, J. Kung, D. M. Kingston, L. S. Kotlyar, B. D. Sparks, P. H. J. Mercier, T. McCracken and S. Ng, *Energy Fuels*, 2010, **24**, 2249–2256.
47. M. Osacky, M. Geramian, D. G. Ivey, Q. Liu and T. H. Etsell, *Fuel*, 2013, **113**, 148–157.
48. L. Konan, C. Peyratout, J.-P. Bonnet, A. Smith, A. Jacquet, P. Magnoux and P. Ayrault, *J. Colloid Interface Sci.*, 2007, **307**, 101–108.
49. T. J. Bandoz, J. Jagiełło, B. Andersen and J. A. Schwarz, *Clays Clay Miner.*, 1992, **40**, 306–310.
50. N. El-Thaher and P. Choi, *Ind. Eng. Chem. Res.*, 2012, **51**, 7022–7027.
51. A. M. Shaker, Z. R. Komi, S. E. M. Heggi and M. E. A. El-Sayed, *J. Phys. Chem. A*, 2012, **116**, 10889–10896.
52. R. Baigorri, M. Fuentes, G. González-Gaitano, J. M. García-Mina, G. Almendros and F. J. González-Vila, *J. Agric. Food Chem.*, 2009, **57**, 3266–3272.
53. A. W. P. Vermeer and L. K. Koopal, *Langmuir*, 1998, **14**, 4210–4216.
54. Q. Zhou, P. A. Maurice and S. E. Cabaniss, *Geochim. Cosmochim. Acta*, 2001, **65**, 803–812.
55. Z. R. Komi, A. M. Shaker, S. E. M. Heggi and M. E. A. El-Sayed, *Chemosphere*, 2014, **99**, 117–124.
56. X. Feng, A. J. Simpson and M. J. Simpson, *Org. Geochem.*, 2005, **36**, 1553–1566.
57. A. W. P. Vermeer, W. H. van Riemsdijk and L. K. Koopal, *Langmuir*, 1998, **14**, 2810–2819.
58. Czarnecki, K. Moran and X. Yang, *Can. J. Chem. Eng.*, 2007, **85**, 748–755.
59. Saadatmand, H. W. Yarranton and K. Moran, *Ind. Eng. Chem. Res.*, 2008, **47**, 8828–8839.
60. G. Gu, L. Zhang, Z. Xu and J. Masliyah, *Energy Fuels*, 2007, **21**, 3462–3468.
61. S. K. Kiran, E. J. Acosta and K. Moran, *Energy Fuels*, 2009, **23**, 3139–3149.

62. T. Jiang, G. J. Hirasaki, C. A. Miller and S. Ng, *Energy Fuels*, 2011, **25**, 545–554.
63. Y. Xu, J. Wu, T. Dabros, H. Hamza and J. Venter, *Energy Fuels*, 2005, **19**, 916–921.
64. X. Feng, P. Mussone, S. Gao, S. Wang, S.-Y. Wu, J. H. Masliyah and Z. Xu, *Langmuir*, 2010, **26**, 3050–3057.
65. X. Feng, Z. Xu and J. Masliyah, *Energy Fuels*, 2009, **23**, 451–456.
66. X. Feng, S. Wang, J. Hou, L. Wang, C. Cepuch, J. Masliyah and Z. Xu, *Ind. Eng. Chem. Res.*, 2011, **50**, 6347–6354.
67. J. T. Davies, A quantitative kinetic theory of emulsion type. 1. Physical chemistry of the emulsifying agent. In: *Gas/Liquid and Liquid/Liquid Interfaces*, Proceedings of 2nd International Congress Surface Activity, Butterworths, London, **1957**, vol. 1, 426–438.
68. S. Wang, J. Liu, L. Zhang, J. Masliyah and Z. Xu, *Langmuir*, 2010, **26**, 183–190.
69. S. Wang, N. Segin, K. Wang, J. H. Masliyah and Z. Xu, *J. Phys. Chem. C*, 2011, **115**, 10576–10587.
70. J. Hou, X. Feng, J. Masliyah and Z. Xu, *Energy Fuels*, 2012, **26**, 1740–1745.
71. J. Peng, Q. Liu, Z. Xu and J. Masliyah, *Energy Fuels*, 2012, **26**, 2705–2710.
72. J. Peng, Q. Liu, Z. Xu and J. Masliyah, *Adv. Funct. Mater.*, 2012, **22**, 1732–1740.

Chapter 2.2

1. C. Angle, in *Encyclopedic Handbook of Emulsion Technology*, ed. J. Sjöblom, CRC Press, 2001, 541–594.
2. K. A. Clark and D. S. Pasternack, *Ind. Eng. Chem.*, 1932, **24**, 1410–1416.
3. J. D. McLean and P. K. Kilpatrick, *J. Colloid Interface Sci.*, 1997, **189**, 242–253.
4. Y. Xu, J. Wu, T. Dabros, H. Hamza and J. Venter, *Energy Fuels*, 2005, **19**, 916–921.

5. Y. Xu, J. Wu, T. Dabros, H. Hamza, S. Wang, M. Bidal, J. Venter and T. Tran, *Can. J. Chem. Eng.*, 2008, **82**, 829–835.
6. R. A. Mohammed, A. I. Bailey, P. F. Luckham and S. E. Taylor, *Colloids Surf. Physicochem. Eng. Asp.*, 1993, **80**, 223–235.
7. Y. Wang, L. Zhang, T. Sun, S. Zhao and J. Yu, *J. Colloid Interface Sci.*, 2004, **270**, 163–170.
8. Y. H. Kim and D. T. Wasan, *Ind. Eng. Chem. Res.*, 1996, **35**, 1141–1149.
9. J. Wu, Y. Xu, T. Dabros and H. Hamza, *Energy Fuels*, 2003, **17**, 1554–1559.
10. T. Sun, L. Zhang, Y. Wang, S. Zhao, B. Peng, M. Li and J. Yu, *J. Colloid Interface Sci.*, 2002, **255**, 241–247.
11. A. M. Atta, A. A. Fadda, A. A.-H. Abdel-Rahman, H. S. Ismail and R. R. Fouad, *J. Dispers. Sci. Technol.*, 2012, **33**, 775–785.
12. P. Alexandridis and T. Alan Hatton, *Colloids Surf. Physicochem. Eng. Asp.*, 1995, **96**, 1–46.
13. N. N. Zaki, M. E. Abdel-Raouf and A.-A. A. Abdel-Azim, *Monatshefte Für Chem. Chem. Mon.*, 1996, **127**, 621–629.
14. I. Kailey and X. Feng, *Ind. Eng. Chem. Res.*, 2013, **52**, 785–793.
15. J. Czarnecki, K. Moran and X. Yang, *Can. J. Chem. Eng.*, 2008, **85**, 748–755.
16. M. Saadatmand, H. W. Yarranton and K. Moran, *Ind. Eng. Chem. Res.*, 2008, **47**, 8828–8839.
17. S. K. Kiran, E. J. Acosta and K. Moran, *Energy Fuels*, 2009, **23**, 3139–3149.

Chapter 3

1. D. Klemm, B. Heublein, H.-P. Fink and A. Bohn, *Angew. Chem. Int. Ed.*, 2005, **44**, 3358–3393.

2. E. Melzer, J. Kreuter and R. Daniels, *Eur. J. Pharm. Biopharm.*, 2003, **56**, 23–27.
3. X. Feng, Z. Xu and J. Masliyah, *Energy Fuels*, 2009, **23**, 451–456.
4. X. Feng, S. Wang, J. Hou, L. Wang, C. Cepuch, J. Masliyah and Z. Xu, *Ind. Eng. Chem. Res.*, 2011, **50**, 6347–6354.
5. X. Feng, P. Mussone, S. Gao, S. Wang, S.-Y. Wu, J. H. Masliyah and Z. Xu, *Langmuir*, 2010, **26**, 3050–3057.
6. S. Wang, N. Segin, K. Wang, J. H. Masliyah and Z. Xu, *J. Phys. Chem. C*, 2011, **115**, 10576–10587.
7. J. Hou, X. Feng, J. Masliyah and Z. Xu, *Energy Fuels*, 2012, **26**, 1740–1745.
8. R. A. Young, in *Textile Science and Technology*, Elsevier, **2002**, vol. 13, 233–281.
9. J. A. Dean and P. Patnaik, in *Dean's analytical chemistry handbook*, McGraw-Hill, New York, **2004**.

Chapter 4

1. Y. Jiang, Z. Wang, X. Yu, F. Shi, H. Xu, X. Zhang, M. Smet and W. Dehaen, *Langmuir*, 2005, **21**, 1986–1990.
2. X. Yu, Z. Wang, Y. Jiang, F. Shi and X. Zhang, *Adv. Mater.*, 2005, **17**, 1289–1293.
3. F. Xia, L. Feng, S. Wang, T. Sun, W. Song, W. Jiang and L. Jiang, *Adv. Mater.*, 2006, **18**, 432–436.
4. J. Wang, J. Hu, Y. Wen, Y. Song and L. Jiang, *Chem. Mater.*, 2006, **18**, 4984–4986.
5. L. Tan, L. Cao, M. Yang, G. Wang and D. Sun, *Polymer*, 2011, **52**, 4770–4776.
6. K. Senshu, S. Yamashita, H. Mori, M. Ito, A. Hirao and S. Nakahama, *Langmuir*, 1999, **15**, 1754–1762.

7. T. Sun, G. Wang, L. Feng, B. Liu, Y. Ma, L. Jiang and D. Zhu, *Angew. Chem. Int. Ed.*, 2004, **43**, 357–360.
8. N. J. Shirtcliffe, G. McHale, M. I. Newton, C. C. Perry and P. Roach, *Chem. Commun.*, 2005, 3135.
9. Q. Yu, X. Li, Y. Zhang, L. Yuan, T. Zhao and H. Chen, *RSC Adv.*, 2011, **1**, 262.
10. J. Lahann, *Science*, 2003, **299**, 371–374.
11. L. Xu, W. Chen, A. Mulchandani and Y. Yan, *Angew. Chem. Int. Ed.*, 2005, **44**, 6009–6012.
12. A. K. Sinha, M. Basu, M. Pradhan, S. Sarkar, Y. Negishi and T. Pal, *Langmuir*, 2011, **27**, 11629–11635.
13. R. Wang, K. Hashimoto, A. Fujishima, M. Chikuni, A. Kitamura, M. Shimohigoshi and T. Watanabe, *Nature*, 1997, 431–432.
14. K. Ichimura, *Science*, 2000, **288**, 1624–1626.
15. P. F. Driscoll, N. Purohit, N. Wanichacheva, C. R. Lambert and W. G. McGimpsey, *Langmuir*, 2007, **23**, 13181–13187.
16. H. S. Lim, D. Kwak, D. Y. Lee, S. G. Lee and K. Cho, *J. Am. Chem. Soc.*, 2007, **129**, 4128–4129.
17. J. Wang, B. Mao, J. L. Gole and C. Burda, *Nanoscale*, 2010, **2**, 2257.
18. Y. Liu, *Science*, 2006, **313**, 958–960.
19. Liang, J. R. Harjani, T. Robert, E. Rogel, D. Kuehne, C. Ovalles, V. Sampath and P. G. Jessop, *Energy Fuels*, 2012, **26**, 488–494.
20. Julthongpiput, Y.-H. Lin, J. Teng, E. R. Zubarev and V. V. Tsukruk, *Langmuir*, 2003, **19**, 7832–7836.

21. M. Motornov, S. Minko, K.-J. Eichhorn, M. Nitschke, F. Simon and M. Stamm, *Langmuir*, 2003, **19**, 8077–8085.
22. P. Uhlmann, L. Ionov, N. Houbenov, M. Nitschke, K. Grundke, M. Motornov, S. Minko and M. Stamm, *Prog. Org. Coat.*, 2006, **55**, 168–174.
23. P.-C. Lin and S. Yang, *Soft Matter*, 2009, **5**, 1011.
24. J. Yang, Z. Zhang, X. Men, X. Xu, X. Zhu, X. Zhou and Q. Xue, *J. Colloid Interface Sci.*, 2012, **366**, 191–195.
25. P. Brown, A. Bushmelev, C. P. Butts, J. Cheng, J. Eastoe, I. Grillo, R. K. Heenan and A. M. Schmidt, *Angew. Chem. Int. Ed.*, 2012, **51**, 2414–2416.
26. B. P. Binks, *Curr. Opin. Colloid Interface Sci.*, 2002, **7**, 21–41.
27. R. Aveyard, B. P. Binks and J. H. Clint, *Adv. Colloid Interface Sci.*, 2003, **100-102**, 503–546.
28. R. J. G. Lopetinsky, J. H. Masliyah and Z. Xu, in *Colloidal Particles at Liquid Interfaces*, eds. B. P. Binks, T. S. Horozov, B. P. Binks and T. S. Horozov, Cambridge University Press, Cambridge, 186–224.
29. B. P. Binks and S. O. Lumsdon, *Langmuir*, 2001, **17**, 4540–4547.
30. B. P. Binks and S. O. Lumsdon, *Langmuir*, 2000, **16**, 8622–8631.
31. B. P. Binks and S. O. Lumsdon, *Langmuir*, 2000, **16**, 3748–3756.
32. B. P. Binks and S. O. Lumsdon, *Langmuir*, 2000, **16**, 2539–2547.
33. L. G. J. Fokkink and J. Ralston, *Colloids Surf.*, 1989, **36**, 69–76.
34. S. Moya, O. Azzaroni, T. Farhan, V. L. Osborne and W. T. S. Huck, *Angew. Chem. Int. Ed.*, 2005, **44**, 4578–4581.
35. N. Stevens, C. I. Priest, R. Sedev and J. Ralston, *Langmuir*, 2003, **19**, 3272–3275.

36. S. Abbott, J. Ralston, G. Reynolds and R. Hayes, *Langmuir*, 1999, **15**, 8923–8928.
37. Y. Shiraishi, G. Nishimura, T. Hirai and I. Komasaawa, *Ind. Eng. Chem. Res.*, 2002, **41**, 5065–5070.
38. Z. Xu, Q. Liu and J. A. Finch, *Appl. Surf. Sci.*, 1997, **120**, 269–278.
39. J. Oszczapowicz and E. Raczyska, *J. Chem. Soc. Perkin Trans. 2*, **1984**, 1643.
40. J. R. Harjani, C. Liang and P. G. Jessop, *J. Org. Chem.*, 2011, **76**, 1683–1691.
41. J. Heldebrant, P. K. Koech, M. T. C. Ang, C. Liang, J. E. Rainbolt, C. R. Yonker and P. G. Jessop, *Green Chem.*, 2010, **12**, 713.
42. L. Phan, D. Chiu, D. J. Heldebrant, H. Huttenhower, E. John, X. Li, P. Pollet, R. Wang, C. A. Eckert, C. L. Liotta and P. G. Jessop, *Ind. Eng. Chem. Res.*, 2008, **47**, 539–545.
43. P. G. Jessop, L. Phan, A. Carrier, S. Robinson, C. J. Dürr and J. R. Harjani, *Green Chem.*, 2010, **12**, 809.
44. F. S. Mohammed, S. Wuttigul, C. L. Kitchens, *Ind. Eng. Chem. Res.* 2011, **50**, 8034.
45. C. I. Fowler, P. G. Jessop, M. F. Cunningham, *Macromolecules* 2010, **45**, 2955.
46. X. Su, C. I. Fowler, C. O'Neill, J. Pinaud, E. Kowal, P. G. Jessop, M. F. Cunningham, *Macromol. Symp.* 2013, **333**, 93.
47. Z. G. Cui, C. F. Cui, Y. Zhu, B. P. Binks, *Langmuir* 2012, **28**, 314.

Chapter 5

1. S.-D. Yeo and E. Kiran, *J. Supercrit. Fluids*, 2005, **34**, 287–308.
2. M. T. Swihart, *Curr. Opin. Colloid Interface Sci.*, 2003, **8**, 127–133.
3. R. Vehring, *Pharm. Res.*, 2008, **25**, 999–1022.
4. R. Vehring, W. R. Foss and D. Lechuga-Ballesteros, *J. Aerosol Sci.*, 2007, **38**, 728–746.

5. R. Arshady, *Colloid Polym. Sci.*, 1992, **270**, 717–732.
6. Guyot and K. Tauer, in *Polymer Synthesis*, Springer Berlin Heidelberg, **1994**, 43–65.
7. S. A. F. Bon, M. Bosveld, B. Klumperman and A. L. German, *Macromolecules*, 1997, **30**, 324–326.
8. L. Peltonen and J. Hirvonen, *J. Pharm. Pharmacol.*, 2010, **62**, 1569–1579.
9. Martín and M. J. Cocero, *Adv. Drug Deliv. Rev.*, 2008, **60**, 339–350.
10. N. Rasenack and B. W. Müller, *Pharm. Dev. Technol.*, 2004, **9**, 1–13.
11. R. Heusch, in *Ullmann's Encyclopedia of Industrial Chemistry*, ed. Wiley-VCH Verlag GmbH & Co. KGaA, Wiley-VCH Verlag GmbH & Co. KGaA, Weinheim, Germany, **2000**.
12. J. W. Barlow and D. R. Paul, *Polym. Eng. Sci.*, 1981, **21**, 985–996.
13. Liu, H. Qin and P. T. Mather, *J. Mater. Chem.*, 2007, **17**, 1543–1558.
14. S. Jiang and S. Granick, *Janus particle synthesis, self assembly and applications*, Royal Society of Chemistry, Cambridge, U.K., **2012**.
15. P. Binks and P. D. I. Fletcher, *Langmuir*, 2001, **17**, 4708–4710.
16. S. Jiang and S. Granick, *J. Chem. Phys.*, 2007, **127**, 161102.
17. Kumar, B. J. Park, F. Tu and D. Lee, *Soft Matter*, 2013, **9**, 6604.
18. M. Linares, A. Formiga, L. T. Kubota, F. Galembeck and S. Thalhammer, *J. Mater. Chem. B*, 2013, **1**, 2236–2244.
19. H. Hu, L. Xiong, J. Zhou, F. Li, T. Cao and C. Huang, *Chem. – Eur. J.*, 2009, **15**, 3577–3584.
20. K. S. Soppimath, L.-H. Liu, W. Y. Seow, S.-Q. Liu, R. Powell, P. Chan and Y. Y. Yang, *Adv. Funct. Mater.*, 2007, **17**, 355–362.
21. J. Peng, Q. Liu, Z. Xu and J. Masliyah, *Energy Fuels*, 2012, **26**, 2705–2710.

22. W.-C. Law, K.-T. Yong, I. Roy, H. Ding, R. Hu, W. Zhao and P. N. Prasad, *Small*, 2009, **5**, 1302–1310.
23. T. Cole, R. A. Scott, A. L. Connor, I. R. Wilding, H.-U. Petereit, C. Schminke, T. Beckert and D. Cadé, *Int. J. Pharm.*, 2002, **231**, 83–95.
24. S. Leopold, *Pharm. Sci. Technol. Today*, 1999, **2**, 197–204.
25. T. Higuchi and A. Aguiar, *J. Am. Pharm. Assoc.*, 1959, **48**, 574–583.
26. J. Malm, J. Emerson and G. D. Hiait, *J. Am. Pharm. Assoc.*, 1951, **40**, 520–525.
27. Y. Kane, J. Rambaud, H. Maillols, J. P. Laget, D. Gaudy and H. Delonca, *Drug Dev. Ind. Pharm.*, 1993, **19**, 2011–2020.
28. Loxley and B. Vincent, *J. Colloid Interface Sci.*, 1998, **208**, 49–62.
29. S. Fujii, D. P. Randall and S. P. Armes, *Langmuir*, 2004, **20**, 11329–11335.
30. J. Drelich, A. Marmur, *Surfaces and Coatings Surf. Innovations* 2014, **2**, 211– 227.
31. W. Dean and D. D. Stark, *J. Ind. Eng. Chem.*, 1920, **12**, 486–490.
32. Melzer, J. Kreuter and R. Daniels, *Eur. J. Pharm. Biopharm.*, 2003, **56**, 23–27.
33. S. Obara, N. Maruyama, Y. Nishiyama and H. Kokubo, *Eur. J. Pharm. Biopharm.*, 1999, **47**, 51–59.
34. Martinac, J. Filipović-Grčić, D. Voinovich, B. Perissutti and E. Franceschinis, *Int. J. Pharm.*, 2005, **291**, 69–77.
35. M. G. Moldenhauer and J. G. Nairn, *J. Controlled Release*, 1992, **22**, 205–218.
36. T. L. Rogers and D. Wallick, *Drug Dev. Ind. Pharm.*, 2012, **38**, 129–157.
37. R. A. Young, in *Textile Science and Technology*, Elsevier, **2002**, vol. 13, 233–281.

38. X. Feng, P. Mussone, S. Gao, S. Wang, S. Y. Wu, J. H. Masliyah and Z. Xu, *Langmuir*, 2010, **26**, 3050–2057.
39. D. W. Fuerstenau, M. C. Williams, *Colloids Surf.* 1987, **22**, 87–91.
40. J. Drelich, *Surf. Innovations* 2013, **1**, 248–254.
41. J. Briscoe, C. J. Lawrence and W. G. P. Mietus, *Adv. Colloid Interface Sci.*, 1999, **81**, 1–17
42. E. Oh, P. E. Luner, *Int. J. Pharm.* 1999, **188**, 203–219.

Chapter 6

1. L. A. Stanford, R. P. Rodgers, A. G. Marshall, J. Czarnecki and X. A. Wu, *Energy Fuels*, 2007, **21**, 963–972.
2. A. Goldszal and M. Bourrel, *Ind. Eng. Chem. Res.*, 2000, **39**, 2746–2751.
3. A. M. Al-Sabagh, S. A. Nehal, M. N. Amal and M. M. Gabr, *Polym. Adv. Technol.*, 2002, **13**, 346–352.
4. J. L. Stark and S. Asomaning, *Energy Fuels*, 2005, **19**, 1342–1345.
5. M. Rondón, J. C. Pereira, P. Bouriat, A. Graciaa, J. Lachaise and J.-L. Salager, *Energy Fuels*, 2008, **22**, 702–707.
6. T. Jiang, G. J. Hirasaki, C. A. Miller and S. Ng, *Energy Fuels*, 2011, **25**, 545–554.
7. M. K. Poindexter and S. C. Marsh, *Energy Fuels*, 2009, **23**, 1258–1268.
8. G. Liu, X. Xu and J. Gao, *Energy Fuels*, 2003, **17**, 625–630.
9. M. Fortuny, C. B. Z. Oliveira, R. L. F. V. Melo, M. Nele, R. C. C. Coutinho and A. F. Santos, *Energy Fuels*, 2007, **21**, 1358–1364.
10. J. H. Masliyah, Z. Xu and J. A. Czarnecki, *Handbook on theory and practice of bitumen recovery from Athabasca Oil Sands*, Kingsley Knowledge Pub., Cochrane, AB, **2011**.

11. J. Czarnecki, in *Encyclopedic Handbook of Emulsion Technology*, ed. J. Sjöblom, CRC Press, **2001**, 497–514.
12. U. G. Romanova, H. W. Yarranton, L. L. Schramm and W. E. Shelfantook, *Can. J. Chem. Eng.*, 2008, **82**, 710–721.
13. C. Angle, in *Encyclopedic Handbook of Emulsion Technology*, ed. J. Sjöblom, CRC Press, **2001**, 541–594.
14. M. A. Krawczyk, D. T. Wasan and C. Shetty, *Ind. Eng. Chem. Res.*, 1991, **30**, 367–375.
15. A. A. Peña, G. J. Hirasaki and C. A. Miller, *Ind. Eng. Chem. Res.*, 2005, **44**, 1139–1149.
16. Y. Fan, S. Simon and J. Sjöblom, *Energy Fuels*, 2009, **23**, 4575–4583.
17. A. Pradilla, S. Simon and J. Sjöblom, *Energy Fuels*, 2015, **29**, 5507–5518.
18. I. Kailey and J. Behles, *Ind. Eng. Chem. Res.*, 2015, **54**, 4839–4850.
19. P. Laplante, M. B. Machado, S. Bhattacharya, S. Ng and S. M. Kresta, *Fuel Process. Technol.*, 2015, **138**, 361–367.
20. E. Pensini, D. Harbottle, F. Yang, P. Tchoukov, Z. Li, I. Kailey, J. Behles, J. Masliyah and Z. Xu, *Energy Fuels*, 2014, **28**, 6760–6771.
21. Y. Si, Q. Fu, X. Wang, J. Zhu, J. Yu, G. Sun and B. Ding, *ACS Nano*, 2015, **9**, 3791–3799.
22. J. Liu, X. Li, W. Jia, Z. Li, Y. Zhao and S. Ren, *Energy Fuels*, 2015, **29**, 4644–4653.
23. Q. Ma, H. Cheng, A. G. Fane, R. Wang and H. Zhang, *Small*, 2016, 1–17.
24. C. Liang, Q. Liu and Z. Xu, *ACS Appl. Mater. Interfaces*, 2015, **7**, 20631–20639.

Chapter 7

1. J. Peng, Q. Liu, Z. Xu and J. Masliyah, *Adv. Funct. Mater.*, 2012, **22**, 1732–1740.
2. J. Peng, Q. Liu, Z. Xu and J. Masliyah, *Energy Fuels*, 2012, **26**, 2705–2710.

3. S. Laurent, D. Forge, M. Port, A. Roch, C. Robic, L. Vander Elst and R. N. Muller, *Chem. Rev.*, 2008, **108**, 2064–2110.
4. M. Mahmoudi, S. Sant, B. Wang, S. Laurent and T. Sen, *Adv. Drug Deliv. Rev.*, 2011, **63**, 24–46.
5. B. Medronho, A. Romano, M. G. Miguel, L. Stigsson and B. Lindman, *Cellulose*, 2012, **19**, 581–587.
6. D. W. Frommer, *J. Am. Oil Chem. Soc.*, 1967, **44**, 270–274.
7. K. Quast, *Miner. Eng.*, 2006, **19**, 582–597.
8. K. Shrimali and J. D. Miller, *Trans. Indian Inst. Met.*, 2016, **69**, 83–95.
9. R. Kargl, T. Mohan, M. Bračić, M. Kulterer, A. Doliška, K. Stana-Kleinschek and V. Ribitsch, *Langmuir*, 2012, **28**, 11440–11447.
10. Z. Liu, H. Choi, P. Gatenholm and A. R. Esker, *Langmuir*, 2011, **27**, 8718–8728.
11. X. Feng, Z. Xu and J. Masliyah, *Energy Fuels*, 2009, **23**, 451–456.
12. X. Feng, P. Mussone, S. Gao, S. Wang, S.-Y. Wu, J. H. Masliyah and Z. Xu, *Langmuir*, 2010, **26**, 3050–3057.
13. J. Hou, X. Feng, J. Masliyah and Z. Xu, *Energy Fuels*, 2012, **26**, 1740–1745.
14. S. Wang, J. Liu, L. Zhang, J. Masliyah and Z. Xu, *Langmuir*, 2010, **26**, 183–190.
15. S. Li, N. Li, S. Yang, F. Liu and J. Zhou, *J Mater Chem A*, 2014, **2**, 94–99.
16. C. Liang, Q. Liu and Z. Xu, *ACS Appl. Mater. Interfaces*, 2015, **7**, 20631–20639.
17. Points of Zero Charge. in *Chemical Properties of Material Surfaces*, CRC Press, **2001**, 731–744.

Chapter 8

1. J.-P. Fortin, C. Wilhelm, J. Servais, C. Ménager, J.-C. Bacri and F. Gazeau, *J. Am. Chem. Soc.*, 2007, **129**, 2628–2635.
2. N. Lee, D. Yoo, D. Ling, M. H. Cho, T. Hyeon and J. Cheon, *Chem. Rev.*, 2015, **115**, 10637–10689.
3. G. P. Willhite, *Waterflooding*, Society of Petroleum Engineers, Richardson, TX, **1986**.
4. S. C. Rose, J. F. Buckwalter and R. J. Woodhall, *The Design Engineering Aspects of Waterflooding*, Society of Petroleum Engineers, Richardson, TX, **1989**.
5. F. F. Craig, *The Reservoir Engineering Aspects of Waterflooding* ed. Henry L. Doherty Memorial Fund of AIME, Richardson, Tex, **1993**.
6. G. Gu, Z. Xu, K. Nandakumar and J. H. Masliyah, *Fuel*, 2002, **81**, 1859–18.

Appendix A. General Background

An overview of the properties of Canadian Oil Sands is provided along with brief descriptions of recovery methods. General concepts in colloid and interface chemistry, relevant extraction process and *in-situ* production methods, are discussed. General concepts and methods in particle engineering are also presented.

A.1 Bituminous (Oil) Sands

Oil sands refer to a specific type of unconventional petroleum deposit. Oil sands represent a significant portion of Canada's petroleum reserves; with an ultimate volume-in-place being estimated to be over 400 billion m³ or 2.5 trillion barrels and the ultimate recoverable volume is estimated to be over 50 billion m³ or 300 billion barrels.¹ Major oil sands deposits are located primarily in the province of Alberta near the Athabasca, Cold Lake and Peace River regions.²⁻⁵ The oil sands deposits were initially marine organisms trapped within the Western Canadian Basin in organic-rich shale deposits, which under high temperature and pressure, were converted into conventional liquid petroleum. During the Cretaceous Period, the light petroleum migrated away from the source rock and was trapped within sedimentary deposits.⁶ In the presence of water and bacteria, the lighter petroleum was transformed into bitumen through biodegradation processes. Due to advanced biodegradation, bitumen is absent of short straight-chain hydrocarbons (*e.g.*, pentane) but rich in high-molecular weight hydrocarbon species (*e.g.*, fused cyclic and aromatic compounds).⁷

A typical Alberta oil sands sample contains approximately 10 wt% bitumen, 85 wt% solids, and 5 wt% connate water.^{8,9} The bitumen is impregnated in the formation within unconsolidated coarse sand grains and fine clay particles. The mineral solids include mainly quartz, feldspar, chlorite, and various types of clays.¹⁰ Mean particle size of the mineral solids in oil sands ore is typically between 80 – 250 µm.⁸ However, oil sands also contain much smaller particles less than 44 µm, known as fines. The amount of fines in oil sands ore varies from less than 10 wt% to approximately 30 wt%, and generally fines have a negative impact on bitumen recovery.⁸ The majority of fines are clay minerals that consist primarily of kaolinite and illite but may also include

variable amounts, although small, of montmorillonite, smectite, and chlorite.⁸ Mechanically dispersed clay aggregates have an average size of about 20 µm whereas chemically dispersed clay platelets have an average size of about 1 µm. The surface of oil sand is hydrophilic and is believed to be surrounded by a thin film of water.^{9,11} Surface water is critical to the success of the Clark hot-water extraction process.

Many factors are responsible for the non-uniformity of oil sands deposits. The underlying Devonian formation is heavily weathered, resulting in highly variable topography with scattered highs and lows.^{2,6} The lack of bitumen mobility also leads to very heterogeneous deposits with bitumen lenses distributed within the formation. The McMurray formation in the Athabasca region shows three distinctive types of sedimentary geology: fluvial in Lower McMurray, tidal-estuary in Middle McMurray, and tidal-marine in Upper McMurray. Electrolytes are also present in the formation due to the aquatic origin of sedimentary deposits. The concentration of ionic species in oil sands ore varies greatly, even within the same geographic region.

Commercial bitumen production in Alberta consists of a surface mining and various *in-situ* production methods.¹² Large-scale surface mining is used to recover bitumen from shallow reserves. Surface mining uses heavy machinery to remove and crush oil sands ore. The crushed ore is subsequently transported as a slurry to an extraction facility, where bitumen is separated and collected.⁸ A simplified illustration of the extraction process is shown in **Figure A-1**. Bitumen from deeper underground deposits cannot be recovered economically by surface mining due to the high cost of removing excess overburden. Conventional production methods cannot be applied to bitumen because of its extremely low mobility. *In-situ* production methods for bitumen are designed to increase mobility by heating and includes: steam-assisted gravity drainage (SAGD), cyclic steam stimulation (CSS), vapour recovery extraction (VAPEX), and toe-to-heel air injection (THAI). Bitumen is a heavily degraded petroleum, which is diluted with low viscosity solvent or upgraded into synthetic crude oil by chemical processes such as vacuum distillation, de-asphalting, cracking and hydrotreating.¹³ These chemical processes require clean bitumen, substantially free of undesirable contaminants (*i.e.*, water, salts and heavy metals) that cause operational issues.

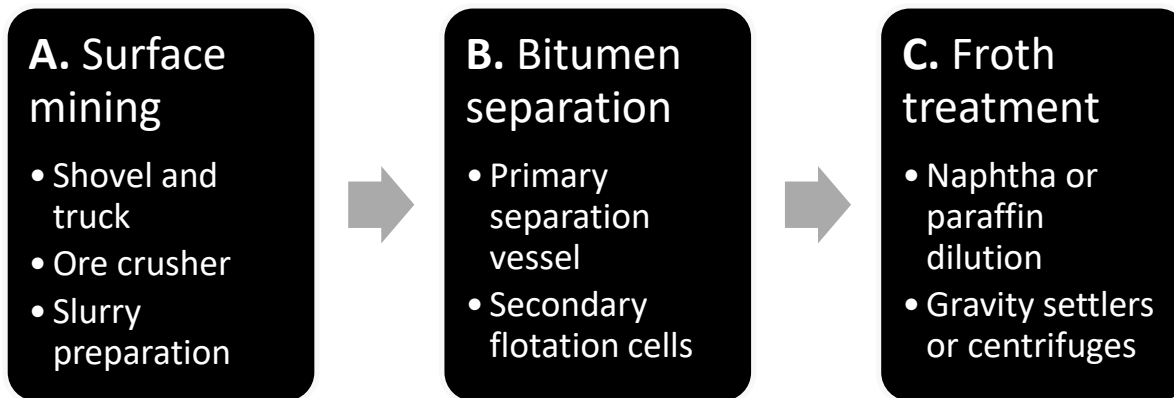


Figure A-1. Schematic representation of the bitumen extraction process used to recover bitumen from oil sands ore. The extraction process includes mining of oil sands ore [A]; liberation and separation of bitumen [B]; and treatment of recovered bitumen-rich froth to remove impurities such as water and solids [C].

A.1.1 Bitumen Properties

Petroleum or crude oil is a complex variable mixture of many different hydrocarbons. The composition and properties of crude oil are dependent on its geological history and the type of reservoir. The quality of a crude oil reserve is generally measured by its heaviness using a hydrometer (*i.e.*, API gravity^b). Light crude oil is more valuable to refineries as it usually contains lower level of contaminants, requires less chemical processing and ultimately yields more high value products. Heavier crude oil is the product of light crude oil partially degraded by microbes and therefore contains a relatively greater proportion of high molecular weight compounds, which are more difficult for microbes to break down.^{14,15} Heavy crude oils can exhibit extremely high viscosity and must often be heated to achieve appreciable flow. Bitumen, an even heavier material compared to heavy crude oil, has a density greater than that of water at ambient conditions. A comparison of typical properties of different types of crude oil is given in **Table A-1**.

^b Degree API is calculated using the following equation:

$$^{\circ}\text{API} = \frac{141.5}{\text{specific gravity at } 15.6^{\circ}\text{C}} - 131.5$$

Table A-1. Typical physical properties of various types of crude oil.

Petroleum	Viscosity (mPa·s)	Density (g/cm ³)	° API	Pour Point (°C)
Conventional oil	< 100	< 0.934	> 20°	< 0
Heavy oil	100 – 10 000	0.934 – 1.0	< 20°	< 0
Bitumen	> 10 000	> 1.0	< 10°	> 10

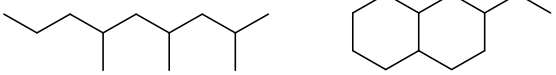
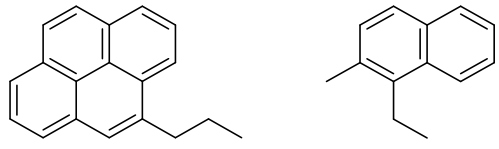
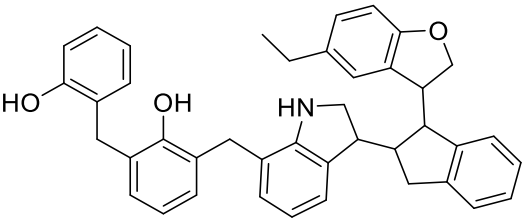
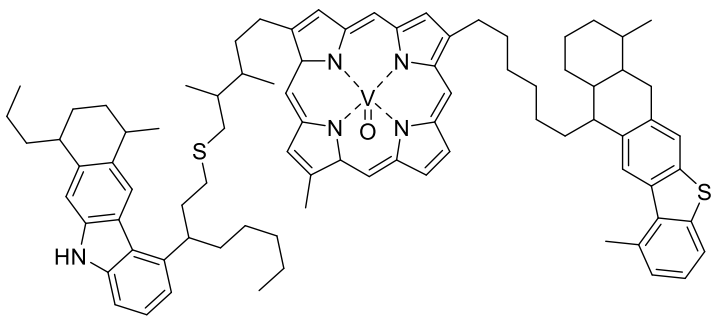
The specific physical properties of bitumen change according to its composition, and thus regional variations exist. Bitumen from the Cold Lake region, for example, is lighter compared to bitumen from the Athabasca region. The density and viscosity of a typical bitumen sample, at different temperatures, are given in **Table A-2**. Bitumen behaves as a Newtonian fluid but is extremely viscous at ambient conditions. Underground bitumen is essentially immobile at reservoir conditions and its viscosity must be reduced for cost-effective *in-situ* production. Fortunately, bitumen viscosity is very sensitive to temperature, and bitumen, once heated, will flow and its mobility is sufficient to sustain production. Gravity separation of water and bitumen is also difficult as both substances have similar density at ambient conditions. The specific gravity of bitumen experiences a peculiar change with increasing temperature. Bitumen slowly rises to the surface between 30 – 100°C but settles above 125°C.

Table A-2. Density and viscosity of bitumen and water at different temperatures.

Temperature (°C)	Density (kg/m ³)		Specific gravity ($\rho_{\text{Bitumen}}/\rho_{\text{Water}}$)	Viscosity (Pa·s)	
	Water	Bitumen		Water	Bitumen
25	998	1000	1.002	8.9×10^{-4}	2.1×10^2
50	988	984	0.996	5.5×10^{-4}	1.5×10^1
75	975	969	0.994	3.8×10^{-4}	1.6
100	958	954	0.996	2.8×10^{-4}	2.3×10^{-1}
150	918	924	1.007	1.8×10^{-4}	9.3×10^{-3}
200	864	894	1.035	1.6×10^{-4}	7.5×10^{-4}

Crude oils are often characterized by chemical composition. The composition of a crude oil is the result of its geological history, and for bitumen, extensive biodegradation. Different components of crude oil are separated based on their solubility and polarity by fractionation.^{7,14,16} The fraction of oil that is insoluble in paraffinic solvent (*i.e.*, *n*-hexane or *n*-heptane) is known as the asphaltenes. The fraction of oil that is soluble in paraffinic solvent, known as the maltenes, is further subdivided into resins, aromatics, and saturates by chromatography using solvents of different polarities. Alberta bitumen typically contains a greater portion of the heavier fractions.¹⁴ The composition of bitumen from a typical Alberta oil sand deposit is summarized in **Table A-3**.

Table A-3. Typical composition of bitumen from oil sands.⁷

Component	Composition (wt%)	C to H ratio	Illustrative exemplary compounds
Saturates	13 – 22	2 – 4	
Aromatics	29 – 49	< 1	
Resins	18 – 32	1 – 2	
Asphaltenes	15 – 21	< 1.15	

Bitumen contains a high concentration of heteroatoms (*i.e.*, nitrogen, oxygen, and sulphur). A typical bitumen sample from the Athabasca region contains 83.1 ± 0.3 wt% carbon, 10.3 ± 0.3 wt% hydrogen, 0.4 ± 0.1 wt% nitrogen, 1.1 ± 0.3 wt% oxygen, 4.6 ± 0.5 wt% sulphur, 220 ppm vanadium and 80 ppm nickel.⁷ Numerous chemical structures of sulphur are found in bitumen, including thiophenes, sulfides, sulfoxide, thiols, sulfones and sulfonic acids. Nitrogen compounds are also found in bitumen as both pyrrole derivatives and basic pyridine derivatives. Sulphur and nitrogen are more abundant in heavier compounds of greater boiling point.¹⁷ Oxygen species in bitumen are mostly carboxylic acids and esters along with phenols, alcohols, ketones and ethers. The most important oxygen-containing species in bitumen are the naphthenic acids (1 – 2 wt%).^{7,18} Naphthenic acids are acidic and interfacially active once ionized at alkaline pH.¹⁸ Bitumen also contains organometallic compounds with heavy metal ions, coordinated to a porphyrin-type structure.^{19,20}

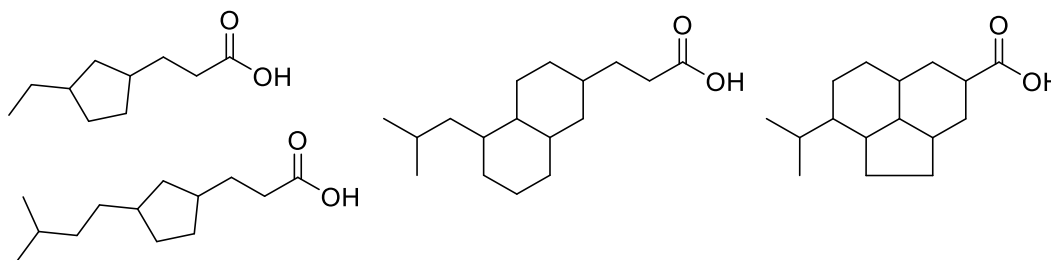


Figure A-2. Typical structures of interfacially active naphthenic acids. ^{7,18}

The surface tension and interfacial tension of bitumen and related materials are given in **Table A-4**. Unlike the interfacial tension of water and pure hydrocarbons, water-bitumen interfacial tension is influenced by pH: decreasing from 23 mN/m (at low pH) to less than 1 mN/m (at high pH).²¹ The change in interfacial tension indicates the presence of pH-sensitive interfacially active species.²² The acidic fraction of crude oil (*i.e.*, naphthenic acids) is especially important to the wettability of the oil sand solids.^{23,24} The average total acid number (TAN) of Athabasca bitumen is around 3.3 mg KOH/g.²⁵ The indigenous surfactants found in bitumen contain carboxylic acid groups (pK_a between 4.2 – 5.2), which are activated at high pH following caustic addition. Compounds found in bitumen also contain other chemical functional groups that ionize at different pH, such as sulfates (pK_a about 1.9), sulfonates (pK_a about 7.0), and amines (pK_a between 9.3 – 11.0).⁷

Table A-4. Surface tension and interfacial tension of bitumen and various fluids.^{26–29}

Component	Temperature (°C)	Surface tension (mN/m)	Interfacial tension (mN/m)
Water	50	67.9	n/a
Toluene	50	24.9	34.3
Hexane	50	15.3	48.1
Bitumen	64	29.6	14.5
	75	28.3	13.5
	104	25.6	11.8

The heat of combustion for bitumen is approximately 41.5 MJ/kg but increases up to 45.7 MJ/kg after blending with a low-viscosity diluent. Thermal properties of bitumen and other materials present in oil sands ore are summarized in **Table A-5**. The variability in thermal conductivity of oil sand, which is between 1.3 – 2.0 W/m·K, appears to be independent of ore composition.^{30,31}

Table A-5. Typical thermal properties of oil sands ore constituents.

Component	Heat capacity (J/kg·K)	Thermal conductivity (W/m·K)
Bitumen	1800	0.2 – 0.5
Sand	800	0.3 – 2.0
Clay	1400	0.2 – 1.8
Water	4200	0.6
Air	1000	0.02

A.1.2 Bitumen Blending

Bitumen cannot be directly transported in pipelines due to its high viscosity at ambient conditions, especially in the regions of colder climate. Although alternative transportation of heavy oil and bitumen by railcar is possible, pipelines remain the most economical and safest method available for moving large volumes of petroleum. Therefore, various strategies have been employed to assist transport of heavy crude oil and bitumen in pipelines. Viscosity of heavy crude oil and bitumen is lowered by heating. However, heating for extended distances is not possible except with special pipelines, which are much more expensive to build, operate and maintain.

Transport of heavy crude oil in pipelines is possible by first producing a low-viscosity oil-in-water emulsion.³²⁻³⁴ The emulsion may be stabilized using a variety of ionic and non-ionic surfactants.^{32,35,36} It is also possible to stabilize emulsions by activating indigenous surfactants using a base.³⁷ Orimulsion®, a 30 wt% emulsion of Orinoco heavy crude in water stabilized by various surfactants, for example, was marketed and sold as a fuel for use in stationary boilers. The additional water reduces the calorific value of combustion as phase separation of Orimulsion® was not feasible. Water is tolerated in combustion processes but incompatible with refinery processes. Dissolved salts in water often lead to accelerated corrosion.

The general limits for viscosity and density, imposed by pipeline operators, are 350 cSt and 940 kg/m³, respectively. Seasonal variations for bitumen blends exist as the viscosity limit is constraining in winter while the density limit may be constraining in summer. In order to meet the specifications of the pipeline, bitumen with a density between 960 – 1020 kg/m³ is diluted with naphtha-based diluents or synthetic crude oil from bitumen upgraders. Suitable diluents for bitumen include light crude, condensates and various refinery cuts. Bitumen diluted with synthetic crude oil costs more but yields greater fractions of high value products during refining.

Table A-6. Typical bitumen blends for pipeline transport.

Type of Blend	Diluent	Diluent Density (kg/m ³)	Diluent (wt%)
DILBIT	Heavy naphtha	650 – 750	> 20%
SYNBIT	Synthetic crude oil	840 – 870	> 50%

A.2 Surface Mining

Surface mining is a massive operation that requires heavy machinery, operating facilities, and related infrastructure.³⁸ Only relatively shallow oil sand formations, concentrated in the Athabasca region, are recovered by surface mining. In order for surface mining to be economical, the ratio of waste (*i.e.*, overburden and interburden) to mineable ore must be less than about 1.0 – 1.5.³⁰ Very large shovels and trucks are used to pick up and transport oil sands ore to a stationary crusher that reduces the ore into smaller lumps. Oil sand deposits are heterogeneous and significant variability is observed in different ore facies. A rich quality ore has more than 15 wt% bitumen and low fines content while a poor quality has less than 8 wt% bitumen and high fines content. Operators will generally blend ores of different quality in order to achieve an average bitumen content of approximately 10 wt%, as poor quality ores generally lead to reduced bitumen recovery. The crushed ore is mixed with hot water and other chemical additives to form a slurry that is transported to the extraction facility through a hydrotransport pipeline. The slurry of oil sands ore is conditioned within the hydrotransport pipeline wherein it is subjected to shear and contact with entrained air. The conditioning process breaks up lumps, disperses loose ore, liberates bitumen from surface of solids, promotes coalescence smaller bitumen droplets and aerates liberated bitumen droplets.

The conditioned slurry enters a large gravity separation vessel at the extraction facility, known as the primary separation vessel (PSV). Inside the PSV, liberated bitumen droplets and air bubbles rise together to the surface, in the form of bitumen froth. Approximately 70 – 90 wt% of recoverable bitumen is collected as froth from the surface of the primary separation vessel. Another 5 – 15 wt% of recoverable bitumen is collected during secondary recovery from middlings stream redirected to secondary flotation cells. Bitumen froth from the primary separation vessel contains approximately 60 wt% bitumen, 30 wt% water, 10 wt% solids, as well as entrained air. The froth is heated to remove entrained air. However, even at high temperature, phase separation of water is extremely slow due to the high viscosity and density of bitumen. A suitable diluent is therefore added to reduce the viscosity and density of recovered bitumen. Although most of the water separates upon dilution, emulsified water droplets and fines remain dispersed. Emulsified water droplets and fines are subsequently removed using a combination of

centrifuges, cyclones and inclined plate settlers. The diluent used during froth treatment must be recovered due to the high cost and limited availability of suitable diluents.

Bitumen extraction tailings emerge from the underflow of the PSV, flotation cells and cyclones. Tailings contain a variety of solids including coarse sand particles and fine clay particles. In addition, tailings contain up to 5 wt% of bitumen, which, along with naphthenic acids, contribute to its environmental toxicity.³⁹⁻⁴¹ Whilst coarse sand particles settle out rapidly from tailings, fine clay particles remain suspended. The mixture of dispersed solids does not densify, even after decades of settling in large tailings ponds. Settling rate is accelerated using both physical and chemical processes. Physical separation of solids is possible using various mechanical dewatering techniques but gravity separation is preferred, due to the large volume of tailings produced. Chemical treatments are available to accelerate the rate of sedimentation by promoting flocculation of small particles. However, chemical treatments are limited by the cost of the additive and its effect on bitumen recovery as the separated water is recycled back into the extraction process.

A.2.1 Bitumen Ore Conditioning

In the original Clark Hot Water Extraction process for bitumen, the oil sands ore slurry was heated to approximately 70 – 80°C and caustic was added to improve extraction efficiency.^{42,43} The conditioning process used in early operations was conducted in a large rotating tumbler with hot steam injection. Numerous improvements to the original process have been made to lower the energy required for bitumen recovery. The modern process operates at lower temperature, typically between 35 – 40°C or between 50 – 60°C, and continues to use a slightly alkaline pH to help condition the ore and liberate bitumen.

Oil sands ore, collected using large shovels, is either transported to the extraction plant by large trucks or as a slurry inside pipelines.³⁸ Hydrotransport of slurry in pipelines has replaced trucking due to its lower cost and the benefits of additional conditioning time. The generalized interconnected processes involved in conditioning of oil sands ore are illustrated in **Figure A-3**. The complex conditioning process consists of digestion of ore lumps, liberation of bitumen from sand grains, as well as coalescence and aeration of liberated bitumen droplets.

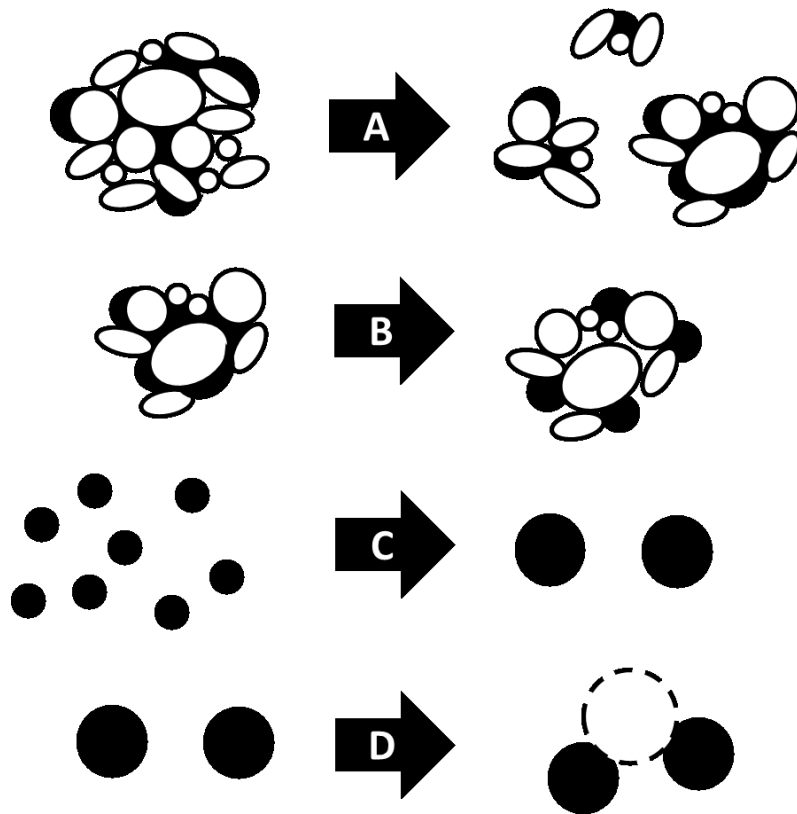


Figure A-3. Schematic representation of oil sands ore conditioning. Conditioning is a general term used to describe several interconnected processes including: digestion of ore lumps [A]; liberation of bitumen from sand grains [B]; coalescence of liberated bitumen droplets [C]; and aeration of bitumen droplets [D].

A slurry is prepared by crushing oil sands ore into smaller lumps (< 0.6 m), which are mixed with recirculated slurry using a cyclofeeder to ensure rapid mixing and effective dispersion of solids. Vibrating screens reject any oversize material but are subject to very heavy wear. Rotary breakers are similar to rotary tumblers with longitudinal lifters along the rotational axis that lift and drop large pieces. The impacts gradually break up the ore. The design of a rotary breaker incorporates a screen that allows small pieces to pass through the screen while oversize material is retained and discharged.

The liberation, coalescence and aeration processes that occur within the hydrotransport pipeline are governed by surface forces and interfacial phenomena. The operating conditions of the hydrotransport pipeline have a critical effect on bitumen recovery.^{44,45} Lumps of ore are

digested along the pipeline with mechanical and thermal energy provided by the carrier fluid. Slurry temperature and hydrotransport distance have an effect on overall bitumen recovery from both high-quality ores and low-quality ores, which often require caustic addition to improve liberation. The disintegration of the ore matrix is more effective at high temperature. At lower temperature, bitumen maintains its shape and helps binds sand grains together, making digestion of lumps more difficult. The length of hydrotransport pipeline required to digest 95% of lumps is greatly reduced at higher temperature wherein bitumen is more fluid.³⁰

Various slurry preparation and conditioning techniques are provided in **Table A-7** for comparison. The use of steam to heat crushed oil sands ores inside a rotating tumbler requires the greatest amount of energy but results in a very hot slurry (> 80°C). The increased residence time of a hydrotransport pipeline lowers the temperature requirement for conditioning the ore, allowing hot water to be used instead of steam to produce a warm slurry (40 – 55°C). Further reduction of slurry temperature (25 – 35°C) using warm water requires addition of hot water (55°C) prior to entering the primary separation vessel (PSV) in order to maintain a temperature of 35°C in the PSV. However, the lower temperature of the slurry during hydrotransport is insufficient for proper conditioning and results in reduced bitumen recovery. Optimum recovery and heating are achieved by first preparing a warm slurry (45 – 50°C) and adding cold water prior to entering the PSV. Bitumen conditioning is more effective when slurry temperature is greater than 35°C. Thus, replacing PSV flood water with colder water does not significantly impact the separation. Reducing the energy requirement of extraction process remains a priority.

Liberation is the process wherein bitumen on the surface of unconsolidated solids begins to recede, agglomerate together, and eventually detach as small droplets. Bitumen recovery is significantly depressed at temperatures below 35°C for all types of ore.⁴⁵⁻⁴⁷ Although temperature does not significantly affect the final contact angle of bitumen on silica, recession of bitumen is much faster at higher temperatures.⁴⁸ The most important effect of temperature is related to reducing bitumen viscosity and the adhesion between bitumen and solids.^{45,49}

The recession and detachment of bitumen droplets, in an aqueous environment, are also strongly influenced by water chemistry.⁴⁴ The surface of sand particles becomes more hydrophilic as silica undergoes hydrolysis at high pH. The change in wettability of solids in oil sands ore from

weathering is a major reason for poor recovery.⁵⁰⁻⁵² In addition, interfacially active compounds with acidic groups are activated under alkaline conditions. The presence of divalent cations (Ca^{2+} and Mg^{2+}) increases the adhesive force between silica and bitumen, while bicarbonate ions have the opposite effect.^{53,54} The ideal surfactant concentration of 0.1 mM occurs around pH of 9.⁵⁵ Therefore, liberation of bitumen is more effective with addition of caustic.

Table A-7. Temperature of different oil sands ore slurry preparations.^{30,56,57}

Slurry preparation and conditioning	Water/steam temperature (°C)	Slurry temperature (°C)	Flood water temperature (°C)	PSV temperature (°C)	Heat requirement (MJ/t)
Tumbler	> 100	80 – 95	n/a	n/a	> 295
Cyclofeeder and hydrotransport	85 – 95	40 – 55	n/a	n/a	> 185
Cyclofeeder and hydrotransport	30 – 40	25 – 35	55	35	> 100
Tumbler/ cyclofeeder and hydrotransport	60 – 70	45	10	35	100

Dispersed bitumen droplets collide with each other and coalesce to form larger droplets. At high temperature, dispersed hydrophobic bitumen droplets may also collide with and attach to air bubbles and even engulf air bubbles. In contrast, hydrophilic sand particles do not interact with air bubbles. The mixture of bitumen and air has a lower specific gravity compared to water and rises to the surface as bitumen froth. Although alkaline condition favours liberation of bitumen, the increased charge on surface of bitumen droplets from ionization of acidic components is detrimental to the attachment of air bubbles on bitumen droplets.

A.2.2 Bitumen Recovery

Liberated bitumen droplets are separated during primary recovery inside a large vessel in a process based on the difference in density between aerated bitumen and mineral solids.⁵⁸ A

stream of conditioned slurry (1450 – 1700 kg/m³) is pumped into the primary separation vessel (PSV), wherein heavy mineral solids quickly settle to the bottom, while bitumen droplets together with entrained air rise to the surface of the pulp. Entrained air, up to 20 – 40 vol% of the collected froth, increases the buoyancy of bitumen. A bitumen-rich froth is produced near the surface of the PSV and contains up to 70 – 90 % of the recoverable bitumen. Hydrophilic materials such as sand particles do not stick to air bubbles and end up mainly in the underflow. The PSV consists of either a thickener-type vessel with a rotating rake or a deep-cone vessel.⁵⁸ The composition of various streams exiting the PSV is summarized in **Table A-8**.

Table A-8. Composition of various streams leaving primary separation vessel.⁵⁸

Primary separation vessel (PSV) streams	Bitumen (wt%)	Water (wt%)	Solids (wt%)
Overflow (bitumen froth)	55 – 65	25 – 35	6 – 12
Middlings	0.5 – 5	60 – 80	20 – 40
Underflow (tailings)	0.2 – 3	20 – 40	50 – 70

The bulk density of mineral solids (*e.g.*, quartz, potassium feldspar, illite and kaolinite) is generally much greater (*i.e.*, between 1300 – 2400 kg/m³) than both water and bitumen. However, sufficiently small particles remain well dispersed due to colloidal stability and energy from motion of carrier fluid. Thus, fines, especially clay particles, tend to accumulate in the middlings stream. Bitumen droplets attached to solids, having higher effective density, cannot rise to the surface and remain dispersed inside the PSV. The composition of the middlings is variable and largely dependent on the quality of the ore. The middlings may contain up to 20 % of the recoverable bitumen for poor quality ores.³⁰ Multiple supplemental separation stages are added to recover additional bitumen from the middlings stream.

Poor processing ores with high fines content generally result in lower bitumen recovery and poorer froth quality.⁵⁹ In a process known as slime coating, clay particles and other solids coat the surface of liberated bitumen droplets and prevent their attachment to air bubbles. Bitumen

depressed by slime coating is less likely to end up in the froth collected from the PSV. Swelling clays such as smectite and weathered solids are especially prone to slime coating.^{60,61} The effect of clay fines on bitumen recovery is reduced with the addition of caustic.⁶⁰ Increasing the temperature also reduces the adhesive force between bitumen and clay fines.⁴⁵

The middlings stream contains some residual bitumen and is diverted to a series of flotation cells, wherein bitumen is recovered by induced air flotation in the secondary recovery process.⁵⁸ Flotation is a separation technique that takes advantage of differences in hydrophobicity; a gas (*e.g.*, air) is used as a carrier to bring hydrophobic material to the surface.⁶² Hydrophobic material attaches onto carrier gas bubbles generated by forcing the gas through small orifice, breaking up air stream using an agitator or *in-situ*. Smaller bubbles are generally more favourable due to greater specific surface area. Flotation is effective in separation of both hydrophilic and hydrophobic minerals from gangue. Flotation of hydrophilic material is possible provided the surface is modified to be hydrophobic using a chemical collector. The use of collectors is critical in selective flotation of minerals such as galena and sphalerite. Collectors include alkoxy xanthates, dithiophosphates, sulfonates, sulfates and carboxylates.⁶³ Kerosene or other liquid hydrocarbons function as a collector in bitumen flotation by coating air bubbles with a hydrophobic layer.^{64,65} In contrast to collectors, chemical depressants are used to modify mineral surfaces to be more hydrophilic, and thus prevent the attachment of these minerals on rising gas bubbles. The response of different minerals to flotation is dramatically affected by process conditions, especially pH due to its effect on surface charge. Particle size is also important for flotation of mineral solids, as larger particles cannot be effectively lifted by air bubbles and smaller particles do not efficiently attach to air bubbles.⁶⁶

Additional separation processes in the tertiary recovery process include the use of gravity settlers, sieve screens, hydrocyclones and thickeners.⁵⁸ Tertiary recovery processes are intended not only to recover additional residual bitumen but also latent heat from tailings stream and recycle process water. Thickeners are large and relatively shallow open cylindrical vessels wherein solids are allowed to settle to the bottom under gravity.⁶⁷ Slow rotating rakes direct the sediment to an opening at the bottom of the vessel for discharge. Under ideal conditions, with chemical additives and sufficient settling time, thickeners can remove solids particles as small as

0.1 μm . Hydrocyclones are much smaller compared to thickeners and have much shorter residence time.⁶⁷ A feed mixture enters tangentially at moderate velocity into a conical vessel away from its apex. The shape of the vessel provides a vortex flow field, resulting in a centrifugal force. Coarse particles experience greater inertia and exit the hydrocyclone through the bottom while finer particles exit through the top along with carrier fluid. Under ideal conditions, hydrocyclones can remove solid particles of about 5 μm .

A.2.3 Froth Treatment

Bitumen froth recovered from the PSV contains up to 40 vol% air; and on air-free basis, approximately 60 wt% bitumen, 30 wt% water and 10 wt% solids. Entrained air is removed inside static deaerating units or at higher temperature inside steam deaerating units. Bitumen froth must remain heated in order to remain fluid. Froth treatment currently consists of diluting the froth with a low-density solvent followed by various mechanical separators including centrifuges and inclined plate settlers. The diluent must later be recovered by stripping the diluted bitumen.

The nature of the diluent has a profound effect on the interfacial properties of emulsified water droplets. A dramatic change occurs above a point known as the critical dilution ratio.^{68–71} At high bitumen concentration, the flexible oil-water interface preserves the spherical shape of droplets upon deflation. Emulsion droplets are more easily formed in this regime wherein the interface is flexible. In contrast, the oil-water interface is rigid at low bitumen concentration and the oil-water interface of droplets crumple when liquid is withdrawn. Droplets with rigid interface flocculate together and settle more rapidly. The addition of diluent to bitumen reduces viscosity and density and therefore accelerates the rate of water droplet sedimentation. Two distinctive solvents (*i.e.*, heavy naphtha and paraffin) are used as diluent in froth treatment processes.^{72–74}

In the naphthenic process, bitumen is mixed with naphtha using a solvent-to-bitumen ratio between 0.65 – 0.70. No precipitation of asphaltenes is observed when bitumen is diluted with naphtha, which contains many aromatic hydrocarbons. The naphthenic process operates at high temperature (70 – 80°C). Dilution with naphtha alone does not result in a high-quality separation as very small residual water droplets (< 5 μm) remain. Subsequent separation units (*i.e.*, centrifuges, inclined plate separators and bitumen cyclones) are required to reduce the water content to about 2.5 wt% and reduce the solid content to about 0.4 wt%.⁷²

In the paraffinic process, bitumen is mixed with paraffin using a solvent-to-bitumen ratio greater than 2.0.⁷⁵ A portion of the asphaltenes precipitate as a result of paraffin addition, as paraffin contains mostly saturates and little aromatics. Asphaltene rejection using pentane begins when solvent-to-bitumen ratio is around 1.0 and increases to over 90% when ratio is around 5.0. The precipitated asphaltenes also carry emulsified water droplets, which are more closely associated with interfacially active components of bitumen. Therefore, the paraffinic froth treatment process produces a product which is very dry, with less than 0.2 wt% water, and virtually free of solids. However, the paraffinic process requires substantially more solvent compared to the naphthenic process, and precipitation of asphaltenes (*i.e.*, 15 – 20 wt% of bitumen) reduces the overall yield of petroleum hydrocarbons.

Chemical additives are added to accelerate phase separation of emulsified water droplets.^{76,77} Chemical demulsifiers function by promoting droplet coalescence and/or flocculating droplets. Coalescence-promoting chemicals weaken the oil-water interface by changing the interfacial properties or by displacing stabilizing material such as indigenous surfactants and biwettable fine solids. Chemical flocculants aggregate droplets and solids together to form larger flocs that settle more rapidly. Many chemical additives used as demulsifiers have a strict window for functional concentration and are prone to overdosing beyond a critical concentration.^{76,77} A study of various classes of polymeric demulsifiers revealed optimal performance when the relative solubility number (RSN) of the additive is between 7.5 – 12.5 and molecular weight is between 7500 – 15000.⁷⁸ In order for a chemical demulsifier to function, it must have sufficient solubility and mobility in the continuous phase so that they can reach the oil-water interface of emulsified droplets.

A.2.4 Tailings Management

The bitumen extraction process uses large amounts of water and produces a waste stream consisting of mineral solids dispersed in process water along with some residual bitumen.⁷⁹ Stockpiles of tailings are traditionally stored in large artificial ponds bordered by sand dykes. Over a course of several weeks to several months, densification of tailings inside large ponds occurs as mineral solids settle under gravity, as shown in **Figure A-4**. Coarse particles (*e.g.*, sand grains) settle relatively quickly and form a sediment at the bottom of the tailings pond. However, smaller

mineral solids (*e.g.*, silt and clay particles) remain suspended, even after several years of sedimentation. Relatively clear water is withdrawn from tailings ponds near the surface and recycled back to the extraction plant. Therefore, chemicals added to the tailings pond in order to accelerate sedimentation must not interfere with bitumen extraction.⁸⁰ The intermediate section of the tailings pond consists of about 85 wt% water, 13 wt% clays and 2 wt% bitumen. The term fluid fine tailings (FFT) formally refers to any fluid with greater than 1 wt% solids and a shear strength of less than 5 kPa. FFT eventually forms mature fine tailings (MFT) after several years of sedimentation, at which point the densification process is essentially at a standstill. MFT consists of up to 30 – 40 wt% solids, comprising primarily of clay particles less than 0.5 μm . The clay particles in MFT form a high viscosity gel network which prevents further densification.⁸¹ Tailings management and disposal remain a significant challenge as it precludes any further land reclamation activity. Hydrocarbons which separate in the tailings pond rise to the surface and represent a significant environmental concern.

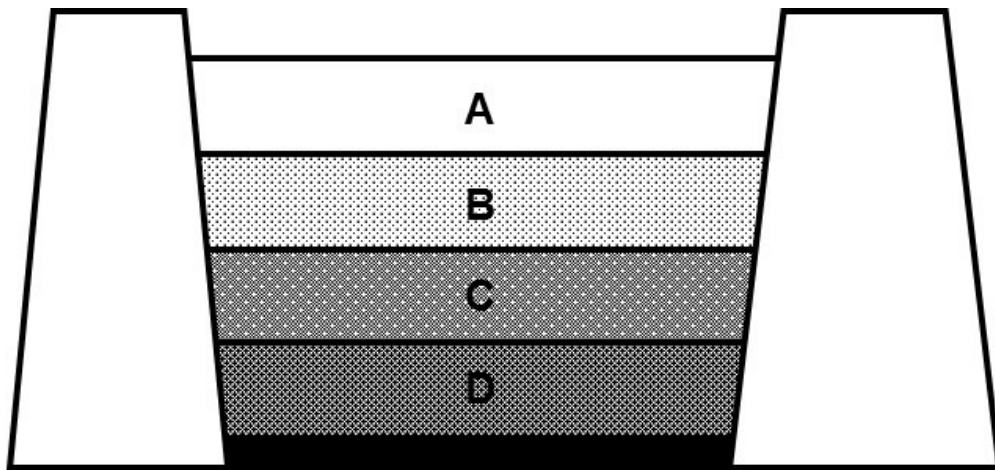


Figure A-4. Cross-sectional diagram of a typical tailings pond. Segregation based on density results in a layer of relatively clear water near the surface [A]; an intermediate layer of fluid fine tailings [B]; a layer of mature fine tailings below [C]; and sediment of coarse particles [D]. The transition between each layer is not usually distinct with transitional regions between each layer.

The colloidal stability of dispersed particles is very sensitive to changes in water chemistry.^{82,83} Colloidal stability provided by strong electrostatic surface charges is reduced by increasing electrolyte concentration. Divalent and multivalent cations (*e.g.*, Ca^{2+} , Mg^{2+}) are very

effective and cause dispersed particles to aggregate. Additives are commonly added to bitumen extraction tailings in order to accelerate the solid-liquid separation process. Chemical flocculants promote formation of aggregates by forming a bridge between particles.⁸⁴ Various technologies for disposing tailings are available.⁸⁵ The cost and technical viability of different disposal methods remain a concern.

A.3 *In-situ* Extraction

Oil sand reserves located deeper underground, with ratio between waste material (*i.e.*, overburden and interburden) and mineable material greater than about 1.5, cannot be economically recovered by surface mining. Unfortunately, conventional production methods are not effective as the high viscosity of bitumen prevents significant primary production.⁸⁶ Therefore, a suitable method of heating the bitumen in place is required in order to increase the mobility of bitumen and induce sufficient flow for economical production.⁸⁷ Viable technologies used to recover underground bitumen include cyclical steam stimulation (CSS) and steam-assisted gravity drainage (SAGD). The geological properties of the specific reservoir are critical to any successful application of an *in-situ* production method. The presence of top gas or bottom water is a challenge for recovery methods based on steam injection, as steam generation represents a significant cost to most *in-situ* production methods and losses must be minimized. Reservoir conformance problems are also present in unconsolidated sand formations.^{88,89}

The majority of wells are drilled using a rotary drilling system, wherein a rotating bit penetrates into the formation. Hydraulic power is delivered from powerful pumps on the surface to the drill bit through a series of interconnected tubular pipes. The bottom hole assembly (BHA) extends from the end of the drill pipe and includes drill collars, subs, sensors, the mud motor and the drill bit. Together, drill collars, drill pipes and the BHA provide the necessary weight-on-bit to penetrate into the formation. The rotation of drill bit and the weight-on-bit from the entire drill string produce a relatively vertical borehole. Non-vertical wells are drilled using a motor with a small bend at the end, as shown in **Figure A-5**. Inclination in a specific direction may be slowly built by rotating the bit alone and sliding the drill string into the formation. Rotary steerable systems are gaining popularity due to higher rate of penetration.

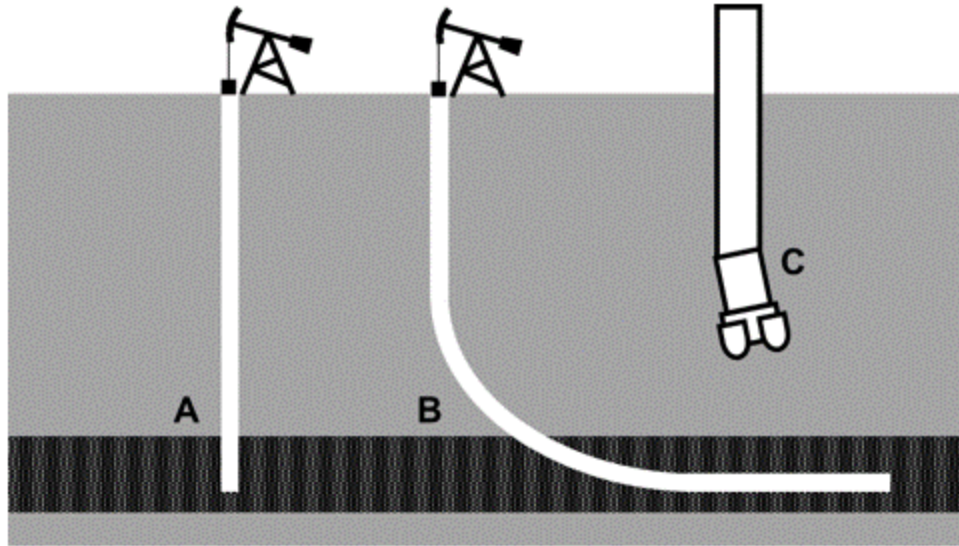


Figure A-5. Diagram of a vertical well [A] and a horizontal well [B]. Directional drilling of non-vertical boreholes along the length of a horizontal deposit is possible using a motor with a small bend [C].

Directional drilling has many advantages including increased length of well section within reservoir pay zone, access to obstructed reservoirs and reduced footprint by drilling multiple wells in a single pad.^{90,91} Directional drilling coupled with real-time logging has greatly improved the placement of wells. Information from downhole compasses and/or gyroscopes is relayed to the surface using various telemetry systems (*e.g.*, pressure, electromagnetic, direct connection).⁹² Various sensors (*e.g.*, temperature, pressure, gamma ray, resistivity, *etc.*) may also be included in the BHA to evaluate the properties of the formation (*e.g.*, density, porosity and saturation) while drilling.⁹² Data acquired in open hole while drilling is usually superior compared to logging after the borehole is cased and cemented. Real-time control of borehole placement based on real-time geotechnical data is known as geosteering and possible using azimuthal formation evaluation sensors.⁹³

Hydraulic fracturing is a method for stimulating a reservoir by inducing cracks within the formation. Fluids move more freely through the formation as a result. Fracturing is therefore especially beneficial in increasing the production rate of formations with low permeability (< 0.1 mD). Hydraulic fracturing is accomplished using a fluid to overcome the effective stress of the formation. Fractures induced by hydraulic pressure propagate in the direction of least resistance

and are perpendicular to the primary stress plane. Horizontal fracturing is only possible to a depth of about 500 – 600 m. At greater depth, only vertical fractures occur due to the overwhelming pressure of the overburden. Open fractures are propped with sand or other solids. Caution must be exercised due to the risk of surface and ground water contamination. Additionally, hydraulic fracturing near active fault lines can trigger seismic activity.

A.3.1 Cyclic Steam Stimulation

The cyclic steam stimulation (CSS) process alternates between an injection phase and a production phase.⁹⁴ During the injection phase, superheated steam is introduced into the reservoir for a period lasting from days to months. The injected steam heats up the formation, lowers the viscosity of bitumen and increases pressure inside the reservoir. During the production phase, bitumen, condensed steam and formation fluids are produced together. The cycle is repeated once the production rate drops, which generally decreases after each subsequent cycle.

CSS wells are relatively simple wells that are made to produce relatively quickly. CSS is fairly versatile and can be used in both single well designs or multi-well designs.⁹⁵ The ultimate recovery for ordinary CSS processes is low but significantly increased by combining CSS with solvent injection, surfactant injection, directional drilling and hydraulic fracturing. Co-injection of solvent improves recovery by enhancing the mobility of the bitumen.⁹⁶ Wetting agents are sometimes injected to modify the wettability of the formation. Injection of surfactant solution forms micelles that help mobilize bitumen through emulsification.

A.3.2 Steam-Assisted Gravity Drainage

The steam-assisted gravity drainage (SAGD) process requires a pair of parallel horizontal wells drilled 5 – 7 m apart; the upper well is used to inject steam into the reservoir while the lower well is used as the production well.^{97–99} A special magnetic ranging tool is used to drill the second well.¹⁰⁰ Injected steam rises in the formation and forms a steam chamber with characteristic wedge shape along the length of the injection well. Steam condenses at the edges of the steam chamber and heats up the bitumen. The mobilized bitumen drains under gravity towards the lower production well where it is carried to the surface.

Recent improvements to the SAGD process are aimed at reducing the energy requirement. Steam and solvent can also be injected together in expanding-solvent steam-assisted gravity drainage (ES-SAGD).^{101,102} The addition of a volatile solvent acts as a diluent and reduces the viscosity of the bitumen at the edge of the steam chamber.¹⁰³ The solvent reduces the temperature at which the bitumen drains into the production well and therefore reduces steam-oil ratio. Other proposed technologies include vapour recovery extraction (VAPEX), which altogether replaces steam with a solvent.^{104,105} The cost and recovery of the diluent are important considerations for solvent-based recovery processes. Electromagnetic heating has also been considered and is currently under development.¹⁰⁶

A.3.3 *In-situ* Combustion

Steam generation represents a significant cost for *in-situ* production and cheaper methods are actively sought. Combustion methods rely on controlled underground combustion of bitumen to generate steam, heat the bitumen and increase mobility.¹⁰⁷ Tow-to-heel air injection (THAI) is a method wherein air is injected into the formation in order to sustain combustion.¹⁰⁸ THAI comprises a vertical injection well located away from the end of a horizontal production well. As the underground combustion process proceeds within the formation towards the base of the horizontal well, mobilized bitumen is produced. Control of the flame front is critical and may require pure oxygen instead of air.¹⁰⁹

A.4 Bitumen Upgrading and Synthetic Crude

Petroleum refineries separate the components of petroleum into various products. Each cut is sold at different prices for different applications. The atom efficiency of a refinery is comparatively high compared to other industries, as nearly all of the material is converted to a valuable product and little of the crude petroleum is wasted. A major operational objective of a refinery is to maximize recovery of most desirable products. Modern refineries are capable of performing a variety of chemical transformations in order to generate a greater amount of the more valuable products. Bitumen cannot be directly processed by conventional refineries and is upgraded into synthetic crudes that have similar characteristics to light sweet crude.^{110–112}

Synthetic crude oil has reduced viscosity and is more valuable compared to bitumen. Bitumen upgrading includes both thermal cracking and hydroconversion processes. Typical bitumen upgraders also remove the majority of sulphur compounds. A wide range of products can be made using various combinations of bitumen upgrading processes.

A.4.1 Separation Processes

The first step in refining is a desalting process. Due to the marine origin of oil and sedimentary deposits, salts are present in the formation and recovered along with petroleum. Chlorides are an especially undesirable contaminant since they react and form very corrosive species. Hydrochloride acid (HCl) gas is formed through hydrolysis of magnesium chloride, calcium chloride and sodium chloride. Furthermore, the acid gas may react with ammonia to produce ammonium chloride and other salts that greatly contribute to fouling. The presence of naphthenic acids influences the generation of HCl inside the refinery.

In desalting units, crude oil is washed with water (up to 10 vol%) at high temperature (up to 150°C). Water and dissolved salt are subsequently removed under high voltage (up to 15 – 35 kV) wherein emulsified droplets move in accordance to the electric field. In alternating current units, adjacent droplets acquire opposite charges, which promote droplet coalescence. Bitumen emulsions are not dewatered effectively using electrostatic methods due to its characteristically high concentration of naphthenic acids, asphaltenes and solids.

Atmospheric and vacuum distillation are classic refinery processes.¹¹³ Separation of compounds by distillation relies on differences in boiling point of different components, which is generally proportional to molecular weight. In a petroleum refinery, a mixture of hydrocarbons is vaporized inside a fractional distillation column. Different cuts, with characteristic boiling point ranges, condense at different intervals along the height of the column. Components with the lowest boiling point exit from the top of the column and the components with the highest boiling point exit from the bottom of the column. Any material which is not vaporized is known as residue. Distillation columns operate at atmospheric pressure or at reduced pressure (1 – 5 kPa). Deasphalting removes all or a portion of asphaltenes through precipitation using a selective solvent (*e.g.*, propane, butane and pentane). Specific fractions of asphaltenes are precipitated using different blends of aliphatic hydrocarbons. Froth treatment using paraffinic solvents is a

form of deasphalting as it removes a portion of asphaltenes. Deasphalting increases the value of the bitumen by removing the heaviest components but leaves a high carbon by-product of little value (*i.e.*, asphalt and/or asphaltenes).

A.4.2 Thermal Cracking and Coking

Thermal cracking of heavy hydrocarbon molecules into lighter products is an essential process for both refineries and bitumen upgraders. In the absence of a catalyst, temperatures in excess of approximately 420°C are required to break C-C bonds. Cracking occurs at lower temperature in the presence of acidic zeolites. Basic nitrogen compounds cause severe catalyst deactivation. Although extensively used in refineries, zeolites are not used in bitumen upgrading due to rapid deactivation and fouling. Thermal cracking occurs through free radical reactions. After initiation, propagation occurs via hydrogen abstraction, β -scission, addition and rearrangement. Thermal cracking without addition of hydrogen does not change the overall C to H ratio; any production of lighter hydrocarbons also produces a proportional amount of heavier hydrocarbons.

Visbreakers are thermal cracking units that lower the viscosity of products.^{114,115} Residue from atmospheric or vacuum distillation is fed into a visbreaker unit operating between 425 – 500°C and 0.7 – 5.0 MPa with a residence time between 60 – 180 s. The process can be operated at lower reaction temperature with increased residence time.¹¹⁶ Reactive unsaturated hydrocarbons are generated by thermal cracking. Polymerization of unsaturated hydrocarbons and formation of insoluble species are undesirable.¹¹⁷ Excessive production of light saturated hydrocarbons is also undesirable as it may induce precipitation of asphaltenes.

Coking processes turn heavy hydrocarbons into fuel oil and petroleum coke. Petroleum coke is a carbon-rich (80 – 95 wt%) solid, which is most commonly used as a fuel. The microstructure of coke varies, depending on the operating conditions of the coker unit and the feed material. Calcined coke with more than 98 wt% carbon and needle-like microstructure is ideal for production of anodes used by the smelting industry. Evolution of gases during coking leads to sponge coke with high void volume well suited for combustion in boilers. Delayed coking is a batch or semi-batch thermal cracking process that heats residual oil in large vessels to about 450 – 500°C.¹¹⁸ Coke accumulates inside the vessel must be removed once the vessel is full. Fluid

coking is a continuous thermal cracking process wherein the feed is injected into a fluidized bed of coke particles heated to about 500 – 550°C. During the fluid coking process, coke particles are continuously withdrawn, stripped with steam and burned to heat the process.

A.4.3 Hydrogen Processes

A variety of chemical processes that add hydrogen to vacuum residues (*e.g.*, hydroconversion, hydrotreating and hydrocracking) are used by different upgraders. Addition of hydrogen lowers the C to H ratio instead of simply disproportioning. Hydrogen is produced by steam-methane reforming, due to the high reaction yield and low cost of natural gas. Steam and methane react together at high temperature (*i.e.*, 800 – 870°C) and moderate pressure (*i.e.*, 2.2 to 2.9 MPa) over a nickel catalyst to form carbon monoxide (CO) and hydrogen gas. More hydrogen is produced by the subsequent water-gas shift reaction, wherein CO is converted to carbon dioxide (CO₂).

The most extensively used catalysts are molybdenum (Mo) sulfides doped with nickel (Ni) or cobalt (Co) loaded on porous γ -alumina (150 – 200 m²/g) in pelletized form (1 – 2 mm). Hydrotreating processes operate at temperatures around or below 400°C and are mainly used to remove sulphur and nitrogen. Hydroconversion processes operate at higher temperatures, in excess of 400°C and with hydrogen pressures in excess of 10 MPa. The high temperature is sufficient to break many chemical bonds. The addition of hydrogen gas suppresses coke formation while the catalyst promotes hydrogenation of aromatics compounds. The hydrocracking process is similar to hydroconversion but utilizes a catalyst that also promotes hydrocarbon cracking. Hydrocracking is usually preceded by hydrotreating in order to remove compounds which would otherwise quickly poison acid catalysts.

A.5 Colloid and Interface Chemistry

Microscopic colloidal and surface forces are responsible for many macroscopic physicochemical phenomena. These physicochemical processes are of critical importance to understanding both bitumen recovery from surface mining as well as *in-situ* production. A fundamental understanding of these forces is the first step towards effective control of multiphase physicochemical behaviour in complex chemical processes with interacting elements.

A.5.1 Surface Activity

Surface activity is a physical phenomenon, which originates from interactions between molecules (*e.g.*, intermolecular forces). These forces include London dispersion forces, induced dipoles, dipole-dipole interactions and hydrogen bonding. Intermolecular forces are much weaker compared to the intramolecular forces which hold molecules together. Nonetheless, they exert a significant influence on physicochemical properties (*e.g.*, solubility, surface tension and wetting). Considering the interface between a liquid and a gas, the imbalance of intermolecular forces at the surface gives rise to a physicochemical phenomenon known as surface tension. Surface tension is defined as the amount of work required to increase surface area at constant temperature, pressure and composition. Surface tension may also be expressed as the force per unit length which resists the change in surface area.

Surface activity may be measured using several different techniques.^{119,120} For liquids, surface tension may be measured directly as the force required to detach from the interface (*e.g.*, the Du Noüy ring and Wilhelmy plate methods) or by measuring its effect (*e.g.*, contact angle or capillary rise). Different correction factors are implemented for different methods to account for non-ideal systems. The Du Noüy ring and Wilhelmy plate method both measure force directly using a balance. The maximum force exerted on the ring or plate before detachment is proportional to the surface tension, which acts over the perimeter of the ring or plate. Typically, platinum and its alloys are used to ensure complete wetting.

Under equilibrium conditions, the gravitational force acting on a liquid inside a capillary is balanced by the capillary force. When the radius of the capillary is small enough, such that capillary forces are dominant, the height of a liquid in a narrow capillary tube is indicative of its surface tension. The contact angle of particles is more difficult to measure. The contact angle of particles may be determined by evaluating the penetration rate of a liquid into a packed column. The rate of penetration for a liquid through a porous body is characterized by the Washburn equation. Solving the Washburn equation for contact angle requires knowledge of the capillary radius which is determined by repeating the measurement using liquids of complete wetting (*i.e.*, zero contact angle). This technique requires that the particle packing remains very consistent.

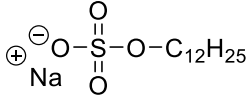
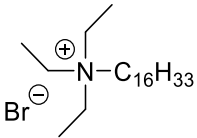
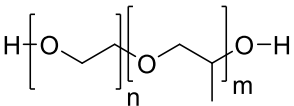
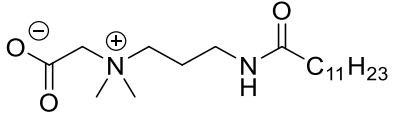
Contact angle may be directly observed for a liquid on a solid surface using the Sessile drop method^{119,120}. The shape of a drop is measured under static conditions after a drop of constant volume is brought into contact with a smooth horizontal surface. A hydrophilic surface is characterized by smaller contact angle ($< 90^\circ$) and a hydrophobic surface is characterized by a larger contact angle ($> 90^\circ$). However, the contact angle measured using a static method can increase or decrease with time due to processes such as evaporation, flux of surfactants or solutes and surface roughness. Dynamic contact angle is measured for a droplet which is advancing by injecting liquid or a droplet which is receding by withdrawing liquid. A marked discrepancy between advancing and receding contact angle is an indicator of a heterogeneous surface. Typically, the contact angle of a droplet on a solid surface is measured while the volume of the droplet is increasing (*i.e.*, advancing contact angle) or decreasing (*i.e.*, receding contact angle). The roughness of a surface has an important role in determining the apparent wettability of a particular surface.^{121,122} For example, water droplets bead on natural materials such as lotus leaves, which would indicate that the surface is hydrophobic with contact angle greater than 90° . However, this phenomenon occurs due to entrapped air pockets on the textured surface. Super-hydrophobic surfaces have been prepared by using various micro-structured surfaces.

A.5.2 Surfactants

Molecules which contain charged or polar functional groups (*i.e.*, carboxylic acids, alcohols, amines, *etc.*) experience stronger intermolecular forces compared to molecules consisting of only non-polar structures (*i.e.*, alkanes, aromatics, fluoroalkanes, *etc.*). Molecules which contain both polar and non-polar character are known as surfactants. Surfactants are transitional molecules due to their limited compatibility in both aqueous and non-aqueous phases. These amphiphilic molecules concentrate at the interface between two immiscible phases and lower interfacial tension. Surfactants have been found to be extremely useful compounds with numerous applications such as emulsifiers, detergents, wetting agents and dispersants. Surfactants are generally categorized by their charge, as shown in **Table A-9**. Surfactants comprising anionic moieties are anionic surfactants while surfactants comprising cationic moieties are cationic surfactants. Surfactants which comprise both positive and negative moieties are zwitterionic surfactants and those that do not contain any charged moieties are non-ionic surfactants. Non-

ionic surfactants are generally polymers made using both hydrophilic monomers and hydrophobic monomers.

Table A-9. Common examples of different surfactants and their chemical structures. Depending on the presence of any charged functional groups, surfactants are classified based on their chemical structures as anionic, cationic, non-ionic or zwitterionic.

Type	Example	Structure
Anionic	Sodium dodecyl sulphate	
Cationic	Cetyl triethyl ammonium bromide	
Non-ionic	PEG/PPG block co-polymers	
Zwitterionic	Cocamido-propyl betaine	

The solubility behaviour of a surfactant in solution is peculiar and very characteristic, as illustrated in **Figure A-6**. At low concentration, surfactant molecules remain dissolved in solution. With increasing concentration, additional surfactant molecules migrate to interfaces. At high concentration, surfactant molecules self-assemble into micelles or other higher order assemblies such as vesicles, cylinders, bilayers, liquid crystals and other structures. The critical micelle concentration (cmc) is the concentration at which micelles begin to form. The measured value of the critical micelle concentration of a surfactant depends on the method of investigation. A surfactant's effect on many physical properties is most pronounced below the critical micelle concentration, where surfactant molecules occupy partially the interfacial areas. Typically, for a molecule to be considered surface active, the slope of the curve in the first region below the cmc should be significant over an effective change in concentration. Short-chain alcohols such as

butanol absorb on the interface but only have a small effect on the physical properties of a biphasic mixture. Surfactants such as carboxylate salts, produced by saponification of fatty acids, are more effective and will more drastically affect the physical properties of a biphasic mixture.

The interfacial concentration of a solute is described by evaluating concentration at the Gibbs' dividing plane. For a binary heterogeneous solution, this imaginary plane is arbitrarily chosen so that the net flux of the majority component is zero. Adsorption of surfactant molecules in the interfacial region as defined by Gibbs' dividing plane leads to changes in surface tension.

Temperature also has an effect on surfactant solubility. For ionic surfactants such as carboxylate salts, there is a minimum temperature, known as the Krafft point below which micelles cannot form.¹²³ For non-ionic polymeric surfactants such as PPO/PEO copolymers and petroleum products, there is a maximum temperature above which the material is no longer soluble, known as the cloud point.¹²⁴ This behaviour results from hydrophilic head segments becoming less hydrophilic as water molecules increase in thermal energy. Polymers such as polyacrylamide and N-isopropylacrylamide have a peculiar response to temperature. At low temperature, the polymers are hydrophilic and hydrated but transition to a less hydrophilic state above the lower critical solution temperature (LCST).¹²⁵

A general method of evaluating a surfactant is to determine the hydrophilic-lipophilic balance (HLB) value.¹²⁶ HLB value may be empirically calculated or experimentally determined by comparing with surfactants with known HLB values. A generally rule-of-thumb known as Bancroft's rule states that the continuous phase is the phase in which the stabilizing surfactant has the greatest solubility. Therefore, high HLB surfactants are more soluble in water and preferentially stabilize oil-in-water emulsions. Conversely, low HLB surfactants are more soluble in oil and preferentially stabilize water-in-oil emulsions. The concept of HLB has been successfully used in formulation of emulsions in the food, cosmetic, and pharmaceutical industries.¹²⁷ Although HLB and Bancroft's rule remain useful concepts, trends based on HLB values should only be taken as qualitative guidelines. Surfactants with different HLB values are used in different applications (see **Table A-10**). A similar concept of relative solubility in different solvent systems is used to evaluate the performance of chemical surfactants, especially non-ionic polymeric surfactant. The relative solubility number (RSN) provides similar information as HLB.¹²⁸

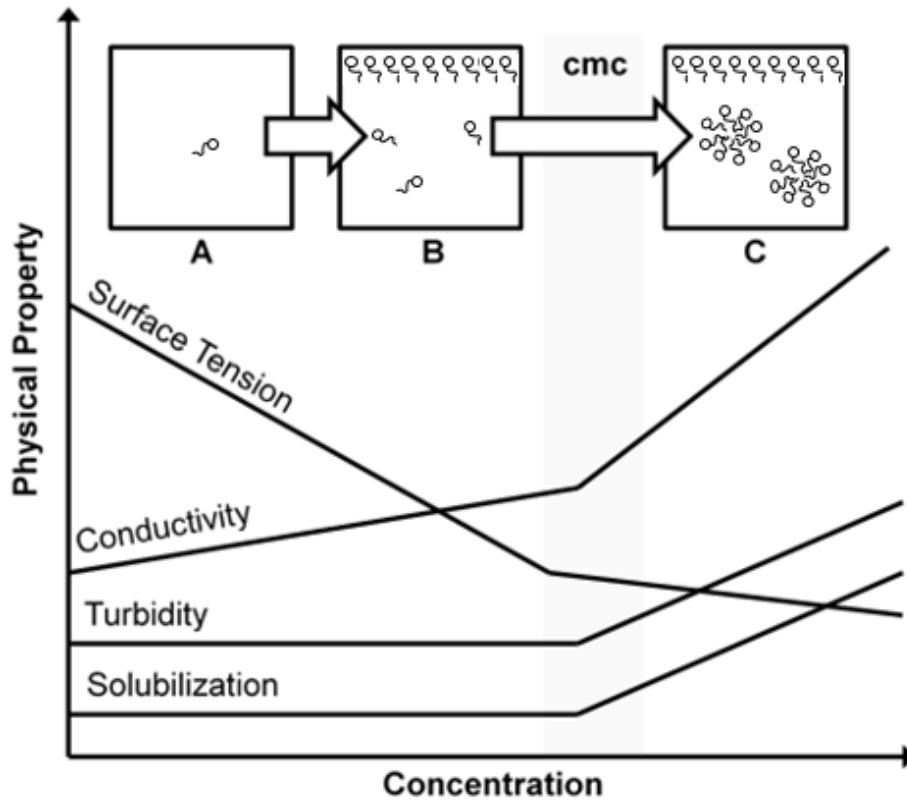


Figure A-6. Illustration of the solubility behaviour of a typical surfactant molecule in solution. At low concentration, the surfactant is dissolved in the solution [A]; as surfactant concentration increases, surfactant molecules preferentially adsorb at interfaces [B]; above a characteristic concentration, surfactant self-assemble and form micelles [C].

Table A-10. Hydrophilic-lipophilic balance (HLB) value used to describe various suitable application of a surfactant.

HLB	Application	Water Solubility
4 – 6	W/O emulsifier	Poor solubility
7 – 9	Wetting agents	Milky dispersion
8 – 18	O/W emulsifier	Milky dispersion
13 – 15	Detergents	Translucent solution
15 – 18	Solubilizing agents	Clear solution

Another important method of evaluating a surfactant based on its structure, shown in **Figure A-7**, is the critical packing parameter ¹²⁹. This quantity is often used to explain and predict self-assembled structures such as spherical micelles, cylindrical aggregates and bicontinuous systems. The relative spatial contributions of the hydrophobic and hydrophilic moieties place limitations on the type of geometry an aggregate system may adopt. Theory behind this model is generally built upon geometric constraints imposed by the higher order structures. Although it is possible to calculate the volume and length of the hydrophobic surfactant tail, the effective area of a surfactant head depends on hydration and other considerations as well.

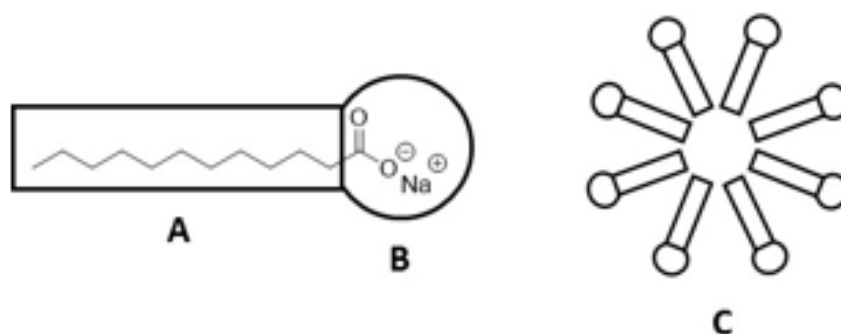


Figure A-7. Surfactant molecules have distinctive hydrophobic [A] and hydrophilic [B] moieties. Surfactant molecules self-assemble into micelles [C] due to the partial compatibility with solvent.

Chemical demulsifiers are widely used in various industries to break or prevent formation of emulsions and foams. Many commercial demulsifier formulations consist of several chemical compounds. For high viscosity water-in-oil emulsions, demulsifiers should possess sufficient mobility in the oil phase in order to reach dispersed water droplets. Generally, demulsifiers may be categorized as high molecular weight or low molecular weight chemicals. High molecular weight demulsifiers (*i.e.*, > 5000 g/mol) are often polymers and/or polyelectrolytes. Small molecular weight demulsifiers are often oil-soluble organic molecules. Active demulsifiers are surfactant molecules which competitively adsorb on the oil-water interfaces and replace stabilizing molecules, thereby providing an antagonist effect on emulsion stability. Indirect demulsifiers modify the effect of stabilizer species by changing the properties of the continuous phase. Interfacial species can therefore be made more or less soluble by addition of an appropriate solvent.

A.5.3 Emulsification

Emulsions are mixtures of immiscible phases, wherein small droplets of one phase are dispersed in another. Emulsions are generally only kinetically stable and will eventually separate, as shown in **Figure A-8**. Although thermodynamically unstable, due to the very large interfacial area, complete phase separation can take hundreds of years for well stabilized systems. The stability of an emulsion is enhanced by the presence of surface active molecules. Surfactant molecules have limited compatibility with both phases and stabilize emulsions by lowering the interfacial tension between the continuous phase and the dispersed phase. Emulsions generally appear opaque because emulsified droplets scatter light.

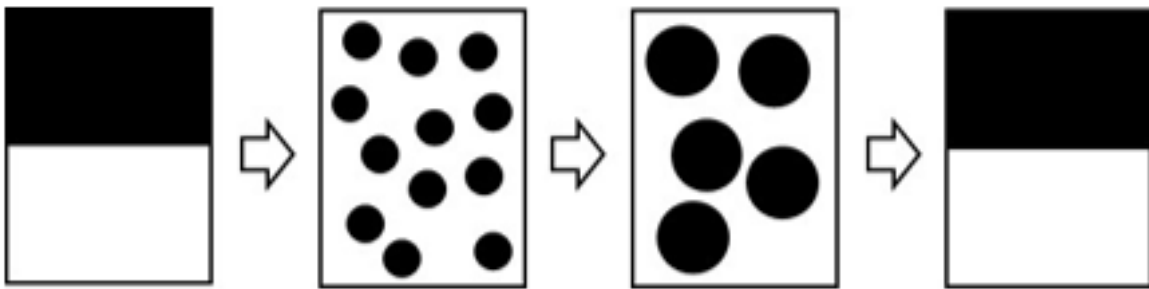


Figure A-8. Illustration of the emulsification process and subsequent droplet coalescence and phase separation. The amount of work required to generate an emulsion is determined by the total interfacial area as well as the interfacial energy between the two immiscible phases.

A simple emulsion consists of a single dispersed phase and a single continuous phase. In addition to the nature of any stabilizing surfactants, the type of emulsion formed is also influenced by the ratio of the immiscible phases, the surfactant (*i.e.*, HLB value), temperature, ionic strength and the presence of additives including small particles. The bulk properties of an emulsion more closely resemble those of the continuous phase. For example, oil-in-water (O/W) emulsions generally exhibit much greater electrical conductivity, while water-in-oil (W/O) emulsions exhibit very low electrical conductivity. Similarly, a drop of an O/W emulsion will disperse readily in water, while a drop of a W/O emulsion will not disperse in water. Complex emulsions also form when droplets are dispersed inside smaller droplets (*i.e.*, W/O/W and O/W/O).

Emulsification is an energy intensive process, in which very large interfacial area is created. The amount of energy required to emulsify a binary system in absence of surfactant is proportional to the surface area and therefore the size of emulsion droplets. Different mechanical devices may be used to provide sufficient energy to generate small droplets.¹³⁰ The presence of a surfactant lowers the interfacial energy, leading to emulsion of smaller droplet size and increased emulsion stability. The curvature of a droplet is indicative of a pressure difference. The Laplace pressure ^c can be significant for very small droplets and particles. Surface curvature can be sufficiently high for very small droplets or particles to prevent homogeneous nucleation.

A.5.4 Emulsion Stability

Most emulsions with droplet size greater than 1 μm are only kinetically stable and phase separation is spontaneous. However, depending on the level of stabilization, phase separation may be instantaneous or require several months; even years.¹³¹ Phase separation occurs by different mechanisms: flocculation, sedimentation, coalescence and Ostwald ripening. These mechanisms are illustrated in **Figure A-9**. Flocculation or aggregation refers to the association of two individual droplets or particles. The rate of flocculation or aggregation is dependent on the magnitude of attractive and repulsive forces. Sedimentation or creaming occurs when there is a density difference between the continuous phase and the dispersed phase. Buoyant forces cause the denser material to sink and the less dense material to rise. The flocculation and sedimentation processes both concentrate droplets but tend to be reversible. Coalescence is the process wherein two droplets combine to form one larger droplet, reducing the total interfacial area. For coalescence to occur, two droplets must collide and fuse together. A thin film of the continuous phase must drain from the vicinity before the two droplet surfaces are in direct contact. If the dispersed material is soluble in the continuous phase, another process driven by differences in molecular diffusivity occurs. Small droplets with high specific surface area and flux

^c The Laplace pressure describes the pressure difference due to curvature of a surface:

$$\Delta P = \gamma \left(\frac{1}{R_1} + \frac{1}{R_2} \right)$$

disappear as larger droplets grow in size. This phenomenon is known as Ostwald ripening. The flocculation, sedimentation and creaming processes concentrate droplets. Complete phase separation occurs through coalescence and Ostwald ripening.

Molecular dispersion forces are applicable to both particles and droplets. This attractive force is due to interactions between dipoles and induced dipoles. The magnitude of dispersion forces can be calculated theoretically or measured experimentally. Typical values for the Hamaker constant range from 10^{-20} J for non-ionic material (*e.g.*, fluorinated polymers) to 10^{-19} J for very polar material (*e.g.*, water). The Hamaker constant of a dispersed system is affected by the interacting medium but an effective Hamaker constant may be calculated.

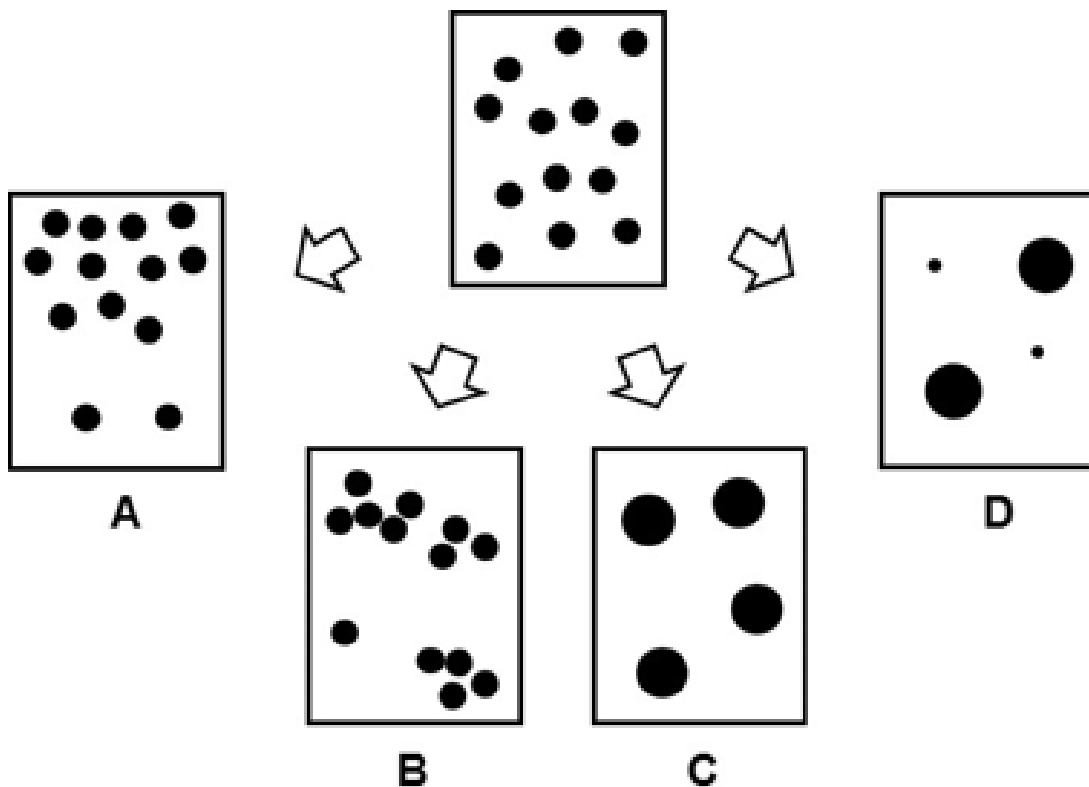


Figure A-9. Illustration of the various mechanisms involved in phase separation of emulsions. Creaming and sedimentation describe the process wherein a lighter material rises and a dense material sinks [A]; aggregation or flocculation concentrates material together as smaller droplets collide and form larger clusters [B]; coalescence describes the fusion of smaller droplets into larger droplets [C]; and molecular diffusion (*i.e.*, Ostwald ripening) is the process wherein larger droplets grow at the expense of the smaller droplets [D].

Dispersed droplets and particles both exhibit surface charge. The electrostatic force between charged ion pairs is described by Coulomb's Law which assumes point charges. The electrostatic force and therefore the degree of ion dissociation in solution is a function of the dielectric constant of the bulk medium. Even non-polar materials (*e.g.*, air bubbles, oil droplets) exhibit charging in water due to the very high dielectric constant of water. Surface charging in solution may occur as ions dissociate from the surface or as ions adsorb onto the surface. The excess charges are the result of differences in ion mobility, solubility and ionization potential. Furthermore, the electric field generated by the charged surface gives rise to a diffuse layer of associating ions directly adjacent to the surface. The distribution of charges further away from the surface is less affected as the strength of the electric field decays with distance. The result is a diffuse double layer, illustrated in **Figure A-10**, consisting of surface ions, neutralizing counter-ions and co-ions, which together remain balanced at equilibrium with its bulk value.

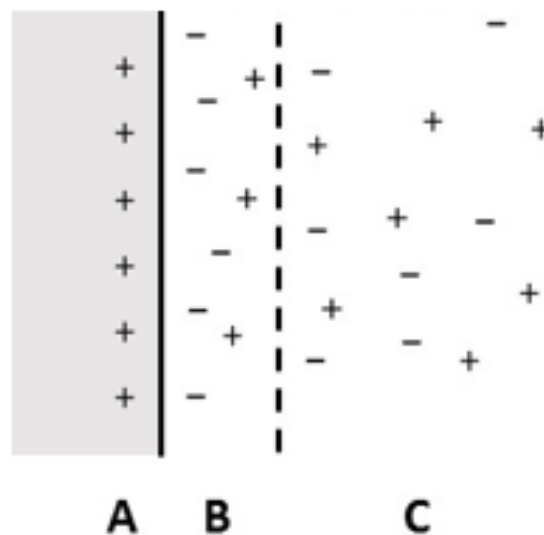


Figure A-10. Illustration of the diffuse electric double layer formed in solution next to a positively charged surface [A]. The diffuse double layer is comprised of an immobile layer, strongly associated with the surface [B]; and a more diffuse layer of counter-ions and co-ions [C], which extends to the boundary of the bulk phase.

Moreover, charged particles are susceptible to be influenced by electric fields. The mobility of a particle under an applied electric field is defined as the electrophoretic mobility. When the

velocity of a charged particle in an electric field is constant, the electrophoretic force is balanced against the drag force, as described by the Stokes' Law. The surface potential calculated by holding a particle at constant speed under an applied electric potential is known as the zeta potential. Electrophoresis is a common technique employed to separate ions or small particles based on their mobility in the presence of an applied electrical potential. Very small particles can deviate from Stokes' Law and require a small correction for the drag force.

A.5.5 Pickering Emulsions

A Pickering emulsion is a special type of emulsion stabilized by solid particles.¹³² The stability of solids-stabilized emulsions is influenced by the wettability, shape and size of the stabilizing particles. In order to stabilize an emulsion, the stabilizing particles must be partially wetted by both the continuous phase and the dispersed phases.¹³³ The irreversible adsorption of particles at the interface creates a physical barrier that reduces coalescence events. The energy of adsorption for particles at the interface is greatest when the contact angle is close to 90° (*i.e.*, for biwettable solids).¹³⁴ Adjusting the wetting characteristics of the stabilizing particles in a Pickering emulsions is similar to adjusting the HLB value of a surfactant in regular emulsions.

Certain solids are known to produce stable emulsions. The equilibrium position of a spherical particle at an oil-water interface is influenced by its wettability, as shown in **Figure A-11**. Hydrophilic material (*e.g.*, fine silica¹³⁵, clay¹³⁶ and iron oxide nanoparticles¹³⁷) are capable of stabilizing oil-in-water emulsions. More hydrophobic materials (*e.g.*, carbon black and polystyrene¹³⁸) are capable of stabilizing water-in-oil emulsions. The wettability of a material arises from surface energy components.¹³⁹ However, surface chemical functionalization can effectively modify their wetting behaviour of various particles. For example, commercially available silane reagents are capable of attaching hydrophobic alkyl, phenyl and halogen groups on the surface of silica particles. Due to the irreversible nature of the adsorption process, emulsions stabilized by solid particles may be stable for extended periods. In order to break a particle stabilized emulsion, the particle must be removed from the interface by either applying a force directly to the particle, as shown in **Figure A-12**, or by inducing a change to the interfacial properties of the stabilizing particles.

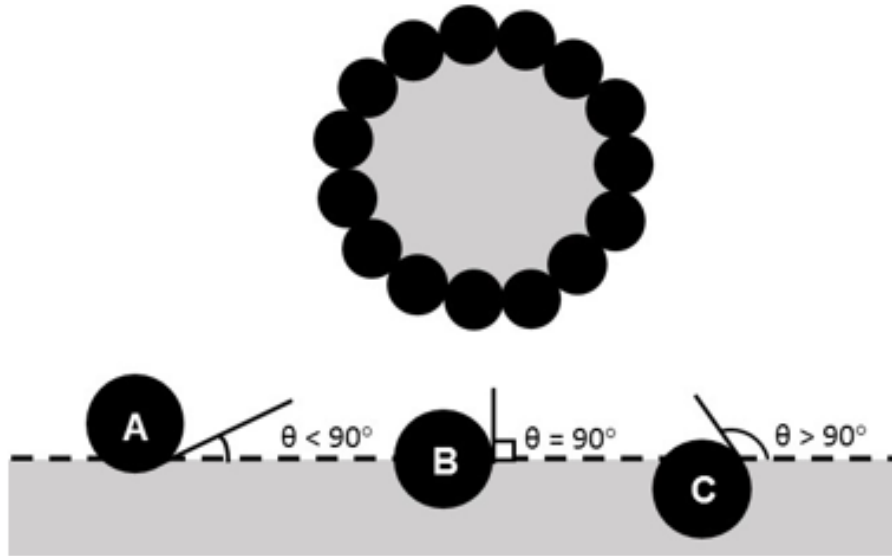


Figure A-11. Illustration of the effect of wetting in stabilizing emulsions with solid spherical particles. Emulsion stabilizing particles effectively reduce the interfacial area. The equilibrium position of the particles on the interface is directly related to the wettability of the particles. Hydrophilic particles [A] have a contact angle, measured through water, lesser than 90° while hydrophobic particles [C] have a contact angle, measured through water, greater than 90° . The most effective stabilizer particles are biwettable [B], having a contact angle close to 90° and equally wetted by both the continuous phase and the dispersed phase.

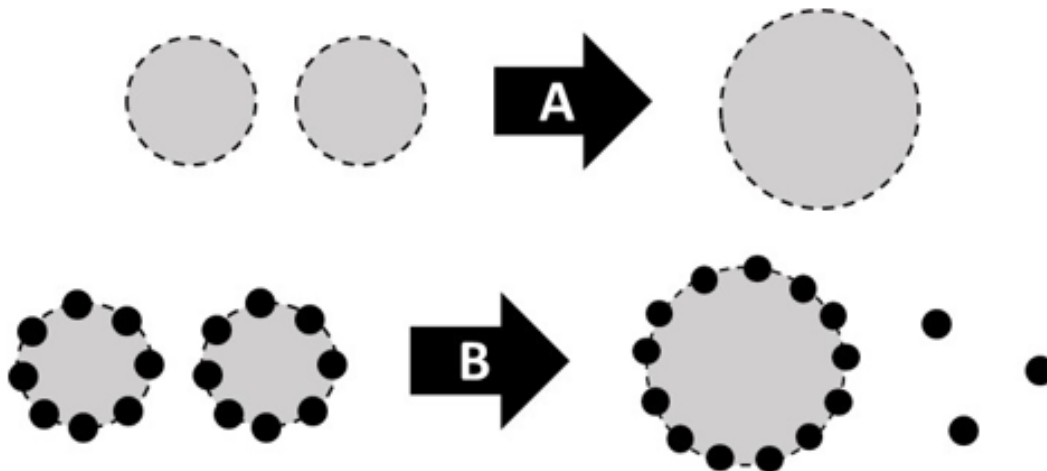


Figure A-12. Coalescence of two emulsion droplets stabilized by either surfactant [A] or solid particles [B]. Desorption of solids after coalescence requires additional detachment energy for particle-stabilized emulsions.

A.5.6 Breaking Emulsions (Demulsification)

Emulsions are sometimes unwanted and must be destabilized using various physical or chemical methods, which include addition of chemical demulsifiers, dilution with solvents, electro-coalescence, centrifugation or combinations thereof.^{8,140–143} Physical methods, such as centrifugation, rely on the difference in density between the two phases and increase the rate of sedimentation by applying a centrifugal force to the system. Heating has a more compounded effect on emulsion stability. By heating, the mobility of emulsified droplets within a viscous continuous phase increases. Additionally, the solubility of different species can change by raising the temperature. Changes in the temperature can also independently affect the density of each phase and accentuate the difference in density between the non-aqueous and aqueous phases. Dilution of an emulsion with low-density solvents also enhances the difference in density between the non-aqueous and aqueous phases. Electrical methods, which deform entrained water droplets under an electric field, are also employed at large scale.

Methods of promoting demulsification are generally classified as physical, electrical or chemical processes. Mechanical processes apply a physical force in order to promote droplet collisions and thus increase the rate of coalescence or increase the energy of collisions in order to overcome the interfacial barrier to droplet coalescence. However, excessive shear must be avoided to prevent further emulsification. Electrical processes generate a strong applied electric field which causes polar molecules to reorient with the field, thus weakening the interfacial film. An applied electric field can also influence the charge of individual droplets and induce electrostatic attraction between oppositely charged droplets. Many demulsification processes act simultaneous on different factors that influence emulsion stability. For example, heating an emulsion reduces the viscosity of the continuous phase, provides additional thermal energy to promote droplet collisions and changes the solubility of indigenous surfactants. Similarly, diluting an emulsion with appropriate solvent reduces viscosity of the continuous phase and, for crude oil emulsions, changes solubility of specific components. There are major drawbacks to demulsification processes based on centrifuging, heating and diluting. Heating and centrifuging are both energy-intensive processes that require expensive equipment. Dilution requires large amounts of costly diluent that must be later recovered to be economical.

Chemical demulsifiers are chemical compounds that have an antagonistic effect on emulsion stability and are commonly used to accelerate phase separation in industrial processes. Chemical demulsifiers are interfacially active, capable of migrating to the oil-water interface and changing interfacial properties of the interfacial layer.^{144–148} A common approach to demulsifier formulation is to select an emulsifier that preferentially stabilizes the opposite emulsion type. An O/W emulsifier will tend to destabilize an emulsion stabilized using a W/O emulsifier and *vice versa*. The performance of chemical demulsifiers can be difficult to predict as performance is affected by numerous variables including temperature, pH, ionic strength, viscosity, solids content and many others. Many chemical demulsifiers are also prone to overdosing beyond a narrow effective operating concentration range.

A.6 Particle Engineering

A particle is a small subdivision of matter defined by physical properties such as morphology, which includes size, shape, structure and surface properties. The properties of solid particles vary according to its structure. For example, the surface of certain materials is catalytically active while its bulk is mostly inert. Particles, having greater complexity than molecules, can be used to produce composite materials that combine the different properties of its constituents. Engineering particles from various materials with specific morphology can greatly impact the properties of the material. Smart particles may be designed by incorporating responsive materials into their structure along with any other materials with beneficial properties.

A.6.1 Particle Properties

The dimensions of complex particles cannot be described using a single numerical value except for regularly shaped particles (*e.g.*, spheres). The aspect ratio describes the ratio between width and height of a particle and can be used to differentiate rod-like particles from plate-like particles. Particle size is often described using an average equivalent diameter determined using a specific instrument based on a model (*e.g.*, sedimentation rate, electrophoretic mobility or light scattering). Equivalent diameters determined by correlating measured physical behaviour to match those of a spherical particle, shown in **Table A-11**, are often used.

Table A-11. Comparison of different measurement techniques used to evaluate particle size. Various techniques give equivalent diameters and different averages depending on the principle of operation and measurement method.

Measurement technique	Equivalent diameter	Type of average
Microscopy	Projected area diameter	Number average
Settling rate	Aerodynamic diameter Hydrodynamic diameter	Mass average
Electrically-induced motion	Electrophoretic mobility	Number average

Particles produced by different methods exhibit different particle size distribution. Milled particles generally have broad distribution while controlled polymerization can produce very narrow particle size distribution. Particles, which contain primarily one particle size, are known as mono-dispersed and exhibit only a single mode. Particle sizes with two predominant particle sizes are bimodal while particles with very broad size range are polydisperse.

Preparation of particles, having various degrees of complexity and organization, is possible by carefully controlling conditions during their assembly and/or applying different transformations after initial particle formation. Complex particles with different types of structure are illustrated in **Figure A-13**, including layered particles with a central void or core, solid particles with either embedded particles or voids and irregular particles. The preparative method used to prepare particles has a great influence on the structure of the resulting particles. Control of process conditions during synthesis can be used to engineer particles with specific properties in order to match their intended function.

Density can be ambiguous for structured and/or complex particles. While true density is determined using the volume of the particle without voids, measured particle density can include both external and internal voids. Bulk density, which is often found in documentation, is typically a measure of powder density and subject to inter-particle forces and sample manipulation. Different environmental conditions can lead to changes in particle size through different aggregation and other growth mechanism or deformation and decomposition processes.

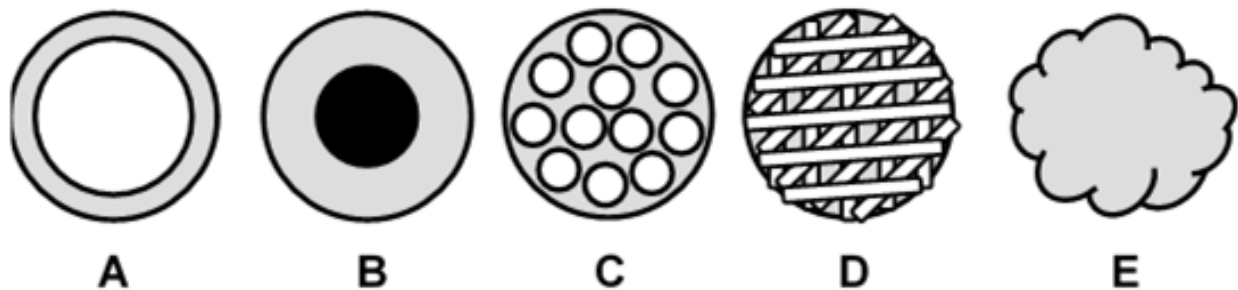


Figure A-13. Illustration of various types of particles prepared with organized structure. Different organizations include: layered particle with central void [A]; layered particle with central core [B]; closed-cell foam [C]; open-cell foam [D]; and irregular [E].

A.6.2 Micro- and Nano- Particles

Discrete particles are known to exhibit different behaviour compared to bulk material.¹⁴⁹ The ratio of surface sites to bulk sites increases for smaller particles. For solids of any shape, a reduction in volume is disproportional to the corresponding change in surface area. The finite number and organisation of individual atoms can lead to unique properties in very small nanoparticles.¹⁵⁰ Smaller particles also typically have more edges and defects on their surface. The structure of a particle can also have an important effect on its function. For many nanomaterials, the properties of certain materials can be tuned by its size and morphology.

Quantum dots are very small particles made of semi-conductor material such as cadmium selenide (CdSe) and cadmium sulfide (CdS). These quantum dots are confined systems and their electronic characteristics are closely related to the size and shape of individual particles.^{151–155} The spectral emission of quantum dots can span the entire colour spectrum and does not suffer from bleaching effects like organic dyes. The behaviour of magnetic particles can change with particle size. Sufficiently small iron oxide particles (Fe_3O_4) possess a single magnetic domain that aligns with an external magnetic field. However, once removed from the magnetic field, energy from Brownian motion is sufficient to reorient the magnetic domain of these small particles. This type of magnetic behaviour makes re-dispersion of recovered material easier.

Catalysts are substances which are capable of accelerating a chemical reaction without itself being consumed by the overall process. Enzymes are biological catalysts with structure-specific functions that enable countless organic transformations required by living organisms. Non-

biological industrial catalysts are generally categorized as homogeneous or heterogeneous, depending on the solubility of the catalyst. Heterogeneous catalysts are vital to the chemical industry and are used in the chemical processes that produce ammonia from nitrogen and gasoline from crude oil. The structure of solid catalysts can contain atomic defects and/or dopants, which are responsible for their superior catalyst activity. The ability of transition metals to catalyze various chemical reactions is also well-known. The activity of homogeneous transition metal catalysts can be directed by attaching specific ligands that interact with the reactants in different ways.

A.6.3 Colloidal Stability

Adhesive and cohesive forces are important when preparing particles and determining whether particles remain individually dispersed or form aggregates. Adhesive forces hold together different materials while cohesive forces hold together the same material. Various forces can hold primary particles together into larger aggregates. Molecular bonding forms very strong links between particles and cannot be easily broken. Various types of inter-particle forces act on different length scales. The van der Waal attraction force which is applicable for all materials is only significant when interacting particles are very close together. Electrostatic forces are present due to polar functional groups and induced dipoles. Hydrogen bonding is a special case where the force can extend relatively far. Hydrogen bonding and electrostatic forces are largely responsible for the high order three-dimensional structures formed by protein and other biological materials.

The magnitude of the adhesive force between two particles is dependent on the contact area between the two particles, as illustrated in **Figure A-14**. Therefore, minimizing contact area is an effective way to prevent adhesion between particles. Small biological particles such as pollen often possess very rough surfaces in order to prevent aggregation. This is advantageous as pollen is generally propagated by wind and large pollen aggregates would not travel as far as smaller individual pollen particles. Another successful strategy employed to prevent adhesion is to maintain a temperature below the glass transition temperature (T_g) of the material. Above its T_g , a material will transform from a hard and brittle state to a rubberier and more deformable state. Particles which are deformable can interact more intimately with each other due to the

greater contact area provided when particles are brought together. Liquid bridging is another mechanism by which particles are held together. In liquid bridging, the presence of a small amount of liquid, usually water, can hold particles tightly together.

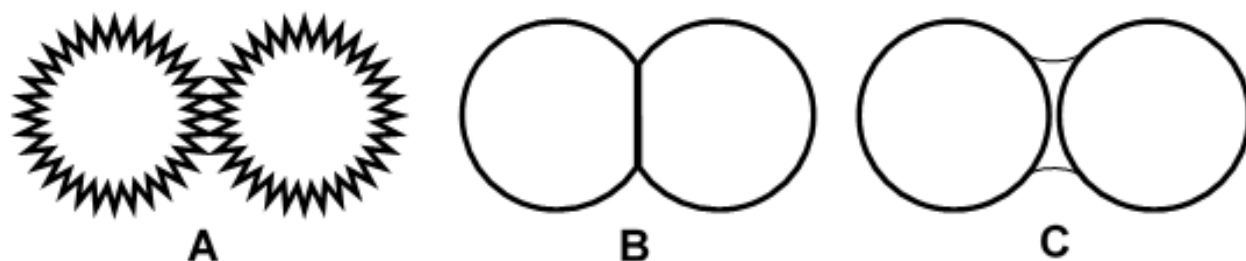


Figure A-14. Illustration of two interacting particles. The adhesive force between two particles is a function of contact area between the two interacting particles. Hard brittle particles with rough surfaces cannot effectively be brought into intimate contact [A]. In contrast, soft rubbery particles deform when brought together and the increase in contact area results in greater interaction between particles [B]. Particles can also be held together by a small amount of liquid, which forms a bridge between particles [C].

The force of electrostatic repulsion between two similarly charged droplets or particles can prevent aggregation. Electrostatic stabilization of dispersed particles in solution is very sensitive to ionic strength of the medium. Steric stabilization between two droplets occurs when there is a physical barrier to coalescence and is less sensitive to ionic strength. The type of surfactant often determines the predominant mode of stabilization. Electrostatic stabilization is the principal stabilization mechanism for ionic surfactants while steric stabilization is more dominant for non-ionic surfactants. Based on the theory of Derjaguin, Landau, Verwey and Overbeek (DLVO), a model was developed by evaluating both the repulsive and attractive forces for two approaching particles or droplets. This model may be used to predict the stability of dispersed systems to flocculation. DLVO theory encounters difficulty in modeling more complex systems such as a clay dispersion.¹⁵⁶ Clay platelets consist of layered sheets with more complex structure. The layered structure results in different charging behaviour, arising from alternate arrangement of siliceous tetrahedral sheets and aluminous dioctahedral sheets.

In aqueous systems, surface charge is a strong function of pH for many types of surfaces including minerals found in oil sands ore. The characteristic pH where the surface charges are completely neutralized is known as the isoelectric point or the point of zero charge. For many dispersed systems, the colloidal stability is lowest in absence of any electrostatic stabilization. Similarly, proteins, which are made of amphiphilic amino acids, are selectively precipitated in separation processes according to their isoelectric points. The point of zero charge for various materials is presented in **Table A-12**. Clay particles are anisotropic with distinctive edges and basal planes that can have opposing charges under certain conditions.^{157,158} In high concentration clay dispersions, a large number of base-edge interactions form a strong gel network that prevents further densification.

Table A-12. The characteristic point of zero charge for different materials.¹⁵⁹

Material	Molecular Formula	Point of Zero Charge
Silica	SiO ₂	2.0 – 3.0
Titania	TiO ₂	6.0 – 7.0
Iron oxide	Fe ₃ O ₄ /Fe ₂ O ₃	6.0 – 8.0
Alumina	γ-Al ₂ O ₃	8.0 – 9.0

A.6.4 Particle Dynamics

The motion of particles through predefined geometries is one method particles of different sizes are classified. Well-defined screen sieves sort particles according to size using a stack of filters with increasingly smaller openings, through which only increasingly smaller particles can pass. Impactors separate particles by taking advantage of particle motion through different geometries such as orifices and elbows. Particles with sufficient inertia will deviate from streamlines and are deposited on different stages inside a cascade impactor. Similarly, a cyclone traps particles which deviate from the streamline, as shown in **Figure A-15**, and is capable of continuous operation. Very small particles (< 15 μm in air) deviate from Stokes' Law and require a correction for friction commonly known as the Cunningham correction factor.¹⁶⁰ Cyclones are also effective in separating droplets or particles suspensions in either water or oil.

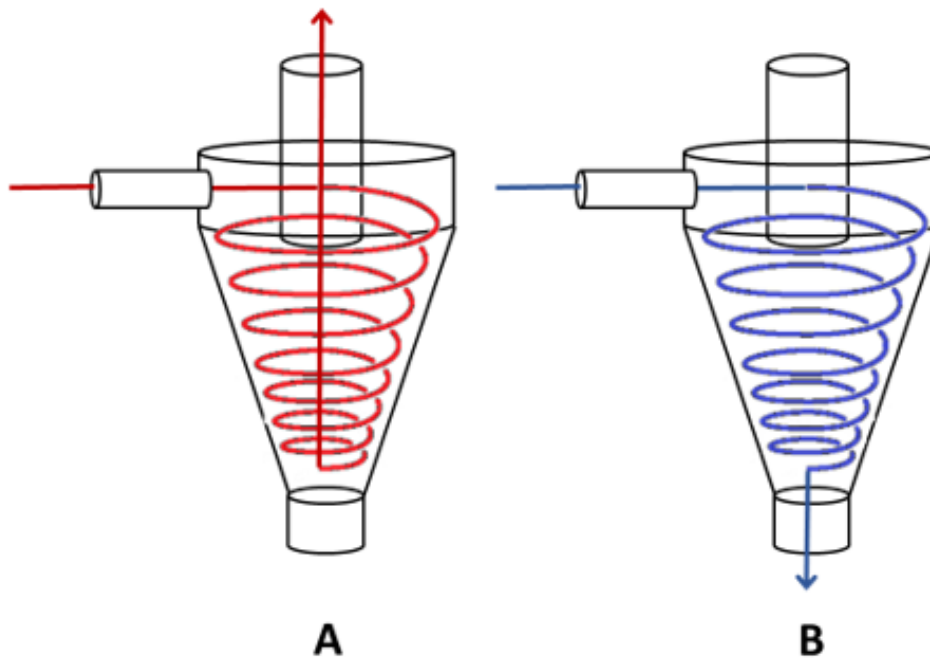


Figure A-15. Illustration of a cyclone separator. Mixture is injected into the cyclone and forms a high speed vortex along the conical wall. Fluid first flows in a helical direction down the cyclone and then up through the centre of the cyclone and exits at the top through an apex finder, in the overflow. [A] Larger particles with sufficient inertia will deviate from the flow stream and exit through the bottom, in the underflow. [B]

Charged particles and droplets are separated based on their electrical charge. A charged particle or droplet can be repelled using a similar charge or attracted using a charge of opposing polarity. The motion of a charged particle or droplet follows the electric field produced by point charges or parallel plates, as illustrated in **Figure A-16**. One method of sorting charged particles involves balancing the inertial and electrical forces acting on the particles. Only particles with a specific charge-to-mass ratio will pass through an opening without depositing on an electrically charged surface. Very small particles can thus be detected using electrozone sensing techniques, wherein a sample is charged using a nuclear source and injected between two rotating cylinders with an applied electrical voltage between the two cylinder surfaces. The inertial and electrical forces acting on the particle must be balanced for a particle to pass through the cylindrical opening. In this manner, particles with specific mass-to-charge ratio are collected and classified by adjusting the potential across the two surfaces and the rotation speed.

Certain electrostatic desalting units generate a large electrical potential to concentrate and/or destabilize charged water droplets. A dilute emulsion mixture is pumped within an array of conductive electrodes that apply an alternating or direct current electric field. Charged particles and droplets move towards the opposite pole while the oscillation of droplets, as the field inverts, promotes droplet interaction and coalescence.

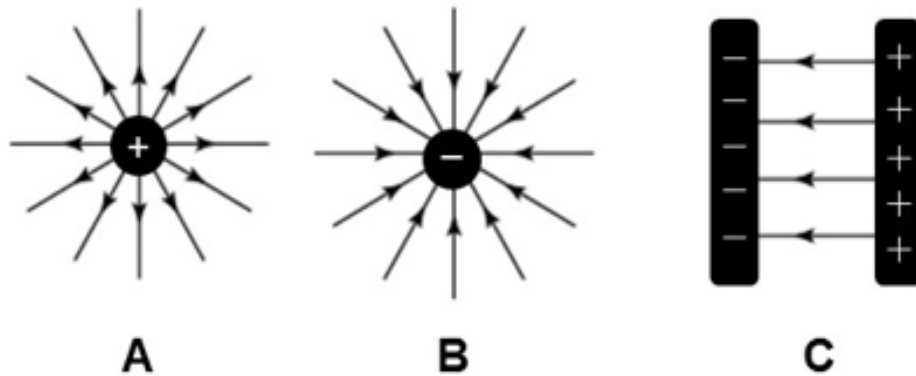


Figure A-16. A charged particle under the influence of an electric field attracted towards oppositely charges or repelled by like charges. Illustration of a positively charged particle moving in an electrical field generated by a positive point charge [A], by a negative point charge [B], or between parallel plates of opposite charge [C].

Magnetic particles are recovered by applying a magnetic field, which can be used to control the motion of magnetically-responsive particles.¹⁶¹ Strong permanent magnetic fields surround certain materials, due to their electronic structure. Magnetic field lines are shown in **Figure A-17**. Electrical current can also generate strong magnetic fields. Direct current electromagnets are similar to permanent magnets but are easily turned off by breaking the circuit or inverted by changing polarity. Continuously oscillating magnetic fields are produced by alternating current electromagnets that operate at specific frequencies.

The magnetic susceptibility of a magnetic material can be very small for paramagnetic and diamagnetic substances or be very large for ferromagnetic and ferro-magnetic substances. Strongly magnetically-responsive material is easily separated and collected under a magnetic field. The ordered magnetic domains within ferri- and ferro-magnetic substances can reorganize randomly above a characteristic temperature, shown in **Table A-13**, and become paramagnetic.

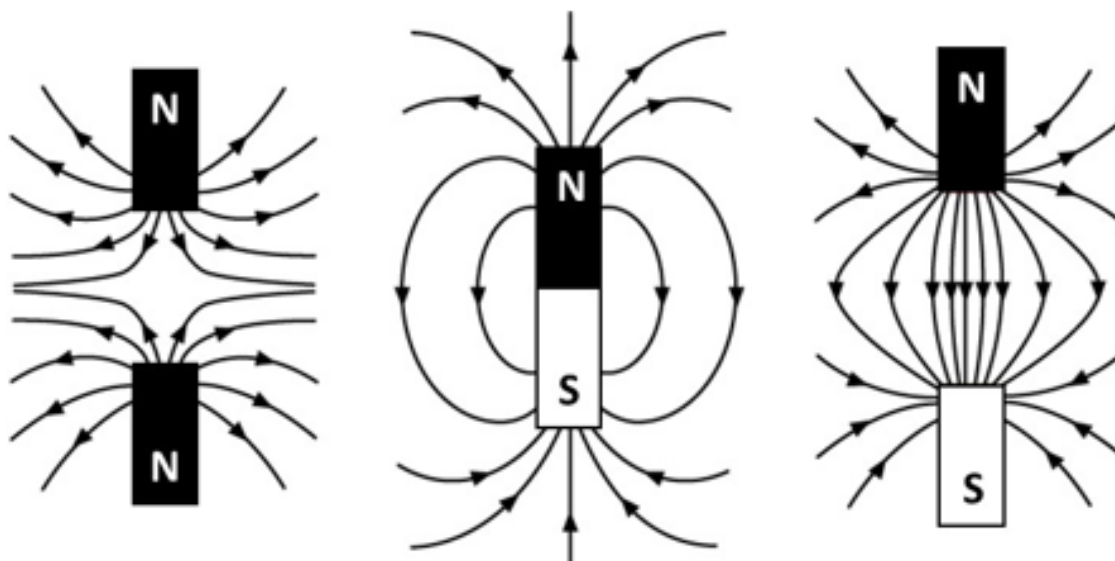


Figure A-17. Illustration of magnetic field lines generated by two magnetic poles in different configuration.

Table A-13. Curie temperature of different magnetic materials.

Material	Temperature (°C)
Iron (Fe)	1043
Cobalt (Co)	1400
Nickel (Ni)	627
Gadolinium (Gd)	292

Superparamagnetic particles that are sufficiently small to have a single magnetic domain acquire magnetization under an external magnetic field. However, once removed from the magnetic field, superparamagnetic particles lose their strong magnetization due to collisions resulting from Brownian motion of solvent molecules. Superparamagnetic particles are only weakly magnetic once removed from the external magnetic field and therefore more easily dispersed. Demagnetization of other magnetic material below the Currie temperature is possible under an alternating current magnetic field but this technique is not suitable for small particles, as small particles tend to spin under an oscillating magnetic field.

A.6.5 Particle Synthesis

Colloidal particle synthesis can be categorized in two general categories: a bottom-up approach or a top-down approach. Different techniques used to prepare particles are summarized in **Table A-14**. Top-down methods focus on breaking up large or bulk material into smaller fragments. Milling, for example, reduces particle size by mechanically breaking up larger material. Bottom-up methods focus on constructing particles from smaller building blocks. Through a sequence of organic chemical reactions, complex molecules are synthesised.

Table A-14. Various techniques used to engineer particles with specific properties or functions. Methods are generally classified as either bottom-up or top-down.

Method	Type	Description
Precipitation	Bottom-up	Induced change in solubility causes a solid to form a supersaturated solution
Crystallization	Bottom-up	Different phases can form under different conditions
Polymerization	Bottom-up	Small molecules combine to form larger insoluble particles
Milling	Top-down	Large particles are broken into smaller particles
Homogenization	Top-down	Breaking up liquid or solid material into a different continuous phase
Atomization	Top-down	Breaking up material dispersed in gas

Particle size reduction takes advantage of different break-up mechanisms including compression, impact and shear. Wet milling, dry milling and cryogenic milling are examples of break-up techniques that can achieve very effective particle size reduction.^{162–165} Particle fragmentation remains very inefficient in part due to the hardness, abrasiveness and toughness of many materials. Cooling a material below its glass transition temperature is critical for many materials, which should remain brittle for optimal break-up efficiency.

Changes to environmental conditions, most often temperature, can trigger considerable changes to the solubility of a substance dissolved in solution. For techniques in which particles are precipitated from a supersaturated solution, nucleation rate and growth rate are important considerations. Very high super-saturation ratios must be typically reached in order for homogeneous nucleation to take place due to the overwhelming high surface energy of very small particles. Therefore, heterogeneous nucleation is more commonly encountered while true homogeneous nucleation is rarely observed. A common method of inducing crystallization is addition of seed particles. The seeds provide a preferential surface for forming solid particles. Seed crystals can also be used to promote the formation of an otherwise kinetically unfavourable phase. In most bottom-up methods, particle growth rate can be controlled and complex structures can emerge from changing reaction conditions.

High-speed mixers and dispersers operate by rotating a rotor through around a stationary stator. The high-speed circular motion of the rotor expels the media through narrow teeth along the stator. Other mechanical homogenizers operate in similar manner by forcing a liquid through a restricted orifice at high pressure. Less efficient blenders operate by rotating a blade through the media. Ultrasonic homogenization occurs through cavitation induced by sonic pressure but cannot be easily scaled up due to impractical manufacturing of large ultrasonic tips. Both high-speed and high-pressure homogenizers are available in high-throughput commercial units.

Atomization and drying methods are also used to produce fine powders. Generally, a material is dispersed or dissolved into a media which is then atomized into much smaller entities. The solvent or dispersant is subsequently removed, leaving residual material as individual particles. This general method can be used in the gas, liquid and even solid phase. In classic emulsion evaporation, a low boiling point solvent is emulsified and then removed by heating the solution beyond the boiling point of the dispersed phase or by reducing the ambient pressure. During spray drying, a stream of solution is passed through a valve along with heated gas. The gas stream helps disperse the solution into a fine mist and provides the necessary energy to evaporate the solvent or dispersant. Complex morphologies can be made by spray drying under different operating conditions.^{166,167} The mobility of different components must be considered due to the rapid rate of solvent removal associated with spray drying.

Polymerisation is a powerful chemical process, wherein small molecules (*i.e.*, monomers) are tethered together in a long chain (*i.e.*, polymer). The result is a high molecular weight compound with one or more regular repeating units. The structure of polymer chains depends on the monomers used as well as the type of polymerization reaction employed. Free radical polymerization is the most common method and applicable to a wide range of monomers but offers relatively little control over structure. Polymers with very well defined structure (*e.g.*, isotactic polymers) can be made using catalytic polymerization reactions (*e.g.*, Ziegler-Natta).¹⁶⁸

A very high level of control over the molecular weight is possible through living polymerization.^{169,170} The increased viscosity of high molecular weight polymers can limit monomer conversion in bulk polymerization. Solution polymerization uses a non-reactive solvent to reduce this effect but still produces a polymer product with a range of molecular weights. Polymerization reactions can also be completed in two-phase system and is especially useful in preparing latex (*i.e.*, dispersed polymer particles). Various modes of dispersed phase polymerization are summarized in **Table A-15** and include emulsion polymerization, dispersion polymerization, suspension polymerization and mini-emulsion polymerization. The different modes of heterogeneous polymerization are distinguished by their kinetics and mechanism of particle formation, the initial state of the mixture and the final shape and size of particles.

Emulsion polymerization is an effective method used to produce dispersed polymer particles characterized by very high molecular weight, high conversion and low bulk latex viscosity. In classic emulsion polymerization, a monomer-in-water emulsion is prepared and stabilized by surfactant. A water soluble initiator starts the polymerization process in the aqueous phase where the monomer has low but finite solubility. Growing oligomer chains quickly lose solubility and migrate inside surfactants micelles. The fast rate of polymerization is sustained by diffusion of monomers from droplets to micelles. Emulsion polymerization is not suitable for excessively hydrophobic monomers that cannot easily diffuse from monomer droplets into nucleated micelles. In contrast, during dispersion polymerization, nucleation occurs and continues in the continuous phase. Growing polymer chains eventually precipitate if solubility of the polymer is poor. The solvency of both the monomer and polymer in the continuous phase is a critical factor that affects both particle size and morphology of resulting particles. Suspension polymerization

is most similar to bulk or solution polymerization. However, the monomer phase is dispersed and droplet remains suspended under continuous mixing. Nucleation occurs within dispersed monomer droplets, which polymerize into spherical beads of approximately the same size. Nucleation also occurs within dispersed droplets in mini-emulsion polymerization. However, droplets are much smaller and require addition of co-surfactant to suppress Oswald ripening.

Table A-15. Various methods of polymerization in dispersed phase for producing latex polymer particles with different properties.^{171–174}

Method	Particle Size Range	Brief Description
Mini-emulsion	< 0.1 μm	<ul style="list-style-type: none"> • Monodispersed particles • Droplet nucleation • Co-stabilizer prevents Ostwald ripening
Emulsion	0.05 – 0.5 μm	<ul style="list-style-type: none"> • Monodispersed particles • Initiator soluble in continuous phase • Micellar nucleation and growth
Dispersion	0.1 – 10 μm	<ul style="list-style-type: none"> • Monodispersed particles • Initiator soluble in monomer • Homogeneous nucleation and growth
Suspension	> 20 μm	<ul style="list-style-type: none"> • Polydispersed particles • Droplet nucleation • Size based on agitation intensity

A.7 References

1. Canada. National Energy Board., *Canada's energy future energy supply and demand projections to 2035.*, National Energy Board, Calgary, **2011**.
2. G. D. Mossop, *Science*, 1980, **207**, 145–152.
3. D. F. Mincken, *The Cold Lake Oil Sands: Geology and a Reserves Estimate*, **1974**, 84–99.

4. S. M. Hubbard, S. G. Pemberton and E. A. Howard, *Bull. Can. Pet. Geol.*, 1999, **47**, 270–297.
5. F. J. Hein and D. K. Cotterill, *Nat. Resour. Res.*, 2006, **15**, 85–102.
6. J. J. Adams, B. J. Rostron and C. A. Mendoza, *Can. J. Earth Sci.*, 2004, **41**, 1077–1095.
7. Alberta Energy Research Institute. and O. Strausz, *The chemistry of Alberta oil sands, bitumens and heavy oils*, Alberta Energy Research Institute, Calgary, AB, **2003**.
8. J. H. Masliyah, Z. Xu and J. A. Czarnecki, *Handbook on theory and practice of bitumen recovery from Athabasca Oil Sands*, Kingsley Knowledge Pub., Cochrane, AB, **2011**.
9. K. Takamura, *Can. J. Chem. Eng.*, 1982, **60**, 538–545.
10. L. Hepler, *AOSTRA Technical Handbook on Oil Sands, Bitumens and Heavy Oils*, Alberta Oil Sands Technology & Research Authority, **1989**.
11. J. Czarnecki, B. Radoev, L. L. Schramm and R. Slavchev, *Adv. Colloid Interface Sci.*, 2005, **114-115**, 53–60.
12. *Oils Sands Technology Roadmap Unlocking the Potential*, Alberta Chamber of Resources, **2004**.
13. M. Gray, *Upgrading petroleum residues and heavy oils*, M. Dekker, New York, **1994**.
14. S. Peramanu, B. B. Pruden and P. Rahimi, *Ind. Eng. Chem. Res.*, 1999, **38**, 3121–3130.
15. M. C. Kennicutt, *Oil Chem. Pollut.*, 1988, **4**, 89–112.
16. J. Bulmer and J. Starr, Eds., *Syncrude Analytical Methods for Oil Sand and Bitumen Processing*, Alberta Oil Sands Technology and Research Authority, Edmonton, **1979**.
17. K. H. Chung, C. Xu, Y. Hu and R. Wang, *Oil Gas J.*, 1997, **95**.

18. J. A. Brient, P. J. Wessner and M. N. Doyle, in *Kirk-Othmer Encyclopedia of Chemical Technology*, ed. John Wiley & Sons, Inc., John Wiley & Sons, Inc., Hoboken, NJ, USA, **2000**.
19. D. Strong and R. H. Filby, in *Metal Complexes in Fossil Fuels*, eds. R. H. Filby and J. F. Branthaver, American Chemical Society, Washington, DC, **1987**, 154–172.
20. J. T. Miller, R. B. Fisher, A. M. J. van der Eerden and D. C. Koningsberger, *Energy Fuels*, 1999, **13**, 719–727.
21. K. Moran, A. Yeung, J. Czarnecki and J. Masliyah, *Colloids Surf. Physicochem. Eng. Asp.*, 2000, **174**, 147–157.
22. L. L. Schramm and R. G. Smith, *Can. J. Chem. Eng.*, 1987, **65**, 799–811.
23. S. Hoeiland, T. Barth, A. M. Blokhuis and A. Skauge, *J. Pet. Sci. Eng.*, 2001, **30**, 91–103.
24. C. Drummond and J. Israelachvili, *J. Pet. Sci. Eng.*, 2004, **45**, 61–81.
25. B. Fuhr, B. Banjac, T. Blackmore and P. Rahimi, *Energy Fuels*, 2007, **21**, 1322–1324.
26. C. W. Bowman, *Molecular and Interfacial Properties of Athabasca Tar Sands*, World Petroleum Congress, **1967**.
27. E. E. Isaacs and K. F. Smolek, *Can. J. Chem. Eng.*, 1983, **61**, 233–240.
28. J. Saien and S. Akbari, *J. Chem. Eng. Data*, 2006, **51**, 1832–1835.
29. S. Zeppieri, J. Rodríguez and A. L. López de Ramos, *J. Chem. Eng. Data*, 2001, **46**, 1086–1088.
30. J. Masliyah, J. Czarnecki and Z. Xu, in *Handbook on Theory and Practice of Bitumen Recovery from Athabasca Oil Sands*, Kingsley Knowledge Pub., Cochrane, AB, **2011**.
31. M. R. Cervenán, F. E. Vermeulen and F. S. Chute, *Can. J. Earth Sci.*, 1981, **18**, 926–931.
32. B. M. Yaghi and A. Al-Bemani, *Energy Sources*, 2002, **24**, 93–102.

33. X. Gutierrez, F. Silva, M. Chirinos, J. Leiva and H. Rivas, *J. Dispers. Sci. Technol.*, 2002, **23**, 405–418.
34. D. Langevin, S. Poteau, I. Hénaut and J. F. Argillier, *Oil Gas Sci. Technol.*, 2004, **59**, 511–521.
35. R. Pal, S. N. Bhattacharya and E. Rhodes, *Can. J. Chem. Eng.*, 1986, **64**, 3–10.
36. N. N. Zaki, *Colloids Surf. Physicochem. Eng. Asp.*, 1997, **125**, 19–25.
37. S. Acevedo, X. Gutierrez and H. Rivas, *J. Colloid Interface Sci.*, 2001, **242**, 230–238.
38. T. Demorest, P. Read, K. Jonah, F. Payne, W. Kosik and Beers, in *Handbook on theory and practice of bitumen recovery from Athabasca Oil Sands*, eds. J. Czarnecki, J. Masliyah, Z. Xu and M. Dabros, Kingsley Knowledge Pub., Cochrane, AB, **2013**.
39. J. S. Clemente and P. M. Fedorak, *Chemosphere*, 2005, **60**, 585–600.
40. V. V. Rogers, *Toxicol. Sci.*, 2002, **66**, 347–355.
41. P. G. Nix and R. W. Martin, *Environ. Toxicol. Water Qual.*, 1992, **7**, 171–188.
42. K. Clark, Bituminous Sand Processing. CA 298058, April 23, **1929**.
43. J. Hou, X. Feng, J. Masliyah and Z. Xu, *Energy Fuels*, 2012, **26**, 1740–1745.
44. J. Masliyah, Z. J. Zhou, Z. Xu, J. Czarnecki and H. Hamza, *Can. J. Chem. Eng.*, 2004, **82**, 628–654.
45. J. Long, J. Drelich, Z. Xu and J. H. Masliyah, *Can. J. Chem. Eng.*, 2007, **85**, 726–738.
46. X. Ding, C. Repka, Z. Xu and J. Masliyah, *Can. J. Chem. Eng.*, 2006, **84**, 643–650.
47. L. L. Schramm, E. N. Stasiuk, H. Yarranton, B. B. Maini and B. Shelfantook, *J. Can. Pet. Technol.*, 2003, **42**.
48. S. Basu, K. Nandakumar and J. H. Masliyah, *J. Colloid Interface Sci.*, 1996, **182**, 82–94.

49. J. Hupka, J. D. Miller and A. Cortez, *Min. Eng.*, 1983, **35**, 1635–1641.
50. S. Ren, T. Dang-Vu, H. Zhao, J. Long, Z. Xu and J. Masliyah, *Energy Fuels*, 2009, **23**, 334–341.
51. S. Ren, H. Zhao, T. Dang-Vu, Z. Xu and J. H. Masliyah, *Can. J. Chem. Eng.*, 2009, **87**, 879–886.
52. S. Ren, H. Zhao, J. Long, Z. Xu and J. Masliyah, *AIChE J.*, 2009, **55**, 3277–3285.
53. H. Zhao, J. Long, J. H. Masliyah and Z. Xu, *Ind. Eng. Chem. Res.*, 2006, **45**, 7482–7490.
54. H. Zhao, T. Dang-Vu, J. Long, Z. Xu and J. H. Masliyah, *J. Dispers. Sci. Technol.*, 2009, **30**, 809–822.
55. L. L. Schramm, R. G. Smith and J. A. Stone, *Colloids Surf.*, 1984, **11**, 247–263.
56. G. Cymerman, S. Ng, R. Siy and J. Spence, in *Proceedings of CIM Vancouver 2006 Conference*, Vancouver, BC, **2006**.
57. G. Cymerman, A. Leung, W. Maciejewski, J. Spence and B. McDonell, *Oil Sand Hydrotransport Tests at Syncrude Canada Ltd.*, Clearwater, FL, **1993**.
58. V. Wolff, in *Handbook on Theory and Practice of Bitumen Recovery from Athabasca Oil Sands*, eds. J. Czarnecki, J. Masliyah, Z. Xu and M. Dabros, Kingsley Knowledge Pub., Cochrane, AB., **2013**.
59. T. Dang-Vu, R. Jha, S.-Y. Wu, D. D. Tannant, J. Masliyah and Z. Xu, *Colloids Surf. Physicochem. Eng. Asp.*, 2009, **337**, 80–90.
60. T. Kasongo, Z. Zhou, Z. Xu and J. Masliyah, *Can. J. Chem. Eng.*, 2000, **78**, 674–681.
61. D. Wallace, R. Tipman, B. Komishke, V. Wallwork and E. Perkins, *Can. J. Chem. Eng.*, 2008, **82**, 667–677.

62. M. C. Fuerstenau, G. J. Jameson and R.-H. Yoon, *Froth Flotation: A Century of Innovation*, SME, **2007**.
63. T. V. Subrahmanyam and E. Forssberg, *Int. J. Miner. Process.*, 1988, **23**, 33–53.
64. B. Albijanic, O. Ozdemir, A. V. Nguyen and D. Bradshaw, *Adv. Colloid Interface Sci.*, 2010, **159**, 1–21.
65. L. Su, Z. Xu and J. Masliyah, *Miner. Eng.*, 2006, **19**, 641–650.
66. R. Crawford and J. Ralston, *Int. J. Miner. Process.*, 1988, **23**, 1–24.
67. E. S. Tarleton and R. J. Wakeman, in *Solid/Liquid Separation*, Elsevier, **2007**, 1–77.
68. A. Yeung, T. Dabros, J. Czarnecki and J. Masliyah, *Proc. R. Soc. Math. Phys. Eng. Sci.*, 1999, **455**, 3709–3723.
69. X. Yang and J. Czarnecki, *Colloids Surf. Physicochem. Eng. Asp.*, 2002, **211**, 213–222.
70. T. Dabros, A. Yeung, J. Masliyah and J. Czarnecki, *J. Colloid Interface Sci.*, 1999, **210**, 222–224.
71. J. Czarnecki and K. Moran, *Energy Fuels*, 2005, **19**, 2074–2079.
72. R. Tipman, in *Handbook on Theory and Practice of Bitumen Recovery from Athabasca Oil Sands*, eds. J. Czarnecki, J. Masliyah, Z. Xu and M. Dabros, Kingsley Knowledge Pub., Cochrane, AB, **2013**.
73. W. E. Shelfantook, *Can. J. Chem. Eng.*, 2008, **82**, 704–709.
74. F. Rao and Q. Liu, *Energy Fuels*, 2013, **27**, 7199–7207.
75. Y. Long, T. Dabros and H. Hamza, in *Asphaltenes, Heavy Oils, and Petroleomics*, eds. O. C. Mullins, E. Y. Sheu, A. Hammami and A. G. Marshall, Springer New York, New York, NY, **2007**, 511–547.

76. R. Grace, in *Emulsions*, ed. L. L. Schramm, American Chemical Society, Washington, DC, **1992**, vol. 231, 313–339.
77. L. L. Schramm, Ed., *Surfactants: Fundamentals and Applications in the Petroleum Industry*, Cambridge University Press, Cambridge, U.K., **2000**.
78. J. Wu, Y. Xu, T. Dabros and H. Hamza, *Energy Fuels*, 2003, **17**, 1554–1559.
79. J. Matthews, in *Handbook on Theory and Practice of Bitumen Recovery from Athabasca Oil Sands*, eds. J. Czarnecki, J. Masliyah, Z. Xu and M. Dabros, Kingsley Knowledge Pub., Cochrane, AB, **2013**.
80. H. Li, J. Long, Z. Xu and J. H. Masliyah, *Energy Fuels*, 2005, **19**, 936–943.
81. O. B. Adeyinka, S. Samiei, Z. Xu and J. H. Masliyah, *Can. J. Chem. Eng.*, 2009, **87**, 422–434.
82. J. Long, H. Li, Z. Xu and J. H. Masliyah, *AIChE J.*, 2006, **52**, 371–383.
83. E. S. Hall and E. L. Tollefson, *Can. J. Chem. Eng.*, 1982, **60**, 812–821.
84. N. Beier, W. Wilson, A. Dunmola and D. Segó, *Can. Geotech. J.*, 2013, **50**, 1001–1007.
85. C. Wang, D. Harbottle, Q. Liu and Z. Xu, *Miner. Eng.*, 2014, **58**, 113–131.
86. A. Shah, R. Fishwick, J. Wood, G. Leeke, S. Rigby and M. Greaves, *Energy Environ. Sci.*, 2010, **3**, 700.
87. S. Thomas, *Oil Gas Sci. Technol. - Rev. IFP*, 2008, **63**, 9–19.
88. D. Zhu, J. A. Bergerson and I. D. Gates, *AIChE J.*, 2015, **62**, 1364–1381.
89. I. D. Gates, J. Adams and S. Larter, *J. Can. Pet. Technol.*, 2008, **47**.
90. Society of Petroleum Engineers (U.S.), *Directional Drilling*, Society of Petroleum Engineers, Richardson, TX, **1990**.

91. I. B. Ishak, R. P. Steele, R. C. Macaulay, P. M. Stephenson and S. M. Al Mantheri, Review of Horizontal Drilling, Society of Petroleum Engineers, **1995**.
92. Measurement While Drilling, Society of Petroleum Engineers, Richardson, TX, **1995**.
93. B. Calleja, J. Market, J. Pitcher and C. Bilby, Multi-Sensor Geosteering, Society of Petrophysicists and Well-Log Analysts, **2010**.
94. J. J. Sheng, in Enhanced Oil Recovery Field Case Studies, Elsevier, **2013**, 389–412.
95. E. Vittoratos, G. R. Scott and C. I. Beattie, *SPE Reserv. Eng.*, 1990, **5**, 19–24.
96. I. D. Gates, *J. Pet. Sci. Eng.*, 2010, **74**, 138–146.
97. C. Shen, in Enhanced Oil Recovery Field Case Studies, Elsevier, **2013**, 413–445.
98. R. M. Butler, *J. Can. Pet. Technol.*, 1994, **33**.
99. D. P. Komery, R. W. Luhning and J. G. O'Rourke, *J. Can. Pet. Technol.*, 1999, **38**.
100. M. S. Bittar, H.-H. Wu and S. Li, New Logging While Drilling Ranging Technique for SAGD: Theory and Experiment, Society of Petroleum Engineers, **2012**.
101. I. D. Gates and N. Chakrabarty, *J. Can. Pet. Technol.*, 2008, **47**.
102. A. Mukhametshina and B. Hascakir, Bitumen Extraction by Expanding Solvent-Steam Assisted Gravity Drainage (ES-SAGD) with Asphaltene Solvents and Non-Solvents. Society of Petroleum Engineers, **2014**.
103. J. Sharma and I. D. Gates, *SPE J.*, 2011, **16**, 503–512.
104. R. M. Butler, I. J. Mokrys and S. K. Das, The Solvent Requirements for Vapex Recovery, Society of Petroleum Engineers, 1995.
105. L. A. James, N. Rezaei and I. Chatzis, *J. Can. Pet. Technol.*, 2008, **47**.

106. M. Koolman, N. Huber, D. Diehl and B. Wacker, *Electromagnetic Heating Method to Improve Steam Assisted Gravity Drainage*, Society of Petroleum Engineers, 2008.
107. A. Turta, in *Enhanced Oil Recovery Field Case Studies*, Elsevier, 2013, 447–541.
108. M. Greaves, A. M. Saghr, T. X. Xia, A. Turtar and C. Ayasse, *J. Can. Pet. Technol.*, 2001, **40**.
109. T. X. Xia, M. Greaves and A. Turta, *Main Mechanism for Stability of THAI- "Toe-to-Heel Air Injection"*, Petroleum Society of Canada, **2003**.
110. M. Gray, *Upgrading Petroleum Residues and Heavy Oils*, M. Dekker, New York, **1994**.
111. J. G. Speight, *Annu. Rev. Energy*, 1986, **11**, 253–274.
112. J. Chrones and R. R. Germain, *Fuel Sci. Technol. Int.*, 1989, **7**, 783–821.
113. R. N. Watkins, *Petroleum Refinery Distillation*, Gulf Pub. Co., Book Division, Houston, 2d ed., **1979**.
114. M. Morimoto, Y. Sugimoto, S. Sato and T. Takanohashi, *Energy Fuels*, 2014, **28**, 6322–6325.
115. J. B. Joshi, A. B. Pandit, K. L. Kataria, R. P. Kulkarni, A. N. Sawarkar, D. Tandon, Y. Ram and M. M. Kumar, *Ind. Eng. Chem. Res.*, 2008, **47**, 8960–8988.
116. L. Wang, A. Zachariah, S. Yang, V. Prasad and A. de Klerk, *Energy Fuels*, 2014, **28**, 5014–5022.
117. A. Zachariah and A. de Klerk, *Energy Fuels*, 2016, **30**, 239–248.
118. A. N. Sawarkar, A. B. Pandit, S. D. Samant and J. B. Joshi, *Can. J. Chem. Eng.*, 2007, **85**, 1–24.
119. J. Webster, *The measurement, instrumentation, and sensors handbook*, CRC Press, Boca Raton, FL, **1999**.

120. J. Ballinger, *Chemical technicians' ready reference handbook*, McGraw-Hill, New York, 5th ed., **2011**.
121. J. Drelich, J. D. Miller, A. Kumar and G. M. Whitesides, *Colloids Surf. Physicochem. Eng. Asp.*, 1994, **93**, 1–13.
122. A. Nakajima, *NPG Asia Mater.*, 2011, **3**, 49–56.
123. M. Nič, J. Jirát, B. Košata, A. Jenkins and A. McNaught, Eds., in *IUPAC Compendium of Chemical Terminology*, IUPAC, Research Triangle Park, NC, 2.1.0 edn.
124. M. Corti, C. Minero and V. Degiorgio, *J. Phys. Chem.*, 1984, **88**, 309–317.
125. R. Pelton, *Adv. Colloid Interface Sci.*, 2000, **85**, 1–33.
126. P. Kruglyakov, in *Hydrophile-Lipophile Balance of Surfactants and Solid Particles Physicochemical Aspects and Applications*, Elsevier, **2000**, vol. 9, 146–266.
127. K. Bouchemal, S. Briançon, E. Perrier and H. Fessi, *Int. J. Pharm.*, 2004, **280**, 241–251.
128. J. Wu, Y. Xu, T. Dabros and H. Hamza, *Colloids Surf. Physicochem. Eng. Asp.*, 2004, **232**, 229–237.
129. J. Israelachvili, *Colloids Surf. Physicochem. Eng. Asp.*, 1994, **91**, 1–8.
130. K. Urban, G. Wagner, D. Schaffner, D. Röglin and J. Ulrich, *Chem. Eng. Technol.*, 2006, **29**, 24–31.
131. W. F. Eckert, J. H. Masliyah, M. R. Gray and P. M. Fedorak, *AIChE J.*, 1996, **42**, 960–972.
132. S. Melle, M. Lask and G. G. Fuller, *Langmuir*, 2005, **21**, 2158–2162.
133. B. P. Binks and S. O. Lumsdon, *Langmuir*, 2000, **16**, 8622–8631.
134. C. Zeng, H. Bissig and A. Dinsmore, *Solid State Commun.*, 2006, **139**, 547–556.
135. E. Vignati, R. Piazza and T. P. Lockhart, *Langmuir*, 2003, **19**, 6650–6656.

136. N. P. Ashby and B. P. Binks, 2000, 5640–5646.
137. J. Zhou, X. Qiao, B. P. Binks, K. Sun, M. Bai, Y. Li and Y. Liu, *Langmuir*, 2011, **27**, 3308–3316.
138. B. P. Binks and S. O. Lumsdon, *Langmuir*, 2001, **17**, 4540–4547.
139. B. P. Binks and J. H. Clint, *Langmuir*, 2002, **18**, 1270–1273.
140. K. J. Lissant, *Demulsification: industrial applications*, M. Dekker, New York, **1983**.
141. C. Angle, in *Encyclopedic Handbook of Emulsion Technology*, ed. J. Sjöblom, CRC Press, **2001**, 541–594.
142. J. Czarnecki, in *Encyclopedic Handbook of Emulsion Technology*, ed. J. Sjöblom, CRC Press, **2001**, 497–514.
143. U. G. Romanova, H. W. Yarranton, L. L. Schramm and W. E. Shelfantook, *Can. J. Chem. Eng.*, 2008, **82**, 710–721.
144. E. Pensini, D. Harbottle, F. Yang, P. Tchoukov, Z. Li, I. Kailey, J. Behles, J. Masliyah and Z. Xu, *Energy Fuels*, 2014, **28**, 6760–6771.
145. J. Wang, F.-L. Hu, C.-Q. Li, J. Li and Y. Yang, *Sep. Purif. Technol.*, 2010, **73**, 349–354.
146. Y. Wang, L. Zhang, T. Sun, S. Zhao and J. Yu, *J. Colloid Interface Sci.*, 2004, **270**, 163–170.
147. W. Kang, G. Jing, H. Zhang, M. Li and Z. Wu, *Colloids Surf. Physicochem. Eng. Asp.*, 2006, **272**, 27–31.
148. Y. H. Kim and D. T. Wasan, *Ind. Eng. Chem. Res.*, 1996, **35**, 1141–1149.
149. P. Christian, F. Von der Kammer, M. Baalousha and T. Hofmann, *Ecotoxicology*, 2008, **17**, 326–343.
150. A. Henglein, *Chem. Rev.*, 1989, **89**, 1861–1873.
151. J. Zheng, C. Zhang and R. M. Dickson, *Phys. Rev. Lett.*, 2004, **93**.

152. M. G. Bawendi, M. L. Steigerwald and L. E. Brus, *Annu. Rev. Phys. Chem.*, 1990, **41**, 477–496.
153. B. O. Dabbousi, J. Rodriguez-Viejo, F. V. Mikulec, J. R. Heine, H. Mattoussi, R. Ober, K. F. Jensen and M. G. Bawendi, *J. Phys. Chem. B*, 1997, **101**, 9463–9475.
154. X. Peng, L. Manna, W. Yang, J. Wickham, E. Scher, A. Kadavanich and A. P. Alivisatos, *Nature*, 2000, **404**, 59–61.
155. W.-C. Law, K.-T. Yong, I. Roy, H. Ding, R. Hu, W. Zhao and P. N. Prasad, *Small*, 2009, **5**, 1302–1310.
156. T. Missana and A. Adell, *J. Colloid Interface Sci.*, 2000, **230**, 150–156.
157. E. Tombácz and M. Szekeres, *Appl. Clay Sci.*, 2006, **34**, 105–124.
158. S. L. Swartzon-Allen and E. Matijevic, *Chem. Rev.*, 1974, **74**, 385–400.
159. Points of Zero Charge, in *Chemical Properties of Material Surfaces*, CRC Press, **2001**, 731–744.
160. E. Cunningham, *Proc. R. Soc. Math. Phys. Eng. Sci.*, 1910, **83**, 357–365.
161. J. Oberteuffer, *IEEE Trans. Magn.*, 1974, **10**, 223–238.
162. E. Merisko-Liversidge and G. G. Liversidge, *Adv. Drug Deliv. Rev.*, 2011, **63**, 427–440.
163. L. Peltonen and J. Hirvonen, *J. Pharm. Pharmacol.*, 2010, **62**, 1569–1579.
164. E. L. Parrott, *J. Pharm. Sci.*, 1974, **63**, 813–829.
165. E. Merisko-Liversidge, G. G. Liversidge and E. R. Cooper, *Eur. J. Pharm. Sci.*, 2003, **18**, 113–120.
166. R. Vehring, W. R. Foss and D. Lechuga-Ballesteros, *J. Aerosol Sci.*, 2007, **38**, 728–746.
167. R. Vehring, *Pharm. Res.*, 2008, **25**, 999–1022.

168. H. G. Alt and A. Köppl, *Chem. Rev.*, 2000, **100**, 1205–1222.
169. O. W. Webster, *Science*, 1991, **251**, 887–893.
170. W. A. Braunecker and K. Matyjaszewski, *Prog. Polym. Sci.*, 2007, **32**, 93–146.
171. R. Arshady, *Colloid Polym. Sci.*, 1992, **270**, 717–732.
172. F. J. Schork, Y. Luo, W. Smulders, J. P. Russum, A. Butté and K. Fontenot, in *Polymer Particles*, ed. M. Okubo, Springer Berlin Heidelberg, Berlin, Heidelberg, **2005**, vol. 175, 129–255.
173. J. M. Asua, *Prog. Polym. Sci.*, 2002, **27**, 1283–1346.
174. C. S. Chern, *Prog. Polym. Sci.*, 2006, **31**, 443–486.